2020

The Temporal and Spatial Dynamics of Fluvial Carbon Cycling in Irish Blanket Peatland Pools and Soils

Mariya Radomski
Technological University Dublin

The temporal and spatial dynamics of fluvial carbon cycling in Irish blanket peatland pools and soils

Mariya Radomski, BSc, MSc

This thesis is submitted in fulfilment of the requirements for the degree of Doctor of Philosophy (Ph.D.)

Technological University Dublin

Supervisors: Dr. Alan Gilmer, Prof. John Cassidy,

Dr. Eugene McGovern & Dr. Vivienne Byers

School of Transport Engineering, Environment and Planning

September 2020

ABSTRACT

Blanket peatlands in Ireland are reservoirs of organic matter and have effects on carbon dioxide (CO_2) flux regulation. Data on dissolved CO_2 in Ireland is limited. In blanket peatlands, the drainage systems are well connected with pools, hummocks and lawns and this connectivity leads to significant variations in outflows of carbon. The excess carbon dioxide in blanket peatlands could originate from soil organic matter decomposition. Dissolved CO_2 could be transported into pools via surface run-off and lateral throughflow. Peatland pools are typically supersaturated in CO_2. As part of a project described in this thesis, the role of spatial and seasonal variables on carbon dynamics at Kippure blanket peatland was assessed. The methods deployed in here included a continuous *in-situ* monitoring of CO_2 using NDIR (nondispersive infrared) sensors in peatland pools, hummocks and a lawn. The monitoring included meteorological parameters and routine hydrochemical sampling. Three stations were established. The study provided data to produce a conceptual model: 'Kippure-PeatHydro-CO_2' of carbon dynamics. Results suggest that CO_2 concentrations were greater in the waters from hummocks (3.74-292.12 mgl^{-1} [C]) and a lawn (1-6.52 mgl^{-1} [C]) compared to that occurring in pools (0.44-0.71 mgl^{-1} [C]). Higher temperatures, the presence of vascular plants, microbial activity, variable water tables and dissolved organic carbon breakdown were among factors correlated with higher levels of CO_2 in hummocks and lawns. The lower values of CO_2 observed in pools were correlated with a lower pH and the aromaticity of organic matter. In general, diurnal levels of CO_2 were correlated with photosynthetic activity (during daytime) and respiration (during night-time). Fluxes of CO_2 modelled in this study were greater in summer 0.28-0.51 $gm^{-2}d^{-1}$ compared to winter estimates. These were correlated with wind driven turbulence of water. Under changing climate, fluvial exports of CO_2 could increase. The 'Kippure-PeatHydro-CO_2' model

could be a valuable tool in simulating blanket peatland dynamics and in providing insight to the eco-hydrological fluxes of carbon under a changing climatic regime particularly in relation to precipitation and temperature. Such a tool will also greatly facilitate the development of appropriate land-use management strategies consistent with Ireland's greenhouse gas emission regulation and water quality control.

DECLARATION PAGE

I certify that this thesis which I now submit for examination for the award of Doctor of Philosophy, is entirely my own work and has not been taken from the work of others, save and to the extent that such work has been cited and acknowledged within the text of my work.

This thesis was prepared according to the regulations for graduate study by research of the Technological University Dublin and has not been submitted in whole or in part for another award in any other third level institution.

The work reported on in this thesis conforms to the principles and requirements of the Technological University Dublin's guidelines for ethics in research.

Technological University Dublin has permission to keep, lend or copy this thesis in whole or in part, on condition that any such use of the material of the thesis be duly acknowledged.

Signature _____ 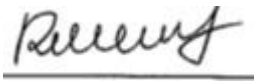 _____ Date _____29/08/2020_____

Candidate

ACKNOWLEDGEMENTS

I would like to thank my spouse Mr. Stanislav Radomski for supporting me tremendously throughout the course of this Ph.D. project. I would also like to thank my supervisor Dr. Alan Gilmer for continuous assistance and guidance throughout the project duration and thereafter.

ABBREVIATION LIST

CO_2	Carbon Dioxide
DOC	Dissolved Organic Carbon
µatm	Microatmosphere
DON	Dissolved Organic Nitrogen
$epCO_2$	Excess Partial Pressure Carbon Dioxide
ER	Ecosystem Respiration
GEP	Gross Ecosystem Production
HumST1	Station one – peat soil
HumST3	Station three – peat soil
LawnST2	Station two – peat soil
NEE	Net flux of Carbon Dioxide
pCO_2	Partial pressure Carbon Dioxide
POC	Particulate Organic Carbon
PON	Particulate organic nitrogen
SAC	Special Areas of Conservation
SD	Standard Deviation
SE	Standard Error
SOM	Soil Organic Matter
ST1	Station one - pool
ST2	Station two - pool
ST3	Station three - pool
TOC	Total Organic Carbon
WT	Water Temperature

TABLE OF CONTENTS

TABLE OF ILLUSTRATIONS AND FIGURES

LIST OF TABLES

CHAPTER 1: INTRODUCTION

1.1 Peatlands

Peatlands are a type of terrestrial wetland ecosystem or a peat-covered terrain with a minimum depth of between 30-40 cm (depending on the country, e.g. Canadian limit is 40 cm and 30 cm is the limit in many other countries) (Lindsay, 1995; Otte, 2003; Rydin & Jeglum, 2013). Wetland ecosystem are typically associated with the simultaneous presence of shallow water bodies and high precipitation levels where the land surface is saturated with water and the inundation of water is sufficient in frequency and duration to support the ecosystem's unique wetland hydrological and hydro geomorphological character (Lindsay, 1995; Otte, 2003; Rydin & Jeglum, 2013). Ecosystem structures that can be classified as wetlands include bogs, fens, marshes, swamps, callows, wet meadows and many lagoons (Lindsay, 1995; Otte, 2003; Rydin & Jeglum, 2013). Peatlands are typically distinguished by an annual accumulation of organic matter (OM) which results where biomass production is greater than annual decomposition (Lindsay, 1995; Otte, 2003; Rydin & Jeglum, 2013). Therefore, peatlands are sedentary systems (formed in place), composed of partially decomposed OM that can include plant (e.g. leaves, woody parts, roots, rhizomes, and parts of bryophytes) and animal remains (e.g. invertebrates, bacteria and fungi), that used to grow or live on the peatland surface or within the peatland soil itself (Lindsay, 1995; Otte, 2003; Rydin & Jeglum, 2013). This partial decomposition is primarily a result of waterlogging, oxygen and nutrient deficiency and high acidity in some cases (Lindsay, 1995; Otte, 2003; Rydin & Jeglum, 2013). The peat layers grow slowly as dead OM is deposited as litter on the surface and covers the older layers of the previous growing period (Rydin & Jeglum, 2013). Some of the dead OM comes from below-ground sources (e.g. roots of plants growing on the mire) and this material also contributes to the growth of the peatland mass (Rydin & Jeglum, 2013).

Peatland classifications

Peatlands can be divided into classes depending on morphology (shape), mode of development (ontogeny) and source of nutrients supplied to vegetation on their surfaces (Lindsay, 1995; Otte, 2003). Three categories of peatlands are found based on their shape (which in turn reflect underlying hydrological/nutrient character), these are fens, raised bogs and blanket bogs (Lindsay, 1995; Otte, 2003) (Figure 1). Based on ontogeny, there are topogenous peatlands that develop as a consequence of impeded drainage that is mediated through features of the landscape (topography) (Lindsay, 1995; Otte, 2003). These peatlands more typically arise where the water-table lies close to the ground surface (Otte, 2003). They may also form in shallow lake basins (Lindsay, 1995; Otte, 2003). Paludification is another developmental classification of peat types – such peat bodies develop where the existing mass of peat grows by accumulation of OM to such a point that it extends out over the surrounding ground surface. This is typically seen around the margins of raised bogs which demonstrate a perched water table which lies permanently above the ground surface (and ground water table) and these margins may often display graminoid species-poor vegetation such as reed-swamps e.g. *Phragmites australis* (common reed) (Lindsay, 1995; Otte, 2003). Mire systems may also arise in freshwater spring settings where the system is water-fed within a topographical depression (Lindsay, 1995; Otte, 2003). Peatlands that develop under the influence of a constant flow of nutrient-rich water are termed soligenous (e.g. blanket peatlands in contact with the underlying mineral soil) while those that develop above groundwater level and under the influence of rainfall are termed ombrogenous (Lindsay, 1995; Otte, 2003).

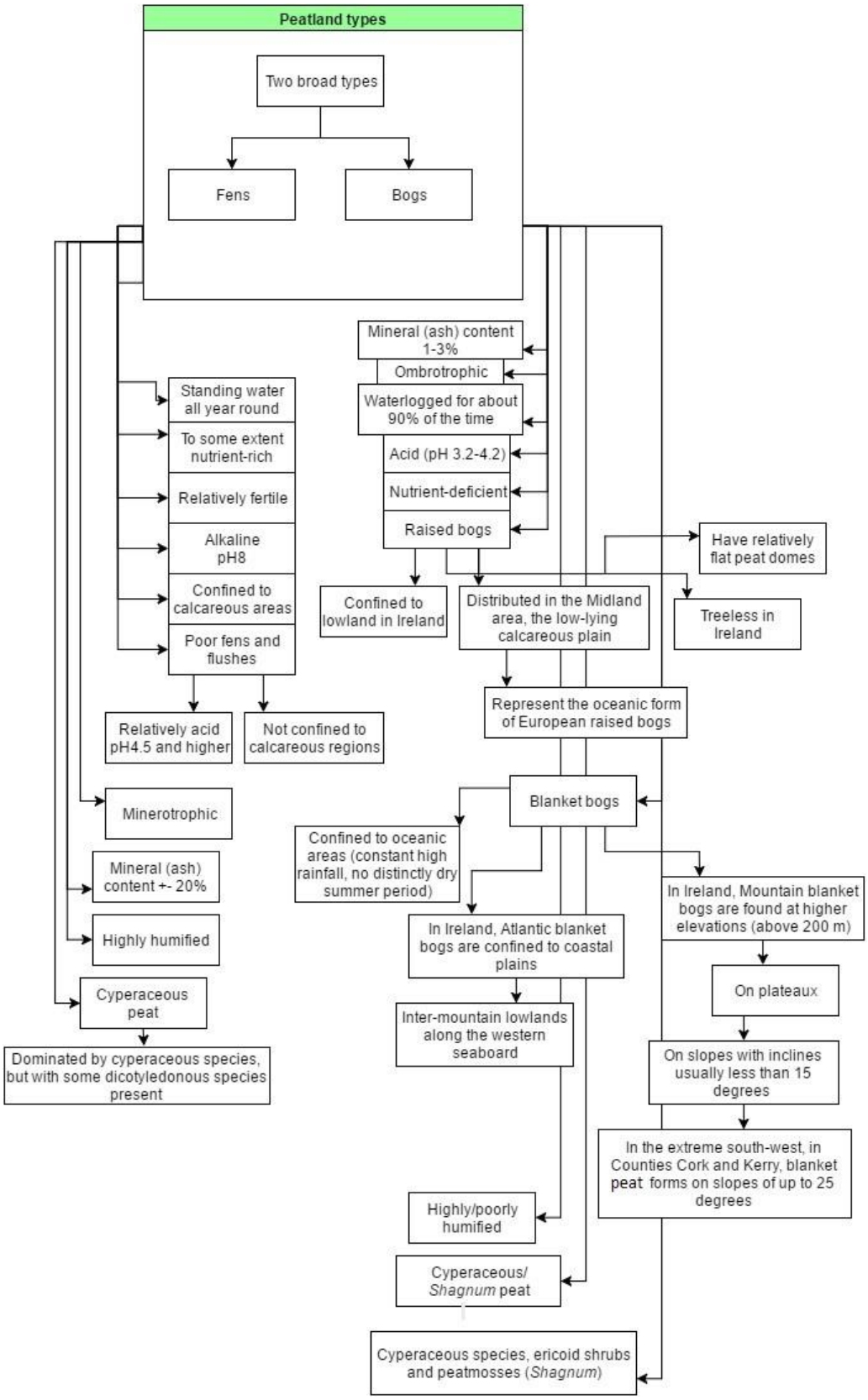

Figure 1 *Peatland types and their characteristics - redrawn after Otte (2003) and Rydin & Jeglum (2013).*

Peatlands can also be classified based on the source of nutrients in the water. Minerotrophic or rheotrophic peatlands are fed by mineral-rich water from outside the system: these are the classical fens (Lindsay, 1995; Otte, 2003) (Figure 1). This is ion contrast with ombrotrophic peatlands (e.g. raised bogs) - nutrient poor, particularly deficient in nitrogen and phosphorus (as well as potassium) and are supplied with nutrients in airborne dust and rainfall (Lindsay, 1995; Otte, 2003; Rydin & Jeglum, 2013) (Figure 1).

Peatlands are extensive in cool humid climatic areas and occur widely in the temperate, boreal and subarctic zones of the Northern Hemisphere (Otte, 2003; Renou-Wilson *et al*., 2011). They are less extensively distributed in the Southern Hemisphere (Otte, 2003; Renou-Wilson *et al.,* 2011). Peatlands are less extensively found in the subtropical and tropical zones, where they are limited to coastal plains and mountain plateaux areas where the climate is humid and surface runoff is impeded (Otte, 2003). It has been estimated that there are about 4.5 million km^2 of peatland in the world, with deep peat deposits retaining about 400 billion tons of peat (Amundson, 2001; Otte, 2003; Schulze & Freibauer, 2005; Bullock *et al.,* 2012; Turner *et al*., 2013). Boreal and subarctic peatlands cover approximately 3% of the Earth's land surface and store about 15–30% (400 to 500 Pg C) of the world's soil carbon while tropical peatlands store approximately 105 Pg C (Limpens *et al*., 2008). Blanket bogs (global cover 1 x 10^5 km^2) are typical of temperate latitude oceanic and mountain regions with high rainfall spread throughout the year, cool summer temperatures and low evaporation rates (Lindsay, 1995). They are features of the landscape in areas along the Atlantic coast of Europe, and are found in Ireland, Great Britain and Norway (Figure 2) (Otte, 2003). Blanket bogs are also found in eastern North America and the Pacific north-west (Otte, 2003).

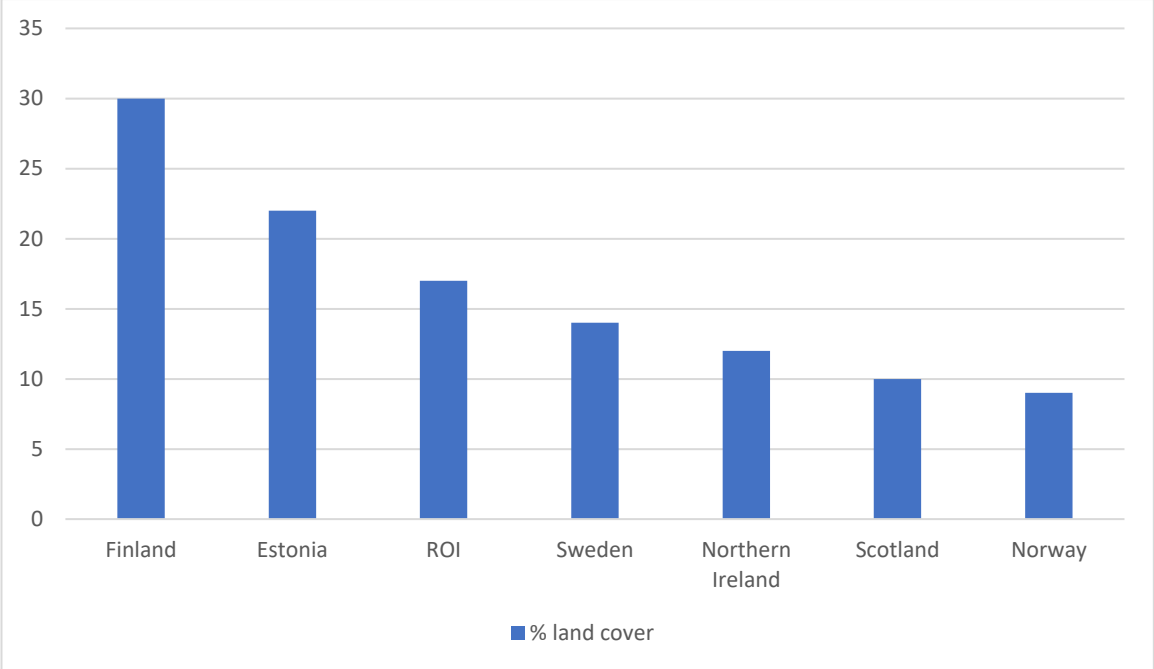

Figure 2 *The extent of peatlands in several countries, expressed as a percentage of total land cover in each location - adapted from Otte (2003).*

1.2 Peatland importance and pressures – globally

Globally peatlands have been acting as sinks of atmospheric carbon dioxide (0.09 to 0.5 Gt C yr^{-1}) for millennia (Limpens *et al*., 2008). In this respect they have a significant impact on climate regulation and through the removal of atmospheric carbon they contribute a negative radiative forcing effect (Limpens *et al*., 2008). If peatlands were to be destabilised, they could potentially emit large levels of carbon dioxide and methane (Limpens *et al.*, 2008). This destabilisation is possible due to a global warming, changes in land use and as result of other anthropogenic practices (Limpens *et al.*, 2008). Extraction of peatland for horticulture is one example of negative anthropogenic practices. This is being practiced extensively in Canada, Ireland and many Baltic countries (Turetsky & St. Louise, 2006). Peat-based growth media is popular in Europe with as much as 90% of it being based on extracted peat as its major or only component

(Joosten & Clarke, 2002). Peat as a base component in growing media is used extensively in the mushroom industry and the overall global trend of usage continues to increase despite a push in certain quarters to see a reduction in this type of use (Renou-Wilson *et al*., 2011). Land-use changes such as peatland afforestation is also altering the dynamic role of peatlands as climate regulators and indeed private afforestation on non-designated sites is unlikely to decline in the near future (Renou-Wilson *et al*., 2011). Afforestation impacts the carbon stock of a peatland by promoting soil aeration, lowering the water table, increasing evapotranspiration and by promoting microbial respiration and organic matter decomposition (Wellock *et al*., 2011). Additionally, peatlands are extensively used as areas for tourism, recreation, sports and even military exercises all of which represent pressures on this land-use type (Renou-Wilson *et al*., 2011). The consequences of tourism include damage by trampling of peatland areas, particularly areas of conservation importance (Borcard & Matthey, 1995). Similar damage to peatlands could be caused by bog visitors, including climbers, cyclists, horse riders and bikers (Renou-Wilson *et al*., 2011). Lack of public awareness, environmental training and the general lack of management plans concerning peatland use are the main reasons for such negative impacts (Murphy *et al*., 2008). But anthropogenic damage is not only occurring through direct interaction but also indirectly through changes in atmospheric chemistry and dynamics associated with changes in the climate patterns (Renou-Wilson *et al*., 2011). Peatlands rely on regimes of atmospheric moisture and precipitation to maintain a stable state (Renou-Wilson *et al*., 2011). Nevertheless, changes to water chemistry including water-borne pollution caused by nutrient runoff (agriculture) could be as damaging as impacts from air-born pollution (Renou-Wilson *et al*., 2011). Nitrogen inputs (air or water-born) from agricultural or urban settings has caused changes in peatland vegetation and promoted shifts in biodiversity (Tomassen *et al*., 2004). It has also been established

that phosphorus enrichment can have a serious impact on peatland dynamics. This can be augmented by clear-felling where phosphorus leaches from afforested peatlands causing a negative impact like that associated with excess nitrogen use (Anderson, 2001).

Peatlands and Development pressures

Infrastructural developments that interact with peatlands can lead to irreversible hydrological changes in the peatland dynamics (Renou-Wilson *et al*., 2011). Significant peatland-based developments include gas pipe networks, wind farms, solar farms, etc. and these developments are becoming more widespread globally (Renou-Wilson & Farrell, 2009). Wind farming is popular in temperate and boreal climates where peatlands are more common (Renou-Wilson & Farrell, 2009). Interreference from development can cause peatland structure to change causing slope failures and exacerbate peatland erosion (Lindsay & Bragg, 2004). Peatland erosion, particularly in the case of mountain blanket peatlands is also greatly affected by the consequence of climate change (Li *et al*., 2018). Increasing temperatures and extreme precipitation events affect soil stability causing bank failures and mass soil movements along with widespread vegetation change which in turn promotes surface erosion (Li *et al*., 2018; Strack *et al*., 2008). While it has been reported that increasing temperatures promote carbon increased sequestration through extending the growing season and enhancing primary productivity it also promotes increased decomposition and evapotranspiration rates (Strack *et al*., 2008). Currently, given the shifting dynamics of the climate system it is unknown whether peatlands will continue their function as net carbon sinks (Limpens *et al.*, 2008). From a precautionary standpoint alone, there is a clear imperative to ensure that the carbon stores of global peatlands are

preserved and protected and where necessary restored through appropriate management practices (Strack *et al*., 2008).

It is significant to note that wetland management plans are being discussed globally and there are many organisations and partnerships across different stakeholders and countries with an interest in promoting their conservation and restoration. The Convention on Wetlands (Ramsar Convention; a treaty signed in the city of Ramsar, Iran), is an intergovernmental treaty that provides a framework for national action and international cooperation designed to promote the conservation (biodiversity) and sustainable use of wetlands and their resources such as water resources (Barthelmes *et al*., 2015). The current programme the 'Forth Ramsar strategic plan 2016-2024' (Ramsar Convention Secretariat, 2016) has four strategic goals: (1) addressing the drivers of wetland loss and degradation, (2) effectively conserving and management of the Ramsar site network, (3) wise use of all wetlands and (4) enhanced implementation of the convention (Ramsar Convention Secretariat, 2016). A complimentary scheme is the Global Peatland Initiative (GPI) which is a collaborative strategy formed and lead by thirteen members who took part in the UNFCCC COP in Marrakech, Morocco in 2016. The primary purpose of the GPI is to promote peatland conservation and prevent further losses of carbon (organic and carbon dioxide) (Global Peatland Initiative, 2016). The GPI initiative is based on two principle approaches: global level actions and national level actions. At the global level the strategy is based on providing and updating an overall assessment of the status of peatlands and their key importance in the global carbon cycle and global economies (Global Peatland Initiative, 2016). At the national level the initiative is based on identifying key counties with significant peatland cover by building a database of peatland occurrence and status, providing sustainable management/action plans and devising options to reduce peatland degradation in those states (Global Peatland Initiative,

2016). The work of the GPI runs parallel to that of the International Mire Conservation Group (IMCG) (National Committee, United Kingdom, 2020) which comprises researchers, consultants and state agencies across 60 countries. The IMCG was established in 1984 in Austria to promote global responsibility in peatland management, including the encouragement and coordination of conservation measures directed at mires and related ecosystems.

1.3 Peatland status: monitoring, conservation and restoration

One of the more significant aspects of peatland conservation is the adequate and accurate monitoring of net ecosystem exchange rates as this essentially determines the sustainability of these systems. This aspect of ecosystem function has been widely addressed (South and North America, Europe, Asia, Africa and Australia) using Eddy Covariance tower techniques with coverage ranging from a few metres to kilometres (Patel *et al*., 2019). This approach directly measures net ecosystem exchange (CO_2 exchange) across the canopy-atmosphere interface by measuring the covariance between fluctuations in vertical wind velocity and the mixing ratio of carbon dioxide (Patel *et al*., 2019). The airflow is considered as a horizontal flow of many rotating eddies each with three-dimensional components (the vertical movement of air is included) representing the turbulent motion of rising and descending air transporting gases including carbon dioxide (Patel *et al*., 2019). There are more than 600 flux towers worldwide located in different ecosystems including peatlands and afforested peatland sites (Patel *et al*., 2019). A global network (FLUXNET), is formed by the combination of regional networks like AMERIFLUX, CARBOEURO FLUX, ASIAFLUX, OZFLUX, and other non-networked sites (Patel *et al*., 2019). Other useful approaches that have been used to monitor carbon dynamics in peatlands include the use of satellite data-driven modelling approaches such

as temperature-greenness, light-use efficiency, and regional-scale Carnegie-Ames-Stanford Approach models (Patel *et al*., 2019). It has been noted that combining Eddy Covariance flux methods and remote sensing data (with modelling approaches) can generate significant insights to the optimization of ecosystem model parameters, output validation, and in up-scaling of CO_2 flux estimates across spatial or temporal scales (Patel *et al*., 2019).

Conservation and the socioeconomic perspective

Recognizing that land-use change may result in significant GHG emissions suggests that avoiding such changes would be beneficial from an overall GHG balance perspective. Preventing land-use change at the socioeconomic level can be associated with various incentives (Strack *et al*., 2008). Incentives may be seen as the avoidance of penalties associated with breaching critical emission levels. This it is argued would incentivise landowners to keep the original land use. Or of course incentives may be seen as positive stimuli where landowners could receive a grant or financial aid if they decide to keep the original land use (e.g. reduced emissions from avoided deforestation and forest degradation initiatives; protection of tropical peatlands) (Strack *et al*., 2008). If land-use change is inevitable or unavoidable then landowners and stakeholders could be incentivised to ensure sustainable management is practiced with respect to hydrology, carbon stocks and water quality (Strack *et al*., 2008). For example, if an undisturbed peatland is to be converted to agricultural use (or forestry), a sustainable management approach would be to reduce the extent and intensity of drainage, reduce the amount of fertilisation, and convert arable cultivation to grasslands, as these measures would either

help minimize or offset peatland decomposition and hence reduce the levels of GHG emissions (Strack *et al*., 2008).

Peatland restoration

There is a growing recognition of the importance of peatland restoration. Various peatland restoration options have been investigated over the years some of which were funded under the EU Life Programme and focused primarily on Natura 2000 sites (Buckmaster *et al*., 2014). Measures that have been evaluated include, drain and ditch blocking to promote hydrological restoration, tree removal, biodiversity restoration, public awareness programmes, large scale restoration and monitoring by remote sensing, the promotion of sustainable grazing, rewetting and controlled burning (Buckmaster *et al*., 2014). In Germany, a pilot project looked at producing *Sphagnum* biomass as an alternative to extracting fossil peat for 'growing media' (horticultural) as a measure to help reduce the loss of pristine bog ecosystems (Buckmaster *et al*., 2014).

Peatland restoration is not only crucial in terms of managing GHG emissions but also in terms of promoting biodiversity conservation (Strack *et al*., 2008). However, measures such as altering the hydrological regime of a peatland through the blocking of ditches requires a detailed assessment of the peatlands hydrology prior to initiating remedial work (Barthelmes *et al*., 2015). It is important to understand how drain blocking might change water flow around the site including water discharge from the site (Barthelmes *et al*., 2015). These dynamics are driven by factors such as slope, the width/size of drains, drain base conditions, accessibility, general topography and the potential impact of other

required engineering structures (Barthelmes *et al*., 2015). Successful blocking of ditches will stop peatland water from draining away and this will have a knock-on effect on peatland oxidation and decomposition (Barthelmes *et al*., 2015). Changes in hydrology will have consequences for species diversity as invasive plant species (shrubs and trees) may establish themselves when conditions are not as wet and acidic (Barthelmes *et al*., 2015).

The peatland rewetting process encourages the growth of peatland forming flora (*Sphagnum*-dominated vegetation) which promotes the re-establishment of the natural peatland state. However, it may also be necessary to reintroduce natural peatland plant communities to restart peatland growth (Barthelmes *et al*., 2015). This may be facilitated by growing plants offsite and then re-introducing when fully developed coupled with direct seeding and then netting of bare peat areas to protect from erosion (Barthelmes *et al*., 2015). It may also benecessary to introduce measures to control or limit nutrient enrichment (e.g. nitrogen and phosphorus) as this helps maintain the peatland flora and protects against the introduction of more aggressive invasive non-peatland plants. (Barthelmes *et al*., 2015).

Although the rewetting of peatlands can create anoxic and reducing conditions which reduce carbon dioxide and nitrous oxide emissions such conditions may also lead to an increase in methane fluxes for short periods of time (Strack *et al*., 2008). Excessive short-term methane emissions associated with the re-wetting process can be offset if the water table is kept low (approx. 10 cm) below the surface (Strack *et al*., 2008). This will promote methane oxidation in the thin oxic layer. In any event the success of peatland

restoration can usually be determined after approximately ten year of rewetting when ideally the carbon dioxide fluxes rates approximate the natural peatland system (Strack *et al*., 2008).

1.4 Conclusion

The role of peatlands in the natural environment is many faceted and the management challenges diverse and complex, yet their significance in terms of maintaining natural biodiversity, their ability and impact on water quality, and most importantly their interaction with climate change underscore the importance of advancing our understanding of their ecophysiological dynamics. In particular there is a need to advance understanding of the factors affecting carbon production and loss from both the terrestrial and aquatic components within peatlands in Ireland. This study seeks to address this challenge in the context of blanket peatlands. This will be addressed through the consideration of three dominant processes:

1. The interaction between temperature, pressure, and precipitation and the levels of CO_2 in the water of pools, hummocks and lawns;
2. The relationship between the fluxing of CO_2 from pools and the speed direction and turbulence of wind;
3. The observable patterns of CO_2 variability across hummocks, lawns and pools with regard to diurnal and seasonal timeframes.

CHAPTER 2: LITERATURE REVIEW

2.1 Peatland development in Ireland

Ireland's temperate climate and topographical features favour saturated conditions and the formation of peatland ecosystems since on average more water falls as precipitation than is lost through evapotranspiration (Otte, 2003). The geomorphology of Ireland also plays a major role in promoting saturated soils as the central regions tend to have a lower elevation than coastal areas which causes many streams and rivers to initially flow inland rather than straight out to sea which facilitates the development of wetlands (Otte, 2003). It is also evident that at the end of the last glacial period (approx. 12, 000 years ago) the retreating ice helped shape the geomorphology in a way that promoted peatland formation (Figure 3) (Otte, 2003). In particular the retreating ice tended to leave extensive networks of drumlins and eskers enclosing poorly drained pockets of land (Otte, 2003; Renou-Wilson *et al*., 2011). These glacial deposits impeded free drainage and hence numerous relatively shallow lakes were formed which gradually infilled through vegetation growth and sediment accumulation (Otte, 2003). The vegetation in deeper water bodies comprised aquatic species such as water lilies and pondweeds while emergent aquatics reeds, sedges, etc., gradually encroached on to the open water from the lake margins (Otte, 2003). Highly productive plant species, such as *Phragmites australis*, produced significant quantities of litter, which sank to the bottom of the lakes and accumulated as poorly decomposed litter. The litter and other sediment deposits (trapped in dead vegetation) eventually filled the entire lake basin up to the original lake water level - producing topogenous basin peat (Otte, 2003). Under constant water supply from the surrounding slopes mineral water fed peat (fen type peats) continued to accumulate material and rise upward (Otte, 2003). Peats growing under the influence of nutrient-rich water are known as soligenous, minerotrophic or rheotrophic. As these peat bodies grew

in size portions of them began to extended out over the original basin template and to cover an ever greater area in a process known as paludification (Otte, 2003).

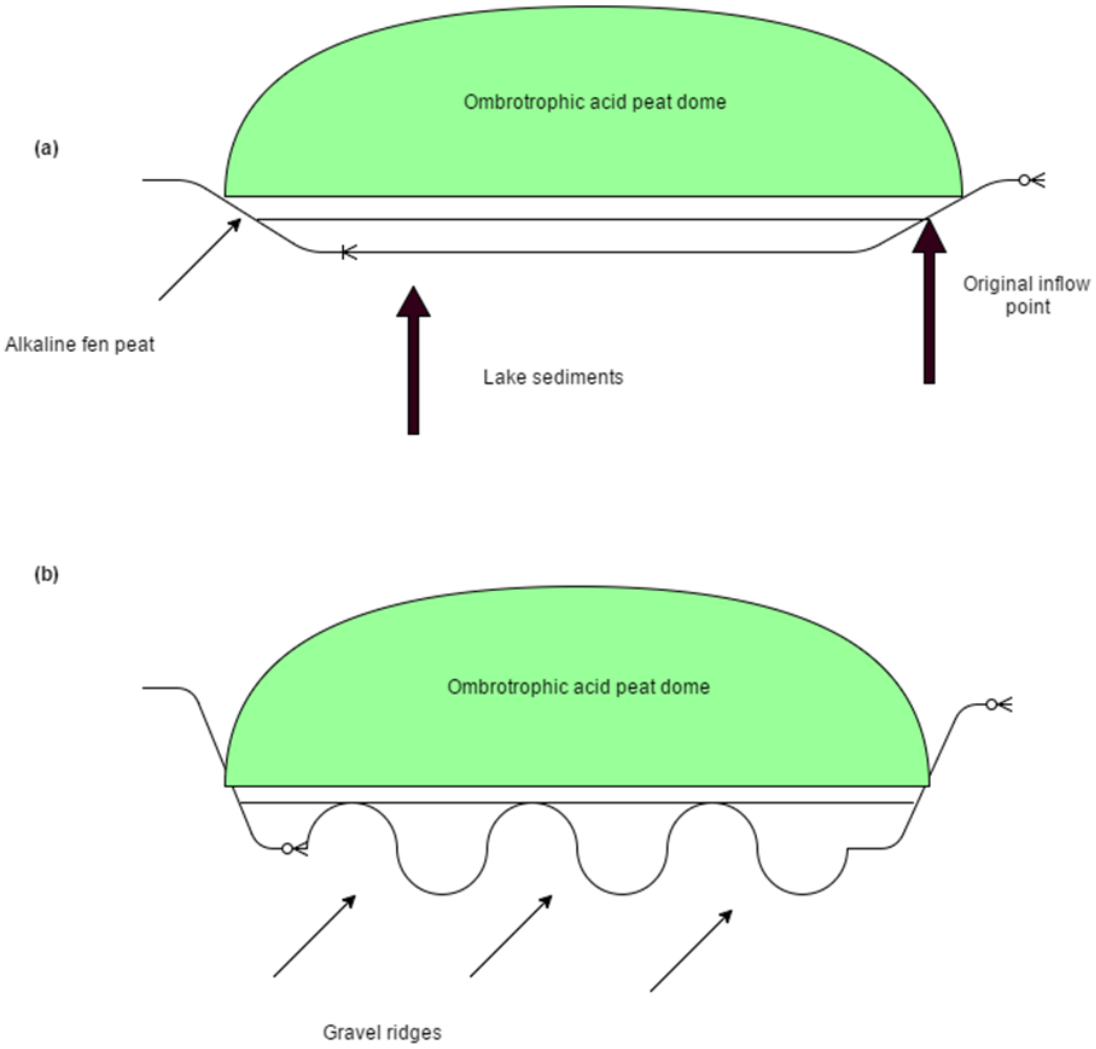

Figure 3 *Development of a typical Irish raised bog: (a) a lake overlaid by fen deposits, reaching as far as the original inflow point and overtopped by an ombrotrophic peat dome; (b) many Irish raised bogs that now have a single dome formed through a coalescing of several smaller domes that spread over intervening gravel ridges - redrawn after Lindsay (1995) & Otte (2003).*

These fens peats are generally shallow but may form peat deposits up to 6 m deep (Otte, 2003). In most places, this fen peat stage was superseded by a further accumulation phase, where peat developed under the influence of rainwater, giving rise to the ombrotrophic peat domes of classical raised bogs (Otte, 2003). Hence the majority of ancient fens are buried beneath the accumulated deposits of the raised bogs. However, there are contemporary examples of fens possible representing the early phases of future raised bogs e.g. Pollardstown Fen in County Kildare (Otte, 2003). Other fens found in Ireland today are more likely to be of recent origin or else have developed on man modified bogs (Otte, 2003).

Many Irish raised bogs followed the form of development from fen to bog as outlined above where the basal (lake) deposits are usually formed of blue-grey, calcareous remains. These are then overlaid by black fen peat deposits containing the readily recognised remains of rhizomes (underground stems) of typical fen plants, such as those of *Phragmites australis* and *Cladium mariscus* (saw sedge) (Otte, 2003). This fen peat is covered by a layer of red brown, humified peat containing the obvious macrofossils of *Eriophorum vaginatum* (harestail cotton-grass), representing the first stage of ombrotrophic bog development (Otte, 2003). In many places, this bog cotton layers gives way to wood peat containing substantial sub-fossils (trunks, stumps and root masses) mainly of scots pine (*Pinus sylvestris*), birch (*Betula pubescens*) and alder (*Alnus glutinosa*). This palaeoeclogical shift reflects a significant environmental change leading to a pronounced drying of the peatlands (a distinctly dry climatic period from 4330 to

4120 BP). This climate shift also shows distinct evidence of fire episodes which either occurred accidentally or were caused by Neolithic peoples in an effort to clear lands of forest for agricultural purposes. In any event this change in environmental conditions promoted the development of pine woodland that spanned the period from about 4300 to 3200 BP (Otte, 2003). Through reversion to a wetter climate, and in some places the impact of fire, the woodland phase gave way to a further episode cooler temperatures and increased precipitation in association with ombrotrophic bog development (Otte, 2003). This is evidenced in a further deposit of *Eriophorum* peat phase, followed by a *Sphagnum* phase, in which *S. imbricatum* (*S. austinii*) was the dominant peat former (Otte, 2003). The development of this *Sphagnum imbricatum* peat phase continued into historical times, when *Sphagnum magellanicum* generally replaced *S. imbricatum* (Otte, 2003). It is now known that *Sphagnum magellanicum* has the ability to regenerate from depths of up to 30 cm below the peat surface and is relatively resistant to fire damage (Otte, 2003). The integrity of the raised peat dome, which is about 90% water, depends entirely on the skin of vegetation that binds the system together and prevents the fluid peat from flowing out of the basin (Otte, 2003). Bog bursts occur where the integrity of the vegetation is destroyed, with the entire peat mass flowing out of its original location (Otte, 2003).

Peat structure

The roots and rhizomes of the vegetation of raised bogs are mainly confined to the uppermost biologically active and relatively well oxygenated colloidal peat layer. This layer is termed acrotelm, and is usually about 30 cm deep (Otte, 2003). This is distinguished from the underlying anoxic and relatively biologically inactive catotelm (Otte, 2003). Raised bogs are the deepest of the Irish peatland types, e.g. Raheenmore in

County Offaly reaches a depth of 15 m and is the deepest known Irish example (Otte, 2003). In contrast blanket bogs are found covering lowland landscapes (Atlantic blanket bogs) in the west of Ireland and highland/mountain landscapes in other locations (Otte, 2003). The ratio of precipitation to evaporation is blanket bog regions is typically greater than 2:1 (Otte, 2003). Blanket peat initiation in Ireland commenced in topographical depressions during the Postglacial/Boreal transition approximately 9000 BP (Otte, 2003). Embryonic soligenous peatlands formed in localised depressions from which blanket bog subsequently spread (Otte, 2003) (Figure 4). These embryonic peatlands were later invaded by and/or surrounded by pine forest, as evidenced by exposed pine stumps found in peat bodies and at the mineral soil/peat interface (Otte, 2003). The two pine layers are observable in many places and are separated by peat layers of up to 60 cm in some places. These pine woodland episodes mimic analogous woodland phases that are recognised in peatlands elsewhere in Europe and are referred to as the Early and Late Atlantic pine forests (Otte, 2003). Following the later pine woodland phase, highly humified, cyperaceous peat accumulated and began to overtake the woodland (Otte, 2003). This peat deposition has continued to occur right uo to the present day, forming a relatively deep blanket of 3.5 m on average, with depths of 7 m in some depressions (Otte, 2003). The timing of blanket peat initiation varied from place to place, spanning several millennia (Figure 4) (Aalen *et al*., 2011; Otte, 2003; Renou-Wilson *et al.*, 2011).

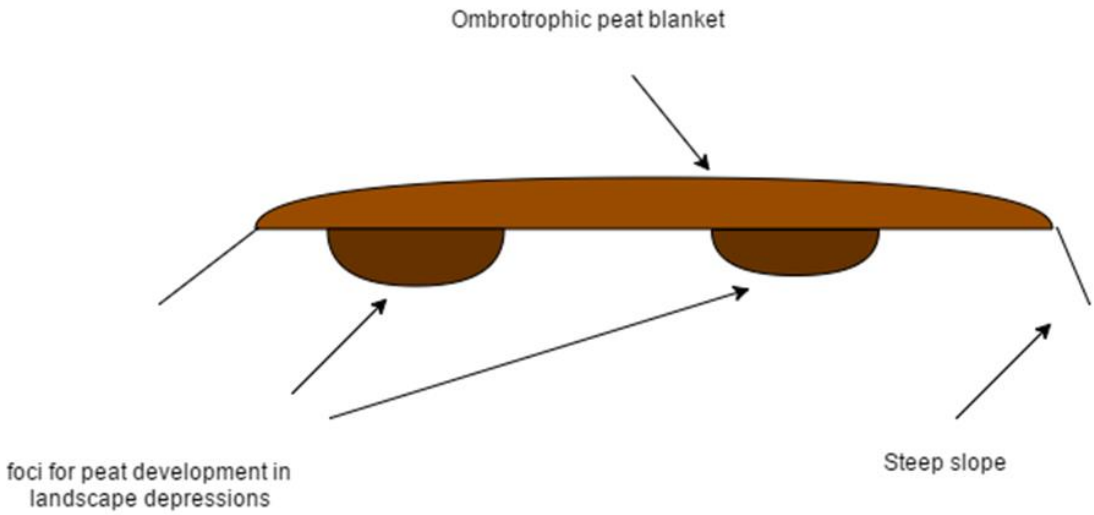

Figure 4 *Blanket bog development: initial development may be confined to depressions on the landscape, peat spreads from these focal points and coalesces to form an apparently uniform peat blanket - redrawn after Lindsay (1995) & Otte (2003).*

2.2 Extent of Irish peatlands

Ireland has peatlands covering 11,456 km^2 or 17% of the land surface of the Republic of Ireland and 16.2% of the island of Ireland. In terms of western European countries only Finland and Estonia have a greater peatland cover (Figure 5). Ireland has the largest cover of blanket bogs in Europe which extended at its maximum to 7,750 km^2 (Hammond, 1979; Conaghan *et al*., 2000). Of all the peatland types Mountain blanket peatlands were the most extensive covering some 5,660 km^2 at their maximum (Hammond, 1979; Renou-Wilson *et al*., 2011). This was followed by Atlantic blanket bogs (3,309 km^2), raised bogs (3,138 km^2) and with fens originally covering about 1,018 km^2. Total peatland cover amounted to 13,125 km^2.

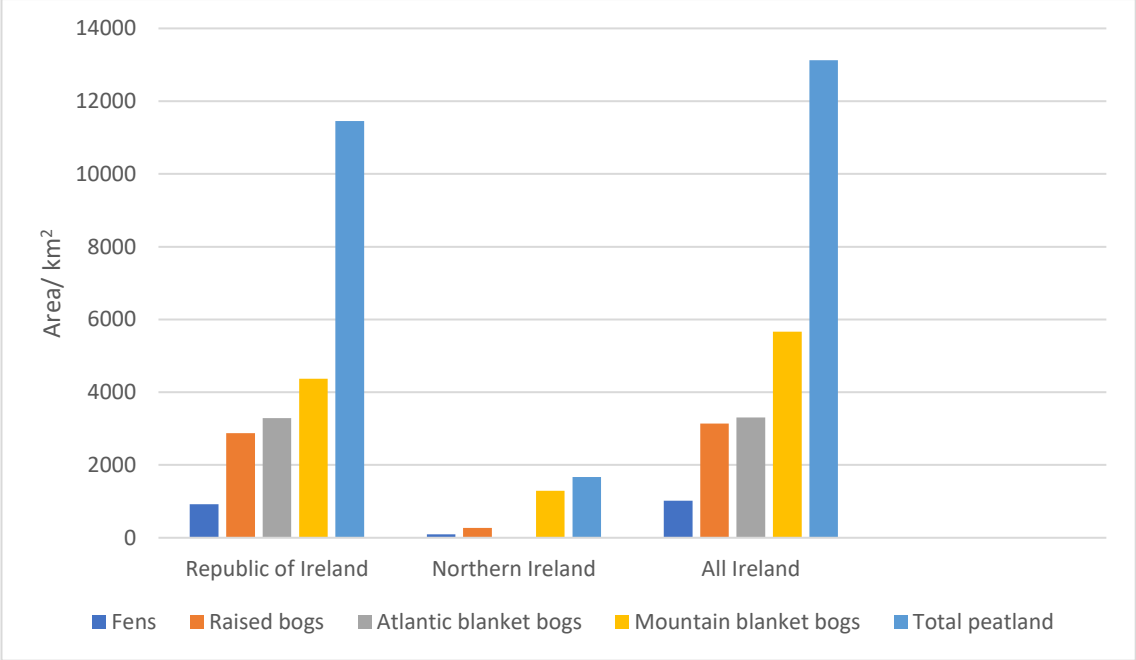

Figure 5 *The original extent of peatlands (km^2) in Ireland - based on data presented by Hammond (1979).*

2.3 Importance of Irish blanket peatlands

Undisturbed blanket peatlands provide many ecosystem functions and services such as nutrient cycling, water filtration, climate regulation, contaminant removal and soil formation roles (Renou-Wilson *et al.*, 2011). Historically peatlands have proven useful as a raw material for fuel and horticulture. However, more recently their importance has been recognised in regulating hydrological systems and atmospheric carbon, supporting biodiversity, and in providing cultural and recreational landscapes. Peatlands in Ireland represent a vital part of the national culture, and have played an important role in Irish history, traditions and economic development (Renou-Wilson *et al.*, 2011). However, peatland resources must be utilised in a way that is consistent with the principles of sustainable development (Scoones, 2007). The sustainability of a system describes its

ability to return to its original normal state after experiencing shock and stress (Scoones, 2007).

Peatlands and sustainable development

The objectives of sustainable development and the UN Sustainable Development Goals are to meet the needs of the present population without compromising the needs (economic, social, cultural and environmental) of future generations (Scoones, 2007; Renou-Wilson *et al.*, 2011). This intrinsic motivation is fundamental to sustainable development, as defined by the Brundtland Commission (WCED, 1987) and encompassed in the United Nations (UN) Sustainable Development Goals (SDGs) (UNEP, 2015). Following the United Nations Conference on Environment and Development (UNCED - Rio de Janeiro, June 1992), several international policies, regulations and action plans were developed to promote and implement sustainable development, such as the European Union Sustainable Development Strategy (EU SDS) (European Council, 2006). According to the EU SDS, member states are required to incorporate sustainable development into various policies, such as those dealing with climate change, green technologies and the low-carbon economy (European Commission, 2009).

In Ireland, the Environmental Protection Agency (EPA) is a body responsible for producing the Framework for Sustainable Development for Ireland. This was developed through research and collaboration and publication in 2012 (Department of Environment, Community and Local Government, 2012; Lehane & O'Leary, 2012). This document highlights how current systems of production and consumption cannot be sustained without excessively impacting on the environment and human health. Indeed, it identifies key areas that need to be tackled in the near future including climate change, biodiversity

loss, water and air quality and pollution. The main objective of this framework have been to promote integration of sustainability principles within general policy development and to initiate effective implementation mechanisms to advance sustainable development (Department of Environment, Community and Local Government, 2012; Lehane & O'Leary, 2012). This has shaped the EPA's 2020 Vision Strategy which seeks to build on that framework in driving climate change adaptation and mitigation, soil and biodiversity conservation, air quality improvements, the sustainable use of resources, water resources protection and the integration and enforcement of environmental policies and regulations (Lehane & O'Leary, 2012).

Globally peatland resources have been degraded over the last 200 years with the loss of many peatland habitats. In Western Europe over 90% of the original mire extent has been lost, while in central Europe the loss of habitat cover is over 50% (CC-GAP, 2005). In Southeast Asia as much as 70% of the tropical peat swamp forests have been significantly degraded (CC-GAP, 2005). It is now estimated that only 15% of the original Irish peatland resource is in a near-intact or pristine state (Renou-Wilson *et al.*, 2011). In Ireland, peatlands have been extracted for fuel and power generation as well as being drained and converted to agricultural use or commercial afforestation. The peat resource has also been used as a raw material in agriculture, horticulture and chemical production (e.g. filters, bedding material and absorbent substrates) (Bullock *et al.*, 2012). Peatlands have also been damaged by atmospheric deposition of pollutants, widespread overgrazing, infrastructural developments, fires and by the introduction of non-native species (Renou-Wilson *et al.*, 2011; Bullock *et al.*, 2012).

Industrial use of peatlands

In Ireland it has been estimated that peat extraction has affected as much as 85% of the original raised bogs and 45% of the original blanket bogs (Malone & O'Connell, 2009). Direct household and industrial burning of peat (fuel source) is releasing 2.1 million tonnes of carbon into the atmosphere per year and this is part of a global picture that is likely to elevate the potential of the atmosphere to trap additional head and raise global average temperatures (Bullock *et al.,* 2012; Rydin & Jeglum, 2013; Turner *et al.,* 2013). Nowadays, blanket peatlands are still widely used for peat extraction in Ireland (Bullock *et al.,* 2012). This extraction uses various techniques including hand harvesting, non-industrial mechanical harvesting and industrial harvesting (Conaghan *et al.,* 2000; Bullock *et al.,* 2012). Hand-harvesting technique have been responsible for losses of approximately 4,700 km^2 of peat and this has been a significant factor in degrading the landscape (Conaghan *et al.,* 2000; Bullock *et al.,* 2012). Approximately 2,500 km^2 of peat has been removed using non-industrial mechanical harvesting (Conaghan *et al.,* 2000; Bullock *et al.,* 2012). Turbary rights govern a major portion of domestic peat extraction and has been carried out for centuries in Ireland - it is estimated that 4,700 km^2 of blanket and raised bogs (including protected areas) have been affected by this practice (Malone & O'Connell, 2009). Technological advancements (hopper, excavator) have led to peat extraction over an even wider area of bog (blanket and raised) and much of this has been what amounts to a semi-commercial basis (Conaghan *et al.,* 2000). This practice has accelerated the degradation of the landscape, promoting decomposition and carbon emissions (Conaghan *et al.,* 2000; Bullock *et al.,* 2012).

2.4 Peatlands, climate change and policy

The relationship between the biosphere and climate is significant and demonstrates a two-way feedback system where the biosphere is controlled by and in turn regulates the climate system. Peatlands are a major biome within the biosphere and hence play a significant part in the regulation of climate and in turn are regulated by climate (Frolking *et al*., 2006). Peatlands require climatic conditions that favour highly saturate soils that promote the accumulation of shallow bodies of water. As peatlands develop, they slowly absorb carbon dioxide from the atmosphere and store this carbon in the fossilised remains of the peat body (Frolking *et al*., 2006). As a result, they tend to exert a net cooling effect on the global climate system which in turn promotes the conditions for lower rates of evaporation and enhanced water accumulation (Frolking *et al*., 2006; Strack, 2008). This is a positive feedback loop. The amount of stored carbon in Irish peatlands is significant and according to estimates based on the depth and density of peat, Ireland's bogs hold approximately 1.08 billion tonnes of carbon (Bullock *et al.*, 2012). However, disturbance leading to peatland degradation is likely to alter the dynamics of these ecosystems to such an extent that they lose their ability to effectively sequester and store carbon. This leads to them becoming carbon emitters which in turn promotes climate warming. Renou-Wilson *et al.* (2011) outlined that disturbed Irish peatlands emit approximately 2.64 Mt of carbon per year directly and only uptake and store 57, 402 t of carbon per annum. The picture gets even more serious if one would consider the amount of the methane and dissolved organic carbon loses along with the carbon dioxide (Connolly & Holden, 2013). Increasing temperatures (around 0.2°C per decade) are expected to increase winter rainfall and reduce summer rainfall causing a reduction in the area of suitable land available for peatland formation by as much as 30% by 2055 (Bullock *et al.*, 2012; Connolly & Holden, 2013).). Higher temperatures can also increase evaporation further

reducing the ability of peatlands to grow – here positive feedback is pushing the system towards a positive radiative force or global warming impact. This complex network of biosphere-climate feedback underscores the importance of ensuring that these extensive ecosystems are carefully monitored, and all appropriate measures are undertaken to ensure they remain stable. Peatland degradation also has other associated impacts including consequences for biodiversity and related systems such as water quality, ecosystems services and land-use (Renou-Wilson *et al.*, 2011).

Globally climate impacts can be seen in the melting of permafrost peatlands (Canada, Finland and Russia) and the changing of vegetation patterns in temperate peatlands (Gunnarsson *et al*., 2002). The Irish BOGLAND project has revealed that climate change impacts on peatlands and their general sensitivity is partly dependent on their geographical location (Renou-Wilson *et al.*, 2011). It has been suggested that mountain blanket peatlands and low-lying midland bogs are particularly vulnerable to an upward shift in global temperatures (Renou-Wilson *et al.*, 2011). These changes will put Irish peatlands under stress causing biodiversity loss, peatland and soil erosion, GHG losses and enhance carbon fluvial losses (Heathwaite, 1993).

Irish peatlands and conservation

In Europe, many peatland habitats are identified as 'priority' habitats under the Habitats Directive (Council directive 1992/42/EEC, 1992). In Ireland, 20% of the total number of bog habitat types (59) have received SAC designation (Renou-Wilson *et al.*, 2011). These special habitats are listed in Annex 1 of the Habitats Directive (Council directive 1992/42/EEC, 1992). According to Douglas *et al.* (2008) there are currently 1,600 km^2 of

peatlands in Ireland that are designated as SAC. Irish peatlands are sources of unique flora and fauna and losses of biodiversity in Ireland would be associated with gene pool loses at national and international levels (Renou-Wilson *et al.*, 2011). Overall peatland habitat status in Ireland has been rated as poor (Douglas *et al*., 2008). There remains a clear need to enhance the conservation status of Irish peatlands including biodiversity protection (European Commission, 2003). In this respect it is acknowledged that society has a significant role to play in that much of the degradation and habitat loss experienced by Irish peatlands has been associated with human activity (Renou-Wilson *et al.*, 2011).

Peatlands fluvial carbon dynamics

It has been demonstrated that climate change and its impact on peatland dynamics has a direct link with acidification in peatlands (Turner *et al.*, 2013). Indeed, Irish peatlands are a key source of dissolved organic carbon (DOC) which has the potential to decrease the pH values in freshwater systems (Mattsson *et al.*, 2007; Feeley *et al*., 2012; Toivonen *et al.*, 2013). In this respect there is an important relationship between water quality and the health status and dynamics of Irish peatland ecosystems. This has clear implications for Ireland's obligations to improve and maintain water quality under the terms of the Water Framework Directive (WFD) 2000/60/EC which seeks to ensure the sustainable management and protection of water resources (Council directive 2000/60/EU, 2000). The restoration and maintenance of freshwater systems free from potentially harmful chemical and microbiological contaminants, is not only a requirement for the preservation and protection of associated ecosystems but is a fundamental requirement for human life (Bridgeman *et al*., 2014).

2.5 Upland blanket peatlands in Ireland

In Ireland mountain blanket peatlands are typically found on mountain plateaux regions throughout the island of Ireland at altitudes exceeding 200 m (Otto, 2003). They can develop on gentle slopes of ≤ 15 degrees but have been found on slopes of 25 degrees in the extreme south-west (Cork and Kerry mountains) (Otto, 2003). In the eastern parts of Ireland, blanket bogs are confined to cooler upland areas (e.g. Wicklow Mountains) over 300-400 meters in altitude and subjected to high levels of precipitation (Conaghan *et al*., 2000). Atlantic blanket bogs have many characteristics in common with mountain blanket bogs although they can be readily distinguished on floristic grounds (Otto, 2003). Mountain blanket bogs are generally graminoids-dominated: the co-dominants are *Eriophorum vaginatum* and *Trichophorum caespitosum* (Otto, 2003). The ericoid component includes *Calluna vulgaris, Erica tetralix, Andromeda polifolia*, the latter missing from Atlantic blanket bog, with an admixture of mountain species such as *Empetrum nigrum* (crowberry) and *Vaccinium myrtillus* (bilberry) that are again absent from Atlantic bogs (Otto, 2003). The vegetation of mountain blanket bog lacks number of the species that are typical of Atlantic blanket bog, including *Schoenus nigricans, Molinia caerulea* (which may occur in areas that are significantly grazed), *Pinguicula lusitanica, Polygala serpyllifolia, Pedicularis sylvatica, Potentilla erecta, Campylopus atrovirens* and *Pleurozia purpurea* (Otto, 2003). The *Sphagnum* cover is often less extensive than in Irish raised bogs (Otto, 2003). Irish examples of mountain blanket bog are closely allied to those found in similar situations in mountainous areas in the UK and Western Norway (Otto, 2003).

In the upland blanket peatlands, the water can move both vertically and laterally, although lateral movement can be quite slow (Otto, 2003). Water that occurs above the peat surface

flows quickly as surface sheet flow. This water can form gullies, pools or channels. Below the peatland surface the water flow rate decreases quickly as it mediates the peatland mass of weakly decomposed organic material (Lindsey, 1995; Otto, 2003). Peatlands have long been recognised as presenting two broad structural zones largely defined by the presence or dominance of the water table. The upper aerobic layer or acrotelm is the aerobic layer while the permanently saturated lower catotelm is the anaerobic layer – the diplotelmic approach (Otto, 2003) (Figure 6). The acrotelm demonstrates greater microbial activity and is the layer where plant growth is dominant, it generally occurs above the lowest level of the water table (Otto, 2003). Different peatland stratigraphical units or positions within the peatland profile (microtopographic units) can be distinguished in relation to the depth of the water table and collectively these determine the variation in the thicknesses of the acrotelm (Otto, 2003). Peatlands with mud-bottoms and carpets of vegetation floating in water can effectively have little or no acrotelm, whereas lawns can demonstrate an acrotelm of 5-20 cm thick, while hummocks can have acrotelm of 50 cm or more (Otto, 2003). The second layer in the peatland structure is the catotelm, which lies below the acrotelm and is anoxic, this layer presents as a more humified darker layer and has the greatest volume (Otto, 2003). The acrotelm is the place where the most intense hydrological and biogeochemical processes occur, because it consists of living and recently dead plant material and it is aerobic (Lindsey, 1995; Otto, 2003). With some exceptions (flow via peatland pipes) the flow of water through the catotelm is much slower than the acrotelm.

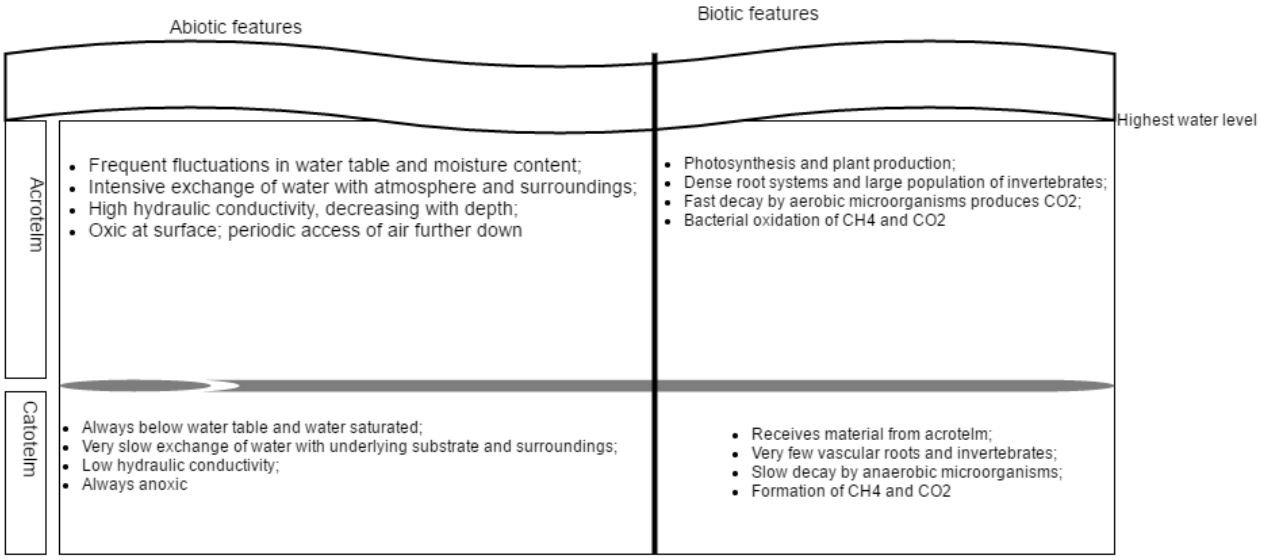

Figure 6 *The acrotelm-catotelm features. Redrawn after Otte (2003) and Rydin & Jeglum (2013).*

Blanket Peatlands and fluvial Carbon

Upland blanket peatlands influence the water quality in the highland and headwater streams. It is known that Irish east coast upland blanket peatlands have been disturbed in the past and that future climatic alterations will further alter their ability to act as carbon sinks and will likely promote losses of dissolved carbon dioxide (CO_2) and dissolved organic carbon (DOC) into the vast watercourses, pools and streams that are a part of these ecosystems. It has been recently acknowledged that globally streams receive significant quantities of terrestrial DOC (4 PgC) and generate about 1.8 ± 0.25 petagrams of CO_2 per year (Battin *et al.*, 2008; Raymond *et al.*, 2013). This is six times greater than what lakes and reservoirs release every year together (Battin *et al.*, 2008; Raymond *et al.*, 2013). The loss of ever larger volumes of carbon into highland streams and watercourses will have detrimental effects on both the hydrochemistry and hydrobiology of these aquatic systems and can also affect regional carbon balances by transporting significant

volumes of terrestrial carbon (organic and inorganic; dissolved and particulate) and promoting the release of CO_2 into the atmosphere (Yang *et al*., 2015; Ruhala *et al*., 2017).

2.6 Peatland microforms: hummocks, lawns and pools

The vegetation in blanket peatlands presents a sequence of topographical microforms. There include raised vegetation features or hummocks which stand about 20-50 cm above the lowest surface level. Below the hummocks are hollows comprising raised lawns which lie about 5-20 cm above the water table blending with lawn carpets which occupy a boundary layer from 5 cm below to 5 cm above the water table. The lowest topographical layers comprise mud-bottoms (inundated) and bog pools - permanently water filled basin (Figure 7). These microforms not only differ in terms of their relative water table position but also in terms of their nutrient composition, oxygen levels and pH. It has been suggested that the difference in elevation between hummocks and hollows is dependent on a positive feedback system between the thickness of the aerated (O_2 rich) peat layer and the rate of peat formation (Belyea & Clymo, 2001). Rates of decomposition of *Sphagnum* spp., water table position and plant species interaction are also linked with the microtopography (Belyea, 1996). Pool formation has been linked to changes in hydrological conditions, where a series of interrelated steps such as higher than normal precipitation results in a rise of the water table which gives rise to ponding in hollows. The new water body causes a reduction in vegetation productivity, while hummocks remain unaffected and are still productive (Belyea & Clymo, 1999). Under conditions of permanent waterlogging, with time, these hollows completely transform into pools and deepen (Belyea & Clymo, 1999). Peatland pool dimensions can vary, ranging from tens of meters to several hundred meters across while their depths may vary from less than a meter to more than two meters (Pelletier, 2014). Most pools are regarded as secondary

features of peatlands as their bottoms are underlain by peat that accumulated prior to pool formation. There are also mineral bottom pools such as those that occur in the Hudson Bay lowlands although these are not common (Hamilton *et al.,* 1994). Peatland pools may also produce a distinct layer of gyttja sediments derived from benthic productivity. These deposits accumulate above the peat prior to full pool formation and are found in a number of locations such as Hammarmossen raised bog in Sweden (Pelletier, 2014). Each microform has its own set of environmental conditions, hummocks have aerated peat, which allows for the growth of dwarf shrubs and *Calluna vulgaris*. *Caluna vulgaris* is the most prominent indicator of the lower limit of the hummock (Rydin & Jeglum, 2013). Lawns are typically characterised by densely growing graminoids (cyperaceous plants, grasses, etc.) such as *Eriophorum vaginatum* (Rydin & Jeglum, 2013). These plant species have bulky, strong and have rhizomes and root networks (Rydin & Jeglum, 2013). Additionally, lawns have a very diversified cover of bryophytes and present high species richness (Rydin & Jeglum, 2013). A sparse cover of cyperaceous plants can be found in places where carpets occur (Rydin & Jeglum, 2013). They have a bryophyte dominant vegetation cover that makes them soft (Rydin & Jeglum, 2013). The mud-bottoms are usually inundated and lacking vascular plants. Here the vegetation cover is limited to creeping mosses, liverworts and to a thin layer of algae covering the bare peat (Rydin & Jeglum, 2013). These units are characteristically soft (Rydin & Jeglum, 2013). Some plant species are found in pools, particularly prominent species such as floating *Sphagnum* (*S. cuspidatum*), which can be found at the pool margins (Rydin & Jeglum, 2013).

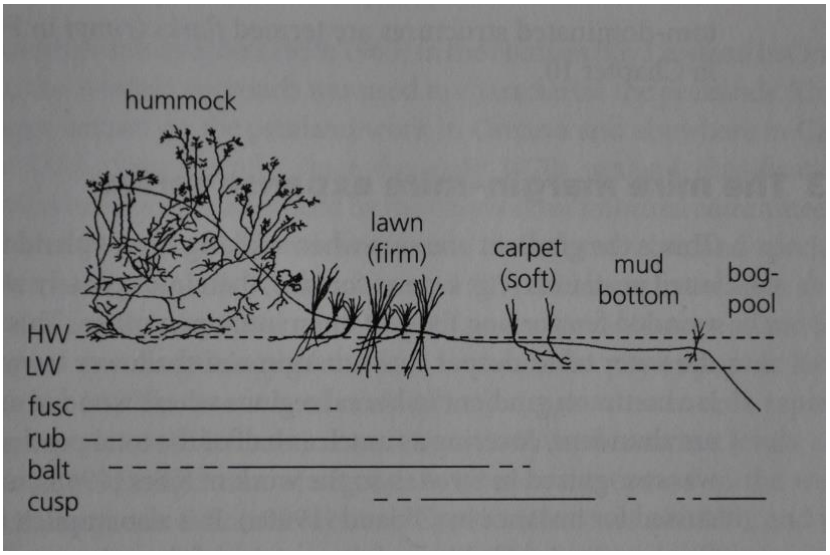

Figure 7 *Microtopographic gradient in a bog. High water (HW) and low water (LW) – approximate levels; peat mosses distribution Shagnum fuscum, S. rubellum, S. balticum and S. cuspidatum. Adapted from Rydin & Jeglum (2013).*

Because each microform has its unique hydrological and biological environment, the structure of peat soil material and its interactions with the atmosphere is dominated by the distribution of microforms making up the peatland surface. The other important factor is the dominant diplotelmic structure of blanket peat since morphological differences within the acrotelm and the catotelm are essential to consider when studying GHG exchange dynamics. The process of GHG movement is driven by diffusion which is heavily influenced by peat porosity (Strack, 2008). Hydraulic conductivity is facilitated where porosity is greater and since porosity is greater in the acrotelm than in the catotelm hydraulic conductivity is greater in this zone. Whereas in contrast the catotelm is characterised by greater water retention due to its smaller pore sized and reduced conductivity (Strack, 2008). It has been noted that the flux rates of carbon are closely regulated by the water table levels, which are in turn related to seasonal changes in peat

surface elevation, peat bulk density, water retention levels and hydraulic conductivity (Strack, 2008).

2.7 Carbon budget

Estimates of carbon accumulation by peatlands (globally) vary from 0.09-0.5 Gt C yr^{-1} (Yu, 2011). That range represents 1-5 % of global annual anthropogenic GHG emissions (Friedlingstein *et al*., 2006). To be able to understand carbon accumulation, it is essential to introduce the concept of carbon balance and budget. The balance between photosynthetic activity or primary production (autotrophic activity) and decomposition (heterotrophic respiration) is the determining factor influencing carbon storage in blanket peatlands (Clymo, 1984). The general model for peatland carbon balance can be represented by $\Delta \mathbf{C = - (NEE + F_{CH4} + F_{DOC} + F_{DIC} + F_{POC})}$, where ΔC is the net change in carbon storage in the ecosystem, NEE (Net Ecosystem Exchange) is the net flux of CO_2 from the ecosystem, F_{CH4} is a net methane flux, F_{DOC}, F_{DIC} and F_{POC} are net fluvial fluxes of DOC, DIC and POC (Strack, 2008). Positive signs (fluxes) represent losses of carbon from peatland. The dominant hydrological loss of carbon from peatlands is in form of DOC (Strack, 2008).

CO_2 is fixed in ecosystems by plants via photosynthesis and represents Gross Ecosystem Production (GEP). Autotrophic respiration drives the incorporation of the CO_2 within the plant biomass. Some of that CO_2 is also returned to atmosphere in this process. Other losses of CO_2 are associated with heterotrophic respiration (decomposition of SOM by microorganisms). Autotrophic respiration represents between 17-50% of total ecosystem respiration (Crow and Wieder, 2005). Ecosystem Respiration (ER) includes both the

autotrophic and heterotrophic processes of respiration. ER is dependent on soil temperature and moisture and the presence of easily decomposable organic material. Based on this NEE can be defined as the difference between photosynthetically fixed CO_2 and emitted CO_2 via respiration: NEE = GEP – ER.

Various studies have evaluated the contribution of peatlands to the global carbon budget. Estimates suggest that on average peatlands emit approximately 4 g CH_4-C m^{-2} yr^{-1} (5.3 g CH_4 m^{-2} yr^{-1}) and are a net sink of atmospheric CO_2 of 42 g CO_2-C m^{-2} yr^{-1} (172 g CO_2 m^{-2} yr^{-1}) (Strack, 2008). Ombrotrophic peatlands have been estimated as representing net sinks of 15±53 g CO_2-C m^{-2} yr^{-1} and a source of 5±4 g CH_4-C m^{-2} yr^{-1} (Strack, 2008). Minerotrophic peatlands have been estimated to contribute a greater proportion of methane at approximately 13 ±10 g CH_4-C m^{-2} yr^{-1} (Strack, 2008). However, it is important to note that these estimates mask considerable spatial and temporal variability. Ecosystem productivity is significantly influenced by vegetation community, nutrient status and hydrology. It has been observed that in subarctic fens the highest rates of productivity occur close to and up to 2 cm below the water table level (Waddington *et al*., 1998). Where high light conditions exist, NEE was greater in rich fens and poor fens than in bogs (Frolking *et al*., 1998). Seasonal temperature is another factor affecting productivity of vegetation. Where growing seasons are longer, due to higher temperatures, higher GEP has been observed. Ecosystem respiration is typically linked with vegetation type and the decomposability of the dead organic matter (DOM), peat substrates and mineral composition. Aerobic conditions stimulate respiration and decomposition, hence lower water table promotes rates of ER. Shifts in vegetation communities affect peat structure and quality, causing variations in rates of ER over time. Additionally, respiration is an enzymatically driven process, positively related with

temperature. Where the peat DOM is more resistant and recalcitrant the peat is subject to lower decomposition rates and therefore ER rates are reduced.

At a peatland scale variations in NEE are measured across the different microforms and plant communities. On the vegetated surface, microforms such as hummocks have greater GEP and ER compared with hollows and drier microforms are generally more effective CO_2 sinks even if respiration rates are greater (Waddington and Roulet, 2000). Peatland pools have been estimated to be net sources of CO_2 to the atmosphere with an annual release ranging from 23 to 419 g CO_2-C m^{-2} yr^{-1} and instantaneous fluxes that range from small uptake of 0.14 g CO_2-C m^{-2} d^{-1} to a release of 16.6 g CO_2-C m^{-2} d^{-1} (Cliché Trudeau *et al*., 2014). CO_2 fluxes ranges of from -7 to -411 g CO_2 m^{-2} yr^{-1} have been noted in undisturbed raised bogs (Canada, Sweden, Siberia) (Strack, 2008). In the blanket bogs of Ireland, CO_2 fluxes have been estimated as ranging between -179 to -223 g CO_2 m^{-2} yr^{-1} (Sottocornola & Kiely, 2005). In some Russian subarctic peatlands hummocks have been noted to emit CO_2 (NEE of 11 g CO_2 m^{-2} yr^{-1}), while hollows and lawns were sequestering CO_2 (hollows: -62 to -158 g CO_2 m^{-2} yr^{-1} and lawns: -110 to -147 g CO_2 m^{-2} yr^{-1}) (Strack, 2008). Similar trends were observed for subarctic peatland in Finland, where NEE was up to -154 g CO_2 m^{-2} yr^{-1} (Strack, 2008). Contrary to this Alaskan subarctic peatland, was emitting CO_2 into atmosphere, up to 312 g CO_2 m^{-2} yr^{-1} (Strack, 2008). Recent data published in paper by Wang *et al*. (2019) suggests that undisturbed temperate ombrotrophic bogs sequester CO_2 when there is no snow cover (-368±211 g CO_2 m^{-2} yr^{-1} in the year 2014-2015 and -242±139 g CO_2 m^{-2} yr^{-1} in the year 2015-2016) and emit CO_2 when under snow cover (200±233 g CO_2 m^{-2} yr^{-1} in the year 2014-2015 and 246±282 g CO_2 m^{-2} yr^{-1} in the year 2015-2016). Overall annual flux was calculated for that peat bog

as -168±132 g CO_2 m^{-2} yr^{-1} in year 2014-2015 and 4±4 g CO_2 m^{-2} yr^{-1} in year 2015-2016 (Wang *et al*., 2019). This illustrates temporal and annual variability in CO_2 fluxes.

Methane production is an anaerobic process. Bacteria that is involved in producing methane is called methanogenic bacteria (Strack, 2008). The gas could be released from the saturated zone inside peatland into atmosphere via diffusion, ebullition (bubbling) and mass flow via plant internal transport network (Strack, 2008). Methanotrophic bacteria can oxidise methane into CO_2 as methane moves from anaerobic to aerobic environment of where plant roots are (Strack, 2008). Peatland temperature and water levels are the main factors influencing emission of methane (Strack, 2008). Production of methane is more temperature sensitive than methane breakdown and oxidation (Strack, 2008). Methane production is affected by quality of substrate, mainly it is produced from new/fresh organic matter leached from the surface of peaty soils into saturated waters of peaty soils lower depths (Strack, 2008). Vascular vegetation can provide fresh substrate for methane production, sites with vascular plants such as fens would have such plants and higher water tables, therefore they would produce higher levels of methane than bogs (Strack, 2008).

DOC fluxes are important to consider since it can breakdown into CO_2 during downstream transport and evade into atmosphere (Billett *et al*., 2004). Saturated peats generally have higher levels of DOC, since decomposition is slower and incomplete (Strack, 2008). Water table fluctuations are important, since DOC concentrations increase if soils are rewetted after drought (Strack, 2008). DOC concentrations are influenced by microbes and therefore temperature is an important factor gathering its extent (Strack,

2008). Temperature response to CO_2 production is greater in extent than that of DOC production (Strack, 2008). Production of DOC from varying types of plants is different (Strack, 2008). Enhanced vegetation productivity in general is linked with higher concentrations of DOC (Strack, 2008).

F_{CH4} varies with peatland type, Irish blanket peatlands could release up to 6 g CH_4 $m^{-2}yr^{-1}$, boreal mires up to 40 g CH_4 $m^{-2}yr^{-1}$, hollows of some subarctic peatlands up to 16 g CH_4 m^{-2} yr^{-1}, thermokarst wetlands and palsa margins up to 33 g CH_4 $m^{-2}yr^{-1}$ (Strack, 2008). The general Canadian peatlands were reported to emit up to 3 g CH_4 $m^{-2}yr^{-1}$ (Strack, 2008). This is in line with recently published data presented in paper by Wang *et al*. (2019). In this paper, annual fluxes of methane from undisturbed ombrotrophic Canadian bogs were 3.08±0.67 g CH_4 $m^{-2}yr^{-1}$ (Wang *et al*., 2019). More recent studies revealed that fluxing extent not only depend on type of peatland and locality but also based on what was the prevailing weather condition (e.g. dry or wet year) (Fortuniak *et al*., 2017; Drollinger *et al*., 2019). In the pine peat bog study by Drollinger *et al*. (2019), fluxes were higher during wetter year (5.24±2.57 g CH_4 m^{-2} yr^{-1}) than during drier year (4.40±2.40 g CH_4 m^{-2} yr^{-1}). In the study by Fortuniak *et al*. (2017) carried out in Poland (lowland temperate mire), similar link was observed. However, the extent of emission was greater. The flux levels were 20±1 g CH_4 m^{-2} yr^{-1} in drier year and 29±4 g CH_4 m^{-2} yr^{-1} in wetter year (Furtuniak *et al*., 2017). Fluxes of methane are also known to be vary when different microforms are considered (Laine *et al*., 2007; Kiely *et al*., 2018). Highest fluxes were recorded from hollow 13±0.1 (SE) g CH_4 m^{-2} yr^{-1}, followed by low lawn (6.1±1.4 (SE) g CH_4 m^{-2} yr^{-1}, high lawn (5.8±1.1 (SE) g CH_4 m^{-2} yr^{-1}) and hummock (3.3±0.5 (SE) g CH_4 m^{-2} yr^{-1}) (Laine *et al*., 2007). Fluxes were greater in winter comparing with other seasons (Laine *et al*., 2007). The annual emission of CH_4 was

estimated between 3.6-4.6 g CH_4 m^{-2} yr^{-1} (six year mean 4.1±0.5 (SD) g CH_4 m^{-2} yr^{-1}) (Laine *et al*., 2007).

DOC export from raised bogs ranges between 4.2-21 g C $m^{-2}yr^{-1}$ (Sweden and Canada) and up to 17 g C $m^{-2}yr^{-1}$ from upland peat complexes (UK) (Strack, 2008). In the paper by Koehler *et al*. (2011), DOC fluxes were estimated from peatland catchments. The annual flux approximations for year 2007 were 14.1±1.5 g C $m^{-2}yr^{-1}$ (Koehler *et al*., 2011) which is in line with levels reported by Strack (2008). Greatest export of DOC coincided with storm events (45% of flux) (Koehler *et al*., 2011). DOC fluxes were found to be reduced from restored peatlands (Waddington *et al.*, 2008; Strack and Zuback, 2013; Strack *et al*., 2015). As reported in paper by Waddington *et al*. (2008), the growing season fluxes (May-October) of DOC were lower (4.8 g C m^{-2}) from restored peatlands compared to unrestored peatlands (10.3 g C m^{-2}). Same author stated that levels reduced even further in both unrestored and restored sites 2 years post restoration (6.2 g C m^{-2} – unrestored and 3.5 g C m^{-2} – restored site) (Waddington *et al.*, 2008). In the paper by Strack and Zuback (2013) it was reported that ten years post restoration, growing season DOC fluxes were 28.8 and 5.5 g C m^{-2} from unrestored and restored peatlands.

Irish data for NEE, is suggesting that annual levels were up to -66 g CO_2-C $m^{-2}yr^{-1}$ and methane 2.5-9.8 g CH_4-C $m^{-2}yr^{-1}$for Atlantic blanket bog (Glencar, Co. Kerry) (Koehler *et al*., 2011; Wilson *et al.*, 2013). In paper by Koehler *et al*. (2011), the NEE at Glencar was measured from 2003- 2008 and the reported estimates were -66.8±5.2 g CO_2-C $m^{-2}yr^{-1}$ (2003) progressively improving until year 2005 (-84.0±4.8 g CO_2-C $m^{-2}yr^{-1}$). In years 2006-2007, NEE were lower (–12.5 ± 3.4 and –13.5 ± 2.3 g CO_2-C $m^{-2}yr^{-1}$) (Koehler *et*

al., 2011). In year 2008, NEE was –42.7 ± 4.7 g CO_2-C $m^{-2}yr^{-1}$) (Koehler *et al*., 2011). Methane fluxes from Glencar as reported by Koehler *et al*. (2011) were similar to those reported in the paper by Wilson *et al.* (2013). In years 2004 and 2008, fluxes were 3.6±1.6 g CH_4-C $m^{-2}yr^{-1}$ and higher levels were estimated in years 2005-2006 (4.5±1.9 and 4.6±2.0 g CH_4-C $m^{-2}yr^{-1}$).

Intact montane blanket bog is net emitter 17-92 g CO_2-C $m^{-2}yr^{-1}$and methane 2 g CH_4-C $m^{-2}yr^{-1}$ (Slieve Blooms, Co. Laois) (Renou-Wilson *et al*., 2011). Raised bog – relatively intact between -53 to 94 g CO_2-C $m^{-2}yr^{-1}$and 12.8 g CH_4-C $m^{-2}yr^{-1}$(Clara, Co. Offaly) (Wilson *et al.*, 2013). Afforested Atlantic blanket bog (Cloosh, Co. Galway) is net emitter 1.4-2.6 g CO_2-C $m^{-2}yr^{-1}$. Drained margins and mechanically cut raised bog are emitters of 122-441 g CO_2-C $m^{-2}yr^{-1}$ (Clara, Co. Offaly) (Renou-Wilson *et al*., 2011). Hand cut and later abandoned Slieve Blooms (Co. Laois) Montane blanket bog is also emitter of 55-170 g CO_2-C $m^{-2}yr^{-1}$and 0.88 g CH_4-C $m^{-2}yr^{-1}$ (Renou-Wilson *et al*., 2011).

2.8 Carbon cycle - primary sources of carbon in upland blanket peatlands

CO_2 in the atmosphere mixes with the rainwater to form a carbonic acid, which is a mild acid (Holden, 2004; Spiro *et al*., 2012). When precipitation infiltrates into the soil, it reacts with the minerals through carbonation and hydrolysis (production of the soluble calcium bicarbonate) (Holden, 2004; Spiro *et al*., 2012). Therefore, the processes of leaching are highly dependent upon dissolved CO_2, and the presence and abundance of dissolved CO_2 is dependent upon concentration of atmospheric CO_2. The relative concentration (partial pressure) of CO_2 below soil cover (e.g. soil air) is typically several hundred times higher than that in an open atmosphere (0.035 % by volume in the atmosphere and 0.15-1 % by volume in the soil air) (Holden, 2004; Hess, 2011; Spiro *et*

al., 2012). The relative concentration of dissolved CO_2 is also higher in the soil in comparison with atmospheric concentration (Holden, 2004; Spiro *et al*., 2012). The partial pressure of CO_2 (pCO_2) is inversely related to temperature, e.g. it falls by approximately 50% between 0-20^oC (Holden, 2004; Spiro *et al.*, 2012). But effects of lowering temperature could restrict biological activity (Holden, 2004). Effects of aridity associated with prolonged freezing of what water is available could also mask effects of temperature on the CO_2 concentration (Holden, 2004). Therefore, dissolved CO_2 in peatlands can have a varied aetiology, it can be derived from the atmosphere (with precipitation), it can be a product of weathering and leaching (carbonation and hydrolysis), or it can be a product of a biological activity (Spiro *et al.*, 2012). Biological activity such as breakdown of organic matter deriving from *Sphagnum* moss is one example of CO_2 production (Medvedeff *et al*., 2015). *Sphagnum* moss tissue chemistry is highly variable (across species), and that affects carbon mineralisation, due to its dominance in the solid peat matrix and through its soluble components (Medvedeff *et al*., 2015). It was also established that *Sphagnum* litter decays at different rates and that DOC (carbon that passes through a 0.45 µm filter) derived from the moss is highly bioavailable relative to other vegetation (Medvedeff *et al.*, 2015). Easily broken components of SOM includes DOC, dissolved organic nitrogen (DON), POC and particulate organic nitrogen (PON) (Tian *et al*., 2015). They are the primary sources of energy for soil fauna and are characterised by rapid turnover (Tian *et al*., 2015).

SOM (soil organic matter) is one of major components of soils that is made from recalcitrant - less efficiently degradable materials and labile components (easily decomposed) (Crowther *et al*., 2015). Large portions of labile matter are lost through respiration as CO_2 (Crowther *et al*., 2015). Within soils, labile matter DOC is mainly

derived from breakdown of lignins which come from leaves and wood but can also coming from plant root exudates (Yu-Lai *et al.*, 2015). Soil DOC is dark and is made of larger molecules with more aromatic rings (hydrophobic) or phenolic, humic and polyphenolic groups (Wooda *et al*., 2011; Yu-Lai *et al.*, 2015). These organic acids in the peat consist of 78% humic and 22% fulvic acids (Kalmykova *et al*., 2008). Humic acids within terrestrial systems promote soil (peat) formation, prevent soil (peat) erosion, slowly release plant nutrients and reduce toxic levels of pollutants (Abouleish & Wells, 2015). Humic acids also act as oxidising or reducing agents under specific environmental conditions, affect photochemical processes, and interact with heavy metal ions (metal exchange processes, metal leaching) organic molecules (synthetic steroid hormones and persistent organic pollutants) and minerals (nitrogen and phosphorus) (Abouleish & Wells, 2015). Humic acids react with environmental contaminants by chemical forces and reactions, including hydrogen bonds, electron transfer, van der Waals and ion exchange (Yu-Lai *et al*., 2015).

DOC concentration in soils and peatlands is dependent on rates of primary production, decomposition, water movement through the soil and sorption by mineral particles (Yu-Lai *et al*., 2015). It varies significantly in different soil classes and is lowest (annual mean 15.4 mgl^{-1}) in the grassland sites and highest (annual mean 54.8 mgl^{-1}) in moorland sites with intermediate levels in heathland sites and forested areas (van den Berg *et al.*, 2012). As result of several studies it was established that DOC concentrations in peatlands could be variable, for instance Billett *et al.* (2012) measured DOC concentrations in a range of 5.60-142.84 mgl^{-1} using total organic carbon (TOC) analyser from the peat pipe water samples. A similar trend of DOC leaching (4-123 mgl^{-1}) was established in study by Schwalm & Zeitz, (2015), where they applied lysimetery method to examine the influence

of land use on DOC concentration. In non-forested sites (UK study), highest DOC concentration was detected in histosol sites (literature DOC range 21.7- 46.4 mgl^{-1}) (van den Berg *et al.*, 2012). In gleysol sites DOC concentration was lower (15.1-18.3 mgl^{-1} mean DOC) (van den Berg *et al.*, 2012). European histosols are soils with the highest carbon content and they produce largest amounts of DOC (van den Berg *et al.*, 2012).

Photosynthetic fixation of CO_2 followed by soil microbial respiration and breakdown of soil organic matter (humification) are two processes producing large volumes of CO_2 that are stimulating carbonation and leaching of dissolved inorganic carbon (DIC) (Figure 8) (Holden, 2004). Therefore, production of biologically derived CO_2 is expected to be higher during summer season because biological activity is high (Holden, 2004). During winter periods, production of gas could be expected to be reduced (Holden, 2004). Diurnal patterns of CO_2 could be also observed; day-time production will be expected to be higher than night-time production (Holden, 2004). The composition of the soil is also important in determining production of CO_2, its spatial variability could be linked with the variable CO_2 dynamics (Holden, 2004). Methane and CO_2 rise to the surface by various ways such as diffusion, bubbles, or root and stem aerenchyma as well as by leaching of POM (Rydin & Jeglum, 2013) (Figure 9).

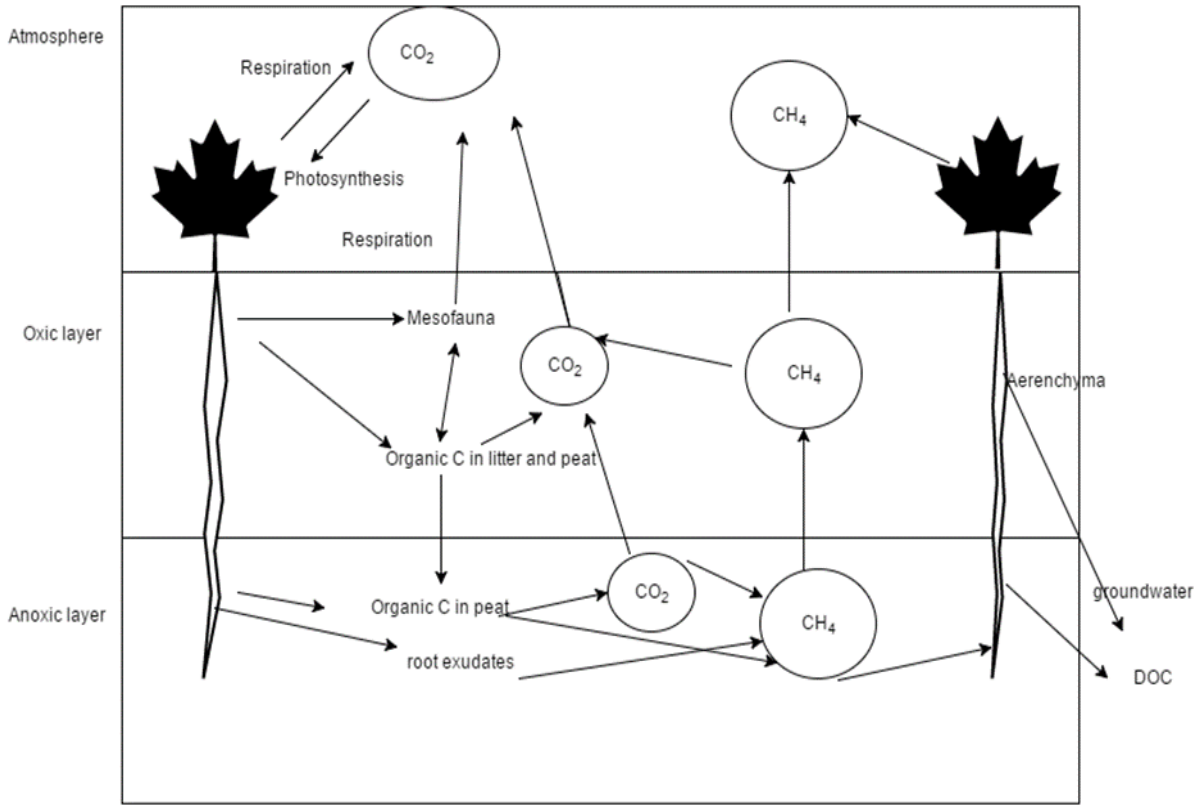

Figure 8 *Acrotelm-catotelm carbon flow. Adapted from Rydin & Jeglum (2013).*

2.9 Aqueous carbon and fluvial exports

Depending on water pH, different species of inorganic carbon might exist, for instance at pH between 1 and 3, CO_2 and the carbonic acid will be predominant, at pH of 3 to 6 bicarbonate will be dominant and above 7 – carbonate will be predominant (Verry *et al.*, 2011). According to Fasching *et al.* (2014) high freshwater concentrations of CO_2 are generated by remineralisation of DOC and POC that occurs after the export from the soils. DOC includes molecules of 100-100 000 Da in size with variable carbon to nitrogen ratio and surface charge (Rowe *et al*., 2014). Phenolic substances are part of the coloured component of DOC (Takeda *et al*., 2013). They contain one or more hydroxyl substituents bounded onto an aromatic ring characterised by strong acidity, mobility and chemical

reactivity (Buondonno *et al.*, 2014). The other humic constituents such as carboxylic acids are polar and soluble (Tsai & Kuo, 2013).

It is well known that in peatland catchments, freshwater dissolved CO_2 concentration usually exceeds 2000 µatm (Baehr & DeGrandpre, 2004). According to multiple investigations, streams draining northern hemisphere peatlands are consistently supersaturated with respect to CO_2 (Dinsmore, 2008; Johnson *et al.*, 2010). Regarding peatland pools, conditions such as negative net ecosystem production, photochemical degradation of DOC or high DIC inflow from peatland soil surface are among conditions responsible for supersaturation (Laas *et al*., 2016). Such supersaturation could be the reason that at some stage these watercourses will act as a sources of CO_2 evasion into the atmosphere and thus may promote global climate warming. In peatland streams, dissolved CO_2 dynamics changes downstream (Neal *et al.,* 1998). Supersaturation and evasion of CO_2 would also change rapidly downstream (Neal *et al.*, 1998). Such changes could be also more frequent in areas of rapidly changing gradient such as changing gradients of headwater streams (Dinsmore & Billette, 2008). In Ireland, such studies were not conducted, and knowledge is limited in that area (Whitfield *et al*., 2011).

Fluvial carbon could be exported in different organic and inorganic forms, that differ morphologically, chemically and could be dissolved or accumulated in solution in a particulate form (Dinsmore *et al*., 2011a & b). The inorganic forms include two major forms: DIC and CO_2. DIC is generally a product of dissolution of CO_2 (carbonic acid) followed by its reaction with bases of carbonate and silicate mineral material (not the case in Kippure bog; bedrock is igneous – magmatic in origin) to yield bicarbonate (Worrall, 2003). Organic forms include particulate organic carbon (POC) and DOC (Worrall,

2003). Fluvial exports of DOC are mainly derived from photosynthetic fixation of atmospheric CO_2 (Ryder *et al*., 2014). DOC molecular structure tends to be different in different soils and under different climatic and ecological conditions (Ryder *et al*., 2014). Spatial and temporal variability of specific peatland site and hydrological pathways (presence of peatland pipes) that would be dominant in specific catchment setting could promote formation and transport of variable types of the carbon into the freshwater streams (Dinsmore *et al*., 2011). Such carbon species would also probably be modified, depending on time spent in the specific location or the compartment within the peatland body (Holden, 2004).

DOC has a specific set of functions in freshwater ecosystems such as carbon cycling, nutrient transport, ultraviolet screening, ameliorating toxicity of many metals and reducing their bioavailability to target surfaces (gills) (Wooda *et al.,* 2011). High concentrations of DOC in a water bodies are associated with increased ecological risks such as interruptions of the endocrine functions in aquatic organisms (Yu-Lai *et al*., 2015). Research conducted in the eastern parts of Ireland using river water samples derived from catchments established that highest levels of DOC were associated with a storm flow (mean: 19 mgl^{-1}) (Feeley *et al*., 2013). DOC production has been linked to increased temperature, reduced water table, increased oxidation, decreased soil acidity, increased microbial activity, switched on activity of enzymes and increased decomposition rates (Scott *et al*., 1998; Freeman *et al.,* 2001a, b; Blodau *et al.,* 2004; Toberman *et al*., 2008; Jager *et al*., 2009; Fenner & Freeman, 2011; Ryder *et al*., 2014).

2.10 Aerial exports of carbon

Mostly all gases present in the atmosphere are non-polar (a type of chemical bond where two atoms share a pair of electrons with each other) (Moss, 2010). Their solubility's decrease with the temperature because temperature increase causes molecular movement that drives gas out of liquid to overlying vapour (Moss, 2010). Therefore, solubility of ions increases with temperature (Moss, 2010). Ionic solubility is not a passive mixing but a chemical reaction (Moss, 2010). However, not all gases behave in a similar way, particularly CO_2 is relatively soluble, because it reacts with water (polar) and exists in equilibrium with ions of carbon: bicarbonate and carbonate in the case of natural waters (Moss, 2010). At the temperature of 15 ^{0}C, in pure water under conditions of one atmospheric pressure of CO_2 it is in equilibrium (CO_2 (water) ⇔ CO_2 (atmosphere)) with atmospheric air (0.03 % CO_2) (Moss, 2010). Carbon dioxide is a major determinant of the acidity of the water and the rainfall (Moss, 2010). When dissolves in water it forms a weak carbonic acid (H_2CO_3): 1) H_2CO_3 (aq)⇔ HCO_3^- (aq) +H^+(aq); 2) HCO_3^- (aq)⇔ CO_3^- (aq) + H^+(aq); 3) HCO_3^- + H^+ ⇔ CO_2 (aq) + H_2O (Moss, 2010). This solubility and reactivity is an acid-base phenomena in the water and involves loss and acceptance of a hydrogen ion (Manahan, 2011). The solubility of the CO_2 is calculated with Henry's Law, which states that the solubility of a gas in a liquid is proportional to the partial pressure of that gas in contact with the liquid (Manahan, 2011). The concentration of gaseous atmospheric CO_2 varies with location, season, it is increasing by about one part per million by volume per year (e.g. 390 ppm (0.0390 %) in dry air; at 25 ^{0}C, water in equilibrium with unpolluted air containing 390 ppm carbon dioxide has a concentration of $1.276*10^{-5}$M) (Manahan, 2011). Therefore, low level of atmospheric CO_2 is associated with water lacking in alkalinity (Manahan, 2011). Consequently, the formation of HCO_3 and CO_3 greatly increases the solubility of CO_2 (Manahan, 2011). The outcome of high

concentrations of free CO_2 in water may impact the respiration and gas exchange of aquatic animals and cause deaths (e.g. should not exceed levels of 25 mgl^{-1} in water) (Manahan, 2011). A large share of the CO_2 found in water is a product of the breakdown of organic matter by microbes (respiration by algae in the absence of light) (Manahan, 2011). In the soil, the seeping water can dissolve a great deal of carbon dioxide from the organic matter produced by the respiration of organisms (Manahan, 2011).

In Irish blanket peatland dominated catchments and the associated waterbodies dissolved CO_2 concentration and evasion could be elevated and or intensified due to high rainfall, frequent occurrence of extreme hydrological and climatic events as these may promote erosion, turbulence, and high downstream carbon fluxes. However, the likelihood, extent and the prospective management measures that should be associated with increased dissolved CO_2 concentration in the Irish streams/pools and the evasion from these sources are not well understood and documented. Moreover, evasion fluxes were not included in the global terrestrial carbon budgets for inland waters (Cole *et al*., 2007). On another side, CO_2 concentration and transport dynamics in the UK peatland streams has a strong correlation with extreme hydrological events and appears to trail behind the storm flow periods (Dinsmore & Billette, 2008). Additionally, peatland streams that are headwaters are complex and tend to have a stronger influence of turbulence on the dissolved CO_2 dynamics and the evasion. These streams have a specific morphological structure that is characterised by a repetition of waterfalls, riffles and pools and these variable gradients, streambed characters, flow constrictions are generating high discharge, turbulence and enhance the evasion of CO_2 (Wallin *et al.*, 2011).

With regards to small and shallow water bodies such as peatland pools, they are often classified as ecological hotspots that exhibit high rates of biogeochemical activities (Gao *et al.,* 2016). They can have a disproportionate impact on global biogeochemical cycles of nutrients, carbon and biological gas emission relative to their areal coverage (Gao *et al.,* 2016). For example, carbon dioxide emission from small ponds has been estimated to be the same order of magnitude as the emissions from larger lakes and reservoirs and can influence regional carbon balances by transporting terrestrial carbon and releasing it into the atmosphere (Yang *et al*., 2015; Gao *et al.,* 2016). The large number of lakes were assessed and it was concluded that approximately 87% of them were supersaturated (net heterotrophic lakes - organic carbon mineralisation exceeds primary production) with respect of CO_2, with an average pCO_2 of about three times the value in the overlying atmosphere, indicating that lakes are sources rather than sinks of atmospheric CO_2 (Yang *et al*., 2015).

2.11 Factors stimulating carbon production and fluxing

As mentioned, one of primary precursors of CO_2 is DOC. DOC production and losses from peatlands are influenced by various biological and surface exchange processes influenced by temperature (Rowe *et al.,* 2014). Excessive DOC production as a result, could be stimulated by global warming and high temperatures (Rowe *et al.,* 2014). For instance, several groups of researchers manipulated temperature in laboratory by increasing it by 4-10 ^{0}C above the seasonal average (Briones *et al.,* 1998; Scott *et al*., 1998; Andersson *et al*., 2000; Kaiser *et al*., 2001; Moore & Dalva, 2001; Wright & Jenkins, 2001; Fenner *et al.,* 2005a, b; Carrera *et al.,* 2009). They determined that DOC concentration varied seasonally, and that highest rate of DOC production was in summer (20 ^{0}C-average air temperature; warm soil). Other groups of researchers speculated that

duration of thermal exposure is also important (Wright & Jenkins, 2001; Clark *et al*., 2005; Bonnett *et al*., 2006; Sarkkola *et al.*, 2009; Tang *et al.*, 2013). Sarkkola *et al*. (2009) established that a 56–71% increase in DOC could be explained by short-term (could be up to a month) temperature increase. But others implied that long-term (months to years) temperature increase is required to promote increased DOC production (Wright & Jenkins, 2001; Clark *et al*., 2005; Bonnett *et al*., 2006; Tang *et al.*, 2013). Long-term temperature increase was also reported to promote increased vegetation cover and litter inputs (Rowe *et al.*, 2014). Higher nutrient input and increased peat oxygenation was inferred to promote increased burrowing activities of peat fauna (Briones *et al*., 1997) and increased microbial activity (Zsolnay, 1996; Kuzyakov, 2002; Freeman *et al*., 2004; Yan *et al*., 2008). Such activity was suggested to trigger increased respiration, activity of phenol oxidase (an enzyme that catalyses degradation of phenolics) and decomposition (Chow *et al*., 2006; Kechavarzi *et al*., 2010; Curtis *et al*., 2014). Faunal and microbial products were found to be the most important sources of high-molecular weight coloured aromatic DOC (Yan *et al*., 2008). This was later supported by Carrera *et al.* (2009) who established that *Cognettia sphagnetorum* (Vejdovsky) abundance and its vertical distribution (greatest effects at 0-3 and 3-6 cm) was strongly correlated with DOC concentration.

Several researchers have been able to establish the link between DOC leaching and drought events (extremes in rainfall patterns) (Briones *et al.*, 1998; Scott *et al*., 1998, Watts *et al*., 2001; Worrall *et al*., 2006). Short-term drought events (days to few weeks) have been associated with positive dynamics of DOC production (Scott *et al.*, 1998; Freeman *et al*., 2001a, b; Blodau *et al*., 2004; Toberman *et al*., 2008; Jager *et al*., 2009; Fenner & Freeman, 2011; Ryder *et al.*, 2014). These drought events cause DOC fluxes

by promoting drier conditions, increasing dissociation of acid functional groups, decreasing soil acidity and ionic strength (Clark *et al.*, 2010; Ryder *et al.*, 2014). Long-term drought (one, two months long) events reduce DOC production and fluxes by increasing ionic strength and acidity driven by sulphur and nitrogen redox reactions (Clark *et al*., 2005 & 2012), decreasing biological activity (Scott *et al.*, 1998; Pastor *et al*., 2003) and diverting decomposition pathways in favour of full mineralisation or production of carbon dioxide (Scott *et al.*, 1998; Preston *et al.*, 2011; Ryder *et al.*, 2014). Toberman *et al*. (2008) hypothesised that phenol oxidase activity could be inhibited due to enzyme malfunction. This enzyme requires oxygen to function (Toberman *et al*., 2008). The reasons for enzyme malfunction include reduced in-flushing of fresh oxygenated water and limited oxygen availability on a micro-scale (Pind *et al*., 1994; Freeman *et al*., 2001a), restricted contact and binding between enzyme and substrate molecules (Aon & Colaneri, 2001; Poll *et al*., 2006) or reduced production due to moisture stress upon the soil biota (restricted nutrient uptake, cell proliferation) (Donnelly & Boddy, 1997; Sharma, 2005). Phenolics will accumulate under anoxic conditions further inhibiting phenol oxidase (Toberman *et al*., 2008). However, it was later established that DOC mobility could be restored when the peatland was subsequently rewetted (Jager *et al*., 2009; Ledesma *et al*., 2012; Tang *et al*., 2013; Turner *et al*., 2013; Monteith *et al*., 2014). The extent of DOC flushing following rewetting of peatlands is strongly dependent on the degree of peat decomposition status (Zak & Gelbrecht, 2007; Cabezas *et al*., 2013; Schwalm & Zeitz, 2015).

Ryder *et al.* (2014) proposed that the effect of water table fluctuations on peat decomposition is not fully understood, because increased rates of decomposition could be induced by both short-term drought and rewetting after the long-term drought. Long-

term research (many years) of rewetted bogs and fens showed a decline in DOC concentrations to near-natural levels (Höll *et al*., 2009; Frank *et al*., 2013; Schwalm & Zeitz, 2015). Furthermore, Toosi *et al*. (2014) established that drought impacts on peat vary with depth, for instance, in deeper peats drought effects on phenol oxidase activity could be associated with changes in oxygenation and soil chemistry and in shallower organic soils reduced water availability could be the primary factor affecting phenol oxidase activity. These finding are important because global climate change is predicted to promote increased numbers of intense drought events, more episodic precipitation and wetter winters in Ireland, UK, Finland, etc. where extensive areas of organic soils occur and this would impact upon the DOC production and fluvial exports and upon the global carbon balance (IPCC, 2007; Jenkins *et al*., 2009; Fenner & Freeman, 2011; Ryder *et al.*, 2014).

DOC transport within peatlands and export from peatlands to watercourses is regulated by peatland hydrology and land use (agriculture, drainage and peat extraction). The understanding of the peatland hydrology could be enhanced by using diplotelmic system approach as previously discussed (Holden & Burt, 2003). The acrotelm is affected by a fluctuating water table (Boylan *et al.*, 2008). It has high hydraulic conductivity (rate of flow) and a variable water content (Boylan *et al.*, 2008). In the catotelm, the water contents are stable (Boylan *et al.*, 2008). Movement of DOC within peat profile is usually through the soil pore water (Limpens *et al*., 2008). The soil pore water is traveling through the peatland profile via macropores (pores with >1 mm diameter) and soil pipes (large, continuous type of macropores) within peatlands (Boylan *et al.*, 2008). Some of the DOC could be also adsorbed and released during the next storm event (Clark *et al*., 2009). The export of DOC from peatlands is associated with leaching, seepage and runoff (influenced by slope angle) through surface layer of peat (top 5 cm) caused by extreme weather events

(storms) as previously mentioned (Hongve *et al.,* 2004). The surface layer of peat is the layer where DOC production is highest, due to highest inputs of organic matter and active decomposition. Therefore, the origin of DOC leached from this layer could be regarded as 'recent' (Blodau *et al*., 2004). The runoff is usually enhanced if peatlands are drained (Van Seters & Price, 2002).

Clymo (1987) and Kuhry *et al*. (1993) implied that the type of vegetation present could influence conditions and resources that could contribute to production and release of DOC including effects on geochemistry of soil water. Furthermore, McNamara *et al*. (2008) speculated that the type of peatland vegetation could also impact on physical properties of the peat such as temperature and water table. Holden *et al*. (2001), Holden (2005, 2009) and Armstrong *et al*. (2012) implied that various physiological characteristics of different plants can cause differences in water table depths in the same hydrological setting by affecting hydraulic conductivities and evapotranspiration. Artz *et al*. (2007, 2008) stated that biota which live within peat could be affected by peatland vegetation due to quality and quantity of plant and litter inputs, including root exudates. Dorrepaal (2007) and De Deyn *et al*. (2008) concluded that those plant characteristics could dictate how plants assimilate and process carbon and further influence soil properties and processes. In peatland ecosystems, the dominant plant types are bryophytes, ericoid dwarf–shrubs and graminoids. They have been shown to correlate with carbon dioxide and methane fluxes (McNamara *et al*., 2008; Ward *et al*., 2009). For instance, *Calluna vulgaris*, widespread in Irish mountain blanket peatlands and contains high polyphenolic, aliphatic acid concentrations and high C: N ratios resulting in litter that is resistant to decomposition (McNamara *et al*., 2008). Another common mountain blanket peatland type of plant is *Eriophorum* spp. It is aerenchymous (allows circulation of gases) and promotes methane

and carbon dioxide emissions due to its physical properties, tissue structure, by supplying labile methanogenic substrates via root exudation and by providing aerobic bacteria with oxygen (to enhance decomposition) to the rhizosphere through their root structures (McNamara *et al*., 2008). *Sphagnum* moss was found to harbour methanotrophic symbionts (McNamara *et al*., 2008). These symbionts are responsible for conversion of methane into carbon dioxide as part of photosynthetic fixation (McNamara *et al*., 2008). Interestingly, Vestgarden *et al*. (2010), Armstrong *et al*. (2012) and Ritson *et al.* (2014) determined that *Calluna* was consistently associated with highest DOC production and leaching from peatlands in UK, Scotland and Netherlands, sedges yielded intermediate DOC and *Sphagnum* low DOC. Overall DOC concentrations ranged from 2.2-120.9 mgl^{-1} with a mean of 24.2 $\pm$18.6 mgl^{-1} (Armstrong *et al*., 2012). These findings were contradictory to what was expected, as more degradable material was likely to give higher DOC production and release in peatlands and *Calluna* is the least degradable material due to its structure and chemistry. Vestgarden *et al*. (2010) also determined that DOC production and fluxes were season and soil depth dependent. The highest concentrations of carbon were detected in shallow layer (0-10 cm) and during the summer period (Vestgarden *et al*., 2010). The reason for lower DOC concentrations at depth of greater than 20 cm could be due to presence of older, more decomposed organic matter or due to weaker adsorption of organic matter (Vestgarden *et al*., 2010). Furthermore, it is likely that synergistic relationship between vegetation, temperature, nitrogen enrichment, hydrology, water table level and peatland morphology was responsible for the observed phenomenon, but this is not fully tested and proved experimentally, however it is known that lower water table depths were linked to higher DOC concentrations. Shrubs and sedges prefer lower water tables, therefore higher DOC concentrations would be expected under shrubs and low in soil water under *Sphagnum* (Armstrong *et al*., 2012).

Peatland to water losses of carbon are important to account for, as overall losses of CO_2 could be intensified from waterbodies if specific condition would prevail (disequilibrium with the atmosphere). There is a need for a very fine-tuned and detailed model that will consider all factors affecting carbon production and losses from both terrestrial and aquatic systems. The following research questions were considered in this study:

1. Is there a correlation between temperature, pressure, precipitation variability and levels of CO_2 in the water from pools, hummocks and lawns?
2. Is fluxing of CO_2 from pools driven by wind influenced turbulence?
3. Could diurnal patterns of CO_2 vary across hummocks, lawns and pools? Are these patterns affected by seasonality?

Two working hypotheses were proposed in this study:

'It is hypothesised that temperature is correlated with levels of CO_2 in all microforms.'

'It is hypothesised that CO_2 concentrations are higher in water from hummock.'

CHAPTER 3: METHODOLOGY

3.1 Study sites

The study area was in the Wicklow Mountains National Park, County Wicklow, Ireland which begin eight kilometres south of Dublin city centre (Figure 9). Wicklow uplands are the most prominent, distinct topographical feature of Leinster and could be visible from distances of up to one hundred kilometres (Aalen *et al*., 2011). They are extensive: between fifteen to thirty kilometres wide and more than forty kilometres in a north/south direction (Aalen *et al*., 2011). The highest mountain in the area is above nine hundred meters (Aalen *et al*., 2011). The gently domed mountains were formed over four hundred million years ago as result of the mixture of different glacial and postglacial processes including weathering, geological uplift, incision and deepening (Aalen *et al*., 2011). The geology in the Wicklow uplands is predominantly granite and is also known as the Leinster batholith (Aalen *et al*., 2011).

(a)

(b)

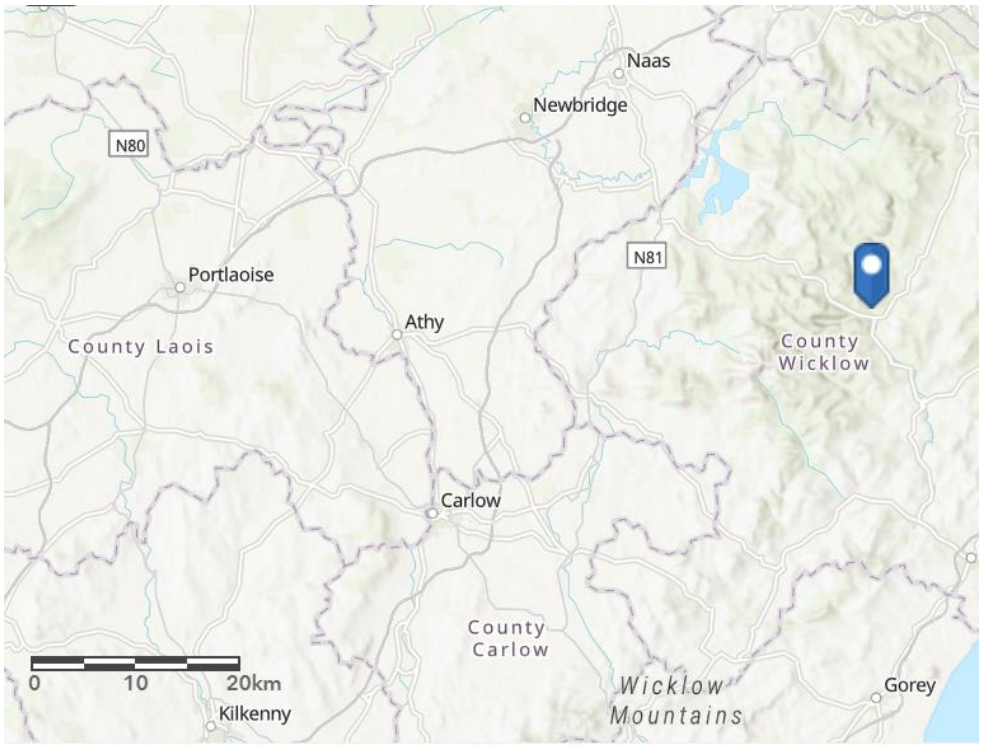

Figure 9 *(a) The map of Ireland; (b) Wicklow Mountains National Park (53°09'10.8"N 6°16'55.7"W) map. Adapted from (a) GeoHive (2017) and (b) ArcGIS (2020).*

The study area was selected based on preliminary survey that was conducted in the approximately 58.6 square kilometre upland blanket peatland located 300-400 metres in altitude in Wicklow Mountains National Park (Conaghan *et al*., 2000) (Figure 10). Kippure or Liffey Head Bog in Wicklow Mountains National Park was selected as the peatland of primary interest (Figure 11). Liffey Head Bog is a headwater bog that is situated in a hollow between three mountains: Kippure, Djouce and Tonduff and that consists of deep and flat blanket peat up to 4.9 metres in depth which is drained by Liffey River and is supported by water (water flows-flushes) from surrounding high ground (Conaghan *et al*., 2000). Apart from Liffey River, this peatland is the origin of the following rivers: Dargle, Cloghoge and Dodder (Figure 10). It is an actively growing peatland and has numerous pool and hollow areas (microforms) which are inhabited by a variety of organisms (Conaghan *et al*., 2000).

Figure 10 *Location of study site - east coast of Ireland (53°09'10.8"N 6°16'55.7"W). Rivers Dargle, Dodder, Cloghoge and Liffey are originating in Wicklow Mountains National Park. Adapted from ArcGIS (2020).*

Drainage of Liffey Head Bog began in 1802 and some areas were subjected to heavy peat extraction during World War II (1939-1945) (Hannigan *et al*., 2011). Nevertheless, the area was never exposed to extensive peat extraction (Hannigan *et al*., 2011). Restoration of the bog was initiated over 15 years ago and included the drainage ditches blocking and subsequent filling with peat blocks from surrounding areas to mirror the natural conditions (Hannigan *et al.,* 2011). Nowadays this upland blanket peatland is a site of the international importance and is a Special Area of Conservation (SAC) (Wicklow Mountains National Parks, 2016). The unique drainage system of this upland blanket peatland supports the plant species that are not common in this type of the environment (Wicklow Mountains National Parks, 2016). Such species are for example *Carex echinata* (M.) or commonly known Star Sedge (Wicklow Mountains National Parks, 2016). These species are adapted to grow in these conditions because such peatlands are prone to water flashes that bring nutrients from the mineral soils below the peat (Wicklow Mountains National Parks, 2016).

Another feature of Wicklow Mountains blanket peatland is the presence of perennial or peatland (bog) pools (Figure 11). Such bog pools could be found in any geographical location where climatic conditions are suitable (e.g. humid zones) (Uhlmann *et al*., 2011). They could be found in both upland and lowland peatlands and could be observed in marshes adjacent to large rivers (Uhlmann *et al*., 2011). These pools could be defined as systems with high species diversity (Uhlmann *et al*., 2011). However, from the point of view of aquatic chemistry, they are poor in electrolytes (Uhlmann *et al*., 2011). As for carbon, these systems are characterised as environments with greater organic carbon

production rather than microbial mineralisation (Uhlmann *et al*. 2011). These slow or incomplete decomposition conditions are favoured under continuous water surplus from atmosphere (precipitation) and from the surrounding terrestrial zone (Uhlmann *et al*., 2011). Low rate decomposition is a permanent feature that is enhanced due to a low oxygen conditions and acidity (Uhlmann *et al*., 2011). This results in peat deposition and siltation in pools (Uhlmann *et al*., 2011).

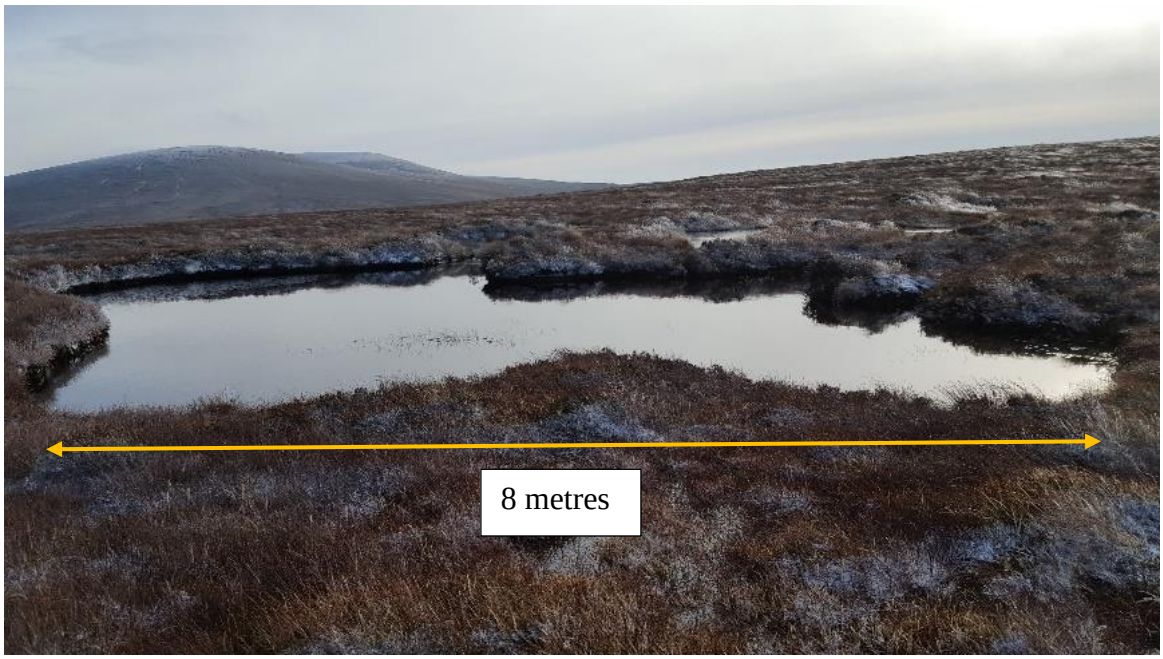

Figure 11 *Close-up view of perennial pool in Wicklow Mountains National Park.*

Within Kippure blanket peatland a suitable study cross-section was selected on the interfluve, e.g. region between valleys of adjacent headwaters: Dargle, Liffey and Cloghoge (Figure 10). The cross-section was selected based on topography, hydrogeomorphology, peatland state (natural and undisturbed) in area and the location. The blanket peatland in this area is positioned on porphyritic granite (Figure 12) and its depth is approximately 2.7-4.9 metres (Hannigan *et al*., 2011).

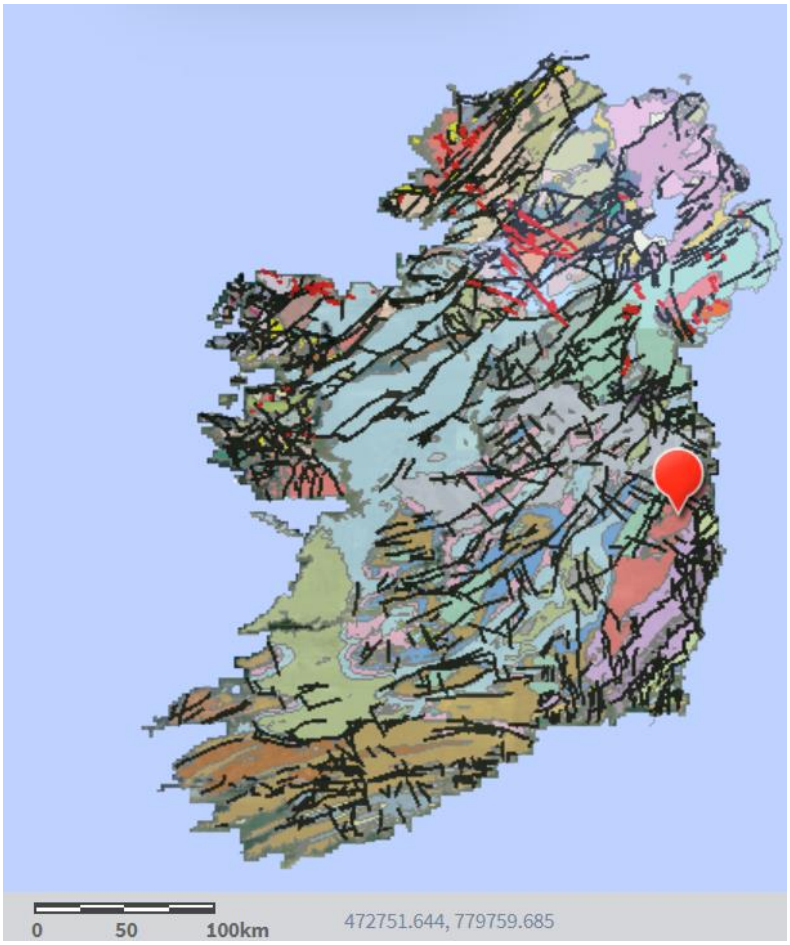

Figure 12 *The bedrock of study area – granite (coloured in red). Adapted from GeoHive (2017).*

Precipitation data was taken from M. Moanbane # 4 weather station located in Wicklow Mountains to determine exact trends in precipitation in the monitoring area (Figure 13). Station was positioned 354 meters above sea level, and it is approximately 13.6 kilometers away from monitoring station one (53° 05.06'N, 6° 26.16'W) (Figure 13). The mean maximum annual precipitation in the area is approximately 2000 mm (The Irish meteorological service online, 2016a).

Figure 13 *Location of weather monitoring station – M. Moanbane # 4 (53° 05.06'N, 6° 26.16'W). Adapted from GeoHive (2017).*

Mean annual air temperature in Ireland ranges from 9 to 11 ^{0}C from northeast to southwest (The Irish meteorological service online, 2016b, c). Mean summer air temperature is about 18 to 20 ^{0}C and winter mean air temperature is about 8 ^{0}C (The Irish meteorological service online, 2016c). To determine exact conditions on site air temperature, pool and peat water temperatures, air pressure and relative humidity were measured throughout the duration of the project (2016-2018). Air temperature was monitored between December-January 2016-2017, May-August 2017 and from November 2017 until August 2018 (Figure 14). It ranged between -5(March 2018) to 23 ^{0}C (June 2017) (Figure 14). Pool and peat water temperatures were measured between December-January 2016-2017, May-August 2017, November-December 2017, January-March 2018 and April-August 2018 (Figure 14). The ranges were 0 (January 2017 &2018) to 21 ^{0}C (June 2017) for pools and 1 (January 2017) to 14 ^{0}C (June-August 2017-2018) for peaty waters (Figure 14). Air pressure was measured between December-January 2016-17, May-June 2017 and November-August 2017-2018 (Figure 14). Overall, between 2016-2018, the air pressure ranged between 917 (March 2018) to 972 hPa (December 2016) (Figure 14). Relative humidity was measured between December-January 2016-2017, December-February 2017-2018 and May-September 2018 (Figure 14). It ranged from 30 (September 2018) to 100% (December-January 2016-2017; January-February 2018) (Figure 14).

a)

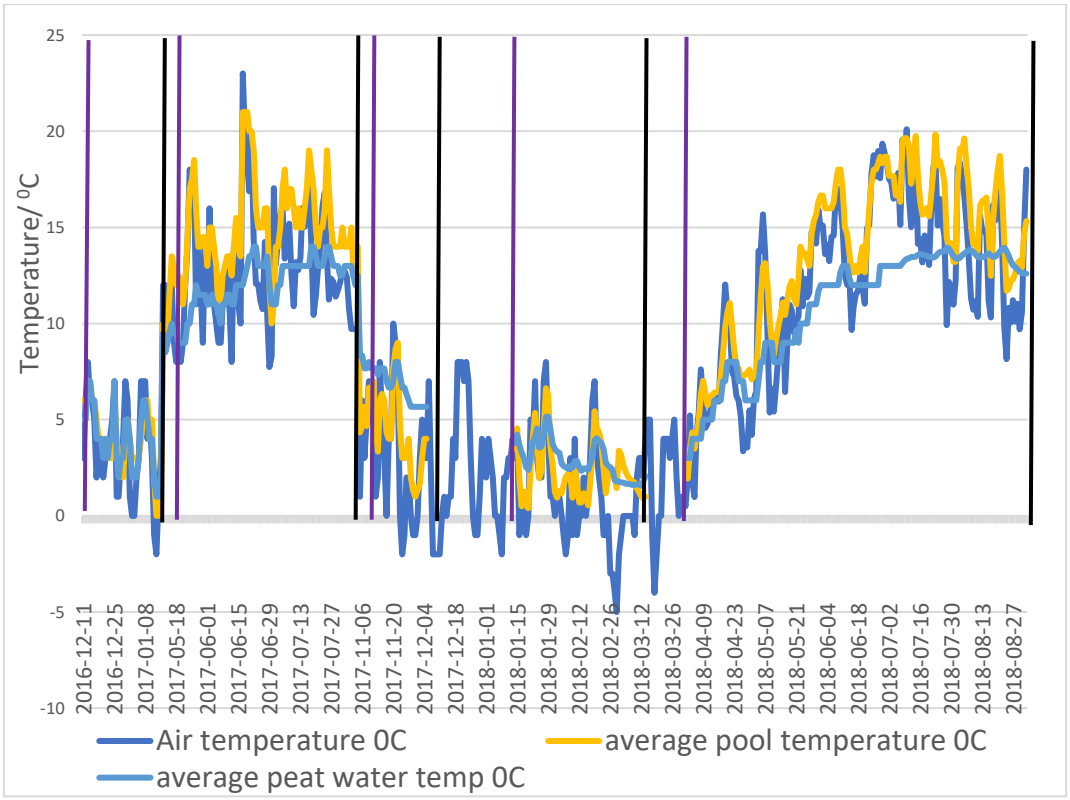
Temperature/ 0C
25
20
15
10
5
0
-5
-10
2016-12-11
2016-12-25
2017-01-08
2017-05-18
2017-06-01
2017-06-15
2017-06-29
2017-07-13
2017-07-27
2017-11-06
2017-11-20
2017-12-04
2017-12-18
2018-01-01
2018-01-15
2018-01-29
2018-02-12
2018-02-26
2018-03-12
2018-03-26
2018-04-09
2018-04-23
2018-05-07
2018-05-21
2018-06-04
2018-06-18
2018-07-02
2018-07-16
2018-07-30
2018-08-13
2018-08-27
Air temperature 0C
average pool temperature 0C
average peat water temp 0C

b)

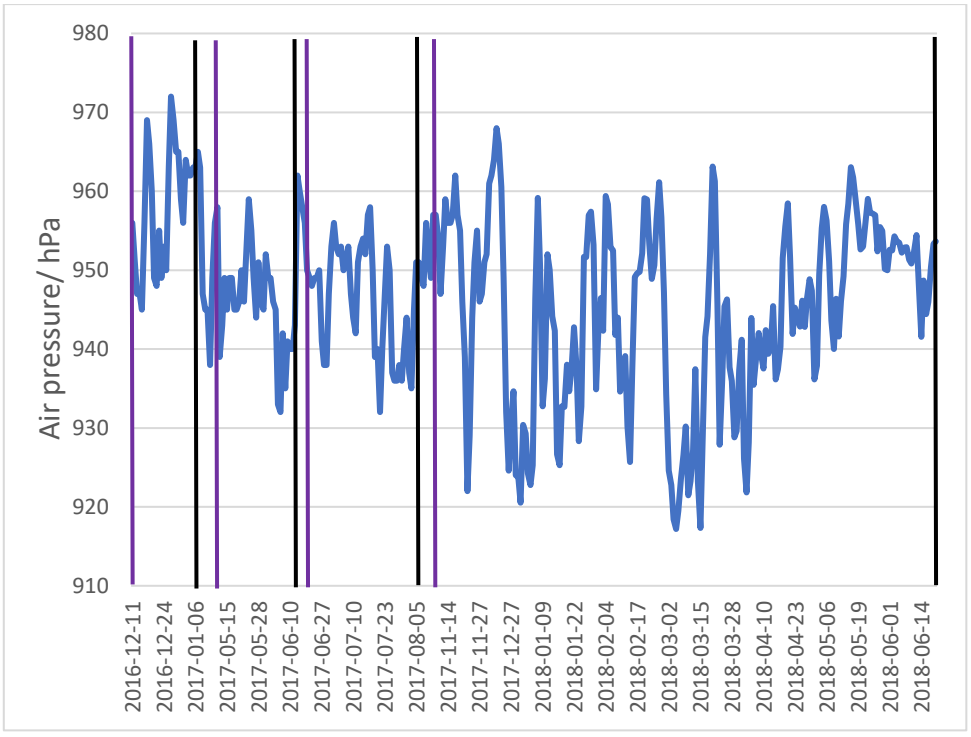
Air pressure/ hPa
980
970
960
950
940
930
920
910
2016-12-11
2016-12-24
2017-01-06
2017-05-15
2017-05-28
2017-06-10
2017-06-27
2017-07-10
2017-07-23
2017-08-05
2017-11-14
2017-11-27
2017-12-27
2018-01-09
2018-01-22
2018-02-04
2018-02-17
2018-03-02
2018-03-15
2018-03-28
2018-04-10
2018-04-23
2018-05-06
2018-05-19
2018-06-01
2018-06-14

c)

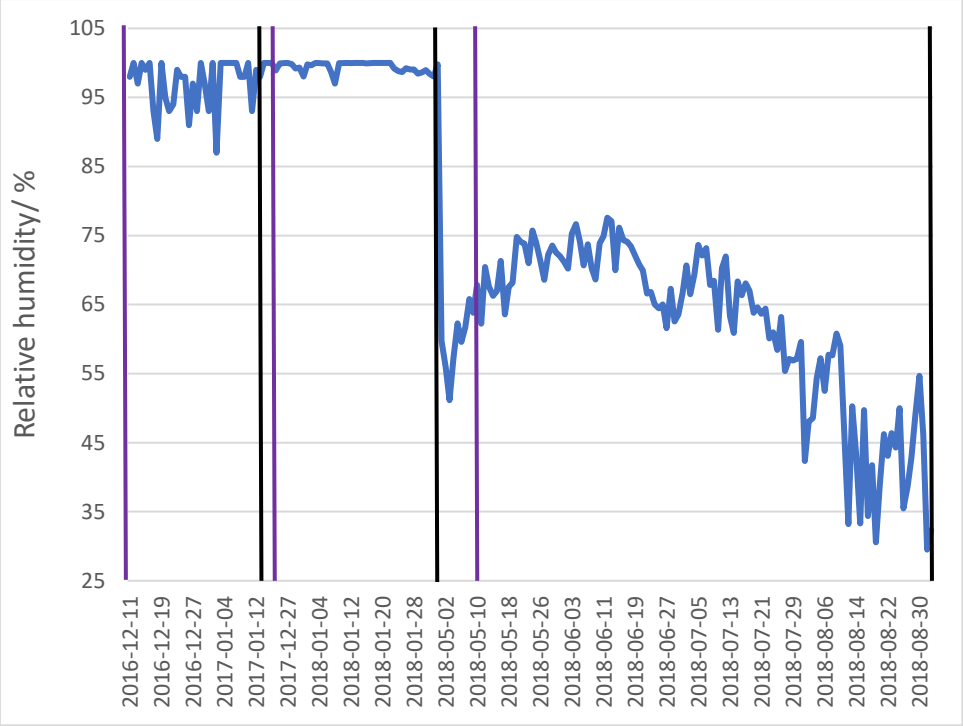

Figure 14 *Showing weather conditions on site throughout 2016-2018: a) air and water temperatures; b) air pressure; c) relative humidity. Water temperature was measured at depth of 0.1 metres in pool water and at level of 0.8 metres in peat soil. Vertical purple lines delineate beginning of monitoring period, black lines – ending.*

Within study area (53° 9.180'N, 6° 16.928'W), suitable peatland pools were selected based on how well they have illustrated bog pools in this type of the environment. These pools were dystrophic in nature (Uhlmann *et al*., 2011). The distinct features of the dystrophic pools are that they were nutrient (e.g. phosphorus and nitrogen) and calcium poor, highly acidic and rich in dissolved humic materials (Uhlmann *et al*., 2011). Bog pools were clear, but brownish in appearance (Figure 15). Their watersheds were small (Figure 15). One of pools was selected as a first point for field installation and *in-situ* experimentation (ST1), second pool was selected as the second point (ST2) and the third station (ST3) was established at later stage of the project (Figure 15a-k). All bog pools

were approximately of same size: one hundred square meters (Figure 15b). Each monitoring station ('Peat-Hydro 1', 'Peat-Hydro 2', 'Peat-Hydro 3') had two sampling/monitoring locations: peat soil zone – hummock and lawn (HumST1, LawnST2, HumST3) and bog pool (ST1-3) based (Figure 15; Figure 16). These points were selected according to literature where these settings were mentioned to be associated with highest and most variable CO_2 and DOC fluxes (Clair *et al.*, 2002).

(a)

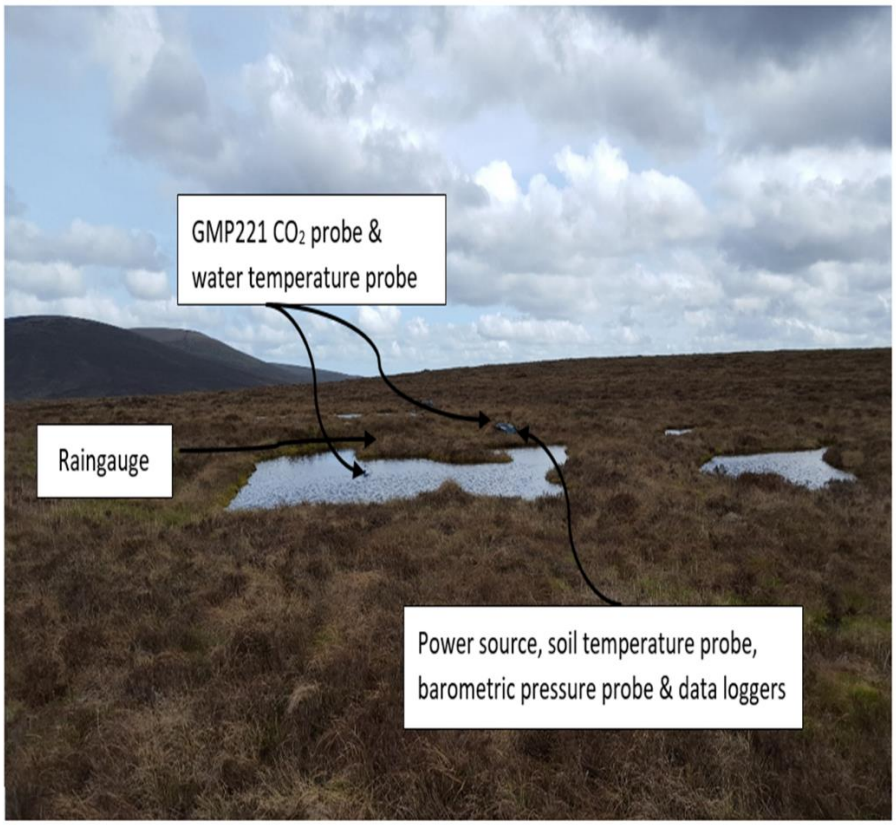

b)

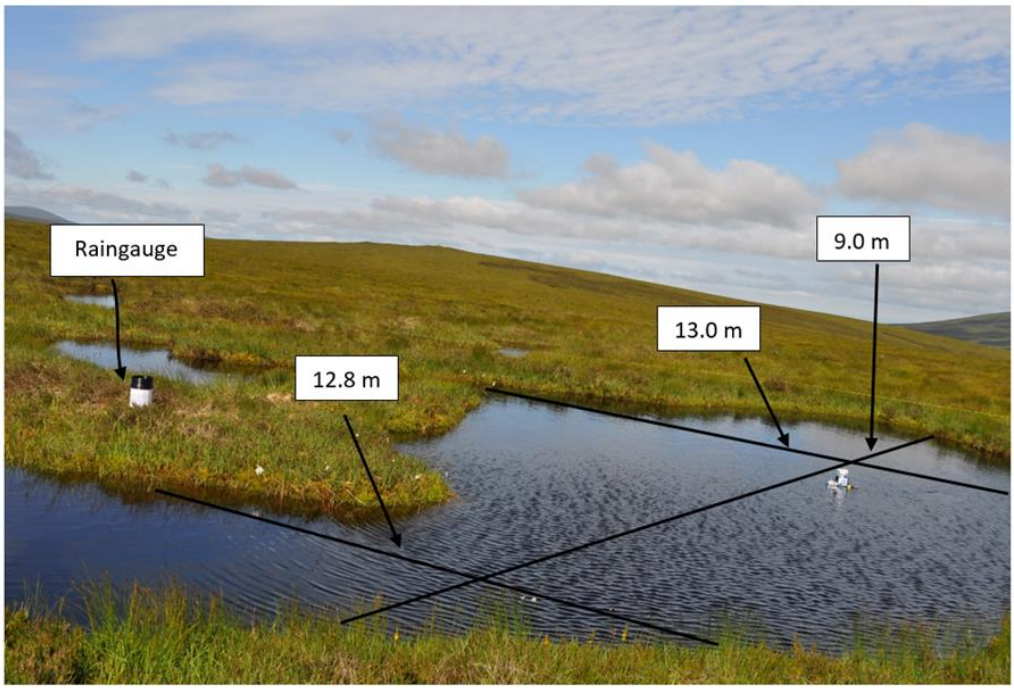
Raingauge
9.0 m
13.0 m
12.8 m

c)

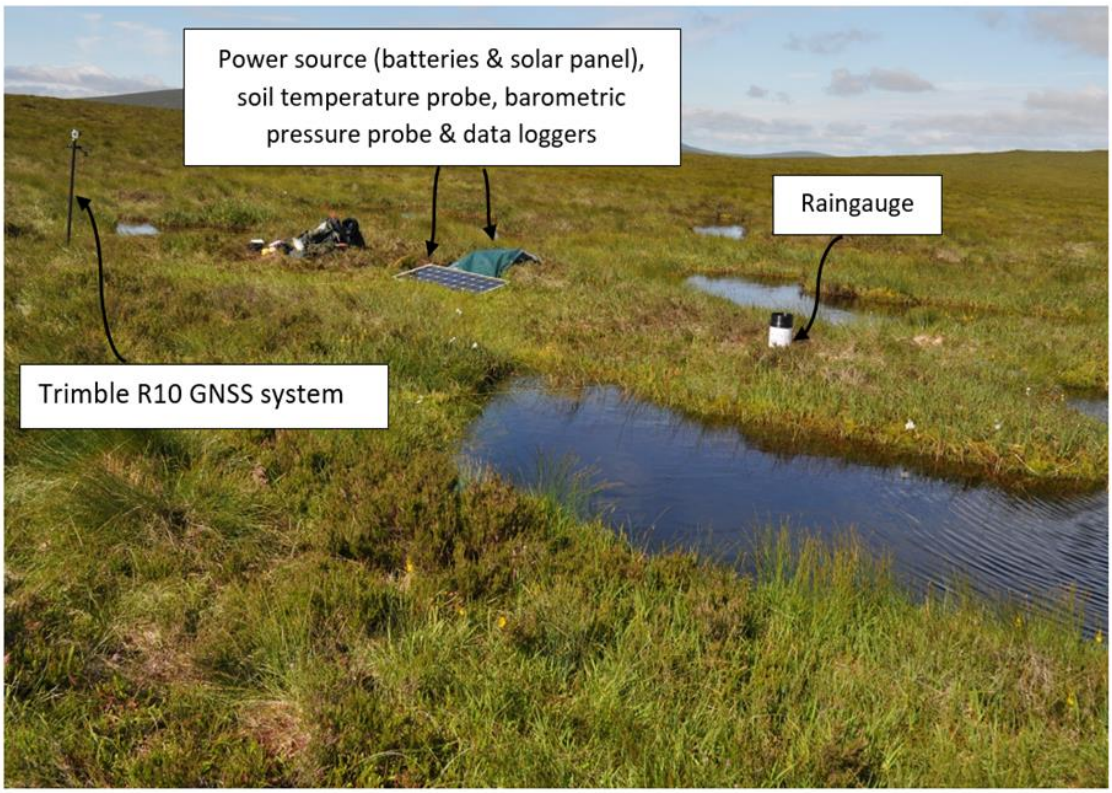
Power source (batteries & solar panel), soil temperature probe, barometric pressure probe & data loggers
Raingauge
Trimble R10 GNSS system

(d)

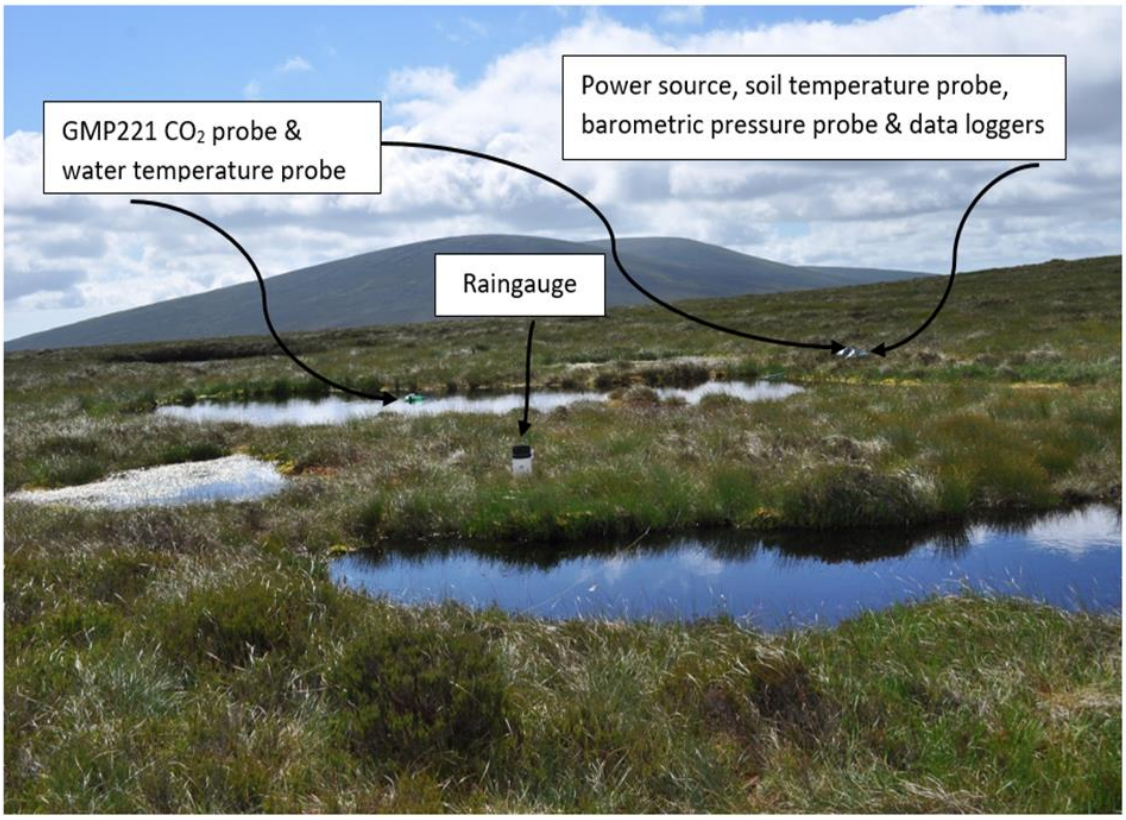
GMP221 CO_2 probe &
water temperature probe
Power source, soil temperature probe,
barometric pressure probe & data loggers
Raingauge

e)

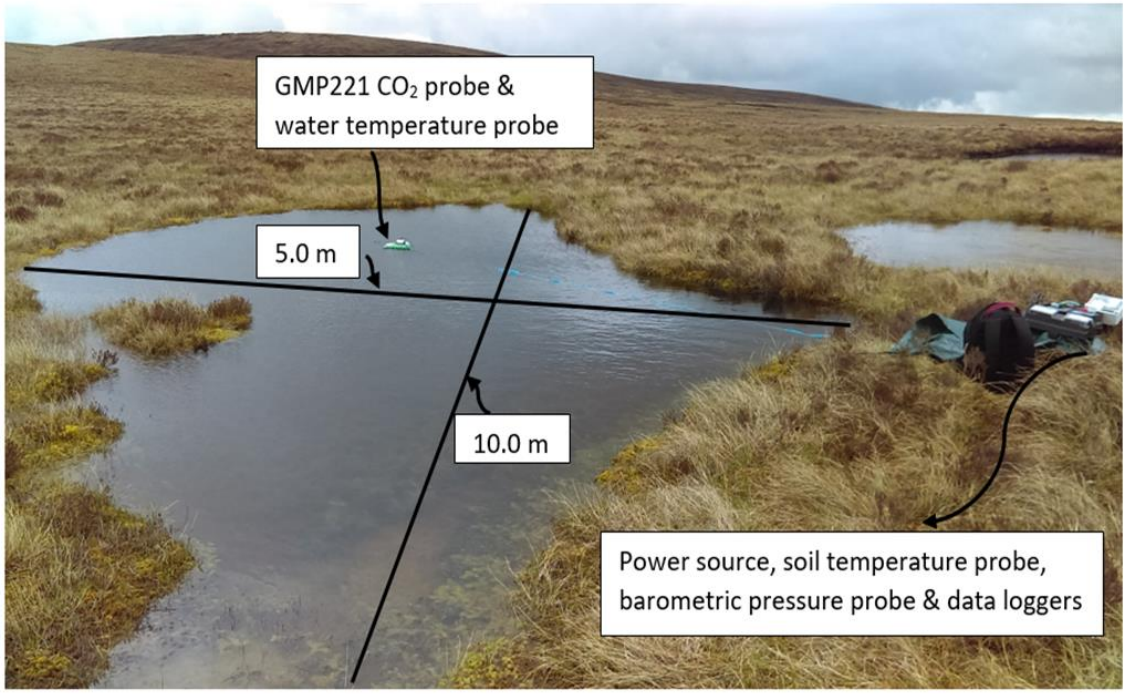
GMP221 CO_2 probe &
water temperature probe
5.0 m
10.0 m
Power source, soil temperature probe,
barometric pressure probe & data loggers

f)

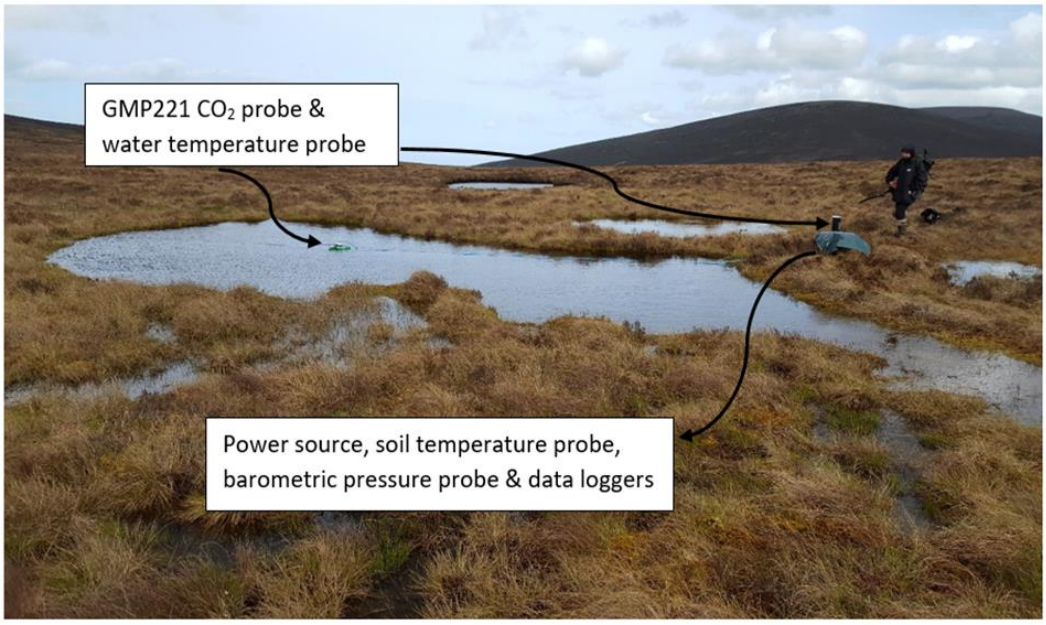
GMP221 CO_2 probe &
water temperature probe
Power source, soil temperature probe,
barometric pressure probe & data loggers

g)

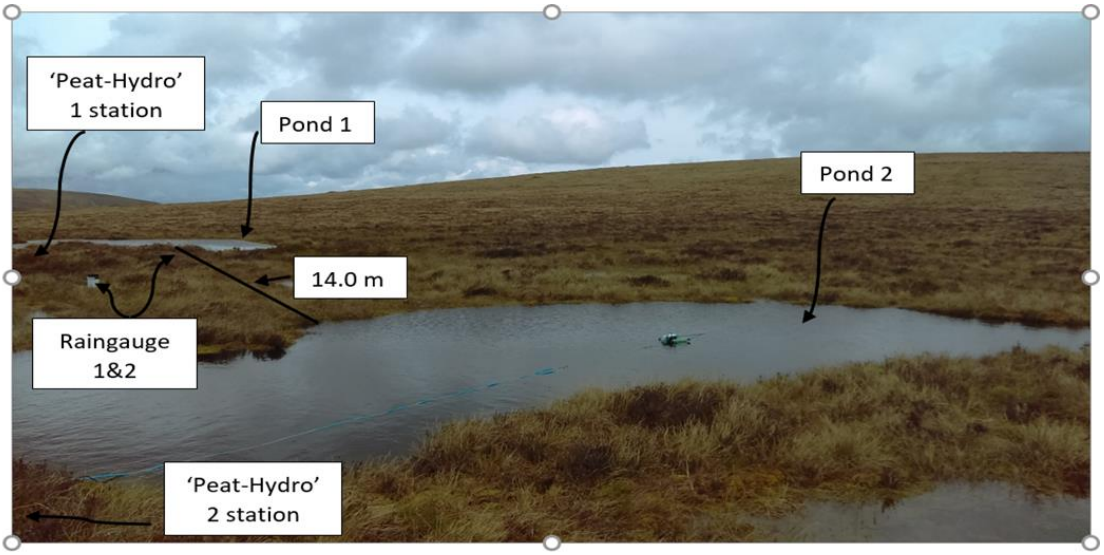
'Peat-Hydro'
1 station
Pond 1
Pond 2
14.0 m
Raingauge
1&2
'Peat-Hydro'
2 station

(h)

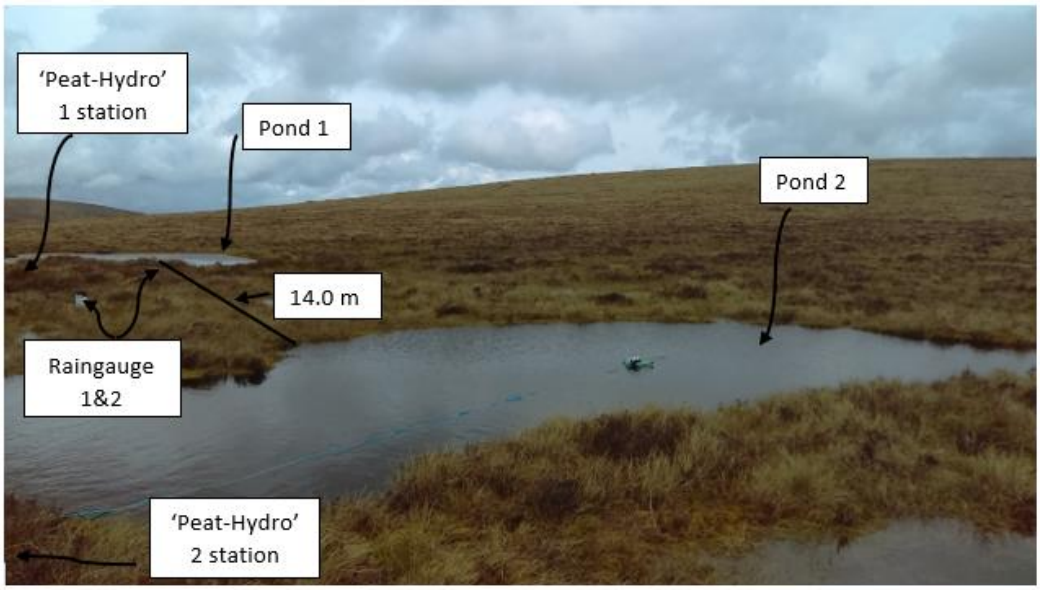
'Peat-Hydro'
1 station
Pond 1
Pond 2
14.0 m
Raingauge
1&2
'Peat-Hydro'
2 station

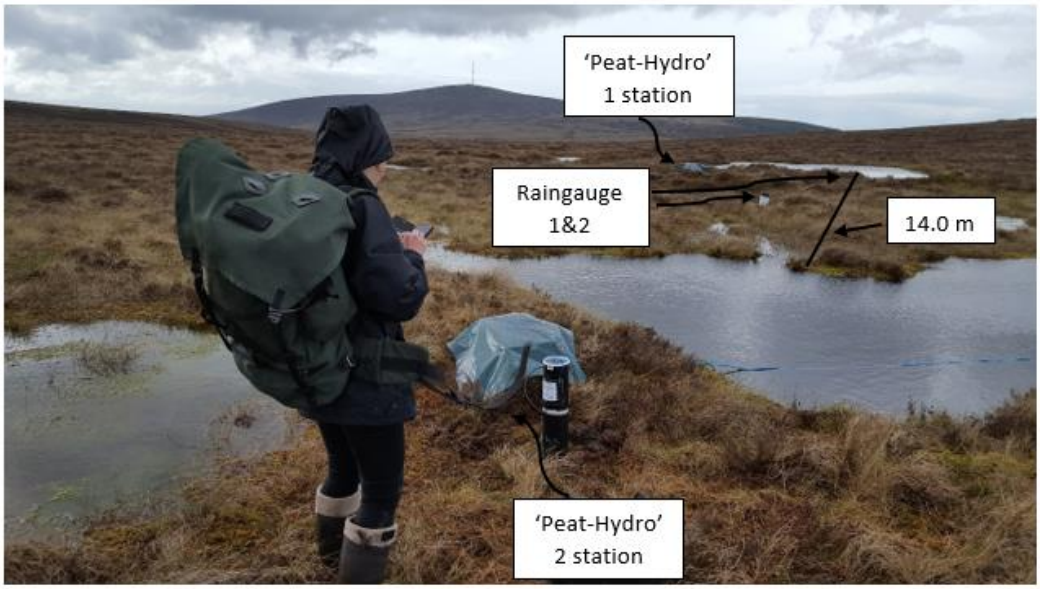
'Peat-Hydro'
1 station
Raingauge
1&2
14.0 m
'Peat-Hydro'
2 station

(i)

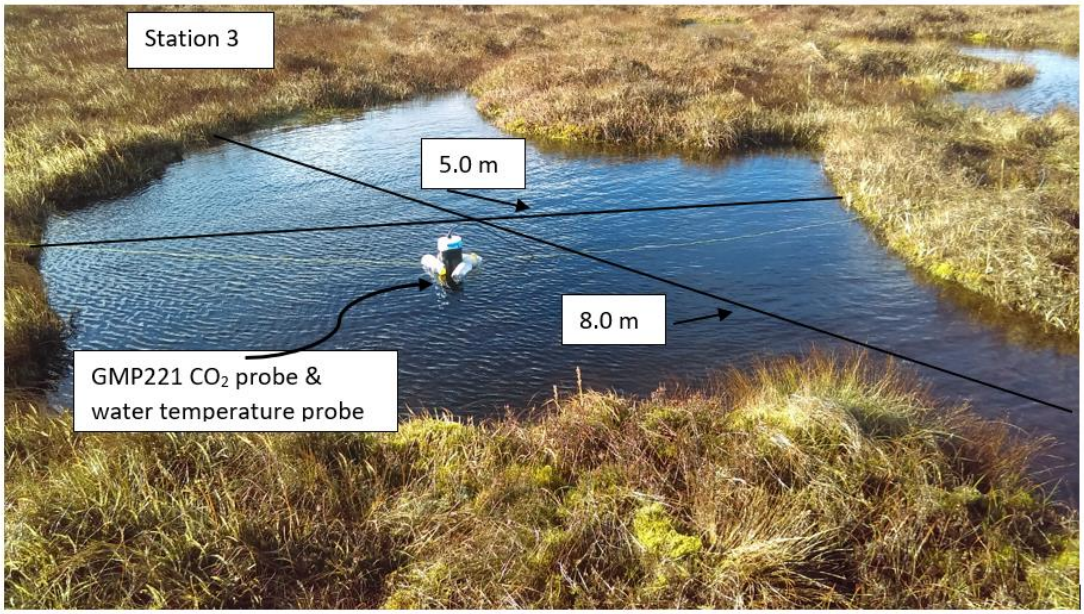
Station 3
5.0 m
8.0 m
GMP221 CO_2 probe &
water temperature probe

(j)

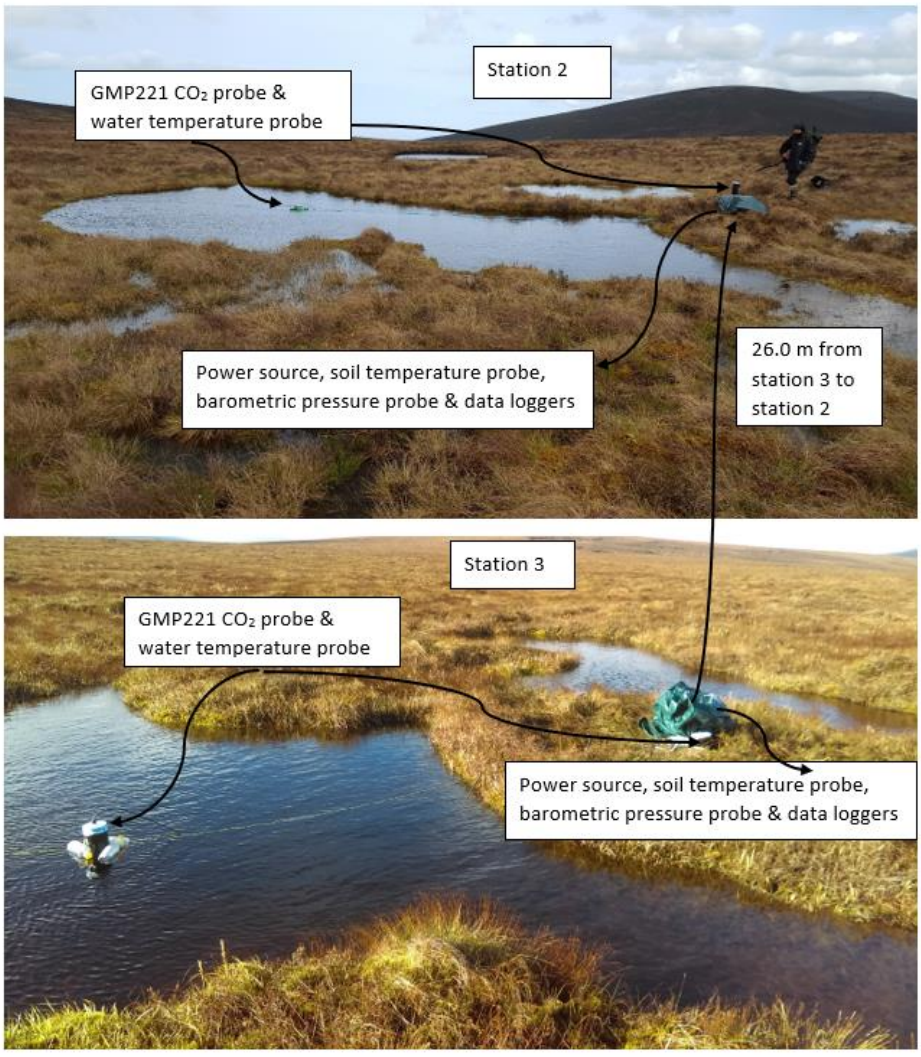
GMP221 CO_2 probe &
water temperature probe
Station 2
Power source, soil temperature probe,
barometric pressure probe & data loggers
26.0 m from
station 3 to
station 2
Station 3
GMP221 CO_2 probe &
water temperature probe
Power source, soil temperature probe,
barometric pressure probe & data loggers

k)

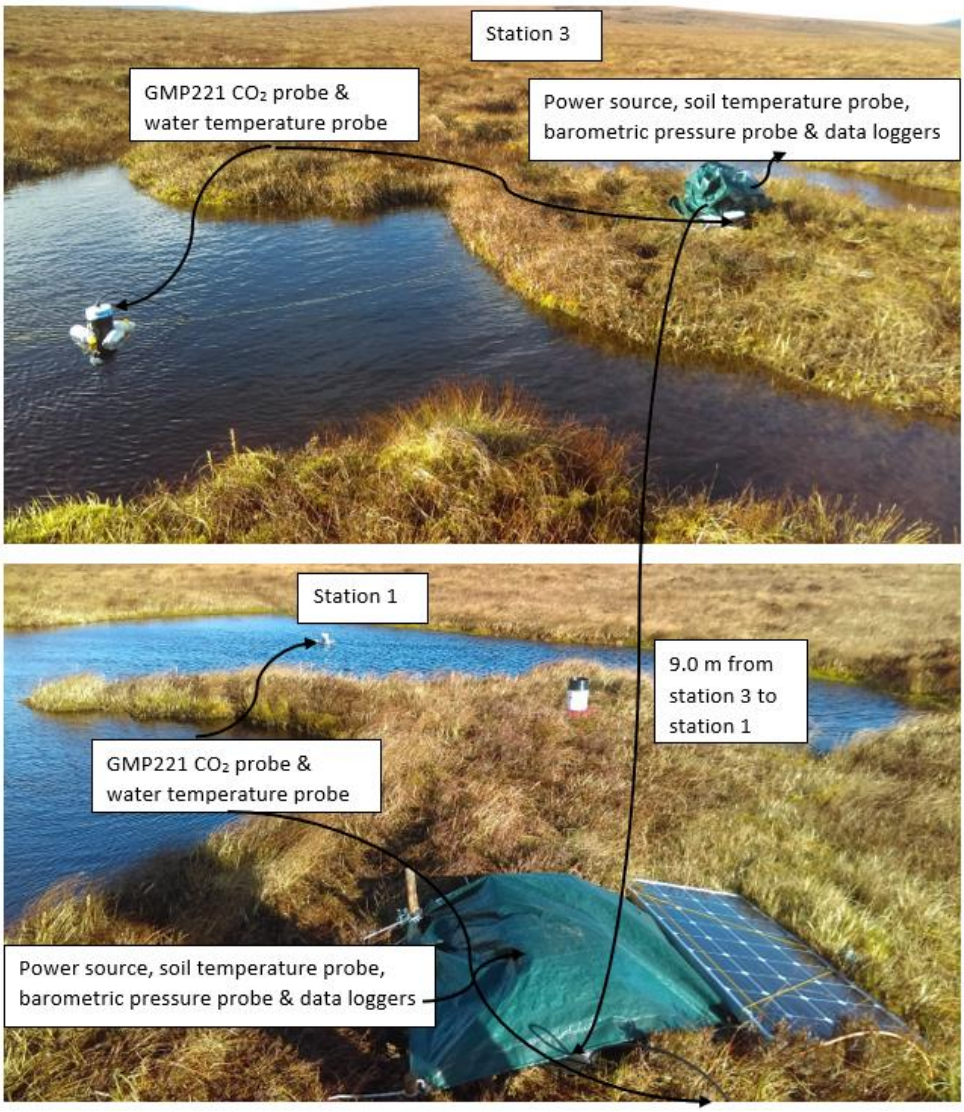

Figure 15 *ST1 (a-c) and ST2 (d-g) and pool dimensions; (h) distance from ST1 to ST2; (k, i) ST3 and pool ST3 dimensions; (k, j) distance from ST3 to ST1-ST2.*

Location: 53° 9.180'N, 6° 16.928'W.

(a) 

(b) 

(c) 

Figure 16 *(a) 'Peat-Hydro 1'; (b) ST1; (c) HumST1.*

The peat zone was characterized according to its dominant floral composition and physical structure. The most abundant species were *Calluna vulgaris*, *Tricophorum cespitosum*, *Narthecium ossifragum*, *Sphagnum spp.* and *Erica tetralix*. Species such as *Eriophorum angustifolium*, *Luzula sylvatica*, *Andromeda polifolia*, *Eriophorum vaginatum* and *Vaccinium myrtillus* were also observed but in smaller quantities. Peat soil collected as per methods (Peatland soil characteristics and parameters), was evaluated by appearance and colour (Figure 17). The soil was between dark brown to black at the surface and more reddish brown towards middle and bottom of soil profile under consideration. Inside the peat there were localised sections where there were remains present of cypearaceous (sedges) plants and other residues (roots, amorphous organic matter, charcoal fragments).

Generally, study site peats derived from hummock and lawn environments were relatively well humified (H7/8; Peatland soil characteristics and parameters). Humification was more profound around 0.8-1 m depth. They were classified as sapric (Peatland soil characteristics and parameters). Hydraulic properties of peaty soils (Peatland soil characteristics and parameters) were assessed and included: rubbed fibre content, soil density, moisture and aeration conditions. Bulk density was calculated for all three sites 0.023- 0.101 g/cm^3. Volumetric water content was 0.101- 0.161 g/cm^3. Soil porosity was on average 96-99%. Soil water filled pore space percentage was 11-16% across all sites.

Figure 17 *Core extracted from monitored peat soil.*

Methodology for this project included continuous monitoring of dissolved CO_2 concentration and water temperature (ST1-3 & HumSt1, LawnST2 and HumST3), air temperature and pressure. Other parameters that were monitored routinely included precipitation, pH (water), water conductivity, TOC, dissolved organic carbon (DOC), nutrients (nitrogen species and phosphorus) and several other elements. CO_2 concentrations were measured from 2016 until 2018. There were five monitoring periods: December-January (2016/17), June-August 2017, November-December 2017, January-March 2018 and April-August 2018. ST1 and HumST1 were in operation throughout entire monitoring period. ST2 was not operational between December-January 2016/17. LawnST2 was not operational in December to January 2016/17 monitoring period, January-May 2018 and in August 2018. ST3 and HumST3 were in operation from November to December 2017 and from May to August 2018. Spot sampling for hydrochemical analyses were conducted on 10th of February 2018, 2nd and 22nd of April 2018, 25th of May 2018, 7th of July 2018 and 5th of September 2018.

3.2 Methods

The most appropriate method for establishment of carbon dynamics of upland blanket peatland discussed in this study is based on continuous monitoring *in situ* of variables such as CO_2 concentrations, water temperature and air pressure. Such method is a suitable approach for long-term application in the environment where CO_2 concentrations vary in time and space. It is also appropriate to use it since carbon dynamics is likely to varying on a diurnal scale (24h clock). From the practical point of view this method allowed us to collect a greater spectrum of direct data and allowed us to conduct a follow-up statistical analysis using data derived from different seasons (winter and summer) and spatial units (pools, hummocks and lawns) in this type of environment.

Historically, methods based on continuous measurement were heavily based on the use of various sensors: pH based, optical (IR for instance) or conductivity-based devices (Orellana *et al*., 2011). The use of pH and conductivity-based sensors to calculate CO_2 concentrations, however, could lead to inaccuracies, as small-scale temperate changes in CO_2 concentrations could be lost during the process of calculations (Johnson *et al*., 2010). As explained in the paper by Takeshita *et al*. (2018) the accuracy of CO_2 estimation based on pH is dependent on three factors: accuracy of the estimated total alkalinity, accuracy of the pH measurement, and the choice of equilibrium constants used for converting pH to CO_2. To complicate this, the probe performance and location could also affect the gas estimation (Pfeiffer *et al*., 2011). In case of pH probe, slight changes in pH readings due to a drifting calibration or sample locale can have a substantial effect in the calculated CO_2 concentration (Pfeiffer *et al*., 2011). Small changes in pH are important because pH is a logarithmic scale (Pfeiffer *et al*., 2011).

On another hand, direct and continuous determination of CO_2 concentrations could give more meaningful results. In this study, the sensor type of choice was a non-dispersive infrared (NDIR) gas sensor that targets wavelength absorption in the infrared spectrum (Vaisala GMM220 CARBOCAP) (Vaisala, 2013) (Figure 18). NDIR technique is in use since 1930s (Dinh *et al*., 2016). It was first used in United States (Dinh *et al*., 2016). This sensor consists of light source, measurement chamber, interference filter, and the detector (Vaisala, 2012) (Figure 20). According to work by Dinsmore (2008; 2011a, b) and Johnson *et al.* (2010) Vaisala CO_2 NDIR sensors are capable of measuring concentrations of CO_2 in the air retained within the headspace of PTFE membrane, which is assumed to be in equilibrium with concentration of CO_2 dissolved in the surrounding water.

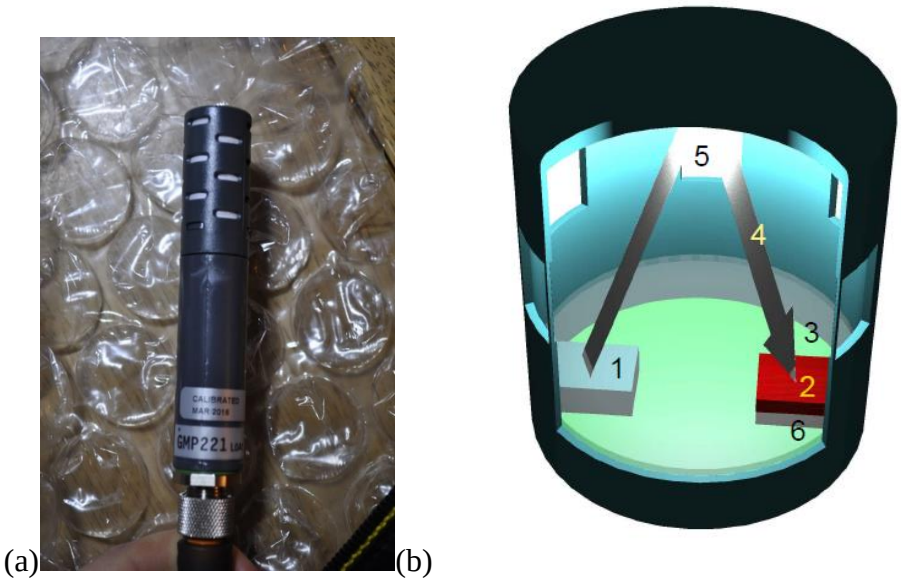

Figure 18 *(a) Vaisala GMM220 (GMP221 probe model) CARBOCAP sensor; (b) Internal structure of Vaisala CARBOCAP sensor: 1 – IR source; 2 – Fabry-Perot Interferometer Filter; 3 – Protective window; 4 - CO_2 IR absorption; 5 – Mirror surface; 6 - Detector.*

The CO_2 gas concentration is detected in the following steps: IR radiation is emitted from the light source; the radiation is passed through the CO_2 gas to the detector and the light intensity is detected and converted into a concentration value (Vaisala, 2012) (Figure 18). The principal that NDIR sensor itself is based on is the Beer-Lambert Law ($I= I_o \times \exp(-kcl)$) (Robinson, 1996; Dinh *et al*., 2016). In this law, I_o parameter is an initial radiation beam intensity, I parameter stands for the beam intensity after traversing the gas to the detector, k- an absorption coefficient, l- sample optical path length or an effective sample chamber length of the sensor and c is the gas concentration (Dinh *et al*., 2016). The Beer-Lambert Law is one of the fundamental laws that relates the degree of absorption by a substance to concentration of its components (Robinson, 1996).

NDIR sensor has many advantages comparing with the other spectroscopy techniques, for instance, it consumes reasonably low amount of energy (power consumption <2.5 W) and it can operate at low temperatures (GMM220 operates at temperature of up to -20 ^oC) (Vaisala, 2012). However, there are some limitations, such as interference (that is said to be largely reduced in VAISALA sensor) and detection limit (GMM220 model range is 0-10% or up to 100 000 ppm CO_2) (Vaisala, 2012). Nitric oxide, carbon monoxide, nitrogen dioxide, nitrous oxide, methane, water vapour, hydrocarbon are all gases that may interfere with CO_2 ad with one another (Sun *et al*., 2016). The absorption spectra of CO_2 located closely with absorption spectra of nitrous oxide, water vapour and carbon monoxide inferring potential interferences (Sun *et al*., 2016). The accuracy of this GMM220 NDIR sensor at 25 ^oC and 1012 hPa is ± 1.5% of range + 2% of reading (applies for concentrations above 2% of full scale) (Vaisala, 2012).

The precision of NDIR sensor shows consistency of results when repeated (Dinh *et al*., 2016). It also has a reasonably short warm-up time of 30 seconds (15 minutes – full specifications) and response time (63%) of 20 seconds (Vaisala, 2012). However, every time the sensor was switching on the corresponding spike was observed on the graph, that was consistent with the sensor warming but was not useful for the purposes of estimating CO_2 (Figure 19). These spikes were removed from the data series, to ensure accuracy when performing gas calculations. The GMM220 sensor type that was used in this study was initially supplied with DC power (two 75 Ah, 12V DC batteries deployed in-parallel) (Figure 20) and an output was recorded with a data acquisition system (Vaisala data-logger; DL4000) (Figure 20). At later stage (Spring-Summer 2017) two pairs of sensors were powered with two batteries that were re-charged with solar panel with capacity of 100 Watt. The sampling interval was every minute from the beginning of project (autumn 2016 until January 2018) after that date the sampling interval was reduced to every five minutes and then data were averaged per hour. The digital timer (Figure 20) was used to cycle sensor on and off for measurements at reduced frequency to conserve power. The timer was set to turn sensor on and off every 15 minutes.

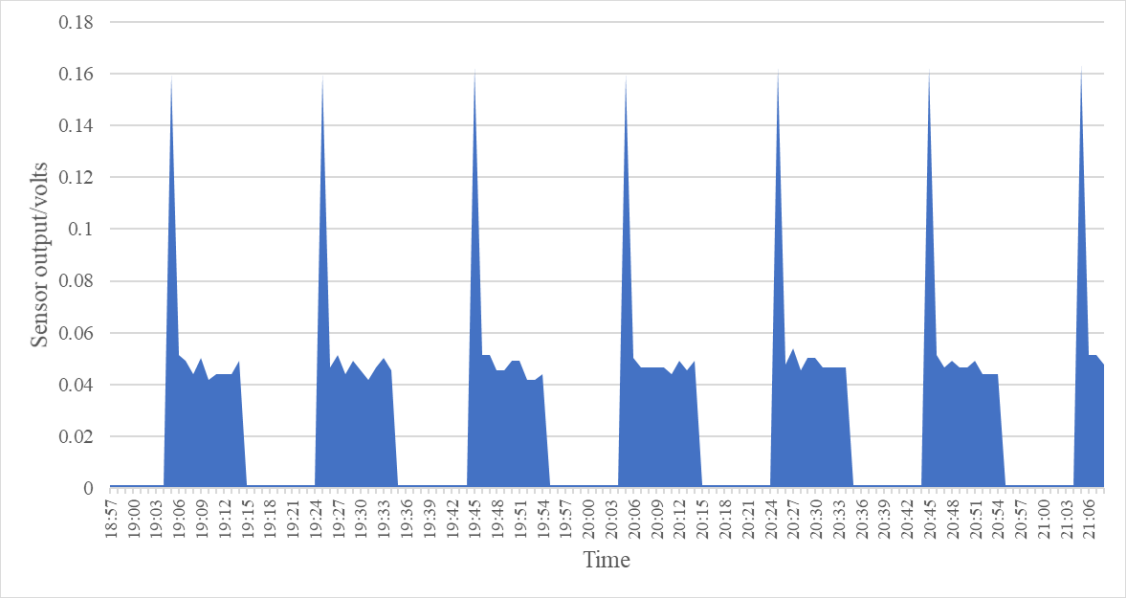

Figure 19 *The sensor activation spikes.*

The rationale behind installing the solar panel was practicality driven. It was installed on site to increase measuring period and prolong the life of batteries (Figure 20). Additional station ('Peat-Hydro 3') was connected during winter 2017 (November-December). Based on performed calculations it was theoretically established that the set-up will work, and that solar panel will provide enough of energy to cover all six sensors on site. After rigorous field-based conditioning, it was established that solar panel was only able to power two batteries and that was only enough for four sensors. This set-up was not adequate to power three stations during wintertime as the cloud cover was significantly reducing solar energy. Therefore, to allow monitoring continuously it was agreed to disconnect (ST3 & HumST3) during winter 2018 and to switch these sensors back during Spring 2018.

(a)

Junction box
DC battery.

(b)

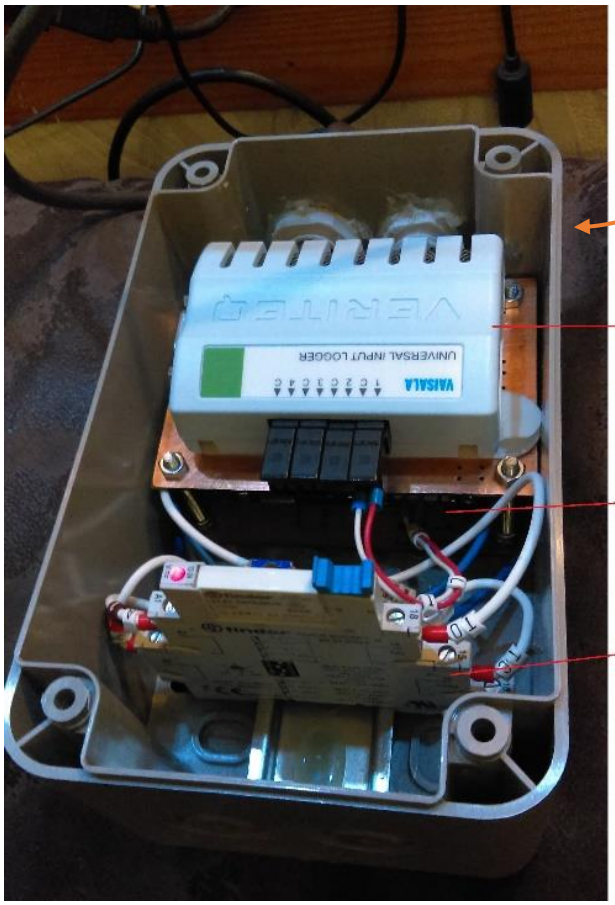

Datalogger

Transmitter

Timer

(c) 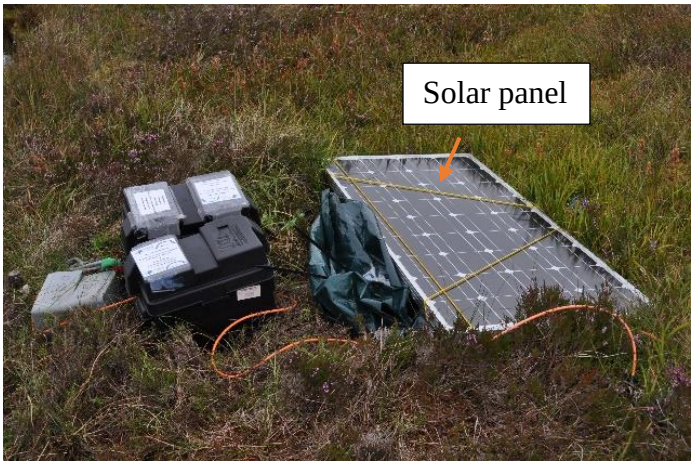

Figure 20 *Equipment used in the study: a) Pair of DC batteries: 75 Ah, 12V DC, b) Junction box containing Vaisala DL4000 data-logger, timer and the transmitter, c) Solar panel power supply.*

Due to pool and peaty soil acidity (low pH values), much of inorganic carbon was in form of dissolved CO_2 (Figure 21). Therefore, other non-biological factors that could have influenced CO_2 concentration in these environments were water temperature and atmospheric pressure. The GMM220 NDIR Vaisala CARBOCAP sensor used in this study did not measure pressure and temperature thus could not automatically compensate for pressure and temperature variations. To measure air pressure and water temperature (HOBO temperature recorder & Omega-RH23 pressure monitor) additional sensors were installed (Figure 22). These meteorological parameters were measured at the same frequency as CO_2, e.g. continuously. To calibrate sensor's output as a partial pressure of CO_2 (pCO_2) based on changes in temperature and pressure Henry's law (universal gas law) was used (Dinsmore, 2008). According to Henry's law, the mass of a gas that dissolves in a definite volume of liquid is directly proportional to the pressure of gas if gas does not react with water: $C_{gas} = K_h \times P_{gas}$ (Plummer & Busenberg, 1982). In this equation, C_{gas} is concentration of dissolved gas, K_h is Henry's law constant that is

temperature dependent (e.g. increases with temperature) and is specific for that gas and P_{gas} is partial pressure of the gas above solution (Plummer & Busenberg, 1982). Based on this law and the instrumental specifications for Vaisala sensor, CO_2 concentration was corrected using the following formula: $C_c = C_m - C_T - C_p$ (Tang *et al*., 2003). In this equation, CO_2 concentration (C) is expressed in μmol mol^{-1}, and the subscripts c, m, T and p mean corrected, measured, temperature corrected, and pressure corrected (Tang *et al*., 2003). The temperature correction was calculated using the formula: $C_T = 14000 (K_T - K^2_T) [\frac{25 - Tc}{25}]$ (Tang *et al*., 2003). In this formula, T_C is the temperature (°C), $K_T = A_o + A_1 \times C_m + A_2 \times C^2_m + A_3 \times C^3_m$, $A_o = 3 \times 10^{-3}$, $A_1 = 1.2 \times 10^{-5}$, $A_2 = -1.25 \times 10^{-9}$ and $A_3 = 6 \times 10^{-14}$ (Tang *et al*., 2003). The pressure correction was calculated using the formula: $C_P = K_P [\frac{P - 101.3}{101.3}]$ (Tang *et al*., 2003). In this equation, P is the pressure (kPa), $K_P = A \times C_m$ and A = 1.38 (Tang *et al*., 2003). The reference pressure and temperature values for the GMM220 were 101.3 kPa and 25 °C.

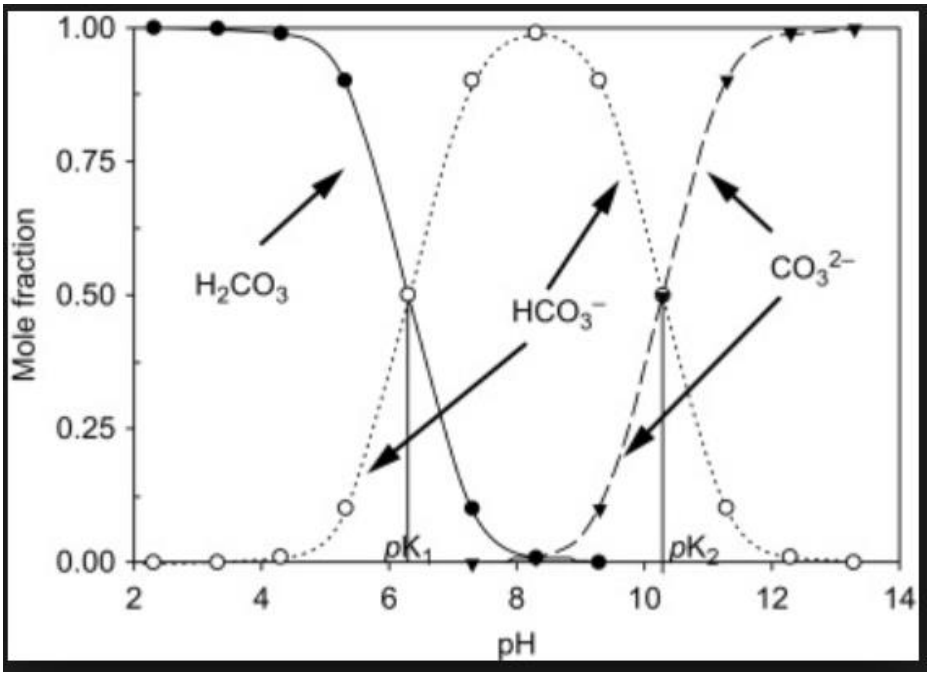

Figure 21 *Carbonate Species Distribution. Adapted from Al Omari et al. (2016).*

(a)

(b)

(c)

Figure 22 *Additional sensing devices: atmospheric pressure and water temperature; a) USB Barometer (UT330CUSB data recorder), b) Water temperature sensor (HOBO), c) Omega-RH23 pressure sensor.*

Concentrations of CO_2 were converted from μmol mol^{-1} to mgl^{-1} [C] to illustrate amount of carbon available in a specific spatial setting. The excess partial pressure CO_2 ($epCO_2$) or quantity of CO_2 contained within environment against concentration present in the atmosphere was calculated ($epCO_2$ = pCO_2/atmospheric CO_2) (NASA Global Climate Change, 2018). $epCO_2$ indicates whether CO_2 is going to be released from the environment. If $epCO_2$ is greater than 1, which usually occurs in supersaturated aqueous conditions then CO_2 is going to be released into the atmosphere (Elayouty *et al*., 2016). $epCO_2$ represents a link between terrestrial and atmospheric carbon cycles (Elayouty *et al*., 2016). Ability of peatland pools to efflux large quantities of CO_2 could have a significant implication on national and global carbon budget. Therefore, it is essential to measure capacity of peatland pools and peatland soil waters of degassing CO_2. It is critical to find the main factors resulting in these losses.

The hummock/lawn microtopography could potentially be associated with different gradients of carbon fluxing. Hummocks could act as hot spots of carbon concentration, accumulations and evasion. Factors such as climatic variability, water table level and peat structure could be of paramount importance with regards to hummocks CO_2 dynamics. Lawns could potentially act in opposite way and sequester carbon at certain periods of the year. Water and oxygen levels in these environments can cause significant variation in soil environmental conditions which causes preferential colonization of hummocks and lawns by distinct plant communities. Such colonization reinforces structural and chemical differences due to topography alone by influencing quantity and quality of soil organic substrate and altering aerobic capacity of the peat by transporting oxygen to the rhizosphere. Plants containing aerenchymous tissue (allows exchange of gases between the shoot and the root; spongy tissue that forms spaces) can also provide a direct pathway

for CO_2 fluxing to the atmosphere, bypassing aerobic peat horizon, and greatly increasing soil-atmospheric fluxes.

Speaking of CO_2 fluxes, they could be measured between peaty soil and the atmosphere. They are commonly measured using a static chamber method (Koster *et al*., 2015). In the study by Koster *et al*. (2015) gas flux measurements were done once a month (summer period) on 48 polyvinyl chloride (PVC) collars (6 collars per plot; diameter 0.22 m and height 0.05 m) installed permanently on the soil in the summer (Koster *et al.*, 2015). The lower edge of the collar was placed at 0.02 m depth in the mor layer above the rooting zone to avoid damaging the roots (Koster *et al.*, 2015). The collars were sealed with a thin layer of sand placed around the collar to reduce leakage of air from below the collar (Koster *et al.*, 2015). All chamber measurements were carried out during the daylight (Koster *et al*., 2015). Vegetation inside the chamber was kept and was maintained intact during the measurements (Koster *et al.*, 2015). The chamber used in the flux measurements was cylindrical (h = 0.24 m and diameter 0.2 m) and was covered with aluminium foil to prevent photosynthesis of ground vegetation during the flux measurements (Koster *et al.*, 2015). It was equipped with a small fan (0.025 m in diameter) for mixing the air inside the chamber (Koster *et al*., 2015). CO_2 concentrations inside the chamber were recorded with NDIR CO_2 probe (GMP343, Vaisala), relative humidity and temperature were measured with RH-/T-sensor at 5 second intervals for 4 minutes during the 5 minutes chamber deployment time (Koster *et al.*, 2015). The first 30 seconds after placing the chamber onto the collars were discarded from the measurement data to exclude the disturbance effects (Koster *et al*., 2015). In this Finnish forested region, CO_2 emissions were significantly higher in August compared with June and July (Koster *et al.*, 2015).

It is a known fact that fluxes of CO_2 from waters could be also measured using the chamber method. In the study by Lorke *et al*. (2015) this method was used to measure fluxes of CO_2 from streams into the atmosphere (Lorke *et al.,* 2015). The chamber cross-sectional area was 0.066 m^2 and the volume was 6.8 litres (Lorke *et al.,* 2015). It was covered by aluminium foil to reduce the internal heating and equipped with a Styrofoam material to keep the chamber body floating on water surface (Lorke *et al.,* 2015). The chamber was equipped with an internal CO_2 logger system that was positioned inside the headspace of the chamber (Lorke *et al.,* 2015). NDIR CO_2 logger was used and it measured CO_2 in range of 0–5000 ppm (Lorke *et al.,* 2015). The logger measured CO_2, temperature, and relative humidity (Lorke *et al.,* 2015). The measurement interval was adjusted to every 30 seconds (Lorke *et al.,* 2015). Some chambers were deployed fixed at a certain position (anchored) and others were freely drifting (Lorke *et al.,* 2015).

According to Davidson *et al*. (2002) and Schneider *et al*. (2009) chamber measurements can be biased when measurements are performed under low turbulence conditions or over too short time periods. These measurements do not integrate fluxes over entire ecosystem and high precision mapping, or remote sensing is needed to extrapolate fluxes and that leads to errors. Therefore, these methods are not applicable for measuring continuously. Floating chambers tend to over-estimate fluxes between two and ten times on small pools when compared to mathematical modelling such as 'Thin boundary layer' referred to below (Vachon *et al.,* 2010). The chamber method is not accurate because the chamber itself causes turbulence that disturbs the air-water interface and the gas exchange as a

result. ‘Thin boundary layer’ method does not disturb that interface and therefore is the method of choice in this project.

In this study, this method was applied to model potential fluxes from peatland pools (ST1-ST3). To follow up the efflux rate of CO_2 and conditions under which these fluxes are significant into the atmosphere, thin boundary layer ($Flux\ [CO_2] = K_x*(C_w - C_a)$) approach (Pelletier, 2014) was used. Where K_x is a gas-specific exchange coefficient found from an expression of the gas-specific Schmid number (Sc), C_w is the pCO_2 in the water and C_a is concentration of gas in the air (Pelletier, 2014; NASA Global Climate Change, 2018). The K_x number was found using the following formulae: $K_x = K_{600}*(Sc/600)^{-b}$, where $b = 0.66$ for the wind speed ≤ 3 m/s or $b = 0.5$ for the wind speed > 3 m/s (Pelletier, 2014). To perform this calculation, Schmid number and K_{600} number (gas exchange coefficient; cm h^{-1}) were calculated (Pelletier, 2014). The Sc number was found using the following equation which is dependent on water temperature (T; ^{0}C): $Sc\ (CO_2) = 1911.1 - 118.11*T + 3.4527*T^2 - 0.04132*T^3$ (Pelletier, 2014). The K_{600} number was normalized for CO_2 at 20 ^{0}C in fresh water with a Sc number of 600 and was approximated as a function of wind speed at 10 m height (U_{10}) using the method by Cole & Caraco (1998): $K_{600} = 2.07 + (0.215 * U_{10}^{1.7})$ for the medium-wind conditions (3-5 m/s) and for the low (< 3 m/s) and high (>5 m/s) using the approach derived from the Wanninkhof (1992): $K_{600} = 0.45*U_{10}^{1.64}$. The reason for using two approaches to calculate the K_{600} was that for low and high winds the relationship by Cole & Caraco (1998) did not correspond well with the relationship that this equation was derived from e.g. Wanninkhof (1992). According to later relationship it was predicted that the K_{600} would be zero at zero wind and that at higher wind speed higher K_{600} values would be expected. The wind speed records were taken from the closest meteorological station that was

measuring wind speed (Casement Aerodrome). This station is located 24.6 km away from the study site. The station was measuring wind at the height of 12 m. Our site was positioned 550 m above the see level and the Casement Aerodrome station was positioned 97 m above the see level. Wind speeds vary greatly on smaller distances. There is an element of uncertainty when modelling wind speeds for locations that are faraway and when sites are at significantly different elevations. To be able to use the wind data to model fluxes of CO_2 wind speed readings at 12 m were used to estimate the U_{10} using the a neutral logarithmic wind profile with a roughness length of 0.001 m: $U_{10} = U_M\ (h_{ref}) * (ln\ (z_1/z_0)/ln(h_{ref}/z_0))$ (Oke, 1987; Howard & Clark, 2007). Where $U_M\ (h_{ref})$is a wind speed at the 12 m, z_1 is a 10 m height and z_0 is a roughness length (Howard & Clark, 2007).

3.2.1 NDIR sensor - laboratory tests

To avoid post-deployment CO_2 concentration correction such as pressure effects on sensor at different water depths, several different (horizontal and vertical) float-based housing designs were tested in laboratory. After the trial, these designs were tested on site for a period of approximately one month (Figure 23). Soon after trials (laboratory and field-based) were finalised the best option was selected. It was agreed that although both designs are suitable, horizontal set-up is more appropriate for fast-flow stream environment. Hence it was decided to select vertical design for the project installation. Regarding the hummocks and lawn-based installation, it was agreed that a different design needs to be considered that is of similar orientation, but more robust and durable.

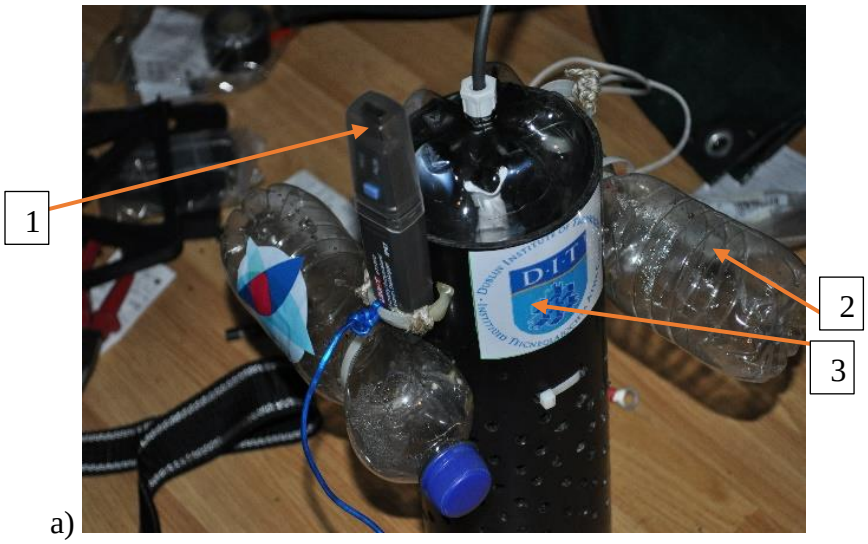

a)

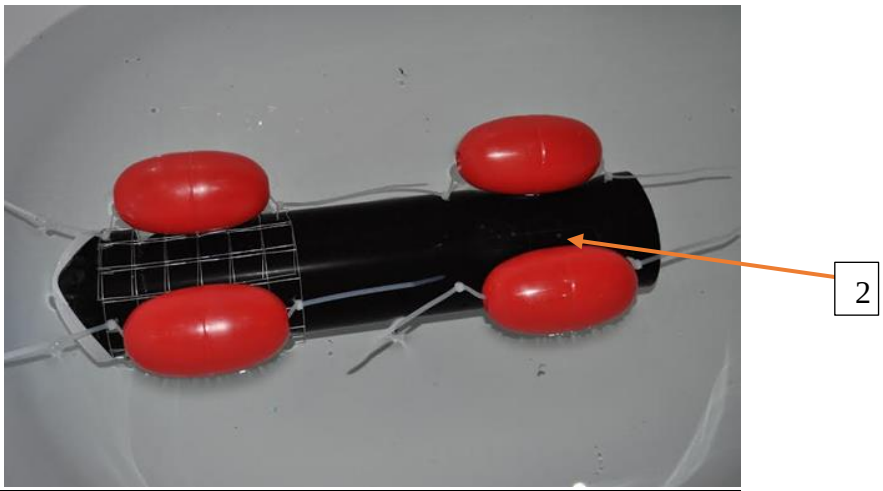

b)

c) 

d) 

Figure 23 *Sensor float housing prototypes: (a) Vertical (1 – pressure probe; 2 – floats; 3 – PVC pipe housing) and (b) Horizontal float housing prototypes – laboratory tests, (c) Vertical and (d) Horizontal float housing prototypes – field based trials.*

3.2.2 Pool-based CO_2 sensors

There were three (approximately 2 cm in diameter by 15 cm long) Vaisala GMM220 CARBOCAP NDIR sensors that were pool-based (ST1-3). By design, these sensors were not suitable to be used in water and needed to be modified. Modification consisted of application of protective expanded polytetrafluoroethylene (PTFE) tube sleeve that is highly permeable to CO_2 but impermeable to water (Figure 24). Applied PTFE sleeves were sealed using Plasti Dip rubberising compound and made impermeable to water at both the cable end and non-cable end. NDIR sensors then were secured inside perforated PVC pipes (Figure 24; Figure 25). The mesh was connected to bottom end of PVC pipes to restrict inflow of debris and therefore to protect PTFE sleeves from the potential damage.

a)

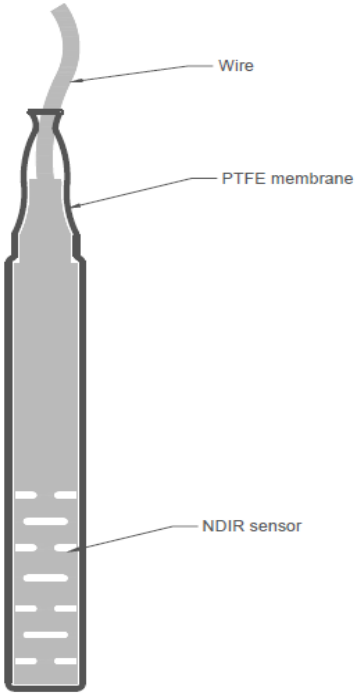

b)

Figure 24 *Pool-based float-housing apparatus for GMM220 sensor: a) detailed illustration of GMM220 sensor enclosed by PTFE sleeve, b) field application of vertical float-housing apparatus with GMM220 (ST1).*

Sensors were mounted vertically within water column and were maintained at a constant depth by a protective float- housing mechanism for periods of different length from the end of 2016 until September 2018. The aim was to capture CO_2 dynamics in all seasons: summer, autumn, winter and spring.

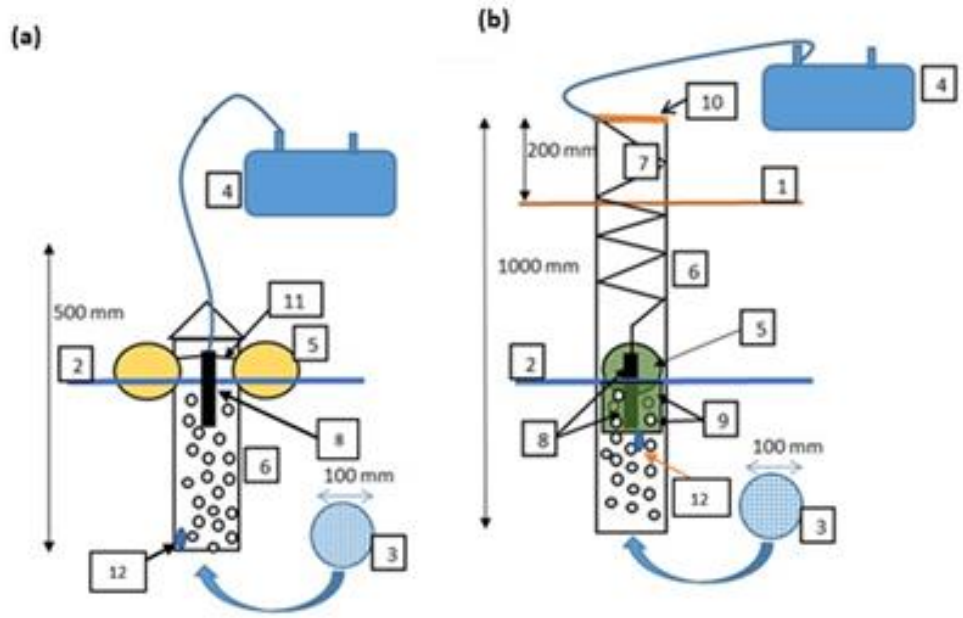

Figure 25 *NDIR module transmitter: component board, cable and a CO_2 probe for field installation (a) pool assembly & (b) peat zone assembly – components labelled* ***1-12*** *(**1** Land surface, **2** Water surface, **3** Mesh-net, **4** Transmitter, data-logger, switch & timer, **5** Float assembly, **6** Perforated PVC pipe, **7** Coiled cable & power line, **8** NDIR sensor, **9** Inner perforated protective housing, **10** Sealing lid, **11** Sensor fastening cables, **12** Water temperature probe).*

3.2.3 Soil water-based CO_2 sensors

There were three Vaisala GMM220 CARBOCAP NDIR sensors that were pool bank-based (hummock conditioned-HumST1 & HumST3 and lawn conditioned-LawnST2). These sensors were analogously modified, enclosed by PTFE sleeves and sealed using Plasti Dip rubberising compound (Figure 26). Sensors then were secured inside perforated PVC pipes (1-metre-long) (Figure 26). Floats were secured at the cable ends of sensors. Plastic coils were aligned with cables and extended down the length of cables. This alteration allowed sensors to move up and down freely in case water table conditions would change inside the wells (Figure 26).

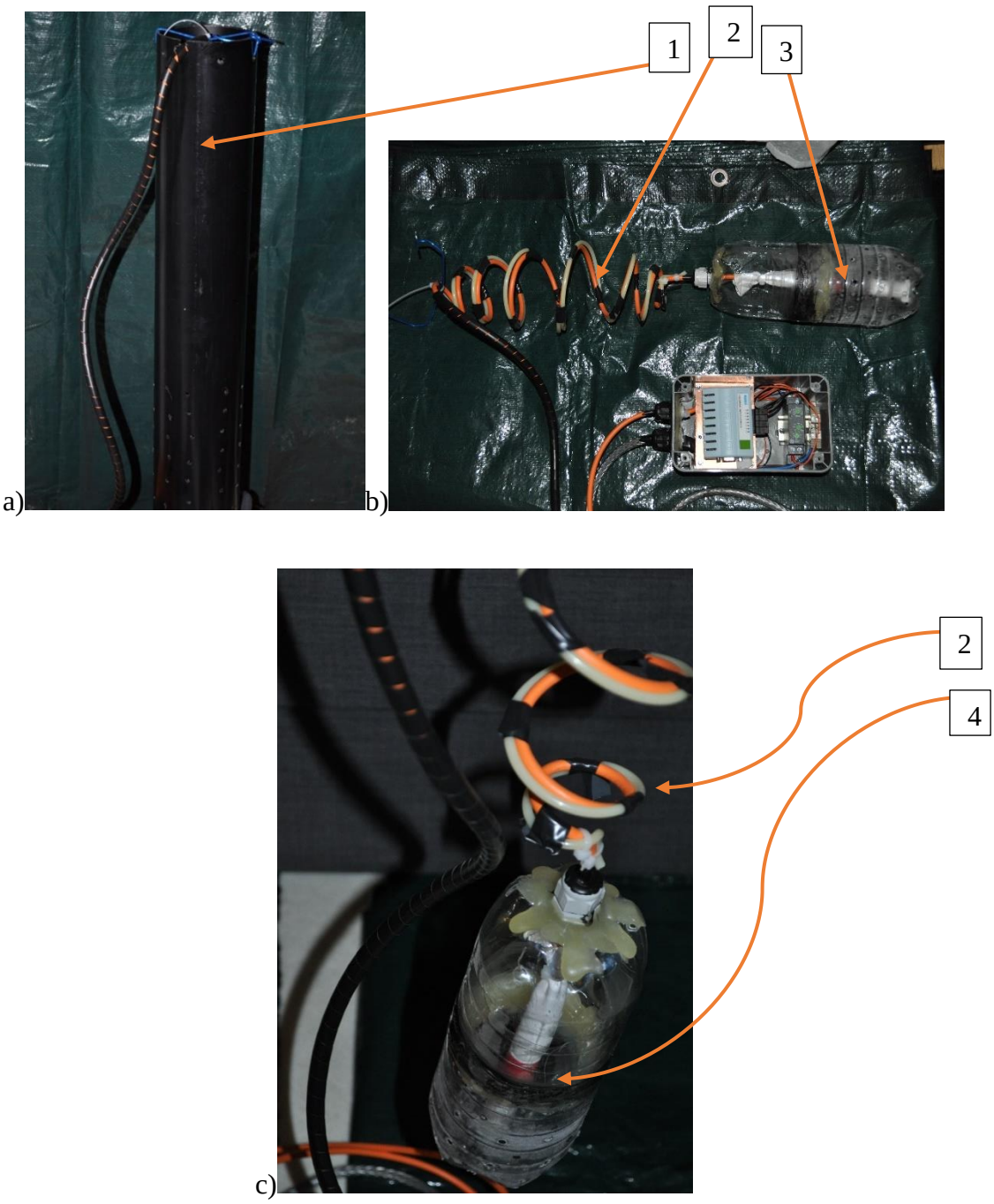

Figure 26 *Peat soil based float-housing apparatus: a) 1-metre-long PVC pipe* ***(1)*** *with the sensor inside, b) Close-up look at the float-sensor set-up (****2*** *– coil;* ***3*** *-float) and the junction box containing: transmitter, data-logger and the timer, c) PTFE enclosed sensor* ***(4)*** *inside the float.*

Approximately 10 mm pore size mesh was connected at the bottom ends of PVC pipes to protect PTFE sleeves from potential damage. Approximately 0.8 m deep wells were excavated using the Edelman auger (Figure 27). PVC pipes were installed vertically (Figure 28). Sensors were left on site for same periods as pool-based sensors for future comparison of CO_2 concentrations on spatial basis (Figure 28).

a)  b) 

Figure 27 *Dip-well preparation on site: a) The auger set, b) Use of an Edelman auger on site.*

Figure 28 *Peat-based set-up: HumST1.*

3.2.4 CO_2 sensor calibration

All Vaisala sensors came pre-calibrated with certificates of calibration. According to manufacturer's certification, every sensor was reading with a small deviation of -0.034 to 0.002 % which is a permissible deviation according to supplier (Appendix A). The manufacturer was indicating that an error of greater than 20% requires attention. Sensors were calibrated in laboratory based on ambient conditions: humidity 34±5 % RH, temperature 23.5±1 ^{0}C and atmospheric pressure 1001±1 hPa. Positive deviation was observed for a calibration with standard reference gas of 0.000 % CO_2 and a negative deviation was observed for a gas with reference of 10.000 % CO_2. The sensor accuracy spot-checking was performed on all six sensors using GMK220 calibrator (Figure 29-30) specifically designed for GMP 220 series probes. It was agreed to perform spot checking using the reference gas: 5% CO_2 110 L calibration gas/ balancing gas N_2. The gas was selected based on manufacturer's recommendations. For that procedure gas should be used with CO_2 concentration within the measuring range of the probe. Probes were measuring up to maximum of 10%.

Procedure involved following steps: 1) the probe (item 1, Figure 29) to be tested had to be removed from PTFE tube, however, there was no requirement to connect the transmitter. When freed of PTFE, it was connected via cable to calibration unit (item 2, Figure 29). Probe was then placed into the chamber (step 2) (item 5, Figure 29) making sure that the sensor is completely inside the chamber. Calibrator was then connected to laptop (step 3) with the serial cable (item 8, Figure 29). Putty software was initiated, connection was set-up (step 4) and settings were checked. Serial line settings for data transfer were: 9600 baud, parity: 8/None, 1 stop bits. Two 12 V (total of 24 VDC/1A) batteries were connected in parallel (step 5) to supply power to connectors (items 9 and

10, Figure 29). When power supply was established the following message appeared in the Putty window on the laptop screen: 'GMT220A – Version: STD 4.08, Copyright: Vaisala Oyj, 1997-2000' (step 6). Calibrator was let to settle for ten minutes (step 7). Pressure regulator (giving about 1 bar pressure: S-Reg regulator) was adjusted to the reference gas and then the siphon was connected to link gas and the calibrator (step 8). In step 9, the flow rate was adjusted to 0.6 l/min with a screwdriver (item 4, Figure 29). The chamber was flashed with gas for five minutes. In step 10, the ambient barometric pressure value was inputted by typing the following command: >MF_PRESSURE 1028 <cr>. The ambient temperature was inputted by typing the following command: >MF_TEMP 230 <cr> (step 11).

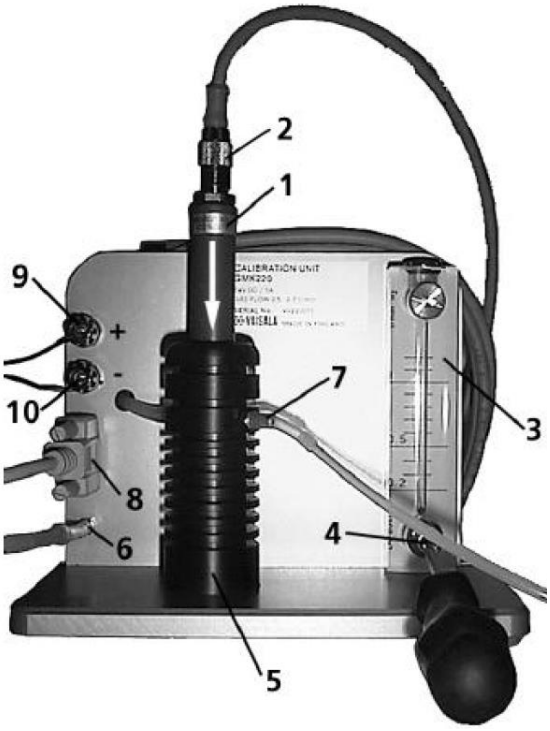

Figure 29 *GMK220 calibrator: 1) probe to be checked; 2) probe connector and the cable; 3) rotameter; 4) flow adjustment screw; 5) chamber (including o-ring, 18.3×2.4 NBR 70 ShA0); 6) gas inlet; 7) gas outlet; 8) serial cable that connects unit with the PC; 9) 24 V supply voltage in (+); 10) ground (-). Adapted from Vaisala (2006).*

In step 12, the following command was typed: >MF_MODE 4 <cr> to list concentrations of CO_2. To stop the output ESC-button was used. The difference between the average reading and actual concentration of reference gas was calculated (Table 1). The gas flow was stopped, and the probe was disconnected upon completion (Figure 30). Results of this spot checking were indicative that probes were operating correctly. Sensors were reading with deviation below the critical maximum of 20 % with a range of -0.04 to 0.11 %. Comparison among individual sensors showed consistent differences, these were corrected by applying a sensor-specific linear correction factor (Johnson *et al*., 2010).

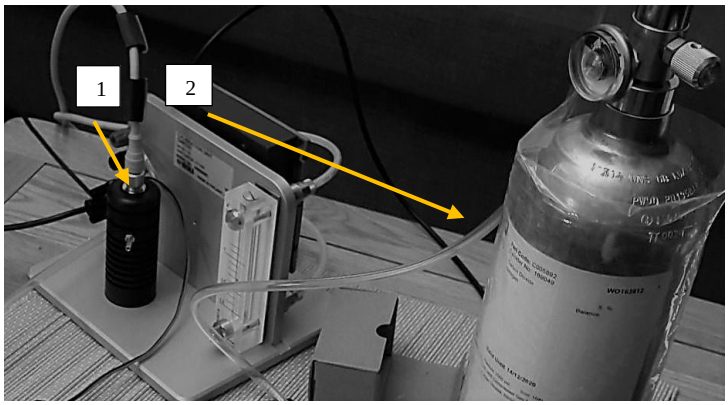

Figure 30 *Showing the calibration procedure: (1) GMK220 calibrator and (2) the reference gas.*

Table 1 *Calibration results: sensors from conditions: HumST1, LawnST2, HumST3 and ST1-3.*

Sensor	HumST1	ST1	LawnST2	ST2	HumST3	ST3
CO_2/%	5.08	5.10	5.13	4.98	5.06	5.01
	5.09	5.09	5.12	4.97	5.07	5.02
	5.10	5.08	5.11	4.96	5.05	5.03
	5.09	5.08	5.10	4.96	5.06	5.02
	5.08	5.07	5.11	4.96	5.07	5.01
	5.11	5.06	5.12	4.95	5.08	5.00
	5.12	5.05	5.12	4.94	5.09	5.01
	5.13	5.06	5.12	4.95	5.10	5.02
	5.12	5.07	5.11	4.96	5.11	5.03
	5.10	5.08	5.10	4.97	5.10	5.04
Average/%	5.10	5.07	5.11	4.96	5.08	5.02
Deviation/%	0.10	0.07	0.11	-0.04	0.08	0.02

3.2.5 ST1 sensor laboratory trial

When ST1 sensor was isolated applying PTFE tube and leak-proofed using PlastiDip rubberizing material (Figure 31) it was tested in aqueous media under controlled laboratory conditions for a period of two weeks before deployment in field environment. CO_2 measuring capabilities of this sensor were tested in simulated freshwater media and freshwater media with intermittently added gaseous CO_2 from the 'Soda Stream' CO_2 cylinder (425 g CO_2) (Figure 31). Sensor was placed almost vertically in the water (water

depth - constant; <10 cm depth) and set to record every minute (7^{th} - 18^{th} of September 2016). From 18^{th} - 22^{nd} of September the sensor was not recording and was just kept in water media to verify that there are no leaks. After laboratory trial, data were collected, analysed and CO_2 concentrations were averaged per day (Laboratory based trial and preliminary monitoring exercise). Concentrations of CO_2 were adjusted according to air pressure where pressure values were taken from Casement Station data (MET eireann, 2019) and per water temperature, that was recorded in the tank using handheld thermometer (TRIXIE) (Trixie, 2019).

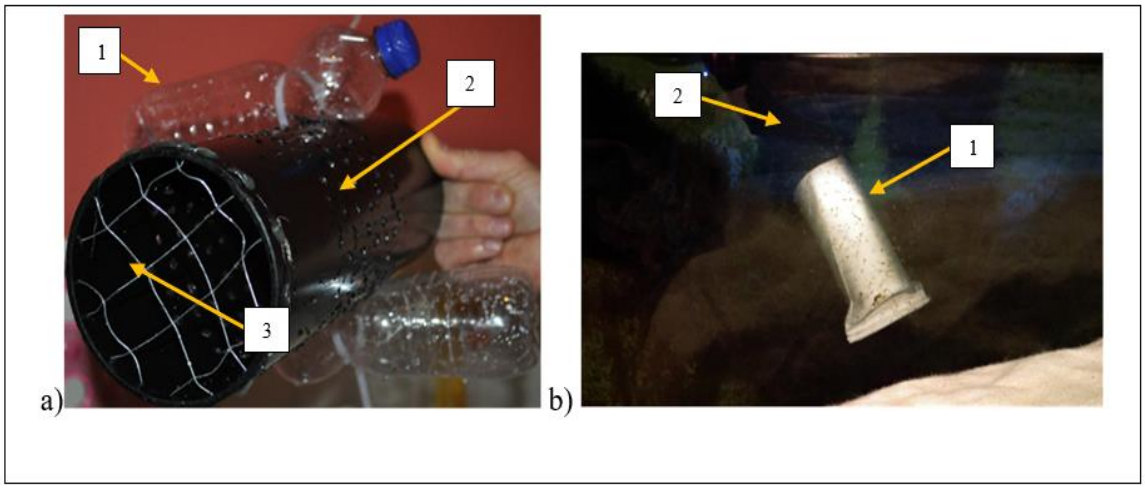

Figure 31 *Preparation to field-based installation: a) Engineering and testing of vertical housing set-up for carbon dioxide probe housing (**1** – floats; **2**- PVC pipe housing; **3** – protective mesh); b) Testing of sensor in an aqueous environment with controlled flow injection of CO_2 gas from the 'Soda Stream' cylinder (**1** – PTFE tube; **2** – NDIR sensor).*

3.2.6 ST1 sensor – preliminary monitoring exercise

Preliminary monitoring exercise was conducted to test reliability and suitability of pool-based CO_2 housing. Air pressure and temperature data were taken from the Casement station (Figure 32). CO_2 probe was conditioned in pool (ST1) and left to measure for a period of three days. Sensor was reading for a period of nineteen minutes (every minute), then was resting for the same amount of time. The time relay was tested in this way. Power supply was known to perform differently under different moisture and temperature conditions; therefore, it was essential to test the set-up to determine the power consumption under different weather conditions.

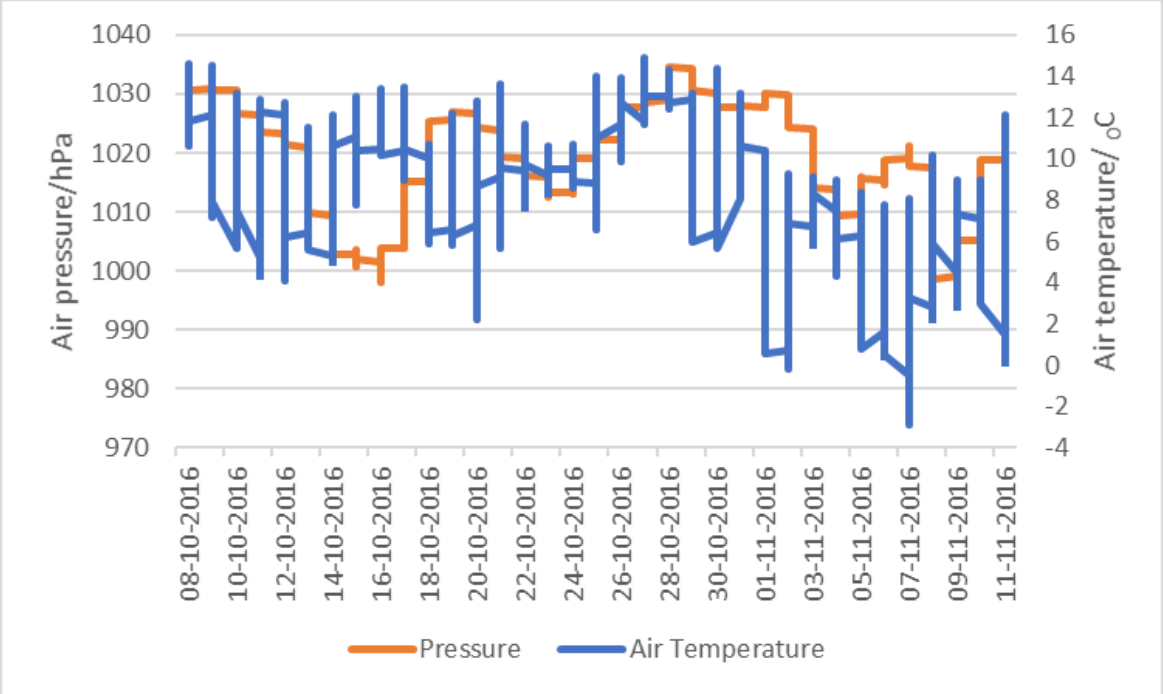

Figure 32 *Data taken from Casement Meteorological station – atmospheric pressure (hPa) and the temperature (^0C): 8th of October to 11th of November 2016.*

3.2.7 Hydrochemical monitoring

Hydrochemical parameters quantified included TOC, particulate organic carbon (POC), dissolved organic carbon (DOC), base cations (Ca, Mg, Na, K), chlorine and nutrients (nitrite, ammonia and phosphorus). The water was sampled on site by grab technique routinely. Plastic bottles (500 ml) were used to collect water. They were rinsed three times with deionised water and then three times with the water from the sampling point prior to collecting the final water sample for analysis. Samples were taken from the surface of the pools (0-10 cm) and from the surface of peat pore water inside wells. Samples of water were transported using the dark container. Cooling bag (at 5 ^{0}C) was used to store the samples while in transit. pH, conductivity, ions, and nutrients were measured either on site or immediately upon the arrival to laboratory (within 24 hours of sample collection). Organic carbon tests were either performed immediately when brought to laboratory, or frozen (-12 ^{0}C) for up to a maximum of three days and then analysed.

There are various approaches for measuring DOC. It could be measured either by combustion or wet oxidation; the former method is more accurate (Sharma *et al*., 2011). Using different methods, such as persulphate oxidation, UV irradiation and or combination of both methods DOC could be quantified (Sharma *et al.*, 2011). Prior to analysis, it is essential to filter the samples of water using 0.45 μm syringe filters or a membrane filter (Qassim *et al*., 2014). In this project water samples were filtered using syringe filters (Figure 33). Then, filtered samples could be analyses for DOC. For example, absorbance measurements (absorbance at 400 or Abs400, 465 or Abs465, and 665 nm or Abs665) could be taken for a basic colour reading (calorimetrically) (Qassim *et al*., 2014). In this project, DOC was quantified using Hach 1900 spectrophotometer (direct method 10173; Test 'N Tube^{TM} vials) at the wavelengths of 430 and 598 nm

(Figure 34) (Hach, 2015). To verify accuracy of method, TOC standard solution was prepared (100 mg/L), exposed to digestion and the resultant sample was then read using Hach instrument along with other samples of water from study sites.

Figure 33 *Syringe with filter - 0.45 µm pore size used for separation of DOC from TOC.*

a) 

b) 

c) 

Figure 34 *Showing the method 10173 followed to quantify DOC/TOC in pool and peat water soil (ST1-3; HumST1, LawnST2, HumST3): a) preparation of Test 'N TubeTM vials for digestion, b) DBR 200 heating block used to incubate test vials with the samples of water, c) DR 1900 Hach spectrophotometer used for quantification of DOC/TOC.*

Apart from quantifying DOC, it's molecular structure could be predicted. Molecular structure provides clues regarding the parent material. Processes of organic matter formation could be also established using molecular structure of DOC. Absorbance to

carbon ratio or a specific absorbance could be gathered by measuring both Abs400 and DOC (Qassim *et al*., 2014). By measuring Abs465 and Abs665, the pH dependent E4/E6 ratio could be determined for all samples, such ratio can be used to measure relative proportions of fulvic acid to humic acid in the DOC and that could indicate upon the degree of humification of samples (Thurman, 1985; Qassim *et al.*, 2014). On another hand, UV-VIS absorbance (350 nm) of DOC could be also measured to quantify DOC ($DOC = 0.905 \times Abs350$), infer aromaticity (254 nm or $SUVA_{254}$) and the molecular weight using dimensionless spectral slope ratio (S_R) (Ruhala & Zarnetske, 2017). To infer aromaticity, Abs254 (only the electron structures associated with aromatic carbon molecules absorb energy at this wavelength) has to be divided by the DOC concentration of the sample ($SUVA_{254} = \frac{Abs254}{DOC\ concentration}$) (Ruhala & Zarnetske, 2017). To predict the molecular weight of DOC, the S_R of the slope of the 275-295 nm ($S_{275–295}$) absorbance spectra has to be divided by the slope of the 350-400 nm ($S_{350–400}$) absorbance spectra ($S_R = \frac{S275nm-295nm}{S350nm-400nm}$)(Ruhala & Zarnetske, 2017). Such slope ratio exhibits a negative correlation with molecular weight (Ruhala & Zarnetske, 2017). SUVA method was used in this project to infer aromaticity of DOC from the water samples. Concentration of DOC was measured using HACH DR 1900 spectrophotometer and UV-VIS absorbance was measured using the UV-VIS spectroscopy method.

According to literature, a small portion (1%) of DOM (dissolved organic matter) can absorb and re-emit light and that specific excitation and emission wavelengths at which fluorescence occurs is dependent on concentration, chemical structure and composition of the substance (Cory *et al.*, 2011). Therefore, fluorescence spectroscopy can be also used to study, infer some properties and measure DOC concentration in the solution. This

method is based on the measurement of DOM in parts per billion (ppb) quinine sulphate equivalents (QSE), using a fluorometer (ppb QSE = $(V_{sig}-V_{CW}) \times SF$)) (Saraceno *et al*., 2009). In this equation, V_{sig} is the output voltage for the sample, V_{CW} is the output voltage for clean water, and SF is an instrument specific scaling factor (Saraceno *et al*., 2009). The potential source of the DOM could be assessed by calculating the fluorescence index (FI) value (FI $=\frac{470nm\ emission\ intensity}{520nm\ emission\ intensity}$) (Fellman *et al*., 2010). Microbial (autochthonous) sources of DOM are associated with high FI values (approximately 1.8) and the terrestrial (allochthonous) sources are associated with the low FI values (about 1.2) (McKnight *et al*., 2001). Additionally, DOC composition in terms of molecular groupings, functions and origin could be assessed using the three-dimensional excitation emission matrices (EEMs) (Ruhala & Zarnetske, 2017). They are produced using the multiple excitation wavelengths and by measuring emission intensities across a range of wavelengths (Cory *et al*., 2011). Therefore, fluorescence spectroscopy could be applied to determine the optical properties of DOM such as protein content, aromatic component, humification status, and the redox index (Bieroza & Heathwaite, 2016).

Other species of carbon were quantified using direct methods, for instance TOC was measured using the HACH DR 1900 spectrophotometer (midrange method). POC could be in theory and practice determined indirectly by loss-on-ignition method (Billett *et al*., 2012). If this method is to be used, the sample needs to be firstly filtered by using the 0.7 µm Whatman GF/F glass micro-fibre filters, then the filtrate should be dried at 105 ^{o}C for 24 hours, and then ignited at 375 ^{o}C for the sixteen hours (Billett *et al*., 2012). POC then could be calculated using a regression equation for non-calcareous soils as per Dawson *et al*. (2002). However, in this project, POC was calculated by using the formula: TOC

mgl^{-1}-DOC mgl^{-1} as per Fiedler *et al.* (2008). Nutrients (nitrite, ammonia and phosphorus) were measured using portable HACH SL 1000 (Figure 35). HACH SL 1000 was also used to quantified total chlorine. Alkalinity (total: WT2002; range: 0-2400 ppm) was measured using the Gran titration method. Base cations (Na, K, Mg, Ca) were measured using inductively coupled plasma mass spectrometry technique (ICP) (Figure 36;Figure 37) (Andersson *et al*., 2000; Chow *et al*., 2005; Dinsmore *et al*., 2011).

Figure 35 *SL 1000 HACH portable spectrophotometer used to quantify nitrite, total chlorine, ammonia and phosphorus.*

Figure 36 *Figure Inductively Coupled Plasma (Varian Liberty 150 ICP-OES) instrument.*

Figure 37 *Row of filtered samples and standards used as parts of ICP analysis.*

3.2.8 Other physical and meteorological parameters

3.2.8.1 Pool water/ peat soil pore water pH & conductivity

There are various methods available for measuring water pH using different types of analytical techniques and devices like electrochemical pH sensors (pH electrodes based on redox reactions; ion-selective electrodes) and optical pH sensors (Orellana *et al*., 2011). In this study, pH of peatland water was measured using three different, pre-calibrated ion-selective pH electrodes (general purpose) with the pH and temperature data logger ((1) EUTECH pH 700, (2) EUTECH pH1 50 and (3) EUTECH-NALCO PC 450) (Figure 38) (RMS, 2020). The field, portable EUTECH pH 150 instrument and EUTECH-NALCO PC450 both had a clear epoxy-bodied pH electrode (length – 150 mm, diameter – 12 mm) with ability to measure entire pH range from -2 to 16 pH units at -10 to 110 ^{o}C (resolution 0.01 and the accuracy ±0.01) (RMS, 2020). This electrode was double junction type electrode. The desktop EUTECH pH 700 had a clear epoxy-bodied electrode with ability to measure pH in range from -1.99 to 16 pH units, had resolution of 0.01 and the accuracy of ± 0.002 (Helago, 2016). These electrodes detect pH by measuring voltage. This is possible because measuring and reference electrodes are completing a circuit through water sample via a permeable porous junction built in the glass wall (Orellana *et al*., 2011). The accuracy of electrodes is highly dependent on external recalibration procedure using the standard solutions of known pH (Orellana *et al*., 2011). The soil pH was measured as part of the peat soil evaluation study based on methods of Riley (1986). To ensure validity and accuracy of results when performing pH measurements, prior to each use electrodes were calibrated with standard solutions: pH 4, 7 and 10.

a)  b) 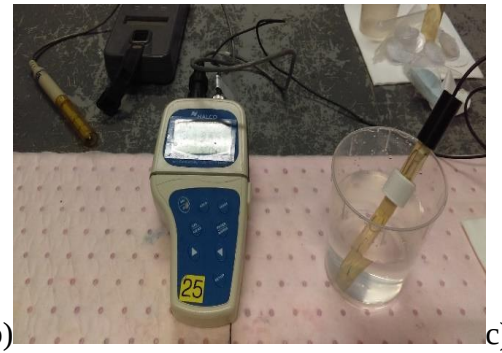 c)

Figure 38 *Range of pH meters used in the project: a) EUTECH pH 150 – portable pH meter; b) EUTECH-NALCO PC 450 – portable pH meter; c) Desktop - EUTECH pH 700.*

Water electrical conductivity was measured in laboratory using conductivity sensors (desktop JENWAY 4520 conductivity meter & NALCO dual probe - EUTECH-NALCO PC 450) (Figure 39) (Jenway, 2020). Desktop instrument had the capacity to measure conductivity, resistivity, salinity and the temperature (Jenway, 2020). Regarding conductivity measurements, the meter was reading ranges from 0 to 19.99S (highest range only with cell constant >5) and had accuracy of ±0.5%±2 digits (Jenway, 2020). It had a resolution of 0.01 µS/0.1 µS, 1 µS/0.01 ms, 0.1 ms and 0.01s (last one only with cell constant >5) (Jenway, 2020). Portable dual probe was reading conductivity in range of 0-200 mS, had a resolution of 0.01 µS to 0.1 mS and a full-scale accuracy of ±1 % (RMS, 2020).

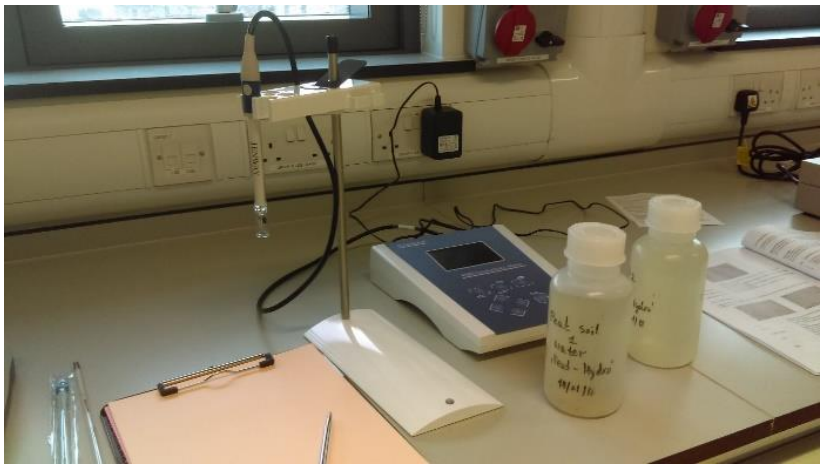

Figure 39 *Desktop conductivity meter - JENWAY 4520.*

3.2.8.2 Water, soil, air temperatures, air pressure, relative humidity & the precipitation

Soil, air and water temperatures were measured continuously *in-situ* using HOBO temperature recorders. UT330CUSB data recorder was used to measure humidity. Omega-RH23 pressure probe was used to record air pressure. HOBO sensors had the time stamp resolution of one second and the time accuracy of ± 1 minute per month at 25°C (Onset computer corporation, 2005-2011). The temperature accuracy of HOBO logger was ±0.54°C from 0° to 50°C, resolution was 0.10°C at 25°C, drift was less than 0.1°C/year and response time: airflow of 1 m/s (2.2 mph): 10 minutes, typical to 90% as per specification (Onset computer corporation, 2005-2011). To verify accuracy of HOBO probes, water temperature readings were correlated (Person correlation). It was established that there was a strong correlation between pool water temperature at ST1, ST2 (0.98), followed by peat pore water temperatures at HumST1 and LawnST2 (0.90)

(Figure 40).

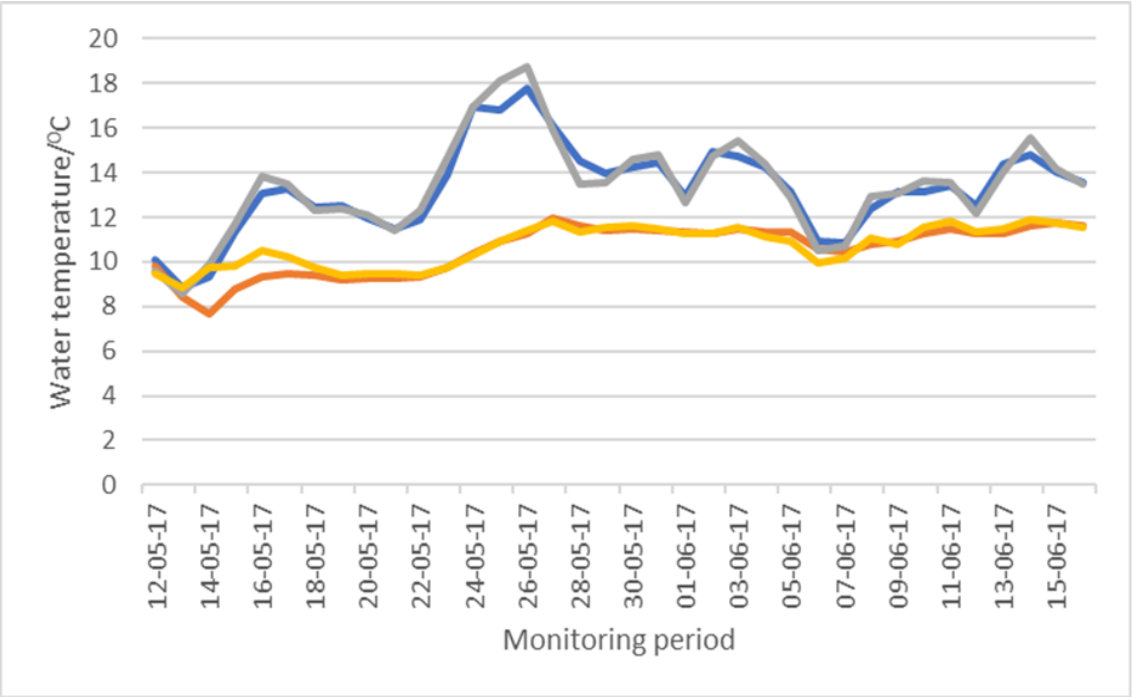

Figure 40 *showing water temperature data recorded continuously with an interval of every ten minutes (blue – ST1 and grey- ST2 lines and red – HumST1 and orange – LawnST2) from 12th of May to 16th of June 2017 using the HOBO temperature probe.*

Precipitation was continuously monitored *in situ* using the rain gauge (tipping bucket mechanism-15.24 cm aluminium bucket) (RG3-M) (Onset computer corporation, 2005-2011) (Figure 41). The rain gauge was able to record the maximum of 12.7 cm per hour as per specification (Onset Computer Corporation, 2005-2011). It had a calibration accuracy of ±1.0% (up to 2 cm per hour for the RG3-M) (Onset Computer Corporation, 2005-2011). It had a resolution of 0.2 mm (RG3-M) (Onset Computer Corporation, 2005-2011). The instrument required annual calibration: can be field calibrated or returned to factory for re-calibration (Onset Computer Corporation, 2005-2011). It was pre-

calibrated in laboratory before the use. Throughout the experimentation period there were two rain gauges available on site. Initially, events were recorded every minute, but from January 2018 onwards, events were recorded every hour for power saving reasons. To convert from tips (precipitation events) to mm of rainfall, each tip was multiplied by 0.2 as per manufacturers specification (Onset Computer Corporation, 2005-2011). Precipitation records from two rain gauges were converted to mm and then were arithmetically averaged using the arithmetic mean method approach: $p_m = \{(p_1 + p_2 + p_3 + \ldots\ldots\ldots + p_n)/n\}$ . . . . (Bhavani, 2013) (Figure 42). In this equation, p_m is the value of mean rainfall over the catchment area; p_1, p_2, p_3,……., p_n are the rainfall values at respective stations in a given period at 'n' number of stations (Bhavani, 2013).

a) 

b) 

Figure 41 *Tipping bucket mechanism RG3-M: a) Side view – rain gauge deployed in situ; b) Inside the rain gauge – data recording device (**1**) and all the wiring.*

a) 

b) 

Figure 42 *Rain gauges deployed in situ: a) Rain gauge #1 covering 'Peat-Hydro 2' territory; b) Rain gauge #2 covering 'Peat-Hydro 1&3'territory.*

3.2.9 Peatland soil characteristics and parameters

The hydraulic properties of peaty soils depend strongly on peatland morphology, e.g. degree of decomposition of plant litter and the vegetation community (Rezanezhad *et al*., 2016). Degree of decomposition and physical quality of the peat varies with depth, age, vegetation and drainage regime (Rezanezhad *et al*., 2016). To evaluate the degree of decomposition and the associated hydraulic properties of peaty soils in this study, peat cores were extracted using the Russian auger (Figure 43;Figure 44). Upon extraction, degree of humification was determined visually using ten classes of humification of the von Post Scale (Table 2) (Verry *et al*., 2011). In this scale, H1 refers to least decomposed

peat and H10 to most decomposed peat (Verry *et al*., 2011). The peatland soil characterisation analysis included assessment of rubbed fibre content (RF), soil density (Bd), moisture and aeration conditions. Materials used to collect soil samples for the peatland soil characterisation analysis included: Russian corer, flat-bladed knife, sealable bags and the marker pen (Figure 43). The approach consisted of analysis of peat soil samples taken from each of the three peat cores taken from ('Peat-Hydro' 1-3) located near the dip wells (Figure 44).

The rubbed fibre content was determined by taking the peat soil volume (35 cm^3) measured in a graduated syringe (Campos *et al*., 2011). The soil was then transferred to a sieve (100 mesh), washed with water until percolated water became clear, then all fibres were rubbed between fingers (thumb and the index finger) under running water until resulting liquid became colourless (Campos *et al*., 2011). At that stage the soil was transferred back inside the syringe and its volume was established. The rubbed fibre percentage value was calculated using the formula: (initial volume of soil/final volume of soil) *100 (Campos *et al*., 2011).

Peatland state, condition and health were evaluated by measuring bulk density. Bulk density affects water infiltration, soil porosity, available water capacity, plant nutrient availability, and soil productivity via activity of soil microorganisms. Bulk density depends on factors such as soil organic matter, soil texture, density of the mineral matter in the soil and the arrangement of the mineral matter in the soil. Bulk density increases with soil depth, because compaction increases, aggregation of soil and penetration of plant roots decreases. Bulk density defined as the weight of dry soil per unit of volume

expressed in g/cm^3. Changes in peatland soil integrity, can affect bulk density and expose soil to excessive erosion by water and wind. Equipment used in laboratory to aid the peatland characterisation analysis included: scale, glass plate and the microwave oven.

To determine bulk density samples of peatland soil were taken near the dip wells (station 1-3) using the Russian corer. The corer was inserted 0.7 metres down into peaty soil, then the core was extracted, corer was opened, peat sample was carefully removed avoiding the loss of soil. Excess soil was cut with the knife, intact core was laid on the plastic bag and carefully sealed and labelled. Cores were placed inside cooling bag and brought to laboratory. Upon arrival to laboratory, the cores were weighted. Empty plastic bag was weighted and then the sub-sample of soil was taken from each core. The sub-sample was cut from the lower section of core, that means that sub-sample was representative of the peat soil present at the level between 0.4-0.5 metres. Then each peat soil sub-sample was placed on the glass plate and weighted. Empty glass plate was also weighted. Every sub-sample on the plate was placed in the microwave and dried on the medium power of 450 W for four minutes. Then sub-samples were re-weighted and dried for four minutes once again. The cycles of drying were continued until the weight was no longer decreasing (3-4 cycles – each four minutes).

To calculate peat soil water content (h) and the peat soil bulk density (i), the following intermediate parameters were measured: (a) weight of the moist peat soil sample plus the plastic bag, (b) weight of the sample plastic bag, (c) weight of the glass clock plate, (d) weight of the glass clock plate plus the moist peat soil, (e) weight of the moist peat soil, (f) weight of dry peat soil and glass clock plate and (g) weight of dry peat soil (Table 3).

The weight of the moist peat soil was calculated using the formula: d-c. The weight of the dry peat soil was calculated using the formula: f-c. The peat soil water content was calculated using the formula: [(weight of moist peat soil-weight of oven dry peat soil)/(weight of oven dry peat soil)]. The bulk peat soil density was calculated using the formula: [(a-b)/(1+h)]/V; where V was the volume of the core calculated using the formula πr^2*h, where h is height. Peat moisture content and aeration extent was then calculated (j-l). Volumetric water content was calculated using the formula: h*i. Soil porosity was calculated using the formula: (1-(i/2.65))*100, where 2.65 is a default value used a rule of thumb based on the average bulk density of rock with no pore spaces (Campos *et al*., 2011). The soil water filled pore space parameter was calculated using the formula: (j/k)*100.

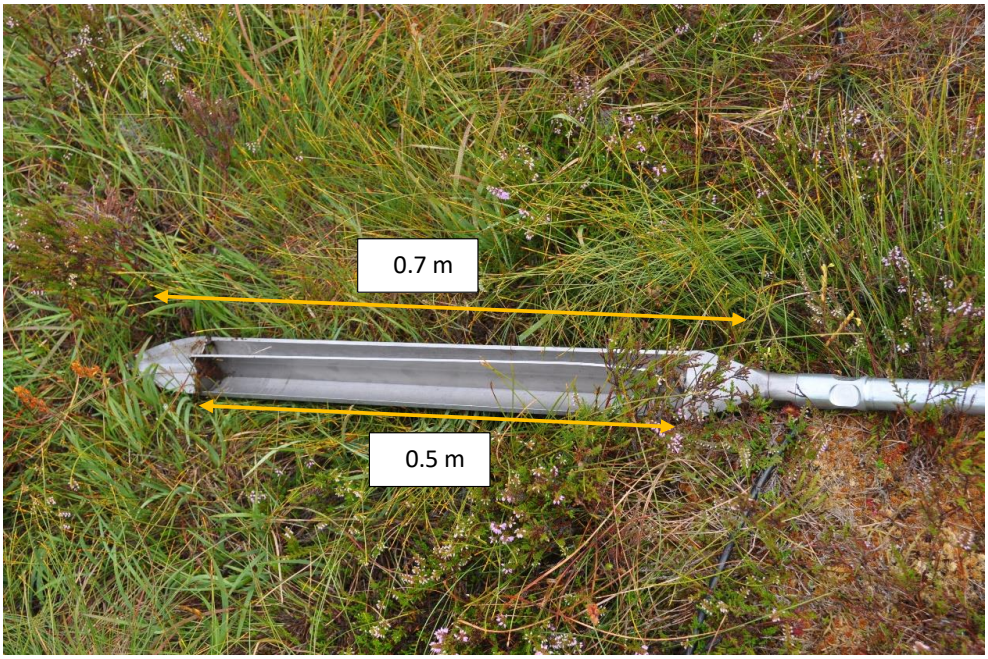

Figure 43 *Russian corer dimensions: external length (0.7 m) and the internal compartment length (0.5 m).*

a) 

b) 

c) 

d) 

Figure 44 *Showing cores extracted from a) HumST1 soil; b) & c) 'LawnST2 soil and d) HumST3 soil.*

Table 2 *von Post field evaluation. Adapted from Verry et al. (2011).*

von Post H Value	**Volume Passing through fingers (%)**	**Additional description of free water expressed to the second hand**
1	0	Expressed water is clear to almost clear and yellow brown in colour. Slowly open the second hand and observe colour as the water depth thins.
2	0	
3	0	Water is muddy brown and retained fibre is not mushy.

4	0	Very turbid, muddy water and retained fibre is somehow mushy.
4.5	1	Amorphous material primarily stays on outside of squeezed fingers.
5	2-10	Use the volume of amorphous material passed. As with H4 and H4.5, water at the edges of the amorphous material is very turbid and muddy.
5.5	11-25	
6	26-35	
6.5	36-45	
7	46-55	Water around the amorphous material is thick, soupy, and very dark.
7.5	56-65	Water around the amorphous material is thick, soupy, and very dark.

8	66-75	There is essentially no free water, it is all amorphous material.
9	76-95	There is no free water associated with the amorphous material.
10	95-100	

Table 3 *Sample table showing the parameters recorded and/ or calculated in the peat characterisation study.*

(a) Weight (moist sample plus the plastic bag)/g
(b) Weight (sample bag)/g
(c) Weight of glass clock plate/g
(d) Weight of glass plate & moist soil/g
(e) Weight of moist soil/g
(f) Weight of dry soil & glass plate/g
(g) Dry weight of soil/g
(h) Soil water content g/g
(i) Soil bulk density/ gcm^{-3}
(j) Volumetric water content/ gcm^{-3}
(k) Soil porosity/ %
(l) Soil water filled pore space/%

3.2.10 Post data collection – C++ programming

To get more accurate, significantly non-intermittent readings of CO_2 concentrations in all conditions (ST1-3; HumST1, LawnST2 & HumST3) measurements were recorded every minute from beginning of the project (autumn 2016) until winter 2017. From January 2018 due to harsh climatic conditions - extreme cloud cover, fogging and extreme snowfalls and due to absence of solar power, recording frequency was reduced to every five minutes. Anyhow, quantity of records streaming from all sensory devices was exceptionally large (CO_2 loggers, temperature loggers, pressure loggers, rainfall loggers). To ensure a more efficient alignment of all readings per time, date, condition and to correct CO_2 concentration according to variations in air pressure and water temperature it was decided to compile a simple programme using the C++ programming language. The purpose of this programming language is to express tasks using a code. The C++ programming language is based on idea of providing direct mapping of build-in operations and types to hardware to provide efficient memory use and efficient low-level operations (Stroustrup, 2013). The C++ is a general-purpose programming language that is designed to support a wide range of users (Stroustrup, 2013). The programme was written in a file using a text editor *Eclipse Neon* that had also a function of a compiler. The editor compiled the source file to produce a corresponding binary executable. Each C++ application that contains a complete code has a main function that is first loaded into memory and then transferred to CPU for execution. The purpose of this C++ programme produced for this project was to allow excess of all excel spreadsheets containing continuous data including air pressure, water temperatures from various settings, CO_2 data from all sensors and precipitation data. Then, using the programme it was also possible to extract data and then align it in a single file per date and time. Following on from that a set of commands was applied to firstly, remove the noise caused by senor

warming-up after turning on. According to sensor specifications, the warm-up time was 30 seconds. These first 30 seconds were removed to ensure they are not used in the calculations. Additionally, the programme was performing array of commands to compensate for variations in air pressure and temperature on CO_2 concentration. The following C++ programme that was used in the study was designed by a colleague from the Engineering Field (Radomski, 2018). It was used regularly, and little modifications and updates were applied to this C++ application to ensure its best performance.

3.2.11 Statistical analysis

Entire data sets in this work were tested to assess normality (Ghasemi & Zahediasl, 2012). The statistical tests such as correlation, regression, t-tests, and analysis of variance assume that the data follows a normal distribution (e.g. Gaussian distribution; Johann Karl Gauss, 1777–1855) (Ghasemi & Zahediasl, 2012). Quite often it is assumed that the populations from which the samples are taken are normally distributed (Ghasemi & Zahediasl, 2012). The concept of normality is critical when constructing reference intervals for variables (Ghasemi & Zahediasl, 2012). To be able to make assumptions about reality it is necessary to consider normality and treat this concept seriously (Ghasemi & Zahediasl, 2012). If the sample size is large enough (>30) noncompliance with the normality assumption should not cause major issues (Ghasemi & Zahediasl, 2012). Parametric procedures could be applied (analysis of variance) even when the data are not normally distributed (Ghasemi & Zahediasl, 2012). The concept of true normality is not completely real, but it is possible to visually illustrate it using normality plots (e.g. Quantile-Quantile or Q-Q plots, boxplots, etc.), or by applying significance tests (e.g. compare the sample distribution to a normal one) (Ghasemi & Zahediasl, 2012). The outcome of that analysis is to ascertain whether data show a serious deviation from

normality (Ghasemi & Zahediasl, 2012). Visual analysis of normality is usually unreliable and does not guarantee that the distribution is normal (Ghasemi & Zahediasl, 2012). To get more accurate representation of reality, the normality tests such as Kolmogorov-Smirnov (K-S) test, Lilliefors corrected K-S test, Shapiro-Wilk test, Anderson-Darling test, Cramer-von Mises test, D'Agostino skewness test, Anscombe-Glynn kurtosis test, D'Agostino-Pearson omnibus test, and the Jarque-Bera test could be used (Ghasemi & Zahediasl, 2012). These tests compare the scores in the sample to a normally distributed set of scores with the same mean and standard deviation (Ghasemi & Zahediasl, 2012). The null hypothesis (H_0) that is being tested: "sample distribution is normal" (Ghasemi & Zahediasl, 2012). If the test outcome is significant (probability <0.05), the distribution is not normal (Ghasemi & Zahediasl, 2012). Smaller sample sizes pass the normality tests more often and the large sample sizes are not - significant results would be derived even in the case of a small deviation from normality (Ghasemi & Zahediasl, 2012).

The K-S test is an empirical distribution function in which the theoretical cumulative distribution function of the test distribution is contrasted with the empirical distribution function of the data (Ghasemi & Zahediasl, 2012). Given **N** ordered data points $\mathbf{Y_1}$, $\mathbf{Y_2}$, ..., $\mathbf{Y_N}$, the empirical distribution function is defined as: EN=n(i)/N (Chakravarti, Laha, and Roy, 1967). In this formula, **n(i)** is the number of points less than $\mathbf{Y_i}$ and the $\mathbf{Y_i}$ are ordered from smallest to largest value (Chakravarti, Laha, and Roy, 1967). According to Chakravarti, Laha, and Roy (1967) this is a step function that increases by 1/N at the value of each ordered data point. The K-S test is defined by:

$$(1)\ D=\max_{1\le i\le N} = (F(Y_{(i)} - \frac{i-1}{N}, \frac{i}{N} - F\left(Y_{(i)}\right).$$

In this formula (1) **F** is the theoretical cumulative distribution of the distribution being tested which must be a continuous distribution and it must be fully specified, and **D** is a test statistic (Chakravarti, Laha, and Roy, 1967). The K-S test is a much used and can be conducted using SPSS or Matlab software's (Matlab, 2018; IBM Corp., 2019). This test (with Lilliefors correction) was used to check the normality of all data sets in this study using SPSS tool. The test is good to use for larger sets of data (>30) according to Ghasemi & Zahediasl (2012). Smaller data sets (<30) were tested for normality applying Shapiro-Wilk test (MathWorks, 1994-2020). The test statistic is defined as:

(2) $W = \frac{(\sum_{i=1}^{n} w_i \, X_i')^2}{\sum_{i=1}^{n}(X_i - \bar{X})^2}$ (Shapiro and Wilk, 1965).

In this formula, the summation is from 1 to n and **n** is the number of observations (Shapiro and Wilk, 1965). The array **X** contains the original data, **X'** are the ordered $\bar{X}$ data, is the sample mean of the data, and **w'**= (**w_1, w_2, ... , w_n**) or (3) $w' = MV^{-1}\,[(M'\,V^{-1})(V^{-1}\,M)]^{-1/2}$ (Shapiro and Wilk, 1965). In this formula (3), **M** denotes the expected values of standard normal order statistics for a sample of size **n** and **V** is the corresponding covariance matrix (Shapiro and Wilk, 1965). According to Shapiro and Wilk (1965), **W** may be thought of as the squared correlation coefficient between the ordered sample values (**X'**) and the **w_i**. In this formula (2) **w_i** are approximately proportional to the normal scores **M_i** (Shapiro and Wilk, 1965). In the formula (2) as per Shapiro and Wilk (1965) the **W** is a measure of the straightness of the normal probability plot, and small values indicate departures from normality. This test was conducted using SPSS software (IBM Corp., 2019). In addition to normality tests, Q-Q plots and boxplots were produced just to add a visualisation element to support test results. The main distinguishing feature of Q-Q plot is that the plot illustrates quantiles (values that split a data set into equal portions) of the data set instead of every individual score in the data

(Ghasemi & Zahediasl, 2012). In case of large sample sizes, it is more convenient to use Q-Q plots as they are easier to interpret (Ghasemi & Zahediasl, 2012). In case of boxplots, the median is shown as the horizontal line inside the box and the interquartile range (range between the 25^{th} and 75^{th} percentiles) is shown as the length of the box (Ghasemi & Zahediasl, 2012). The lines extending from the top and bottom of the box are called a whisker's and they represent the minimum and maximum values when they are within 1.5 times the interquartile range from either end of the box (Ghasemi & Zahediasl, 2012). In case where scores are greater 1.5 times the interquartile range are – outliers (out of the boxplot) and those greater than 3 times the interquartile range – extreme outliers (Ghasemi & Zahediasl, 2012). The normally distributed data would appear as a symmetric boxplot with the median line at the centre (approximately) of the box and with symmetric whisker's (Ghasemi & Zahediasl, 2012).

Following completion of normality assessment, descriptive statistics was carried out using complete time series to calculate seasonal averages of CO_2 using Microsoft Excel. Where an average value was quoted, the ± value referred to the standard error of the mean unless stated otherwise. All-time series such as CO_2 concentrations, temperatures, and pressure measurements were assessed for presence of autocorrelation (describes the correlation between values of variable in question at different points in time, as a function of the time difference (Hodzic & Kennedy, 2019). This is important as many parametric statistical procedures such as ANOVA, linear regression, etc. assume that the errors of the models used in the analysis are independent of one another (the errors are not correlated) (Cong & Brady, 2012). The presence of autocorrelation increases the variances of residuals and estimated coefficients, which reduces the model's efficiency (Cong & Brady, 2012). This is a common issue when using a single device to record a

parameter in time instead of using multiple devices at one point in time, this results in errors and any assumptions made regarding significance of statistical relationship could be inaccurate unless some corrective measures are implemented (Cong & Brady, 2012). In this study the time correlation analysis was performed as this produces a variety of useful information about periodicity and correlation strength among data samples of a given quantity (Hodzic & Kennedy, 2019). Autocorrelation (temporal) produce the measure of self-correlation of a data series (Angell & Korshover, 1981; Stojanova, 2012; Hodzic & Kennedy, 2019). The autocorrelation for a data time series x(t), t = 1, 2, …,N, such as relative temperature, pressure, wind speed or CO_2 concentrations is defined as: $R_{xx}(m)=\sum_t x(t)x(t-m),\ \ t=1,2,\dots,N$ (Hodzic & Kennedy, 2019). In this equation, **m** stands for the lag (delay), and m=1, 2,…,N-1 (Hodzic & Kennedy, 2019).

Performing autocorrelation test along is not the only way to identify an autocorrelation, there are other options such as visual examination of residuals (plotting average predicted model against actual model), applying a Durbin-Watson Statistic test ($DW_Y = \frac{\sum_{t=2}^{T}(e_t - e_{t-1})^2}{\sum_{t=1}^{T}(e_t)^2}$, where $e_t = \hat{Y}_t - Y_t$ is the residual associated with the observation Y_t at time t and T is the number of temporal units considered) and running the Ljung-Box Q test (Cong & Brady, 2012). In SPSS, the Ljung-Box Q test is integrated as a default test as part of autocorrelation method. The Ljung-Box Q test formula is: Q-Statistic=$T(T+2)\sum_{k=1}^{L}(\frac{p(k)^2}{T-k})$ (Stojanova, 2012). In this formula, **T** is the sample size, **L** is the number of autocorrelation lags, and **ρ(k)** is the sample autocorrelation at lag k (Stojanova, 2012). According to Stojanova (2012), the Ljung-Box Q-Statistic assesses the null hypothesis that a series of residuals exhibits no autocorrelation for a fixed number of lags **L**, against the alternative that some autocorrelation coefficient **ρ(k), k** = 1,...,**L**, is non-zero. To apply

this test correctly, it is essential to use correct range of lags, if **L** is too small, the test will not detect high order autocorrelation; if it is too large, the test will lose power when a significant correlation at one lag is washed out by insignificant correlations at other lags (Stojanova, 2012). As per Stojanova (2012) the default value of **L** = min[20,**T** −1] for the input lags.

When autocorrelations are being detected it is essential to remove them from time series. It is important to assess the trend that time series exhibit. Plotting autocorrelation graphs allows to see these behaviours. If there is a potential repeatable trend, it needs to be smoothed or reduced (prewhitened) by transforming data (differencing, logarithmic transformation, square root transformation, etc.). Differencing (subtracting previous observation from the current observation; 1,2,3 etc.) can help stabilize the mean of the time series by removing changes in the level of a time series, and so reducing or eliminating trend and or seasonality (Stojanova, 2012). There are other more rigorous methods to further adjust time series and reduce autocorrelation, for example, it is a common practice to apply ARIMA model (autoregressive integrated moving average model) (Probst *et al*., 2012). The ARIMA model have been used to deal with autocorrelation in different types of time series data (Stojanova, 2012). The model could be defined using the following formula: $\hat{Y}_t = \sum_{i=1}^{M} a_i Y_{t-i} + \sum_{i=1}^{N} b_i E_{t-i} + \varepsilon_t$ (Stojanova, 2012). In this formula, the first summation is the autoregressive part (AR), the second summation is the moving average part (MA), whereas the last part is an error term that is assumed to be a random variable sampled from a normal distribution (Stojanova, 2012). The AR consists of weighted past observations and the MA consists of weighted past estimation errors (e.g. difference between the actual value and the forecasted value in the previous observation) (Stojanova, 2012). According to Stojanova (2012) the ARIMA models

require lengthy time series and the impulse-response function specification aligns time lags (to achieve stationarity) of a response variable with those of a covariance. As was mentioned above, prior to applying this model, the data must be prewhitened. This measure is essential to remove spurious correlations based on temporal dependencies between adjacent values of the input time-series and removes these influences from the output time-series (Probst *et al.,* 2012). This can be achieved when input time-series and an output time-series are fitted using ARIMA model using SPSS (Probst *et al.,* 2012).

The outputs of ARIMA model are orders of the AR and MA components those are determined by the temporal lags, at which the partial autocorrelation function (PACF) and the autocorrelation functions (ACFs) are significant (Probst *et al.,* 2012). The difference between the ACF and PACF is that ACF is a representation of correlations between a time-series and the lagged versions of itself and the PACF is a representation of the correlations between values of a time-series against the values at lag removing the influences of the values between x_t and x_{t-L}(Probst *et al.,* 2012). As per Probst *et al.* (2012) after defining the ARIMA order p (order of AR), d (differencing-transforming a non-stationary time series into a stationary one), and q (MA parameters) and estimating the AR and MA parameters, the residuals of the estimated ARIMA model are checked for autocorrelation. In this study when differencing or natural log transformation along did not remove autocorrelation completely the ARIMA model was constructed. The model was constructed on case by case basis as per methods described in the article by Peixeiro (2019).

The cross-correlation analysis is another analysis performed in here. According to Hodzic & Kennedy (2019) this analysis can be used to compare two discrete time data series x(t) and y(t) such as relative temperature and CO_2 concentration and is defined as: $R_{xy}(m) = \sum_t x(t)y(t+m), m = -N+1, \ldots, -2, -1, 0, 1, 2, \ldots, N-1$. In this equation, m stands for the lag (delay) and t = 1, 2, …, N (Hodzic & Kennedy, 2019). These two formulas could be implemented in various ways depending on the software tool being used (SPSS, Matlab, R or Python) (Hodzic & Kennedy, 2019). In this study the software being used was SPSS (IBM Corp., 2019).

SPSS tool has only one cross-correlation forecasting function that only allows to perform a general cross-correlation test (IBM Corp., 2019). Matlab and R software's are more sophisticated as it is possible to perform a normalised cross-correlation. The most important feature of normalised cross-correlation analysis is that normalisation is being applied to produce an accurate estimate and determine statistical significance (Stojanova, 2012; MathWorks, 1994-2020). Additionally, the normalised cross-correlation allowed to establish the time delay between two variables (e.g. temperature and CO_2 concentrations). In the paper by Hodzic & Kennedy (2019), they approached this by locating the maximum value point for R_{xy} and locating the corresponding argument (time lag) between relative temperature and CO_2 concentration: $\tau_{delay} = \arg\max_m R_{xy}(m)$. It is also possible to calculate correlation coefficient to avoid the need of calculating cross-correlation point by point (Hodzic & Kennedy, 2019). The correlation coefficients (Spearman, Pearson and Kendal) are single numbers and they can be used as a simple measure of cross-correlation intensity between two variables (Stojanova, 2012; Hodzic & Kennedy, 2019). The syntax used to determine the time shift (lag) in this study using the Matlab was:

(1) TT2=lag(TT1)

(2) TT2=lag(TT1,n)

(3) TT2=lag(TT1,dt).

The first command above shifts (time lag) the data in each variable in TT1 forward in time by one-time step (MathWorks, 1994-2020). The command (2) shifts data by n time steps, e.g. if n is positive, then lag shifts the data forward in time and if n is negative, then lag shifts the data backward in time (MathWorks, 1994-2020). The third command shifts data by dt, a time interval (duration or a calendar duration) (MathWorks, 1994-2020). Complete time series of trends in CO_2 from different spatial settings (ST1-3 and HumST1, LawnST2 and HumST3) were compared using One-way ANOVA. Seasonal and diurnal trends were compared by selecting time series (similar) and date series (samples equally sized) and then applying One-way ANOVA. Precipitation values were compared with CO_2 and DOC levels using Pearson correlation test.

CHAPTER 4: RESULTS

4.1 Laboratory based trial and preliminary monitoring exercise

Laboratory trial results suggested that sensor was performing well under changing conditions (with and without addition of CO_2). Response time was minimal, and sensor was reacting almost immediately to changes in CO_2 (Figure 45). Preliminary monitoring exercise results suggested that vertical housing for probe was adequate for this type of environment. The time relay device used in this project was appropriate, and sensor had sufficient power supply throughout the entire monitoring period. Average concentration of CO_2 during this period was 0.47 mgl^{-1} (range: 0.31-0.65 mgl^{-1}) (Figure 46).

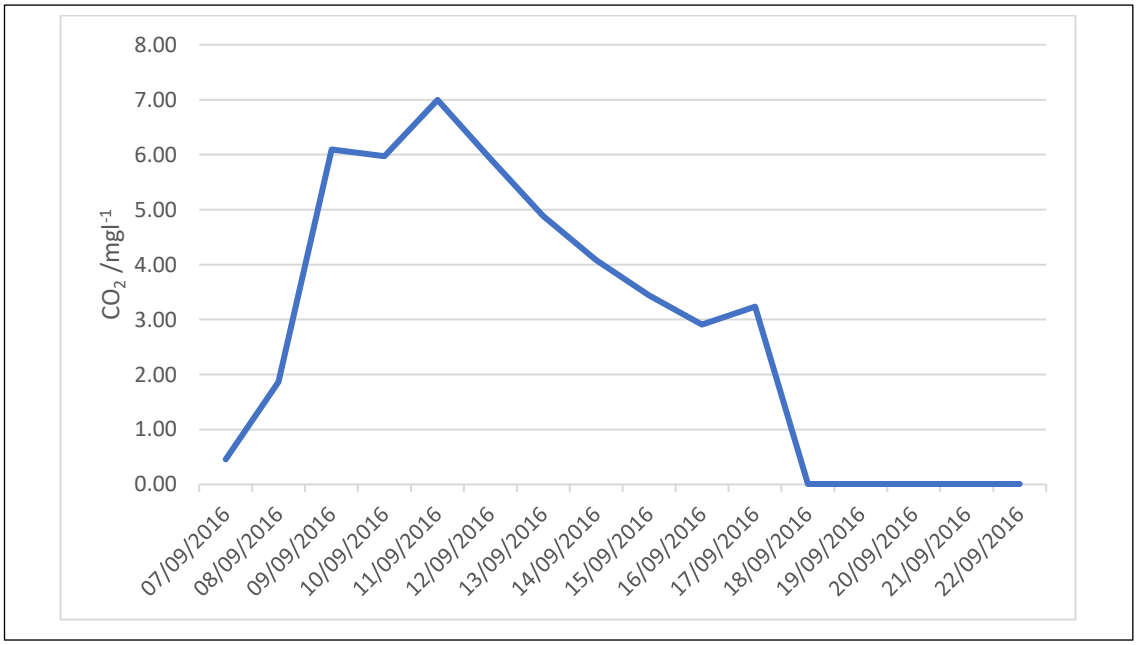

Figure 45 *Sensor #1 two weeks laboratory trial under exposure to 'Soda Stream' CO_2 – periodical controlled injection from 7th of September to 22nd of September 2016: CO_2 mgl^{-1}.*

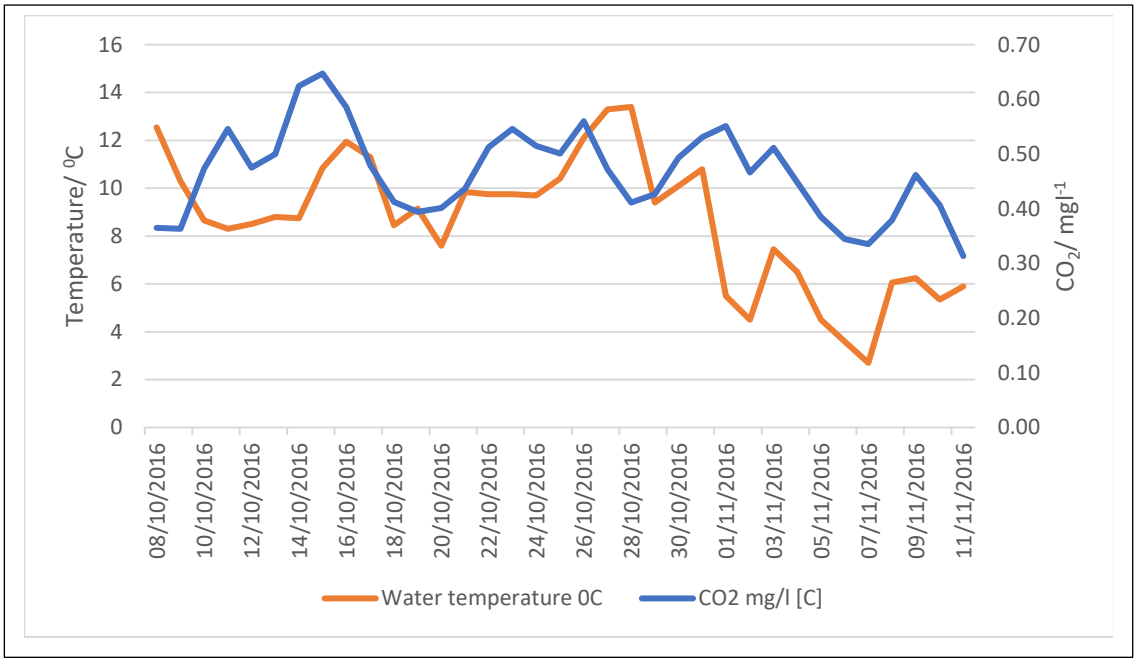

Figure 46 *Sensor #1 continuous field-based monitoring of CO_2 concentration in blanket peatland pool (ST1): October to November 2016.*

4.2 Hydrochemical analysis of water from hummocks, lawns and pools

The pH values in these waters were between 1- 4.92 in 2018 (Figure 47). Lowest and highest values were recorded in water samples collected in May (**Error! Reference source not found.**). Electrical conductivity ranged between 17.66-271.6 µS/cm (Figure 16). Lowest value was measured in July and highest in September. Nitrite level was in range 0-0.002 mgl^{-1} and total chlorine was between 0.02-0.04 mgl^{-1}. Ammonia was between 0-0.73 mgl^{-1} (greatest from July sample) and orthophosphate was between 0-4.72 mgl^{-1} (greatest from May sample). The following quantities of ions were found: calcium (average: 4.76 mgl^{-1}), potassium (0.50 mgl^{-1}), magnesium (0.40 mgl^{-1}) and

sodium (1.40 mgl^{-1}) in these peaty waters (Inductively coupled plasma mass spectrometry - ICP). Total organic carbon (TOC) levels were between 6-53 mgl^{-1} (greatest from September) (Figure 47).

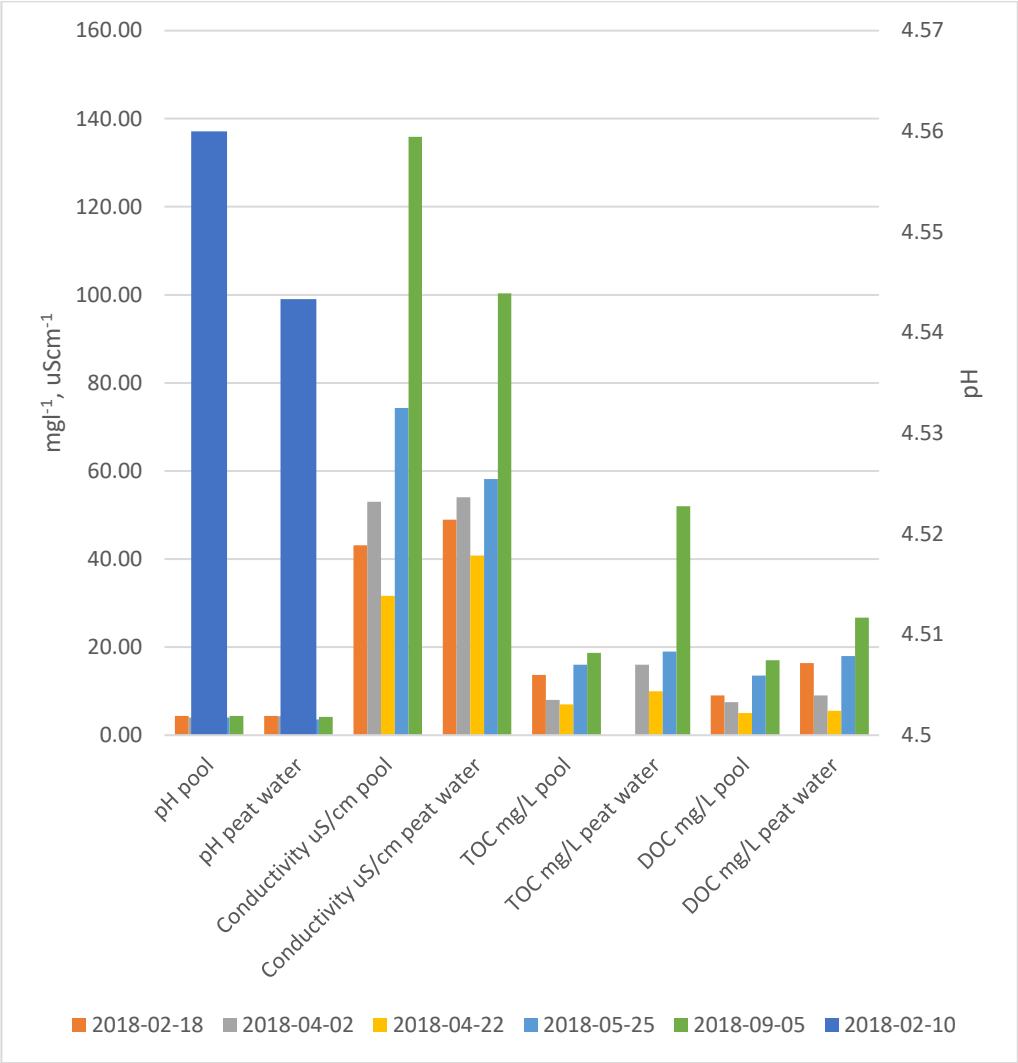

Figure 47 *Study area – hydrochemistry.*

4.3 Normality testing using SPSS

Out of 26 data sets (Table 4) analysed only three (PoolST1 WT/ ^{0}C, PoolST2 WT/ ^{0}C and HumST3 WT/ ^{0}C) did not pass normality tests. The PoolST1 WT/ ^{0}C normality assessment results were D(5) =0.473, $p<0.05$ and D(5)=0.552, $p<0.05$ (based on

Kolmogorov-Smirnov & Shapiro-Wilk tests; D – test statistic; 5 -degrees of freedom) (Table 4). The PoolST2 WT/ ^{0}C normality assessment results were D(5) =0.367, $p<0.05$ and D(5)=0.684, $p<0.05$ (based on Kolmogorov-Smirnov & Shapiro-Wilk tests) (Table 4). The HumST3 WT/ ^{0}C normality assessment results were D(5) =0.367, $p<0.05$ and D(5)=0.684, $p<0.05$ (based on Kolmogorov-Smirnov & Shapiro-Wilk tests) (Table 4). In all three cases, H_0 hypothesis was rejected as $p<0.05$. Contradicting result was obtained when analysing HumST1 CO_2 mg/l [C] data set (Table 4). When applying Kolmogorov-Smirnov test, the result was suggesting not normal distribution: D(5)=0.367, $p<0.05$, however when Shapiro-Wilk test was performed the result indicated the normal distribution: D(5)=0.816, $p>0.05$ (Table 4; Figure 48). This could be attributed to differences in sensitivity of tests, Shapiro-Wilk test is best to use for sample sizes in range from <50 and up to 2000 and Kolmogorov-Smirnov test performs at its best with sample sizes between 30-100 (HumST1 CO_2 mg/l [C] sample size was >100) (Ghasemi & Zahediasl, 2012). Additionally, normality plots (Figure 48) illustrate presence of outliers in data. Normality was observed among data points from remaining 22 data sets (Table 4; Figure 49). The H_0 hypothesis was not rejected ($p>0.05$) (Table 4).

Table 4 *Tests of Normality results performed using SPSS.*

Tests of Normality						
	Kolmogorov-Smirnov[a]			Shapiro-Wilk		
	Statistic	df	Sig.	Statistic	df	Sig.
ST1 CO_2 mg/l [C]	0.164	5	0.200*	0.986	5	0.965
ST2 CO_2 mg/l [C]	0.190	5	0.200*	0.947	5	0.719
ST3 CO_2 mg/l [C]	0.296	5	0.176	0.779	5	0.054
Pressure/ hPa	0.299	5	0.163	0.872	5	0.276
PoolST1 WT/^{0}C	0.473	5	0.001	0.552	5	0.000
PoolST2 WT/^{0}C	0.367	5	0.026	0.684	5	0.006
PoolST3 WT/^{0}C	0.237	5	0.200*	0.961	5	0.814
ST1 CO_2 $gm^{-2}d^{-1}$	0.245	5	0.200*	0.958	5	0.792
ST2 CO_2 $gm^{-2}d^{-1}$	0.332	5	0.075	0.808	5	0.094
ST3 CO_2 $gm^{-2}d^{-1}$	0.280	5	0.200*	0.778	5	0.053
HumST1 CO_2 mg/l [C]	0.367	5	0.026	0.816	5	0.109
LawnST2 CO_2 mg/l [C]	0.249	5	0.200*	0.920	5	0.529
HumST3 CO_2 mg/l [C]	0.151	5	0.200*	0.982	5	0.947
HumST1 WT/^{0}C	0.241	5	0.200*	0.821	5	0.119
LawnST2 WT/^{0}C	0.231	5	0.200*	0.881	5	0.314
HumST3 WT/^{0}C	0.367	5	0.026	0.684	5	0.006
Air temperature ^{0}C	0.345	5	0.053	0.863	5	0.238
Relative humidity/%	0.221	5	0.200*	0.902	5	0.421
Precipitation/mm	0.162	5	0.200*	0.981	5	0.942

pH pool	0.247	5	0.200*	0.829	5	0.136
pH peat water	0.307	5	0.139	0.797	5	0.077
Conductivity uS/cm pool	0.238	5	0.200*	0.866	5	0.252
Conductivity uS/cm peat water	0.340	5	0.060	0.810	5	0.097
DOC mg/L pool	0.214	5	0.200*	0.958	5	0.794
DOC mg/L peat water	0.170	5	0.200*	0.966	5	0.848
Soil temp/^{0}C	0.221	5	0.200*	0.902	5	0.421

*. This is a lower bound of the true significance.

a. Lilliefors Significance Correction

a)

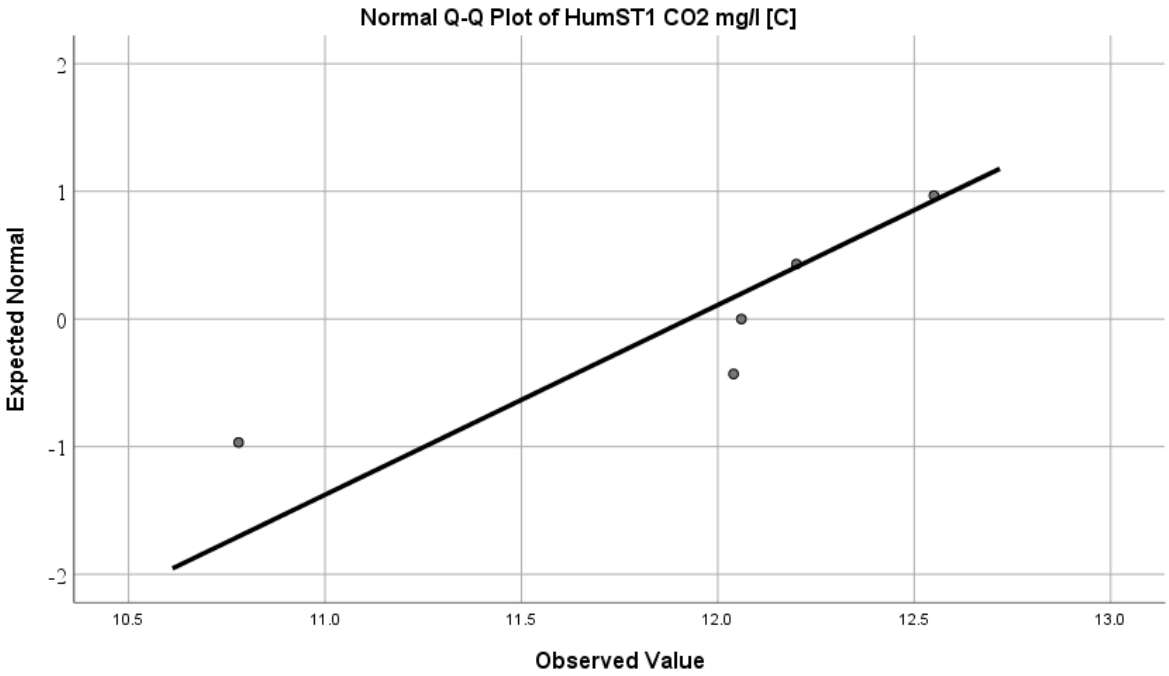

b)

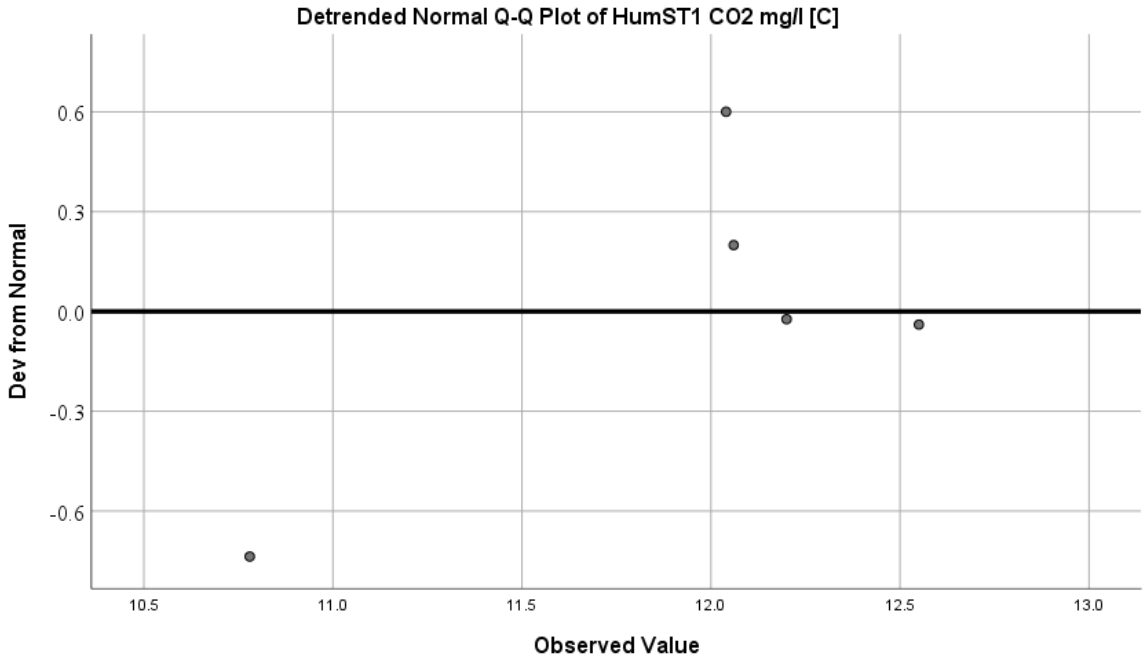

c)

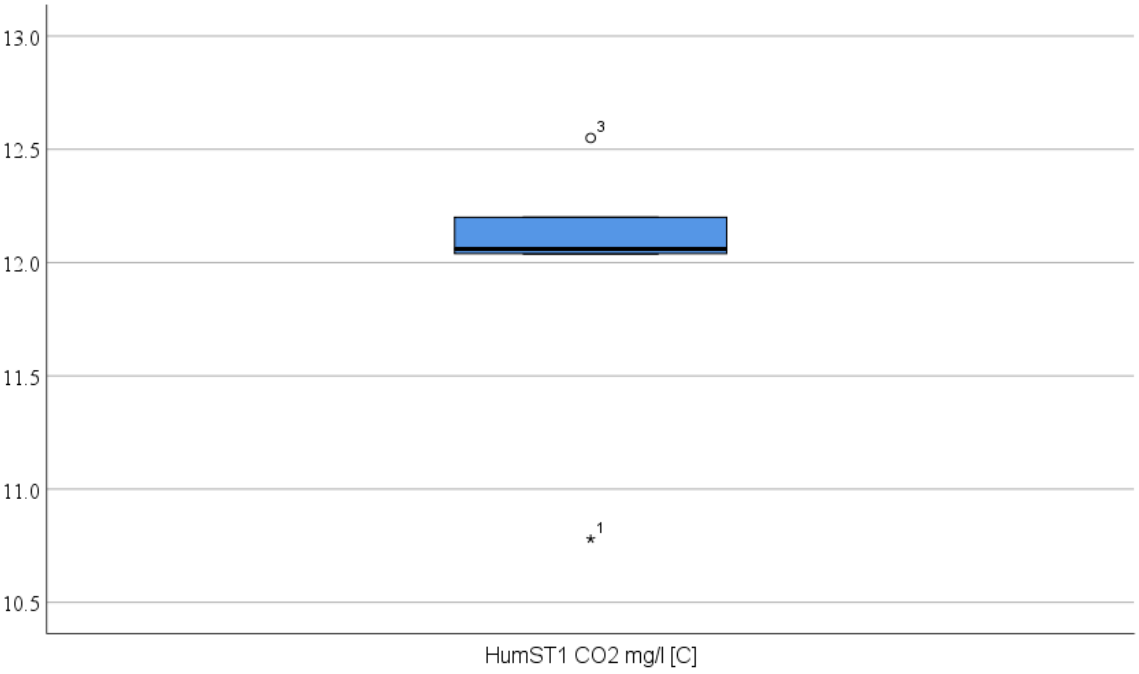

Figure 48 *Normality plots: a) Q-Q plot of normality; b) Detrended Q-Q plot – deviation from normality; c) boxplot of normality. HumST1 CO2 mgl-1 [C] data – entire data set.*

a)

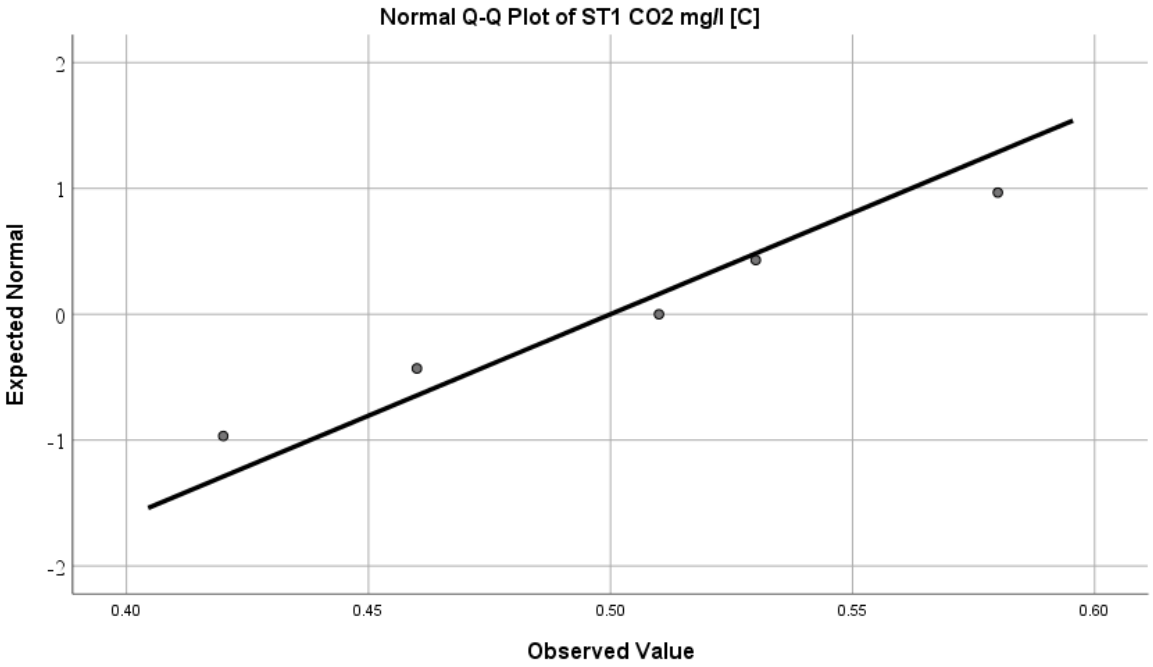
Normal Q-Q Plot of ST1 CO2 mg/l [C]
Expected Normal
2
1
0
-1
-2
0.40
0.45
0.50
0.55
0.60
Observed Value

b)

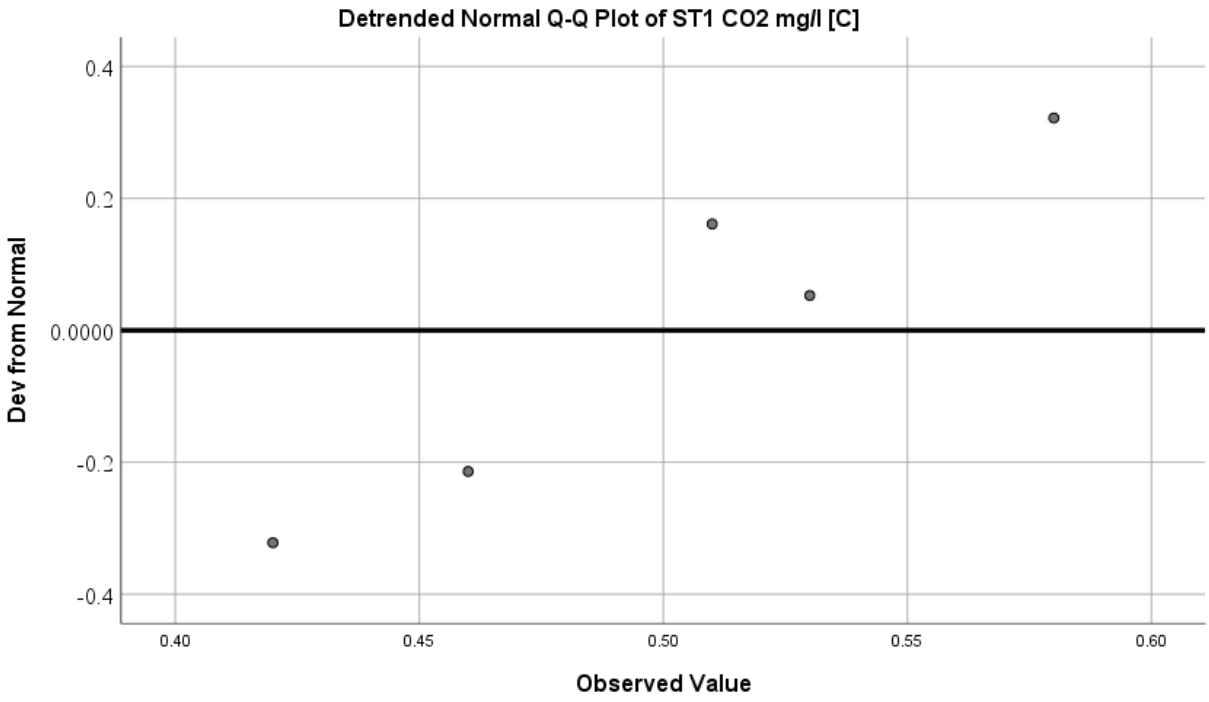
Detrended Normal Q-Q Plot of ST1 CO2 mg/l [C]
Dev from Normal
0.4
0.2
0.0000
-0.2
-0.4
0.40
0.45
0.50
0.55
0.60
Observed Value

c)

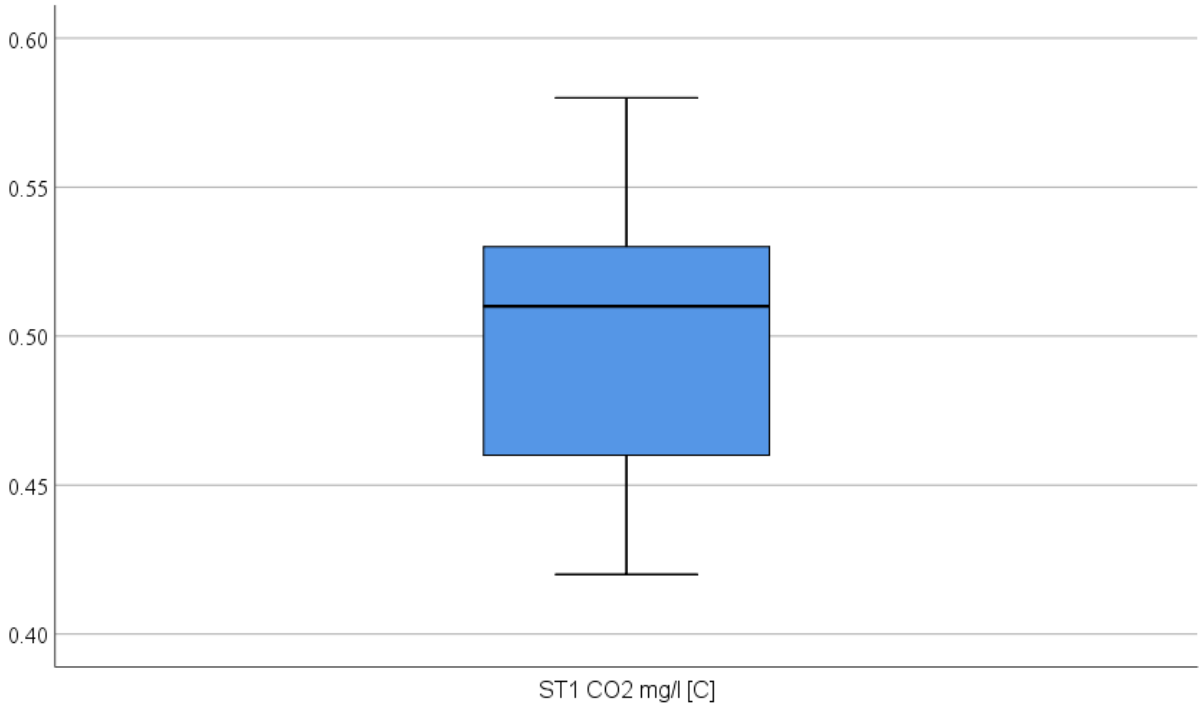

Figure 49 *Normality plots: a) Q-Q plot of normality; b) Detrended Q-Q plot – deviation from normality; c) boxplot of normality. ST1 CO2 mgl^{-1} [C] data – entire data set.*

4.4 Autocorrelation analysis

The Durbin Watson Statistic test was performed to establish the presence of Lag1 autocorrelations in time series (Table 5 The Results of Durbin Watson Statistic test. The time series from the project.). The results indicated that time series contained positive autocorrelation at Lag1 (Table 5). All Durbin Watson Statistic values were between 0-2 (Table 5). This was performed on non-transformed data (non-differenced data; data with no hidden internal or seasonal trends being removed). The general autocorrelation

(forecasting) analysis was performed to obtain autocorrelation graphs to get insights in terms of trends and time series behaviour. In every case time series autocorrelation plots were indicative that there was a trend and that data were not stationary (Figure 50).

Table 5 *The Results of Durbin Watson Statistic test. The time series from the project.*

Location	Type	Period	Durban Watson Statistic
ST1	CO_2 mgl^{-1}	1	0.477
ST1	WT ^0C	1	0.694
ST1	CO_2 mgl^{-1}	2	1.019
ST1	WT ^0C	2	0.409
ST1	CO_2 mgl^{-1}	3	0.661
ST1	WT ^0C	3	0.654
ST1	CO_2 mgl^{-1}	4	0.476
ST1	WT ^0C	4	0.079
ST1	CO_2 mgl^{-1}	5	0.127
ST1	WT ^0C	5	0.542
HumST1	CO_2 mgl^{-1}	1	0.078
HumST1	WT ^0C	1	0.855
HumST1	CO_2 mgl^{-1}	2	0.230
HumST1	WT ^0C	2	0.542
HumST1	CO_2 mgl^{-1}	3	0.822
HumST1	WT ^0C	3	0.657
HumST1	CO_2 mgl^{-1}	4	0.163
HumST1	WT ^0C	4	0.482
HumST1	CO_2 mgl^{-1}	5	0.172

HumST1	WT ^{0}C	5	0.067
ST2	CO_2 mgl^{-1}	1	0.252
ST2	WT ^{0}C	1	0.153
ST2	CO_2 mgl^{-1}	2	1.161
ST2	WT ^{0}C	2	0.803
ST2	CO_2 mgl^{-1}	3	0.115
ST2	WT ^{0}C	3	0.612
ST2	CO_2 mgl^{-1}	4	0.211
ST2	WT ^{0}C	4	0.153
ST3	CO_2 mgl^{-1}	1	1.262
ST3	WT ^{0}C	1	0.965
ST3	CO_2 mgl^{-1}	2	0.248
ST3	WT ^{0}C	2	0.322
LawnST2	CO_2 mgl^{-1}	1	0.274
LawnST2	WT ^{0}C	1	0.578
LawnST2	CO_2 mgl^{-1}	2	0.773
LawnST2	WT ^{0}C	2	1.105
LawnST2	CO_2 mgl^{-1}	3	0.170
LawnST2	WT ^{0}C	3	0.175
HumST3	CO_2 mgl^{-1}	1	0.487
HumST3	WT ^{0}C	1	0.942
HumST3	CO_2 mgl^{-1}	2	0.128
HumST3	WT ^{0}C	2	0.175
Kippure	Air T ^{0}C	all	0.757

Kippure	Soil T ^{0}C	all	0.333
Kippure	Air pressure hPA	all	0.398
Casement	Wind speed m/s	1	0.833
Casement	Wind speed m/s	2	1.337
Casement	Wind speed m/s	3	1.579
Casement	Wind speed m/s	4	0.863
Casement	Wind speed m/s	5	0.952
Casement	Wind speed m/s	6	0.888
ST1	CO_2 $gm^{-2}d^{-1}$	1	1.053
ST1	CO_2 $gm^{-2}d^{-1}$	2	1.523
ST1	CO_2 $gm^{-2}d^{-1}$	3	1.374
ST1	CO_2 $gm^{-2}d^{-1}$	4	0.675
ST1	CO_2 $gm^{-2}d^{-1}$	5	1.026
ST1	CO_2 $gm^{-2}d^{-1}$	6	1.339

a)

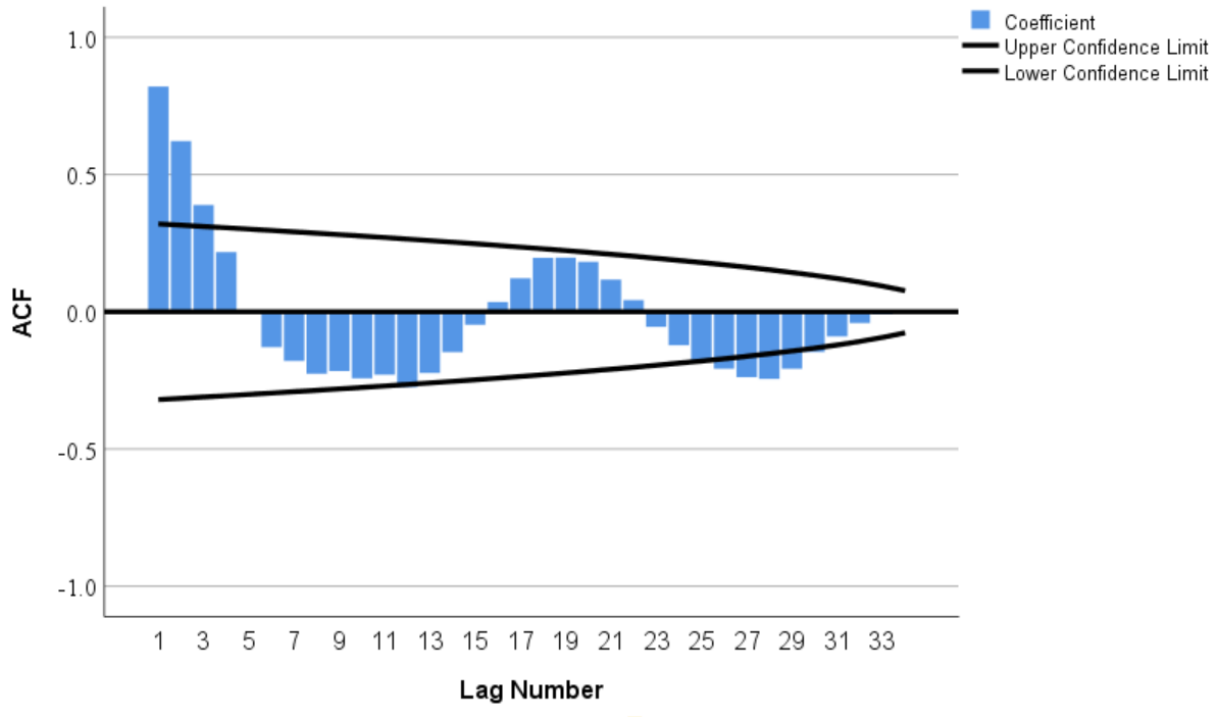
Coefficient
Upper Confidence Limit
Lower Confidence Limit
ACF
1.0
0.5
0.0
-0.5
-1.0
1 3 5 7 9 11 13 15 17 19 21 23 25 27 29 31 33
Lag Number

b)

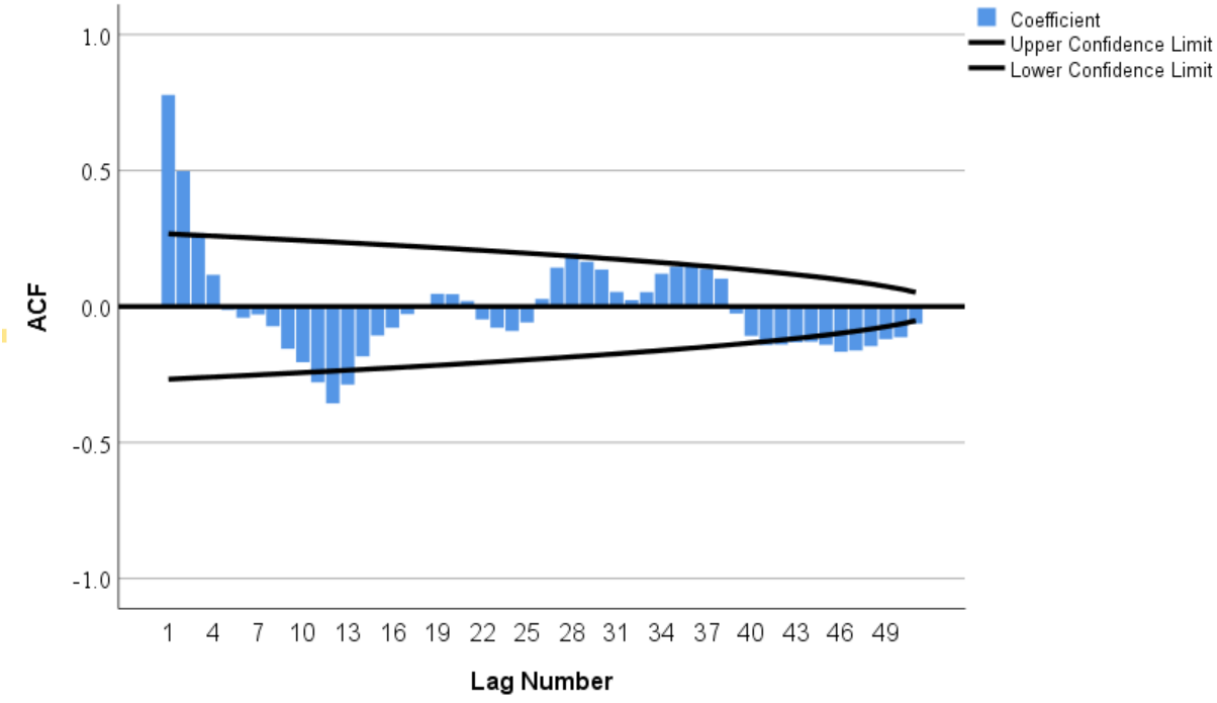
Coefficient
Upper Confidence Limit
Lower Confidence Limit
ACF
1.0
0.5
0.0
-0.5
-1.0
1 4 7 10 13 16 19 22 25 28 31 34 37 40 43 46 49
Lag Number

c)

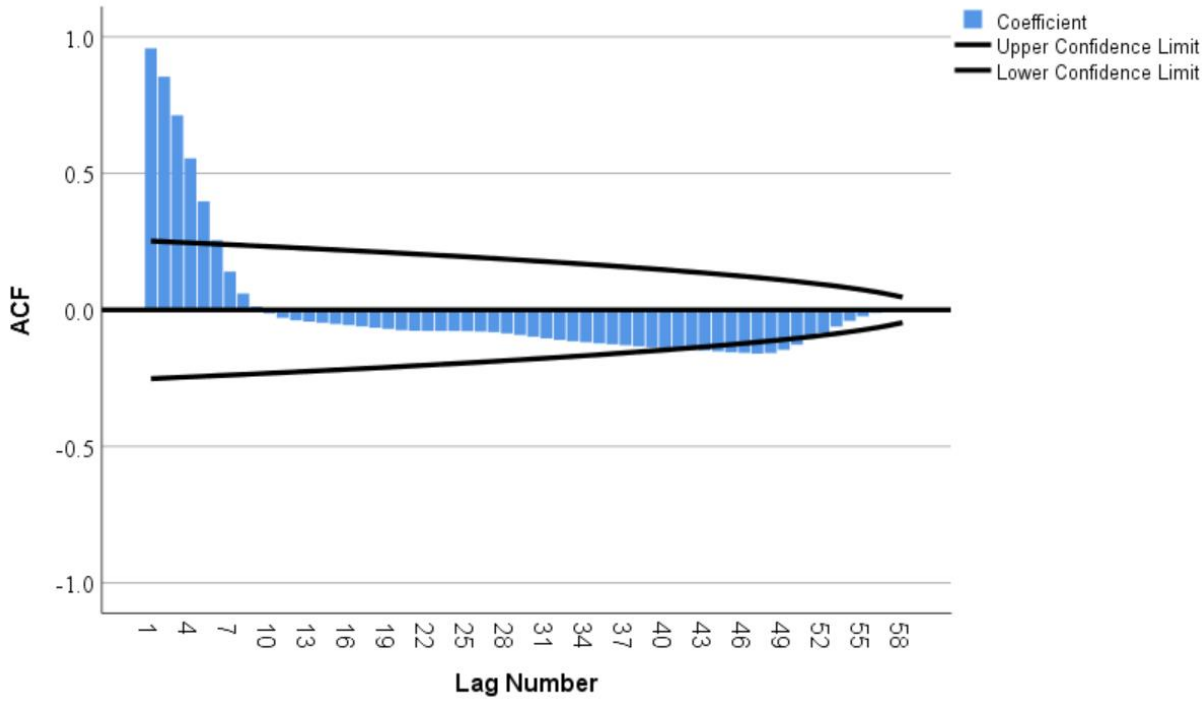
Coefficient
Upper Confidence Limit
Lower Confidence Limit
ACF
1.0
0.5
0.0
-0.5
-1.0
1
4
7
10
13
16
19
22
25
28
31
34
37
40
43
46
49
52
55
58
Lag Number

d)

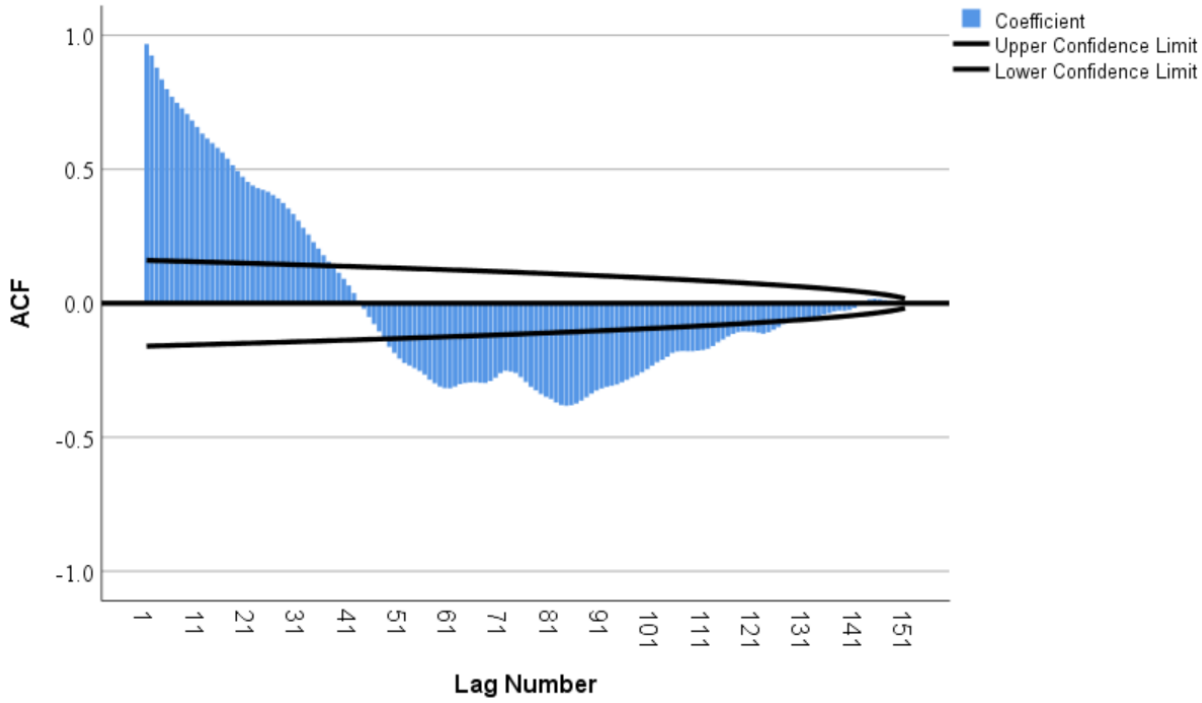

Figure 50 *The autocorrelation plots: (a) ST1 CO_2 mgl^{-1}-period 1; (b)ST1 WT ^0C – period 2; (c) ST1 CO_2 mgl^{-1}-period 4; (d) ST1 WT ^0C – period 5. NB: ACF – Autocorrelation factor (coefficient).*

The autocorrelation analysis (data transformation: differencing of order 1) was performed to obtain stationary time series and potentially remove existing autocorrelations in the time series (CO_2 data, water temperature data, air temperature, air pressure, soil temperature, wind speed). Below are presented results from ST1 and HumST1 data sets (5 periods: (1) winter 2016-2017; (2) summer 2017; (3) winter 2017; (4) winter-spring 2018; (5) summer 2018) (Figure 51; Figure 52). No significant ($p>0.05$) autocorrelations were detected when period 1 CO_2 and water temperature data were analysed (Figure 51a, b). The maximum non-significant autocorrelations of -0.336 and -0.275 were detected at lag 12 and 13 when looking at CO_2 and water temperature data sets at ST1 (Figure 51a,

b). Non-significant ($p>0.05$) autocorrelations were detected when period 2 CO_2 data were analysed (e.g. the maximum autocorrelation of -0.227 at lag 18 at ST1) (Figure 51c). With respect to water temperature data from period 2 at ST1, there were several significant ($p<0.05$) weak autocorrelations detected at lags 28, 32, 34, 35 and 36 (0.167, -0.150, 0.161, -0.027 and 0.002) (Figure 51d). No significant ($p>0.05$) autocorrelations were detected when period 3 CO_2 data were analysed (e.g. the maximum non-significant autocorrelation coefficient was 0.264 at lag 11) (Figure 51e). Several weak but statistically significant ($p<0.05$) autocorrelations were detected when water temperature data from period 3 were analysed (Figure 51f). From lags 9-18 with the autocorrelation coefficients of -0.301, -0.230, 0.139, 0.088, 0.301, -0.086, -0.071, -0.020, -0.109 and 0.122 (Figure 51f). Period 4 data were analysed to determine autocorrelations. The CO_2 data analysis indicated that autocorrelations occurred from lags 1-57 and were all significant ($p<0.05$), strongest autocorrelation was found at lag 1 (0.736) (Figure 51g). The water temperature data analysis indicated presence of weak non-significant ($p>0.05$) autocorrelations at lags (2-6) the autocorrelation coefficients were -0.220, -0.245, -0.197, 0.001 and -0.006 (Figure 51h). The statistically significant ($p<0.05$) but weak autocorrelations were detected when analysing CO_2 data from period 5 at lags from 115-136 (all autocorrelation coefficients were <0.1; highest coefficient was -0.082 at lag 121) (Figure 51i). Several statistically significant ($p<0.05$) but weak autocorrelations were detected when analysing water temperature data from period 5 (Figure 51j). These were detected at lags 1-38, 71-80, 82 and 86-97(Figure 51j). The highest autocorrelation coefficient was observed at lag 1 (0.226) (Figure 51j).

a)

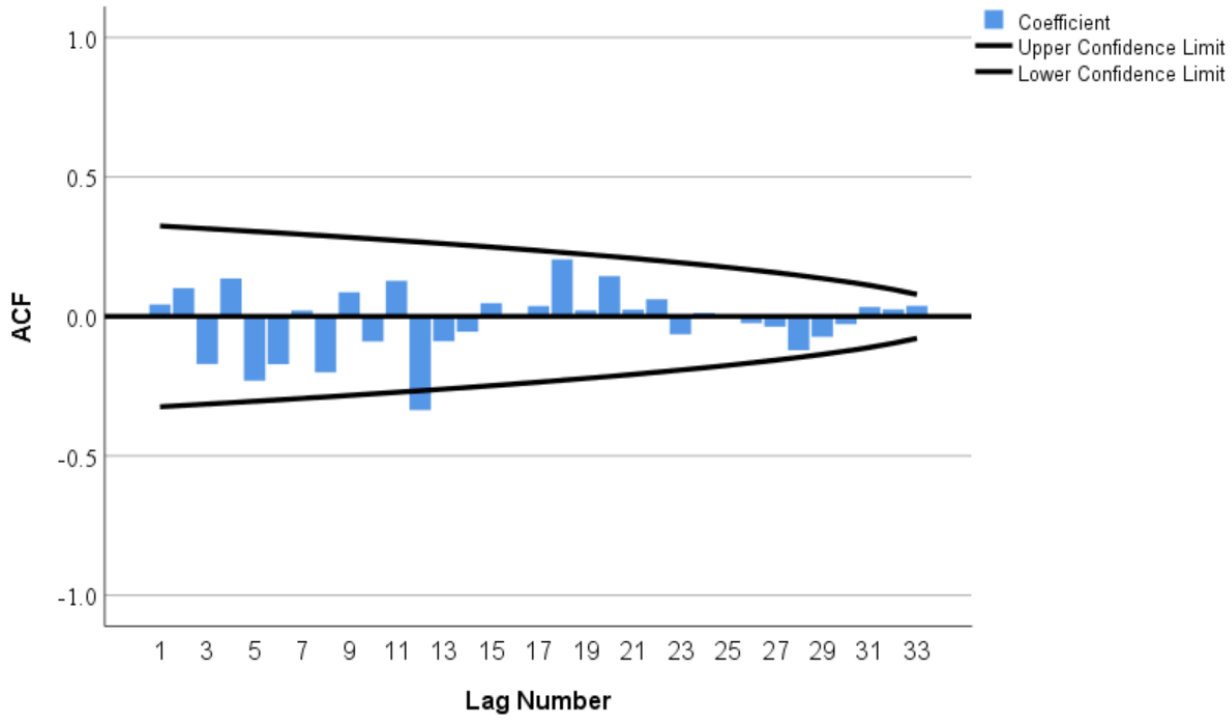
Coefficient
Upper Confidence Limit
Lower Confidence Limit
ACF
1.0
0.5
0.0
-0.5
-1.0
1 3 5 7 9 11 13 15 17 19 21 23 25 27 29 31 33
Lag Number

b)

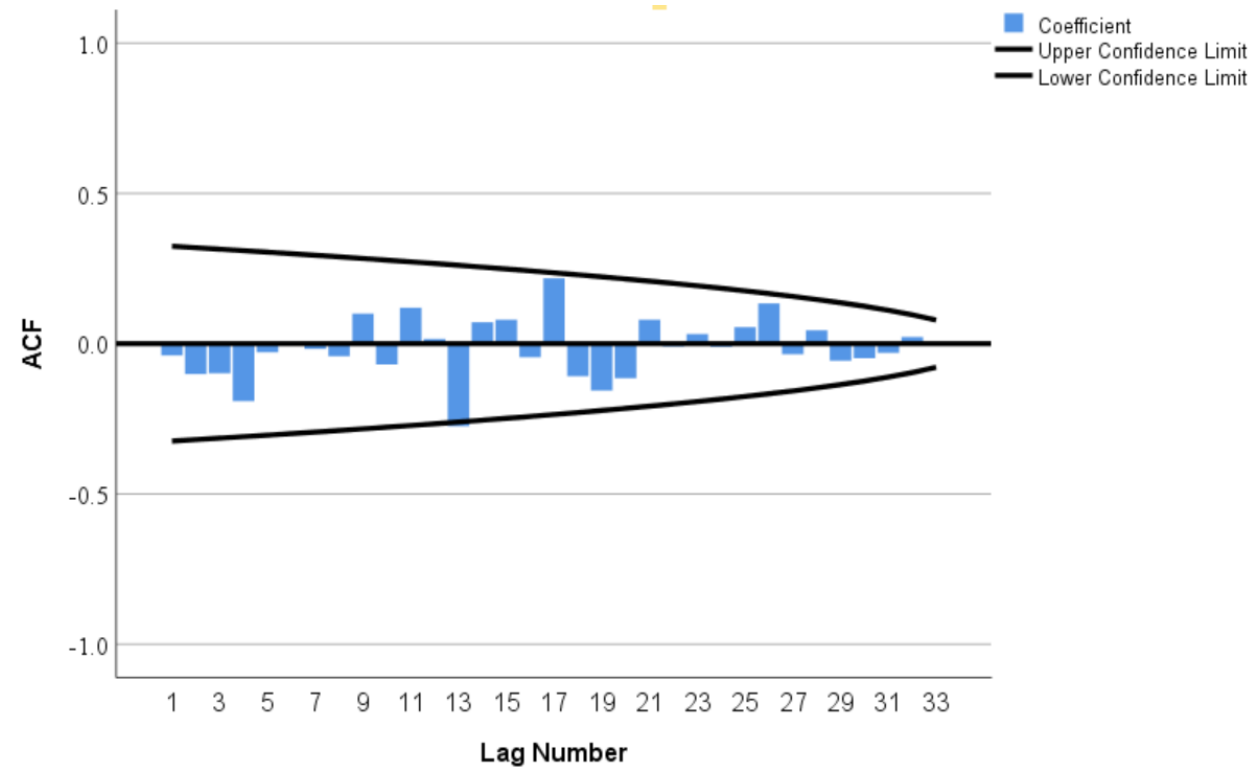
Coefficient
Upper Confidence Limit
Lower Confidence Limit
ACF
1.0
0.5
0.0
-0.5
-1.0
1 3 5 7 9 11 13 15 17 19 21 23 25 27 29 31 33
Lag Number

c)

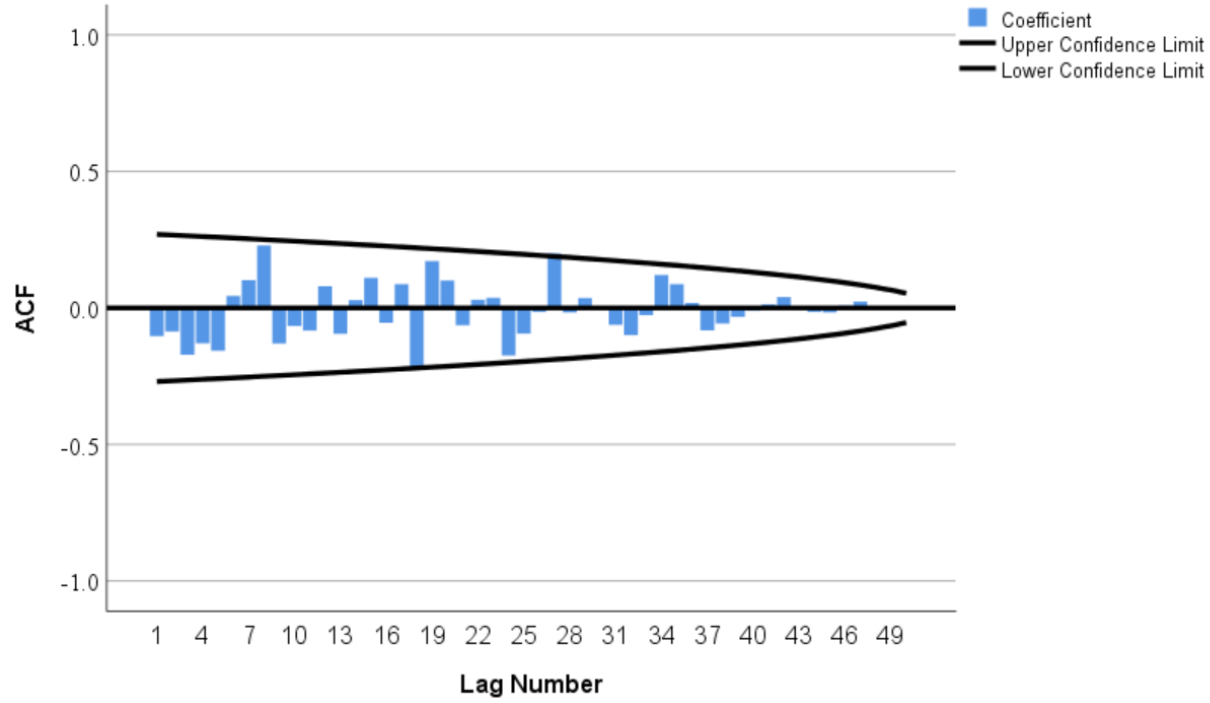
Coefficient
Upper Confidence Limit
Lower Confidence Limit
ACF
1.0
0.5
0.0
-0.5
-1.0
1 4 7 10 13 16 19 22 25 28 31 34 37 40 43 46 49
Lag Number

d)

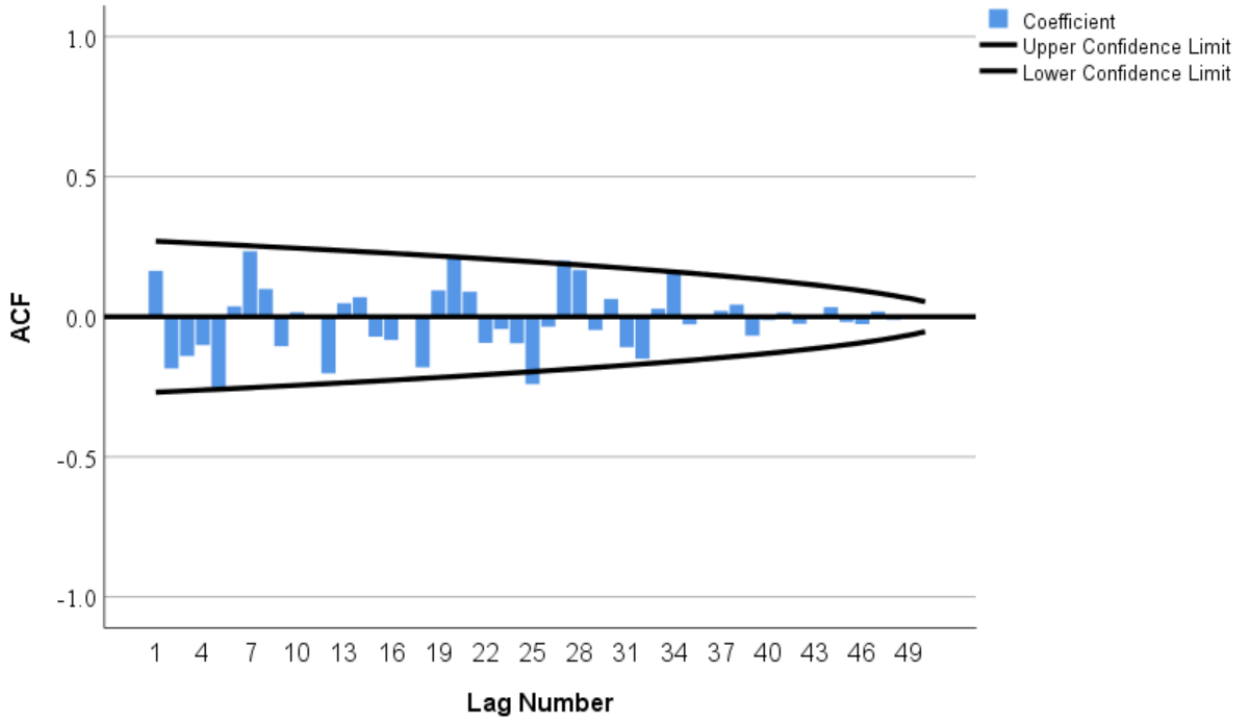
Coefficient
Upper Confidence Limit
Lower Confidence Limit
ACF
1.0
0.5
0.0
-0.5
-1.0
1 4 7 10 13 16 19 22 25 28 31 34 37 40 43 46 49
Lag Number

e)

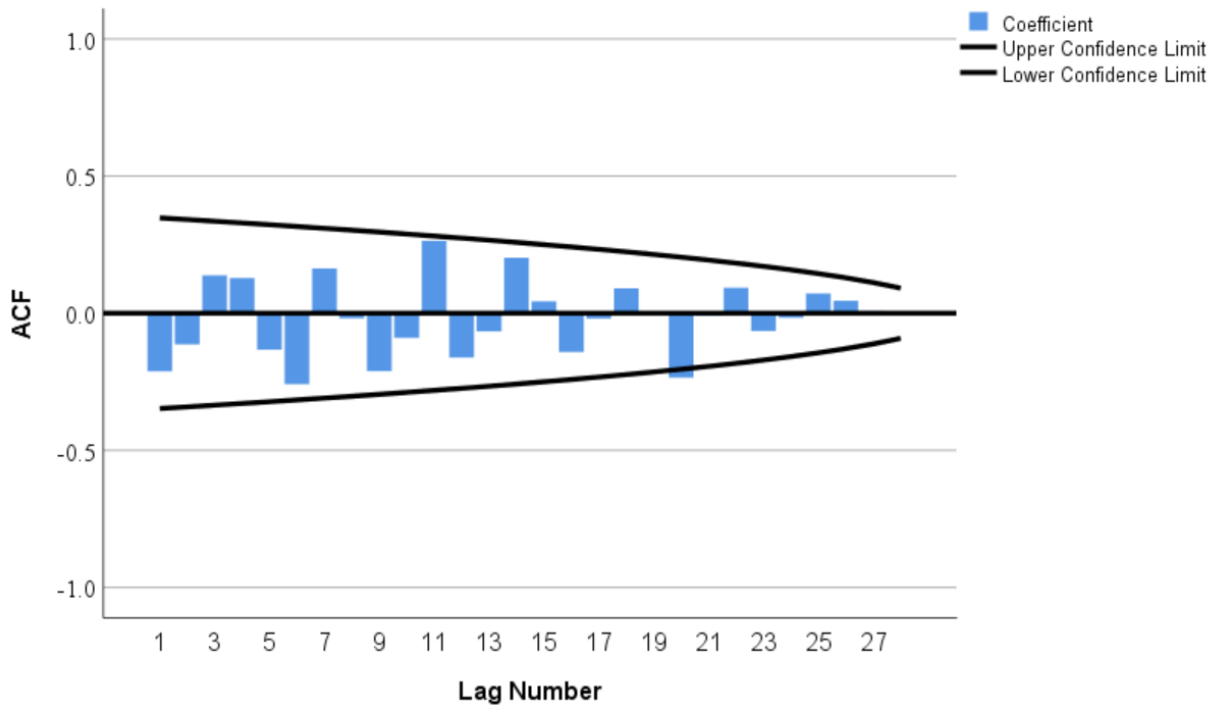
Coefficient
Upper Confidence Limit
Lower Confidence Limit
ACF
1.0
0.5
0.0
-0.5
-1.0
1 3 5 7 9 11 13 15 17 19 21 23 25 27
Lag Number

f)

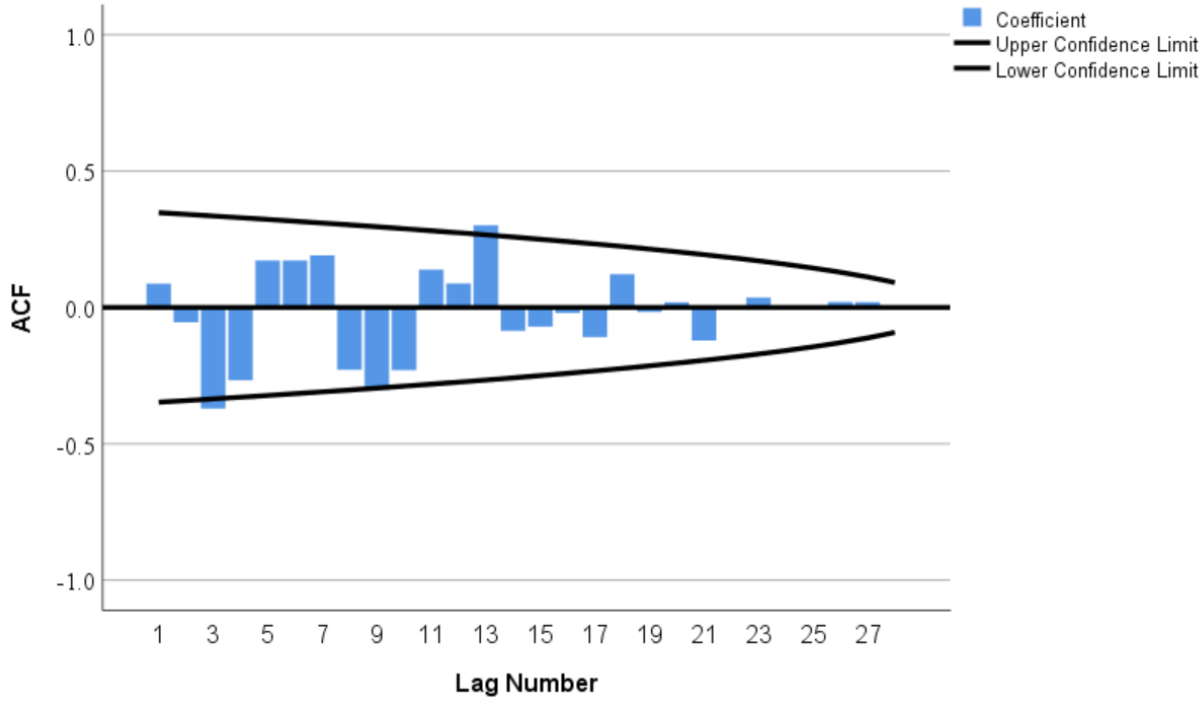
Coefficient
Upper Confidence Limit
Lower Confidence Limit
ACF
1.0
0.5
0.0
-0.5
-1.0
1 3 5 7 9 11 13 15 17 19 21 23 25 27
Lag Number

g)

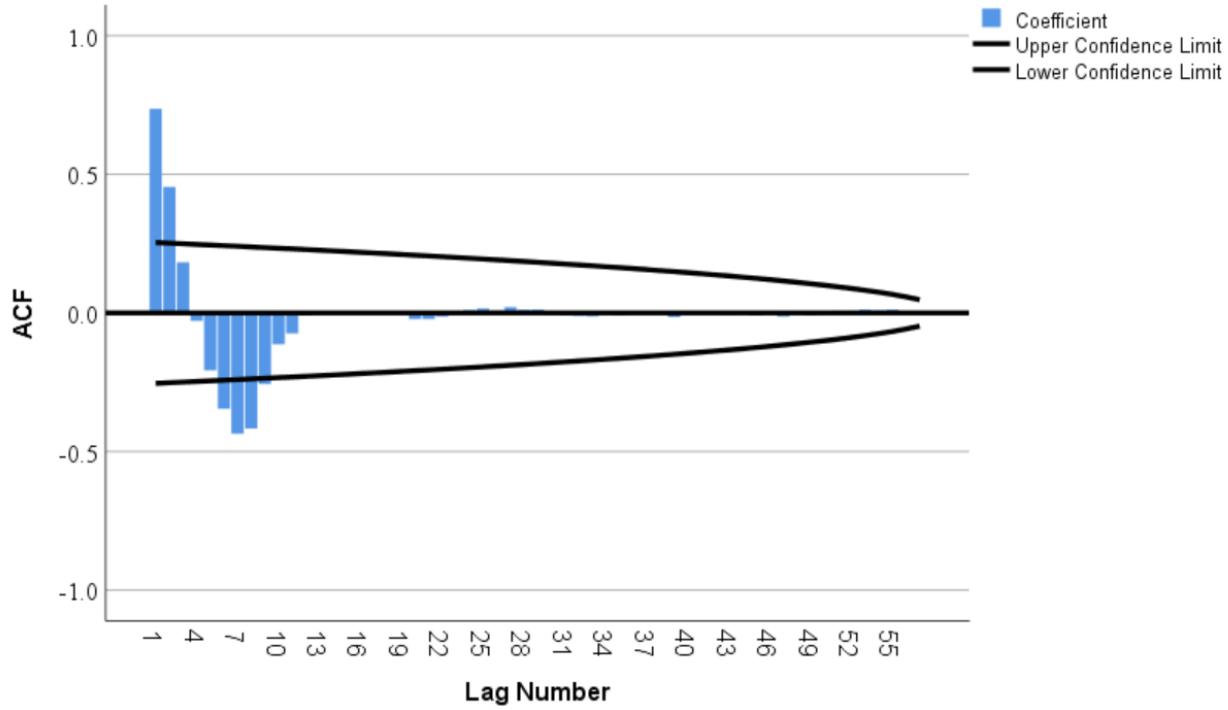
Coefficient
Upper Confidence Limit
Lower Confidence Limit
ACF
1.0
0.5
0.0
-0.5
-1.0
1 4 7 10 13 16 19 22 25 28 31 34 37 40 43 46 49 52 55
Lag Number

h)

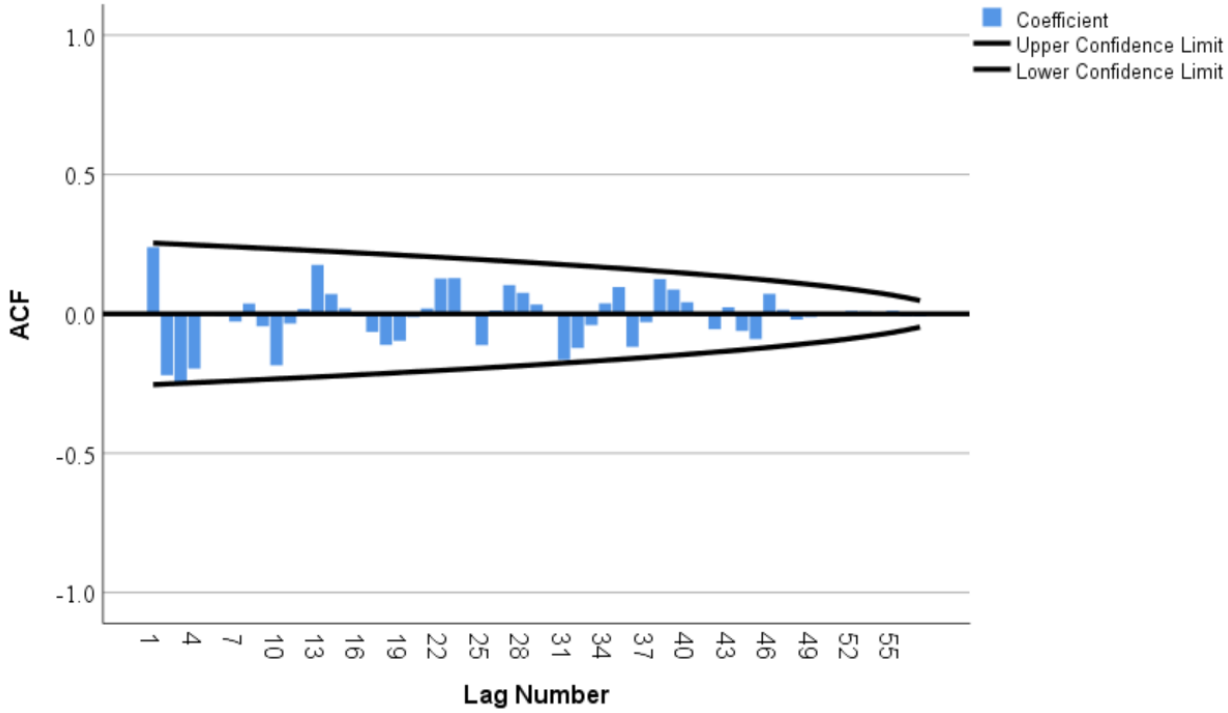
Coefficient
Upper Confidence Limit
Lower Confidence Limit
ACF
1.0
0.5
0.0
-0.5
-1.0
1 4 7 10 13 16 19 22 25 28 31 34 37 40 43 46 49 52 55
Lag Number

i)

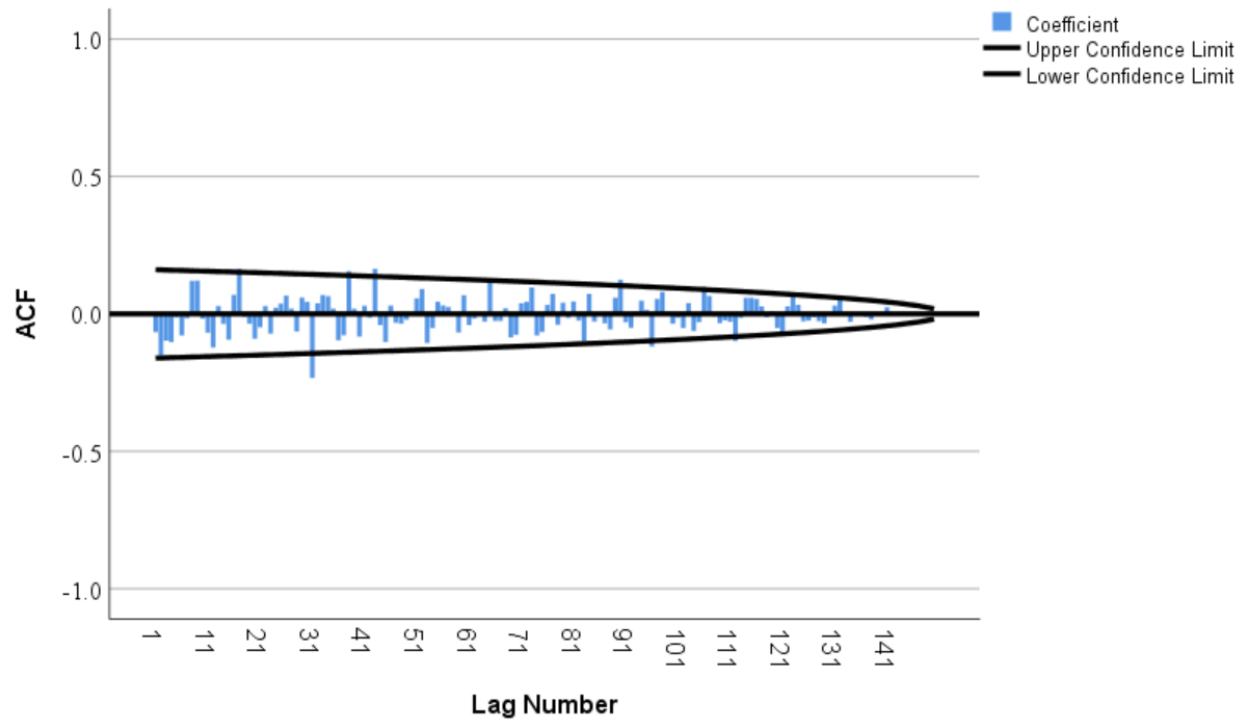
Coefficient
Upper Confidence Limit
Lower Confidence Limit
ACF
1.0
0.5
0.0
-0.5
-1.0
1
11
21
31
41
51
61
71
81
91
101
111
121
131
141
Lag Number

j)

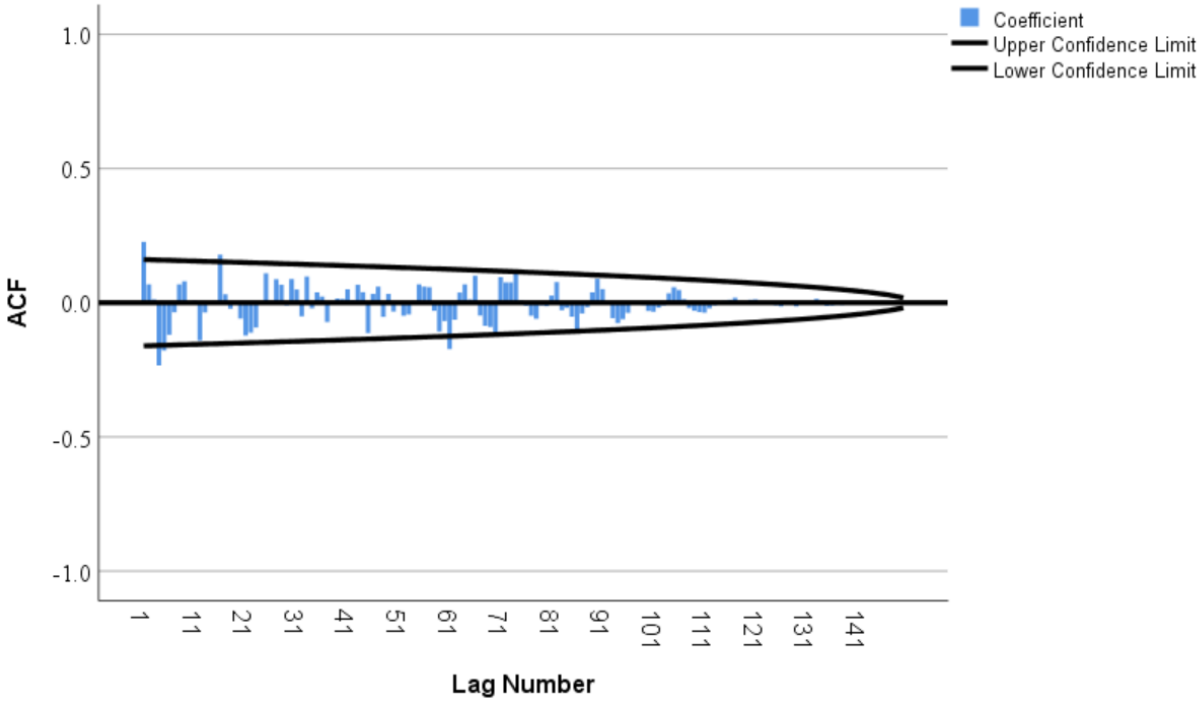
Coefficient
Upper Confidence Limit
Lower Confidence Limit
ACF
1.0
0.5
0.0
-0.5
-1.0
1
11
21
31
41
51
61
71
81
91
101
111
121
131
141
Lag Number

Figure 51 *The CO_2 concentrations (a, c, e, g, i) and water temperature (b, d, f, h, j) time series autocorrelation analysis plots: monitoring periods 1-5 (e.g. a & b – period 1), ST1 time series. NB: ACF – Autocorrelation factor (coefficient).*

At HumST1 similar period were analysed (1-5) (Figure 52). The data that was analysed from period 1, indicated that HumST1 CO_2 time series were autocorrelated at lags 1-33, this observation was statistically significant ($p<0.05$), the strongest autocorrelation was 0.763 at lag 1 (Figure 52a). The peat water temperature analysis did not show any statistically significant autocorrelations ($p>0.05$), the biggest autocorrelation coefficient of -0.258 was observed at lag 4 (Figure 52b). The period 2 CO_2 data were analysed and several significant ($p<0.05$) weak autocorrelations were detected from lags 2-5 and one moderately significant autocorrelation was determined at lag 1 (0.404) (Figure 52c). No statistically significant ($p>0.05$) autocorrelations were detected when peat water temperature from period 2 was analysed (biggest autocorrelation coefficient was -0.232 at lag 18) (Figure 52d). No statistically significant ($p>0.05$) autocorrelations were observed among CO_2 time series from period 3 (biggest non-significant autocorrelation coefficient of -0.396 at lag 2 was detected) (Figure 52e). The only single significant ($p<0.05$) autocorrelation at lag 5 (-0.299) was detected when peat water temperature time series were analysed from period 3 (Figure 52f). The period 4 data analysis indicated statistically significant ($p<0.05$) autocorrelation from lags 1-44 with the biggest autocorrelation coefficient of 0.462 (moderate) at lag 1 (CO_2 data) and from lags 3-57 with the largest autocorrelation coefficient at lag 3 (-0.410 - moderate negative) (peat water temperature data) (Figure 52g, h). No statistically significant ($p>0.05$) autocorrelation were found when data from period 5 (CO_2 and peat water temperature) were analysed (Figure 52i, j). The greatest non-significant autocorrelation coefficients

were detected at lag 20 (-0.172 – weak negative) from CO_2 time series and at lag 7 (-0.205 – weak negative) from peat water time series (Figure 52i, j).

a)

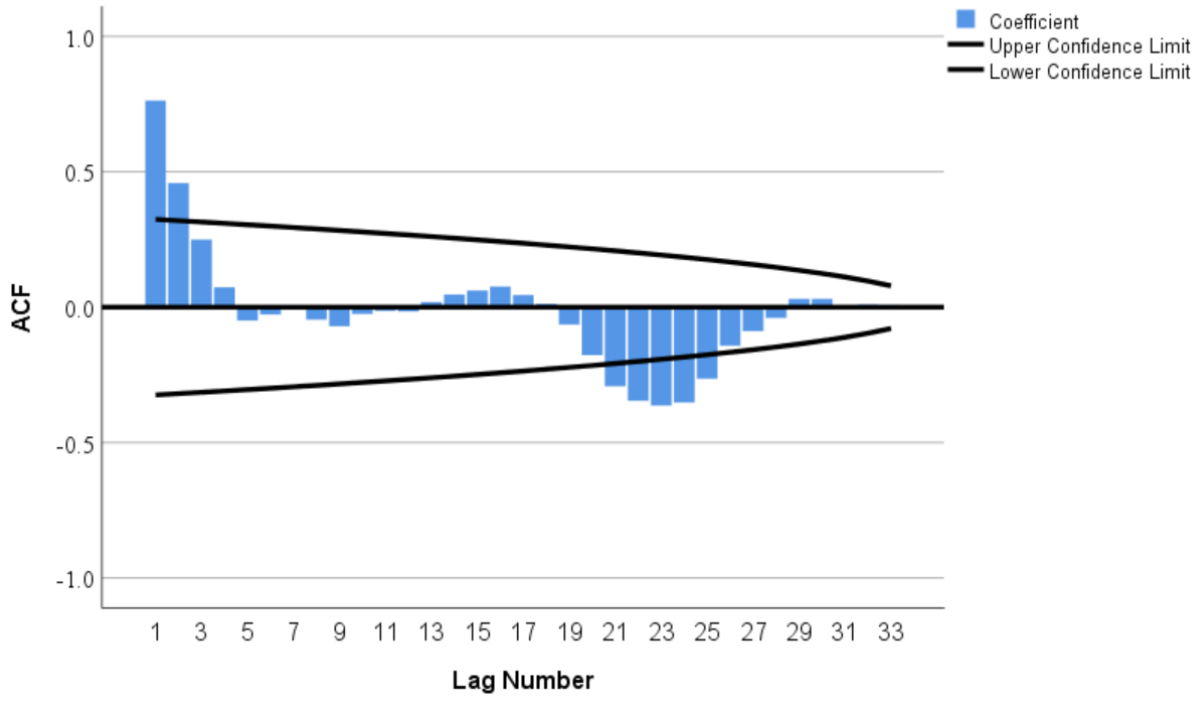

b)

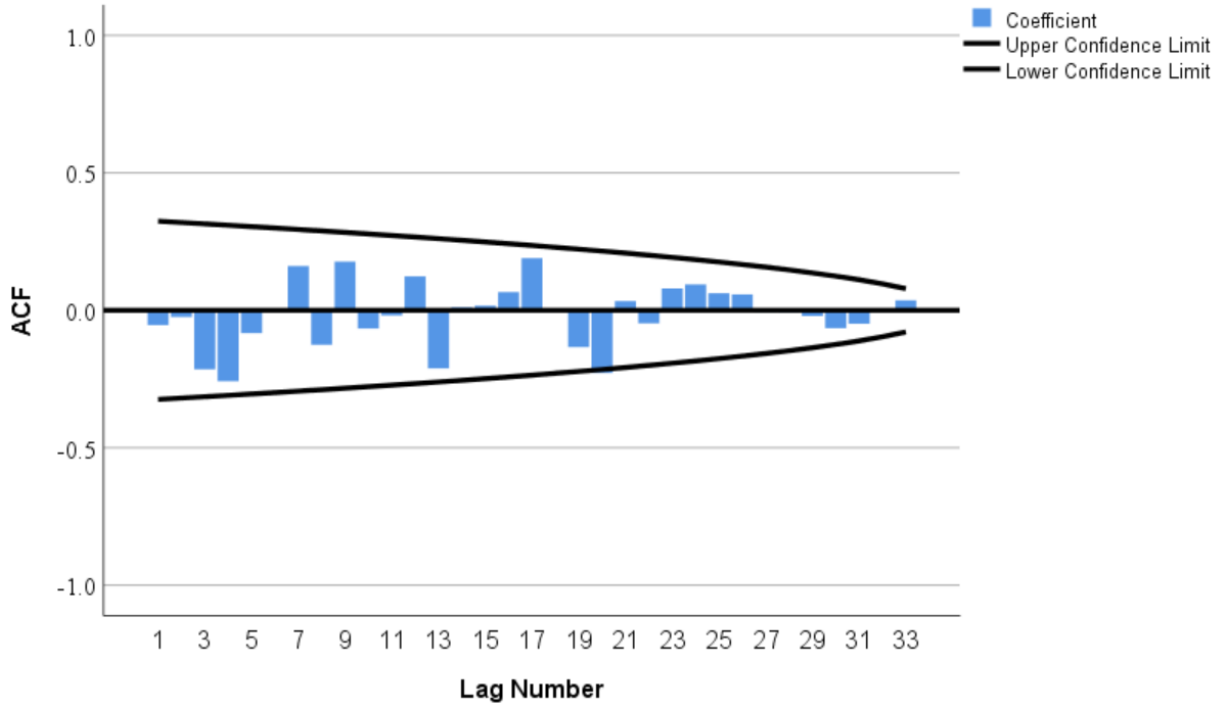
Coefficient
Upper Confidence Limit
Lower Confidence Limit
ACF
1.0
0.5
0.0
-0.5
-1.0
1 3 5 7 9 11 13 15 17 19 21 23 25 27 29 31 33
Lag Number

c)

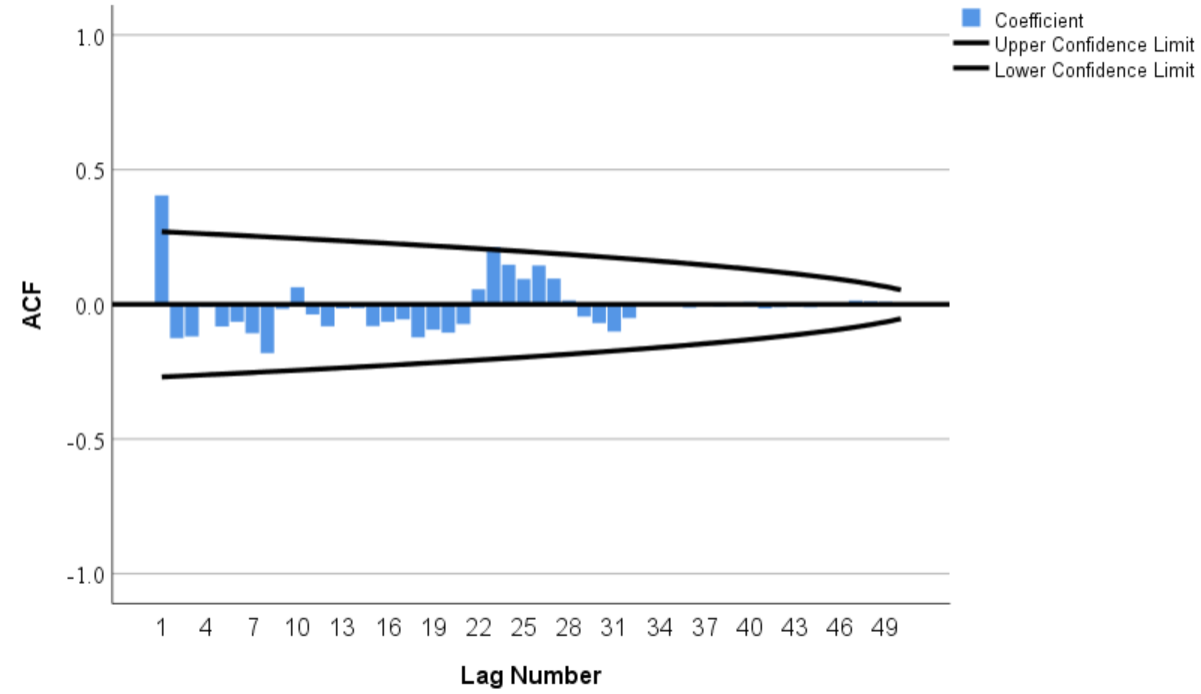
Coefficient
Upper Confidence Limit
Lower Confidence Limit
ACF
1.0
0.5
0.0
-0.5
-1.0
1 4 7 10 13 16 19 22 25 28 31 34 37 40 43 46 49
Lag Number

d)

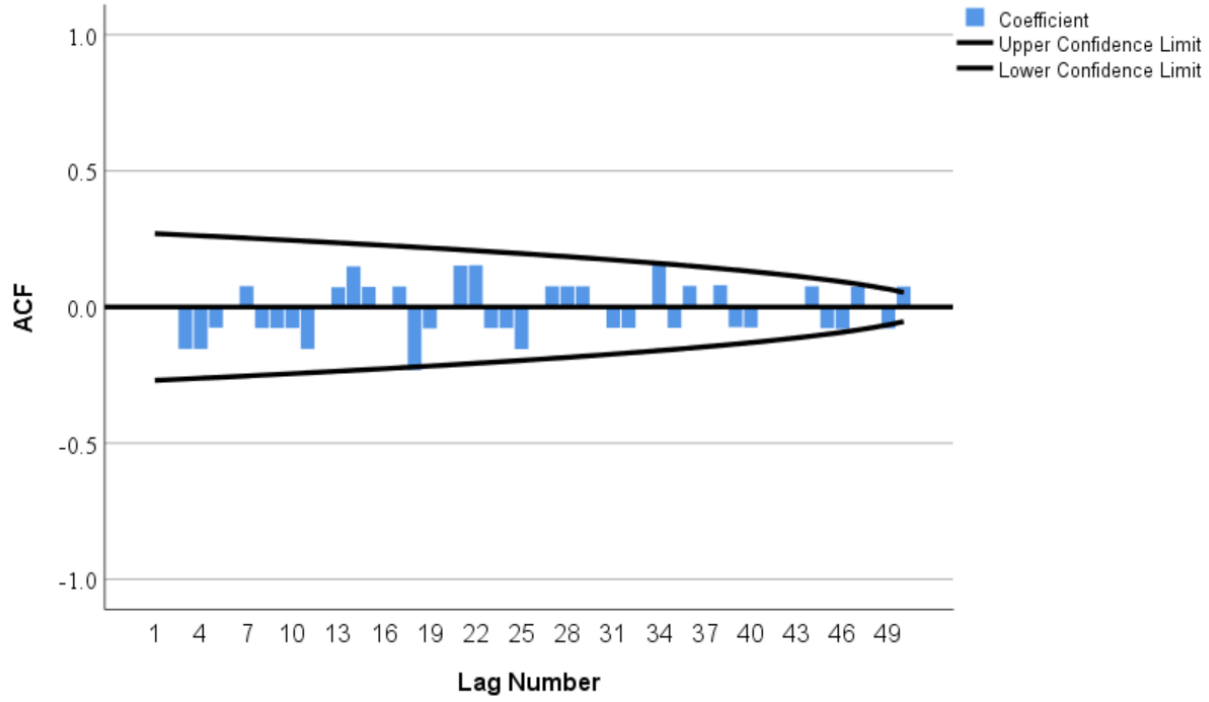
Coefficient
Upper Confidence Limit
Lower Confidence Limit
ACF
1.0
0.5
0.0
-0.5
-1.0
1 4 7 10 13 16 19 22 25 28 31 34 37 40 43 46 49
Lag Number

e)

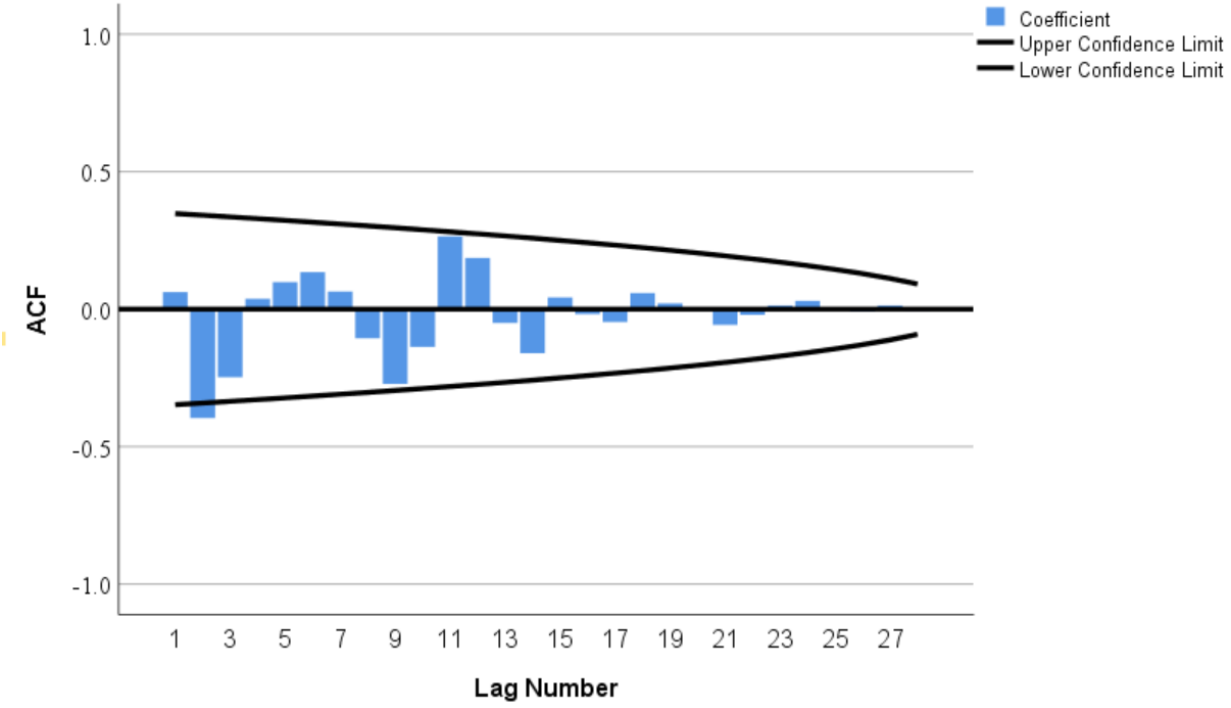
Coefficient
Upper Confidence Limit
Lower Confidence Limit
ACF
1.0
0.5
0.0
-0.5
-1.0
1 3 5 7 9 11 13 15 17 19 21 23 25 27
Lag Number

f)

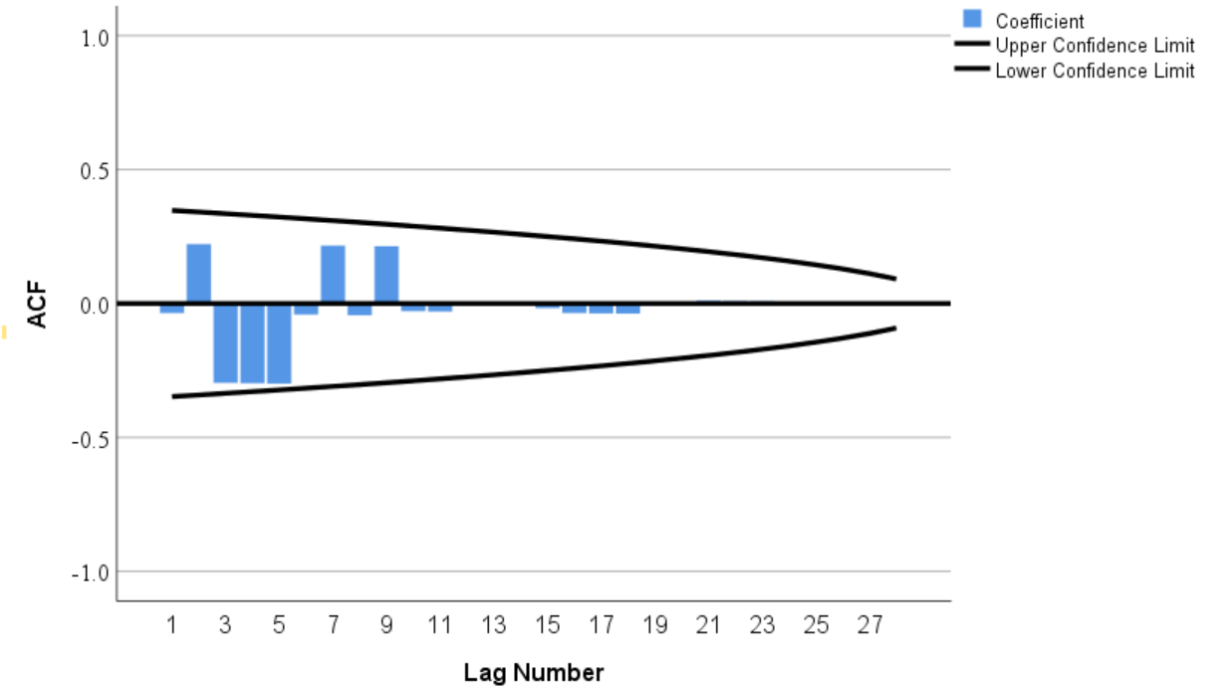
Coefficient
Upper Confidence Limit
Lower Confidence Limit
ACF
1.0
0.5
0.0
-0.5
-1.0
1 3 5 7 9 11 13 15 17 19 21 23 25 27
Lag Number

g)

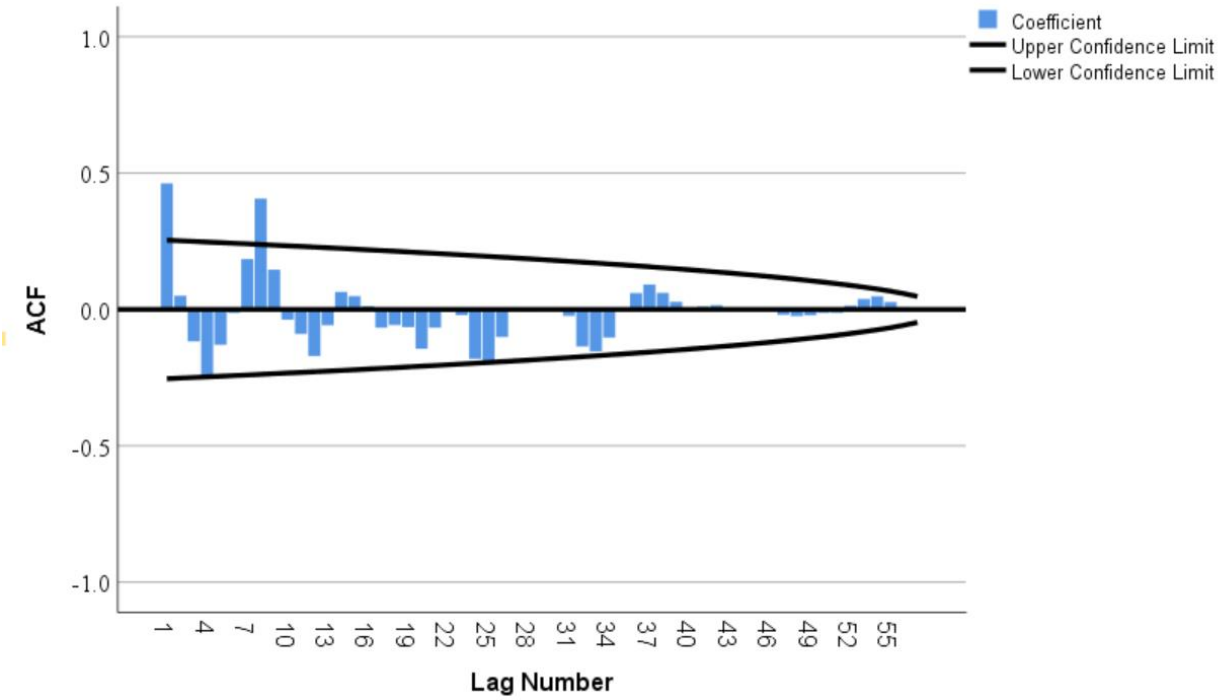
Coefficient
Upper Confidence Limit
Lower Confidence Limit
ACF
1.0
0.5
0.0
-0.5
-1.0
1 4 7 10 13 16 19 22 25 28 31 34 37 40 43 46 49 52 55
Lag Number

h)

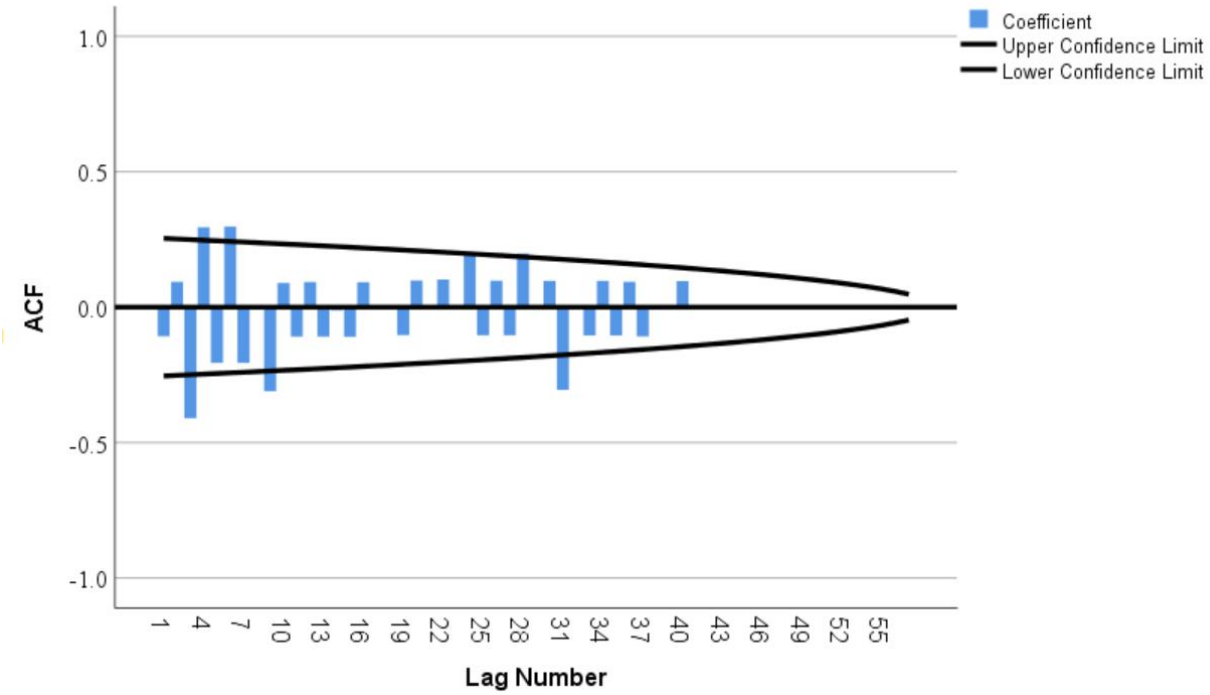
Coefficient
Upper Confidence Limit
Lower Confidence Limit
ACF
1.0
0.5
0.0
-0.5
-1.0
1
4
7
10
13
16
19
22
25
28
31
34
37
40
43
46
49
52
55
Lag Number

i)

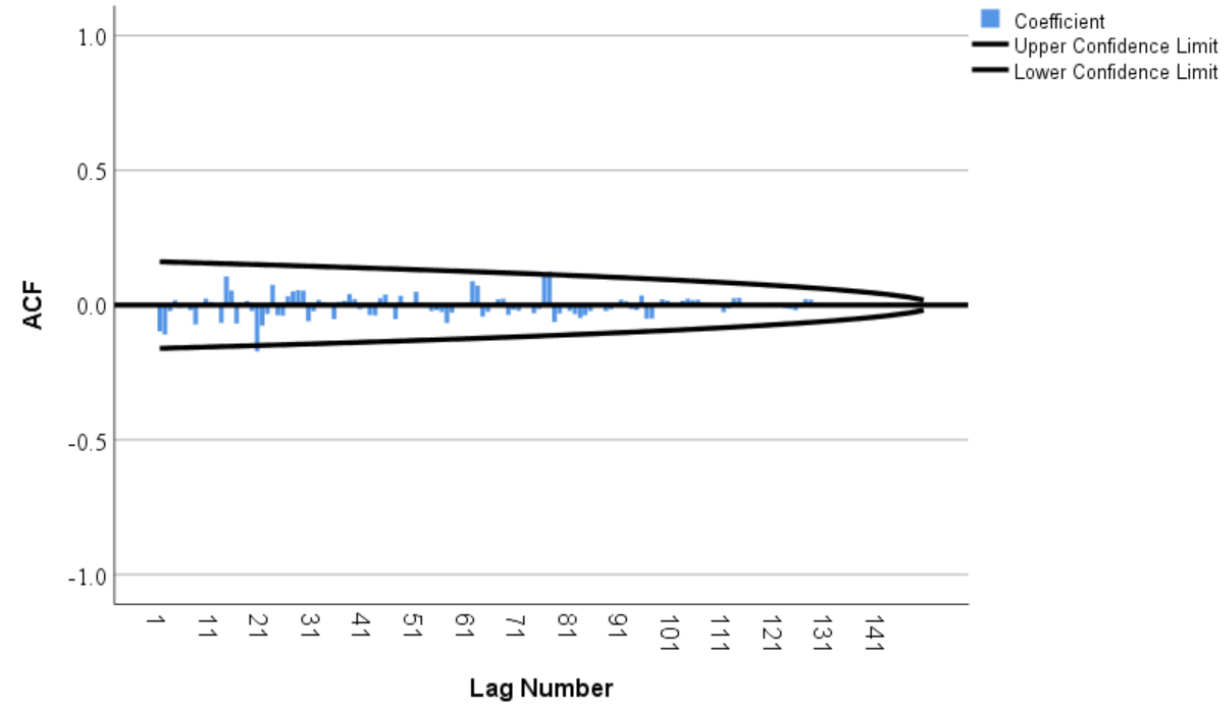
Coefficient
Upper Confidence Limit
Lower Confidence Limit
ACF
1.0
0.5
0.0
-0.5
-1.0
1
11
21
31
41
51
61
71
81
91
101
111
121
131
141
Lag Number

j)

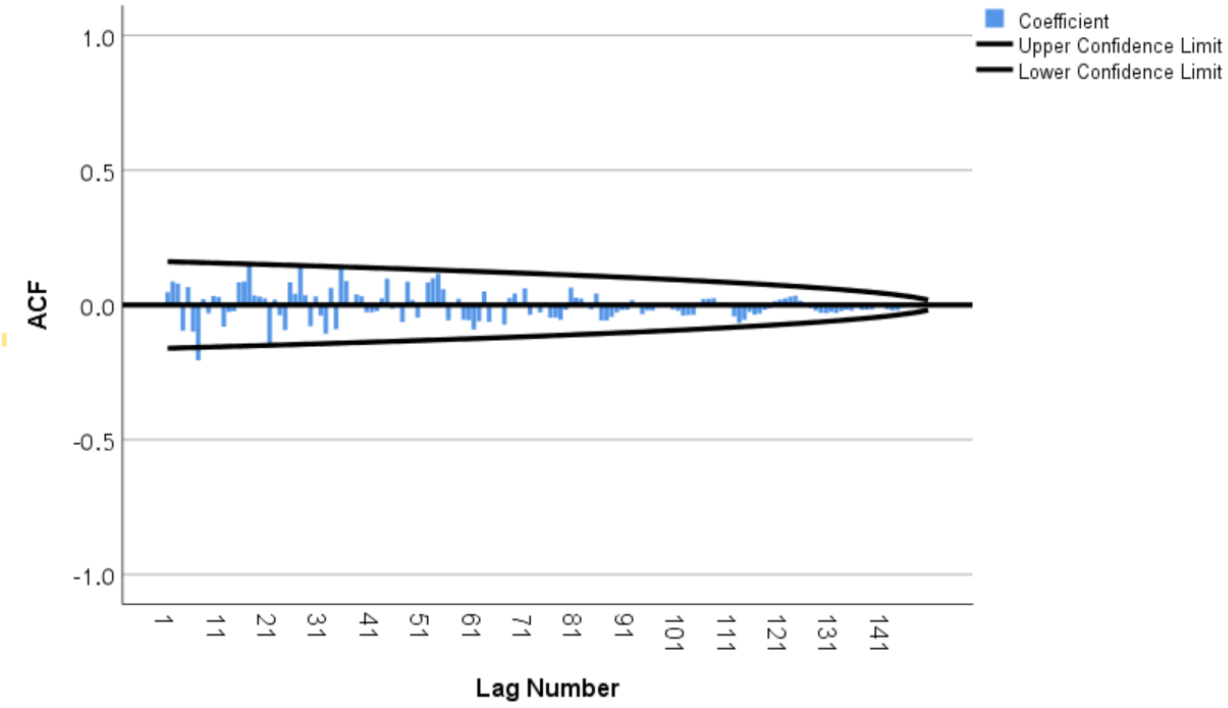

Figure 52 *The CO_2 concentrations (a, c, e, g, i) and water temperature (b, d, f, h, j) time series autocorrelation analysis plots: monitoring periods 1-5 (e.g. a & b – period 1), HumST1 time series. NB: ACF – Autocorrelation factor (coefficient).*

The autocorrelation analysis was also performed on data from ST2 and ST3 time series (CO_2 and water temperature). The data from ST2 consisted of four periods: (1) summer 2017; (2) winter 2017; (3) winter-spring 2018 and (4) summer 2018. The statistically significant ($p<0.05$) difference was observed at several lags when ST2 CO_2 time series (period 1) were analysed, highest autocorrelation of -0.212 (weak negative) at lag 4 was detected. Similar observation was made when water temperature time series were analysed (period 1), the statistically significant ($p<0.05$) autocorrelation of 0.274 (weak positive) was detected at lag 1. The time series (CO_2) data analysis from periods 2-4 revealed presence of statistically significant ($p<0.05$) autocorrelations at several lags, but largest coefficients were recorded at lags 1 (period two: -0.504 – moderate negative; period three: 0.624 – moderate positive) and at lag 8 (period 4: 0.226 – weak positive).

As for water temperature data series analysis revealed the statistically significant ($p<0.05$) autocorrelations with biggest coefficient of autocorrelation visible at lags 3 (period two: -0.531 – moderate negative and period three: -0.293 – weak negative) and at lag 1 (period four: 0.372 – moderate positive). The ST3 data series consisted of two periods: (1) winter 2017 and (2) summer 2018. Analysis of time series from period 1 had illustrated absence of statistically significant ($p>0.05$) autocorrelation when CO_2 data were assessed (-0.298 – weak negative, non-significant autocorrelation coefficient maximum at lag 2). The period two analysis of CO_2 data revealed statistically significant ($p<0.05$) autocorrelations at several lags with the largest coefficient detected at lag 5 (-0.314 – moderate negative). The water temperature analyses of data from periods one and two revealed several autocorrelations that were significant at different lags with the largest autocorrelation coefficient observed at lag 3 (-0.508 – moderate negative at period 1) and at lag 5 (-0.240 -weak negative at period 2).

When LawnST2 time series data (periods: (1) summer 2017; (2) winter 2017 and (3) summer 2018) were analysed, no statistically significant ($p>0.05$) autocorrelations were found when peat water temperature (periods 1-3) were analysed and CO_2 data (periods 2-3) were analysed. The weak negative, non-significant autocorrelation coefficients (largest from statistics data table) were recorded: -0.296 at lag 4 (period 1; water temperature), -0.254 at lag 2 (period 2: water temperature) and -0.177 at lag 5 (period 3; water temperature). The weak negative, non-significant autocorrelation coefficients (largest from statistics data table) were also recorded when CO_2 data were analysed: -0.207 at lag 10 (period 2) and -0.215 at lag 20 (period 3). The only statistically significant ($p<0.05$) autocorrelations were detected when CO_2 data from period 1 was analysed, several lags contained autocorrelation, and the biggest coefficient was detected at lag 1 (0.285 – weak positive). The HumST3 data consisted of two periods: (1) winter 2017 and (2) summer

2018. The autocorrelation analysis revealed non-statistically significant ($p>0.05$) autocorrelations when peat water temperature was analysed. The largest non-significant autocorrelation coefficients were -0.477 at lag 3 (period 1) and -0.169 at lag 5 (period 2). Both coefficients were negative and weak-moderate in strength. When CO_2 time series were analysed, the period 1 data appeared to contain the autocorrelations that were statistically significant ($p<0.05$) at several lags, with the largest coefficient found at lag 1 (0.367 -moderate positive). And period 2 data contained non-statistically significant ($p>0.05$) autocorrelations, the largest coefficient was found at lag 14 (0.225 – weak positive, non-significant).

Entire air temperature (2016-2018), soil temperature and air pressure time series (with no period splitting) were analysed for presence of autocorrelations (Figure 53). The air temperature time series analysis revealed presence of several weak but significant ($p<0.05$) autocorrelations at different lags with the maximum autocorrelation coefficient found at lag 5 (-0.169) (Figure 53a). Similar trend was observed when soil temperature and air pressure time series were analysed (Figure 53b). The autocorrelations were found at several lags in both cases, these were significant as per Q-test ($p<0.05$), the maximum autocorrelation coefficients were found at lag 31 (-0.191 – weak negative; soil temperature) and at lag 33 (-0.179 – weak negative; air pressure) (Figure 53b).

a)

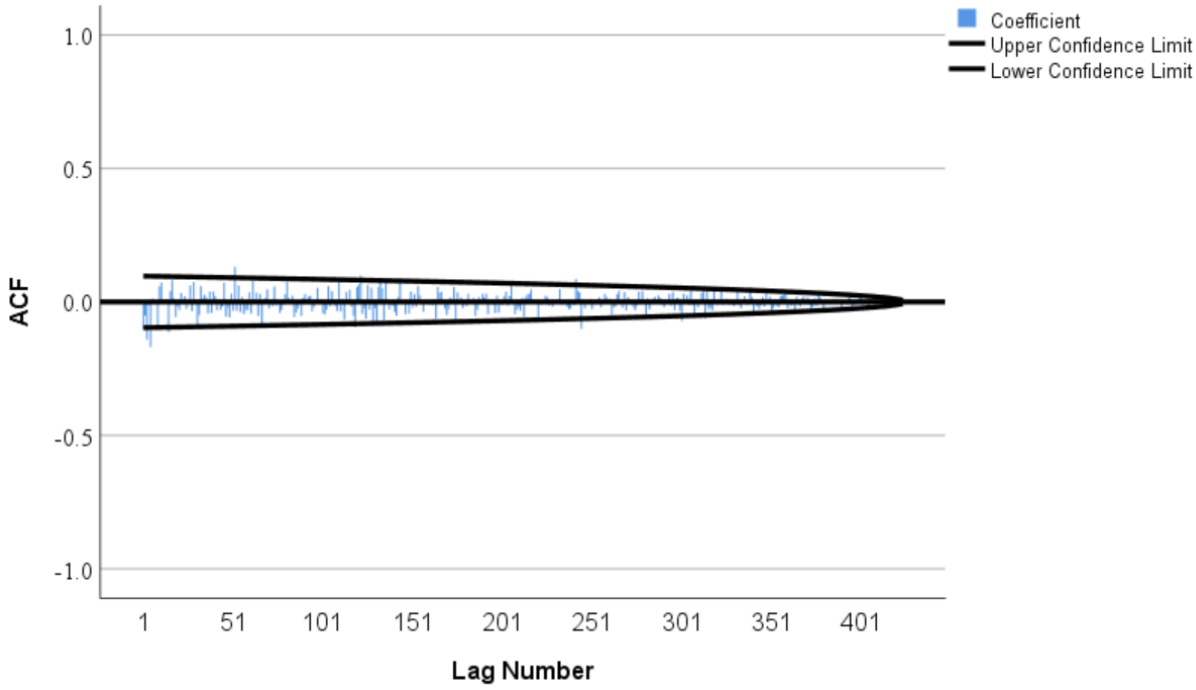
Coefficient
Upper Confidence Limit
Lower Confidence Limit
ACF
1.0
0.5
0.0
-0.5
-1.0
1
51
101
151
201
251
301
351
401
Lag Number

b)

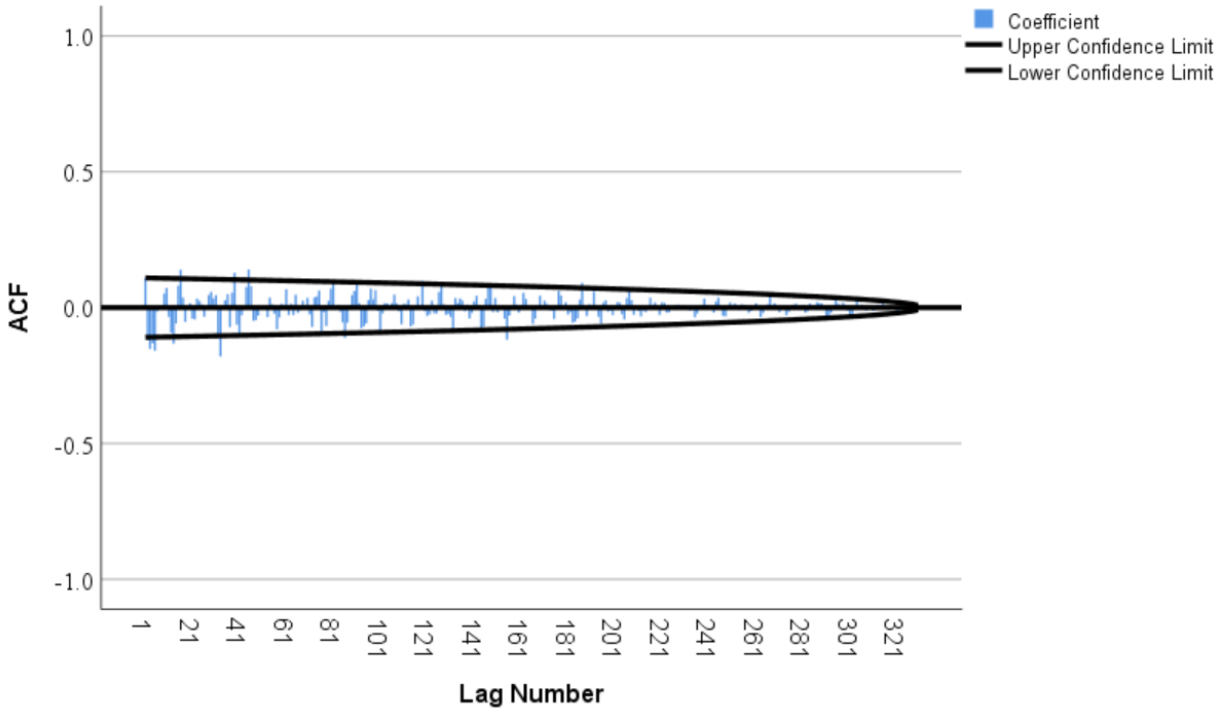

Figure 53 *The air temperature (a) and (b) air pressure time series autocorrelation analysis plots: entire data sets (2016-2018). NB: ACF – Autocorrelation factor (coefficient).*

To assess the potential autocorrelations in wind speed and CO_2 flux time series, the ST1 data from 6 periods were analysed ((1) – winter 2016/2017; (2) summer 2017; (3) winter 2017; (4) winter 2018; (5) spring-summer 2018 and (6) summer 2018). The wind speed time series were analysed, two of time periods (2 & 3) analysed appeared to contain significant autocorrelation ($p<0.05$) at lag 1 (-0.303 – moderate negative) and at lag 5 (-0.343 – moderate negative), and the remaining time series did not show any significant autocorrelations. All autocorrelations (significant and non-significant) were negative weak to moderate in extent (Figure 54a). The CO_2 flux time series from period 2-5 contained significant ($p<0.05$) autocorrelations with maximum autocorrelation coefficient detected at lag 1 (-0.341-moderate negative; period 2), lag 1 (-0.372 –

moderate negative; period 3), lag 2 (-0.353 – moderate negative; period 4) and at lag 1 (-0.221 – weak negative; period 5). Non-significant autocorrelations (p>0.05) at period 1 and 6 were weak negative (Figure 54b).

a)

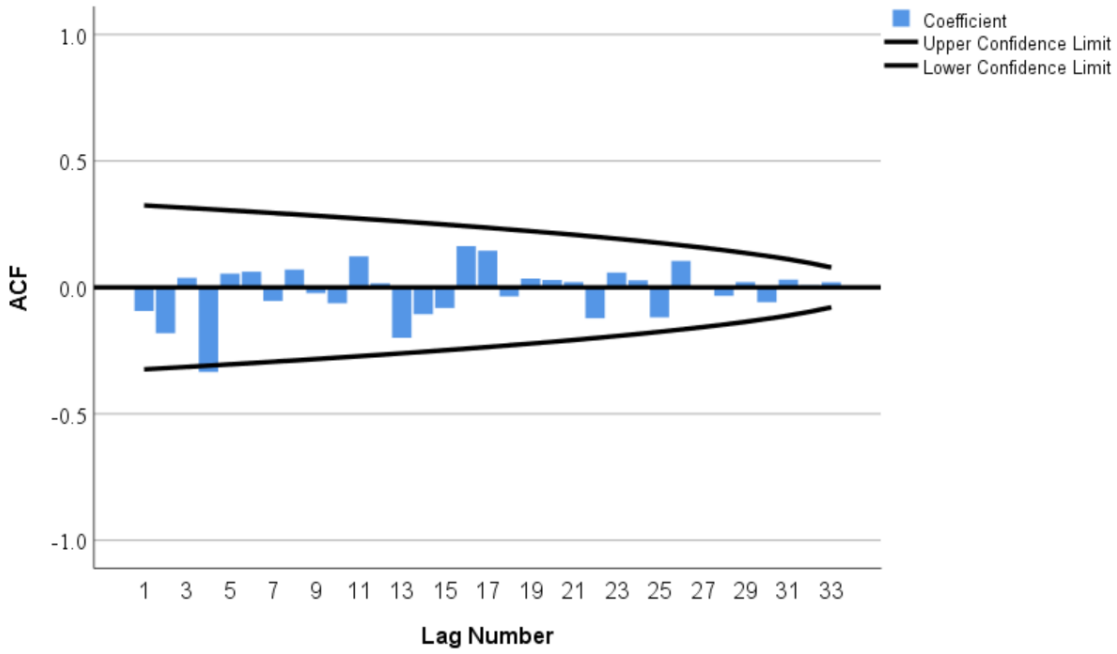

b)

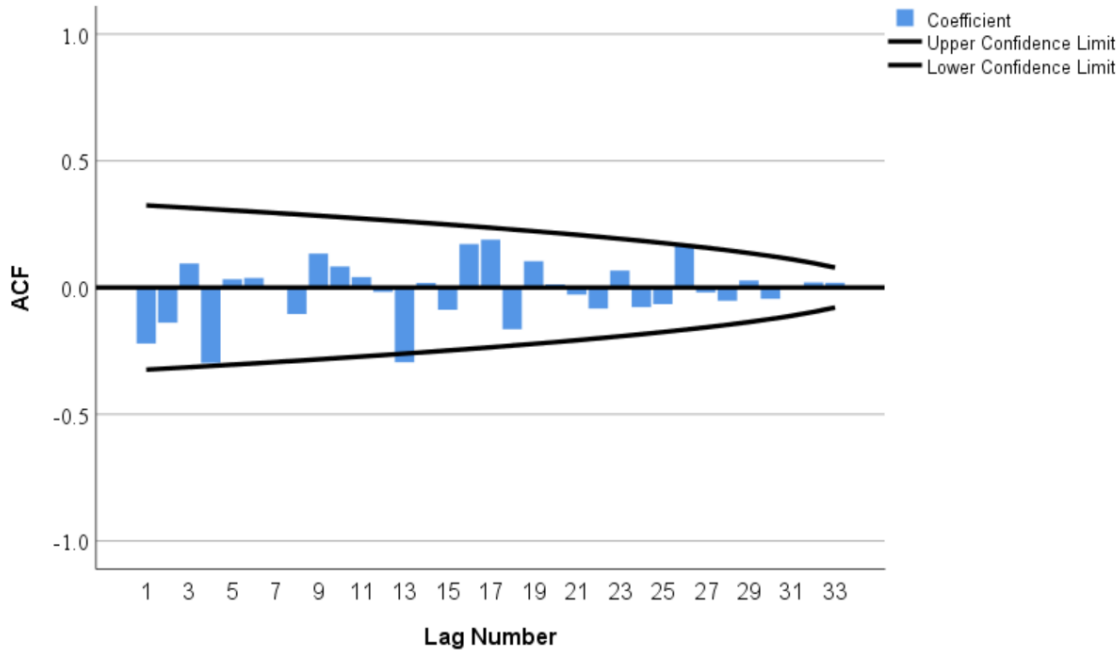

Figure 54 *The wind speed (a) and (b) CO_2 flux time series (ST1) autocorrelation analysis plots: the period 1. NB: ACF – Autocorrelation factor (coefficient).*

First order differencing method did not smooth, reduce trends in all the time series. Therefore, it was required to perform other prewhitening measures (natural log transformation, etc.) or higher order differencing on those time series that contained autocorrelations. With respect to WT ST1 (periods 2-3) time series, the natural log transformation with differencing of order 1 was enough to remove autocorrelations (Figure 55).

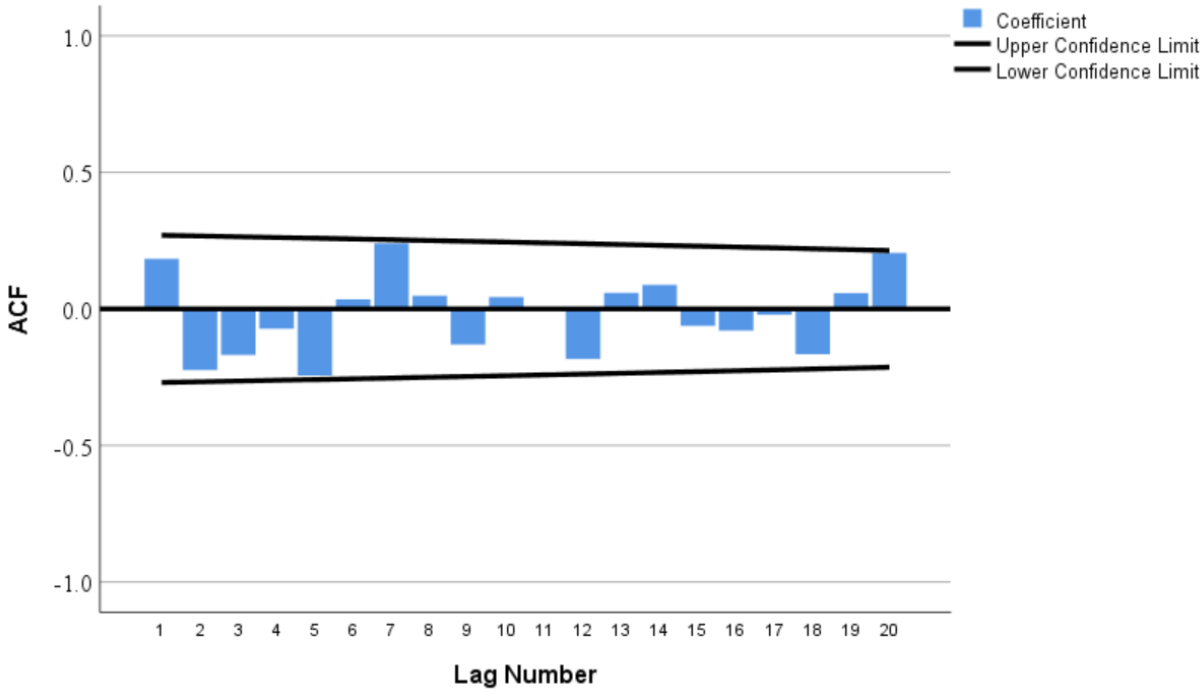

Figure 55 *The autocorrelation plot showing prewhitened WT ST1 time series from period 2.*

The ARIMA models were created to remove autocorrelations in all remaining cases. The ARIMA (2,1,7) was constructed to remove autocorrelations from CO_2 time series (ST1; period 4). To test the goodness fit of the model, the following two parameters were measured: coefficient of determination (R^2) and the root mean square error (RMSE). The RMSE was 0.285 and R^2 was 0.971 indicating excellent performance of ARIMA (2,1,7). The normal distribution of time series was observed ($p>0.05$) (Figure 56a). The ST1 period 5 WT and CO_2 time series were modelled applying ARIMA (0,0,4) and ARIMA (1,1,11). In case of WT times series, prior to modelling, the seasonal differencing (order 1) was applied to reduce the influence of seasonality. The results of fitting of the ARIMA model were R^2 = 0.083, RMSE = 1.029. The time series were showing independent distribution ($p>0.05$) (Figure 56b). The ARIMA (1,1,11) model was applied to CO_2

(period 5; ST1) time series. The time series were transformed (natural log). The results of the model (R^2 = 0.644; RMSE = 0.064; p>0.05) were indicative that this model was suitable in reducing autocorrelation in time series (Figure 56c).

a)

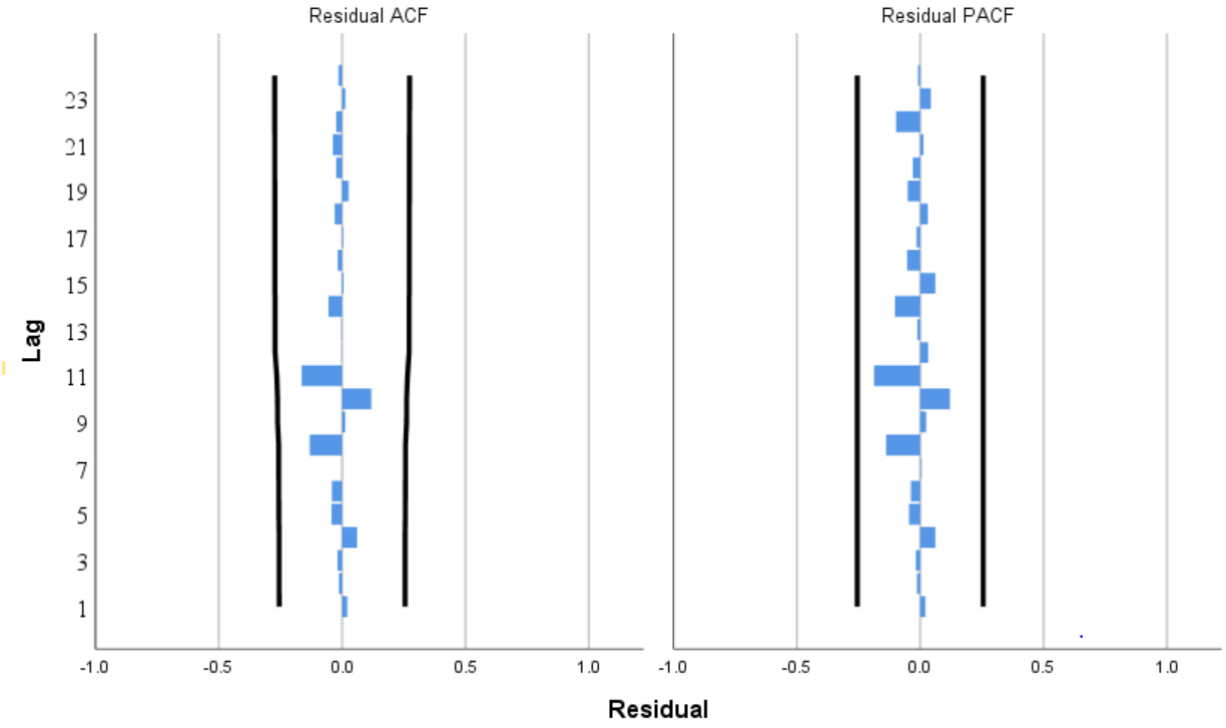

b)

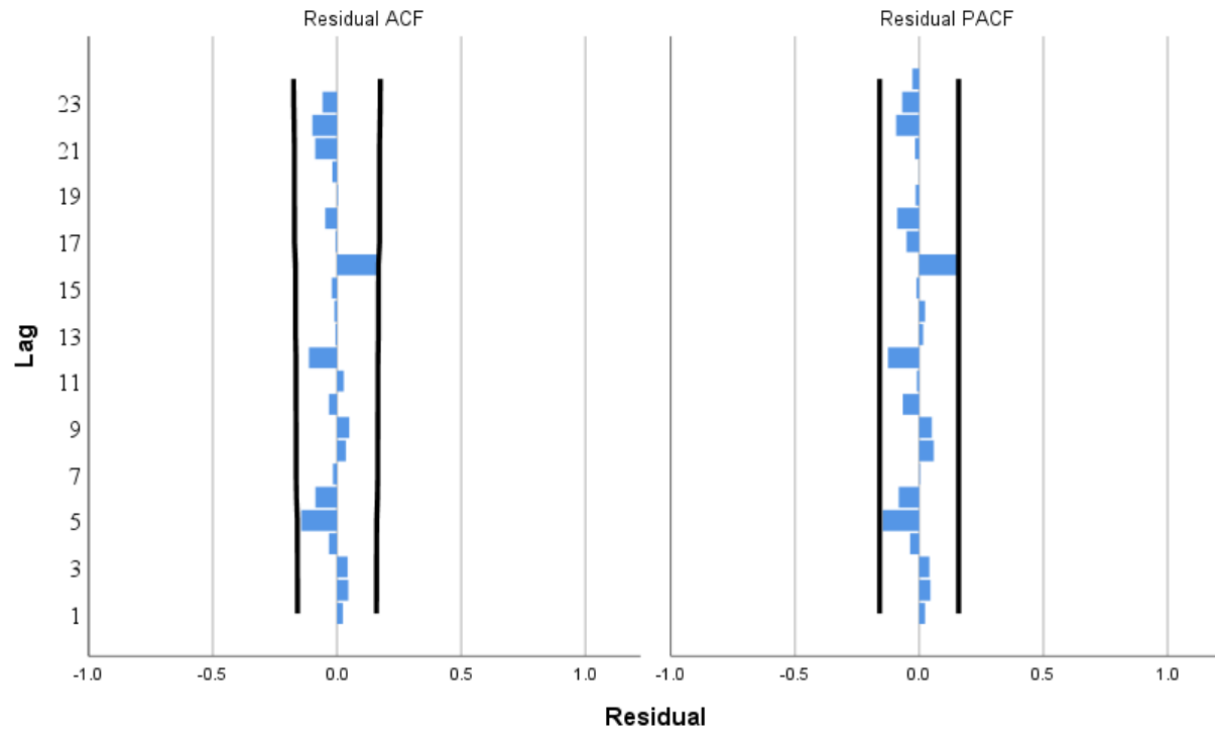

c)

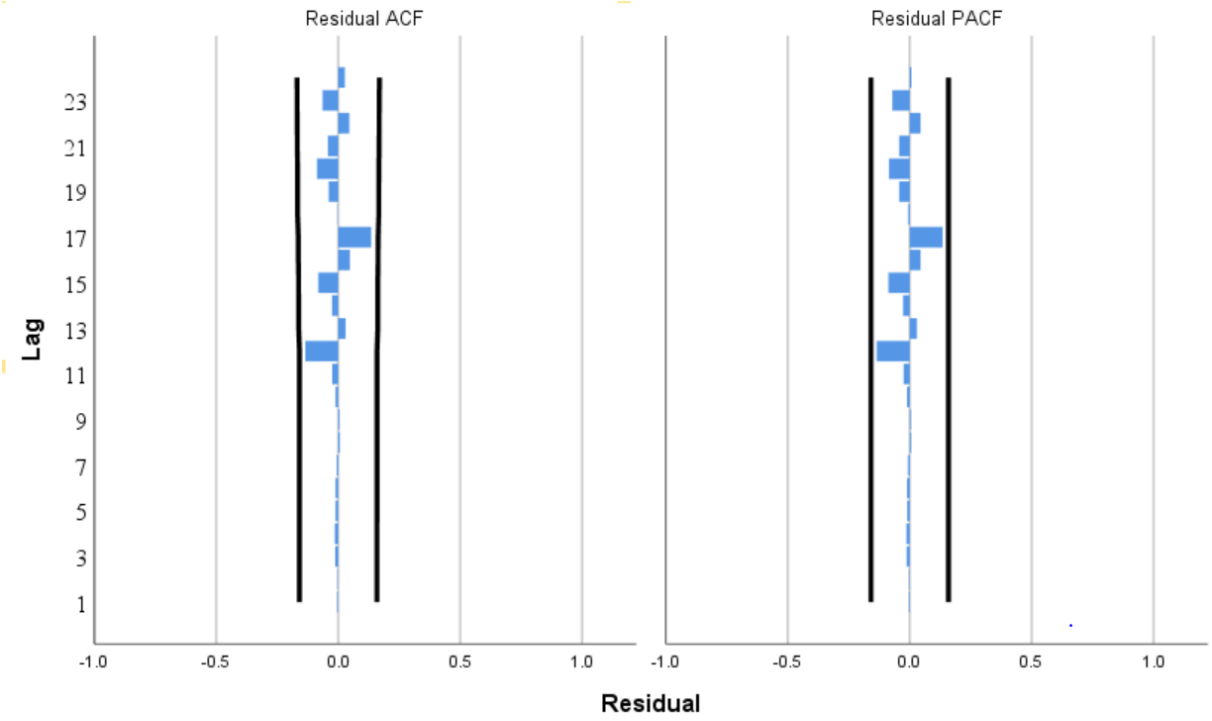

Figure 56 *The results of fitting ARIMA models: (a) (2,1,7) ST1 CO_2 mgl^{-1}-period 4; (b) (0,0,4) WT ^0C-period & (c) (1,1,11) CO_2 mgl^{-1}-period 5.*

The higher differencing was applied with regards to HumST1 CO_2 mgl^{-1}(period 1) time series. The data were natural log transformed and a differencing of the order two was applied to remove autocorrelations. This was successful ($p>0.05$) (Figure 57a). The CO_2 time series from period 2 (HumST1) were natural log transformed and the ARIMA (2,1,5) model was applied to remove autocorrelations. The results of the model were: $R^2 = 0.836$, RMSE = 5.623 and the model was appropriate ($p>0.05$) (Figure 57b). The ARIMA (1,1,7) model was fit to prewhitened (natural log transformed) time series from period 3 (WT HumST1). The model was successful at removing autocorrelations ($R^2 = 0.844$ and RMSE = 5.547; $p>0.05$) (Figure 57c). The ARIMA (1,1,8) model was applied to transformed (natural log) time series from period 4 HumST1 (CO_2 and the water temperature). The model results were $R^2 = 0.897$ and RMSE = 0.614 (WT) and $R^2 = 0.858$ and RMSE = 0.369 (CO_2). The model application was successful in both instances ($p>0.05$) (Figure 57d & e).

a)

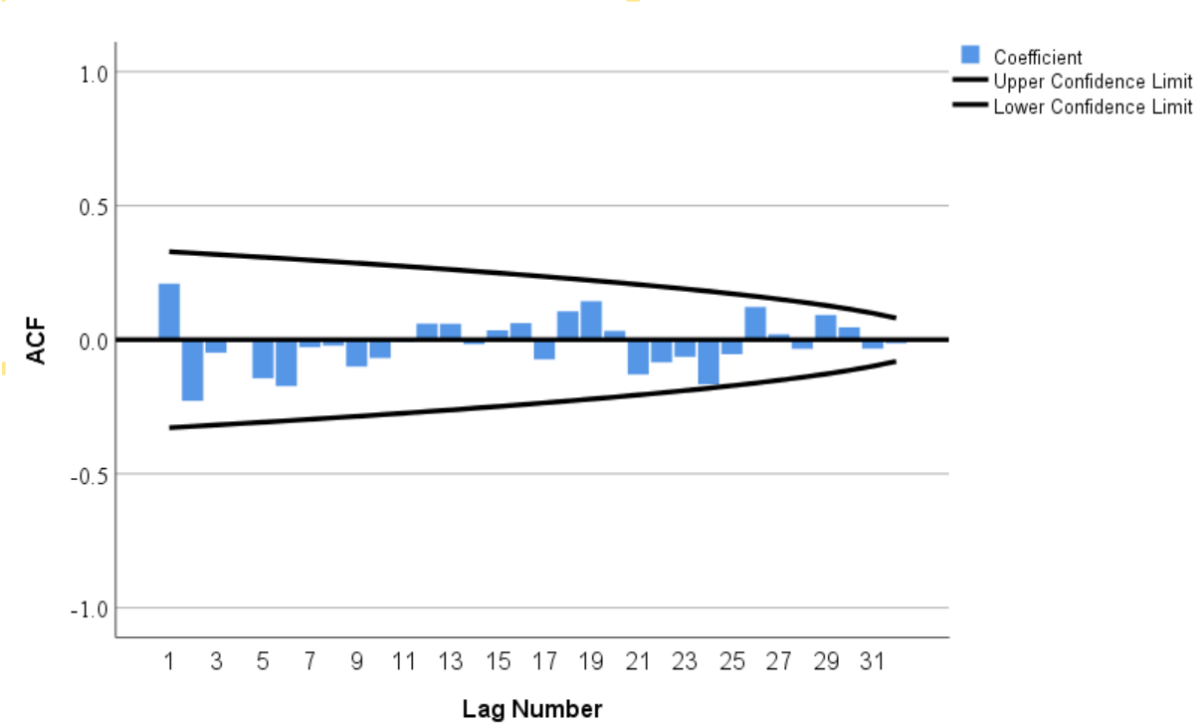

b)

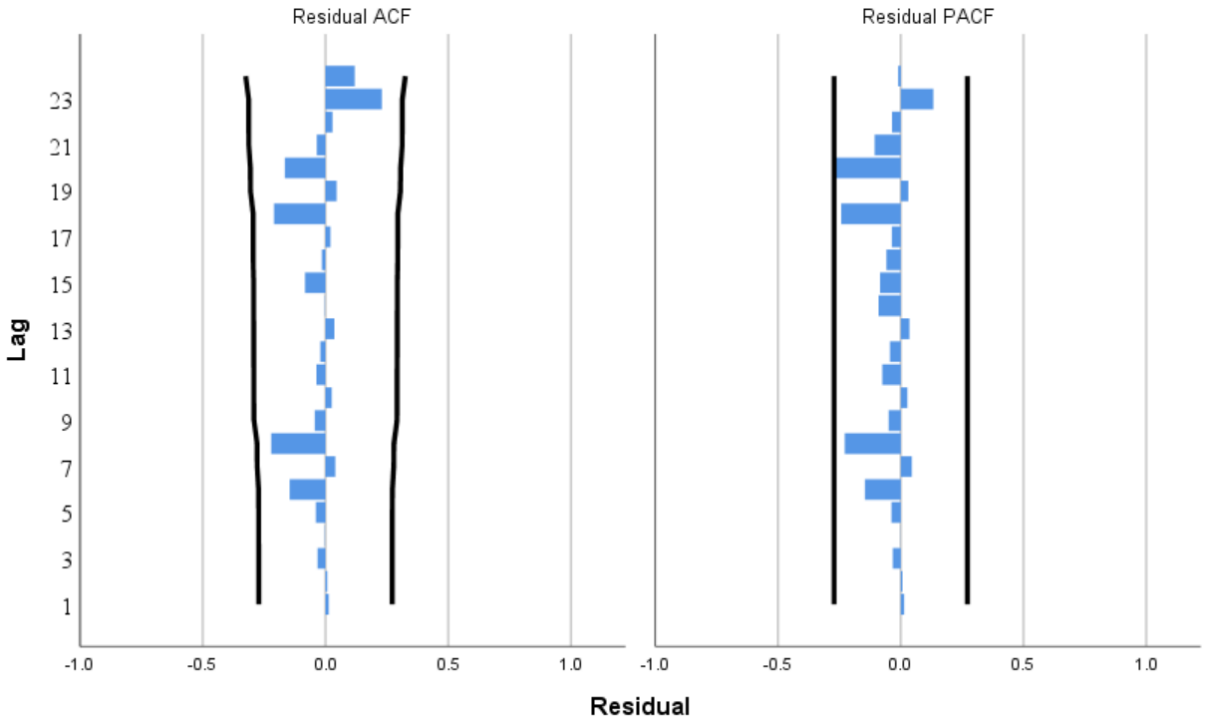
Residual ACF
Residual PACF
Lag
23
21
19
17
15
13
11
9
7
5
3
1
-1.0
-0.5
0.0
0.5
1.0
Residual

c)

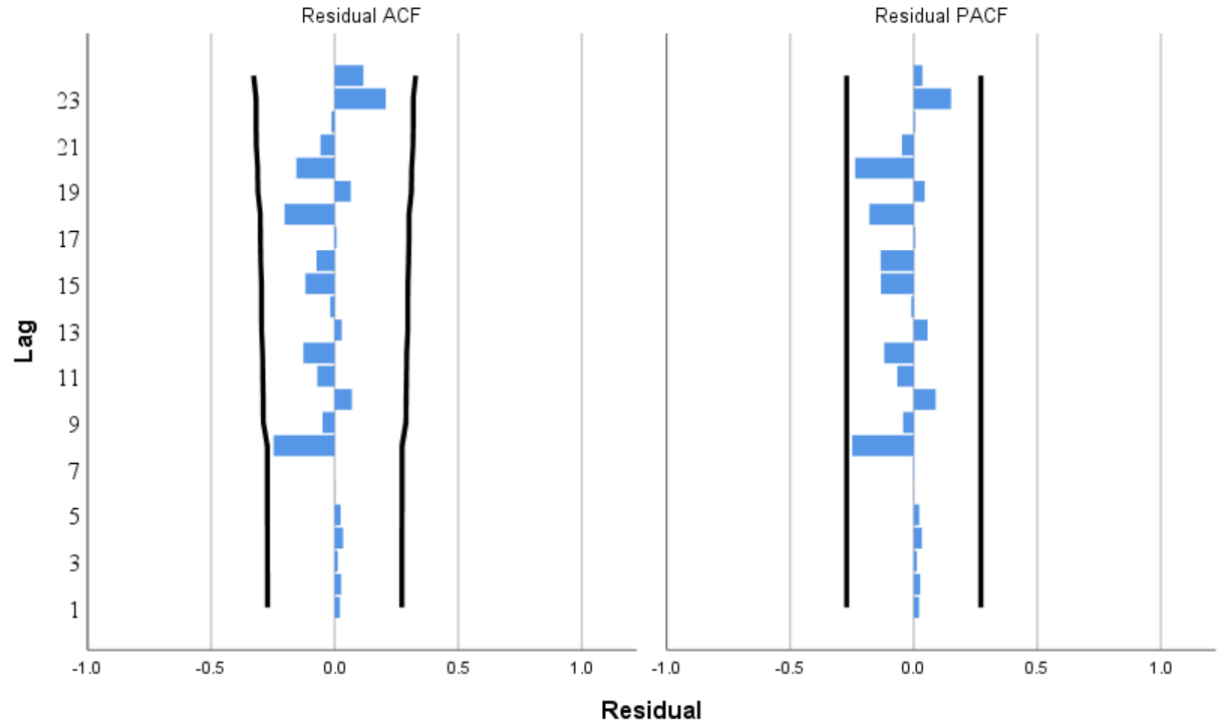
Residual ACF
Residual PACF
Lag
23
21
19
17
15
13
11
9
7
5
3
1
-1.0
-0.5
0.0
0.5
1.0
Residual

d)

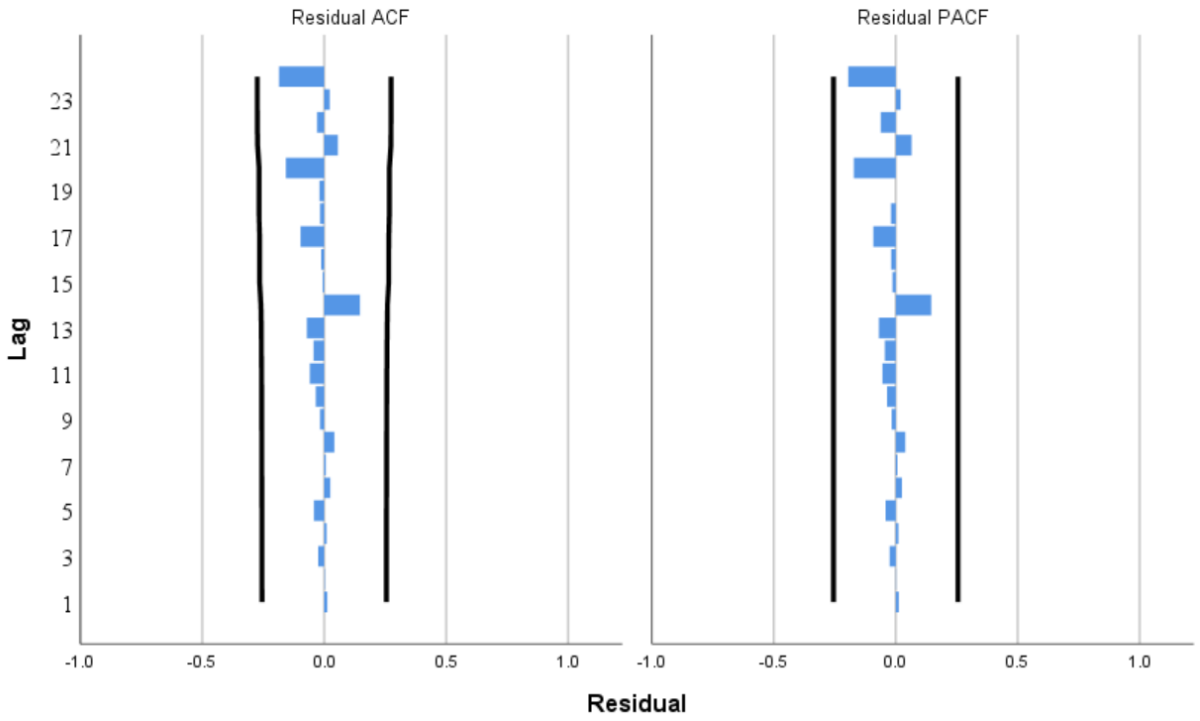

e)

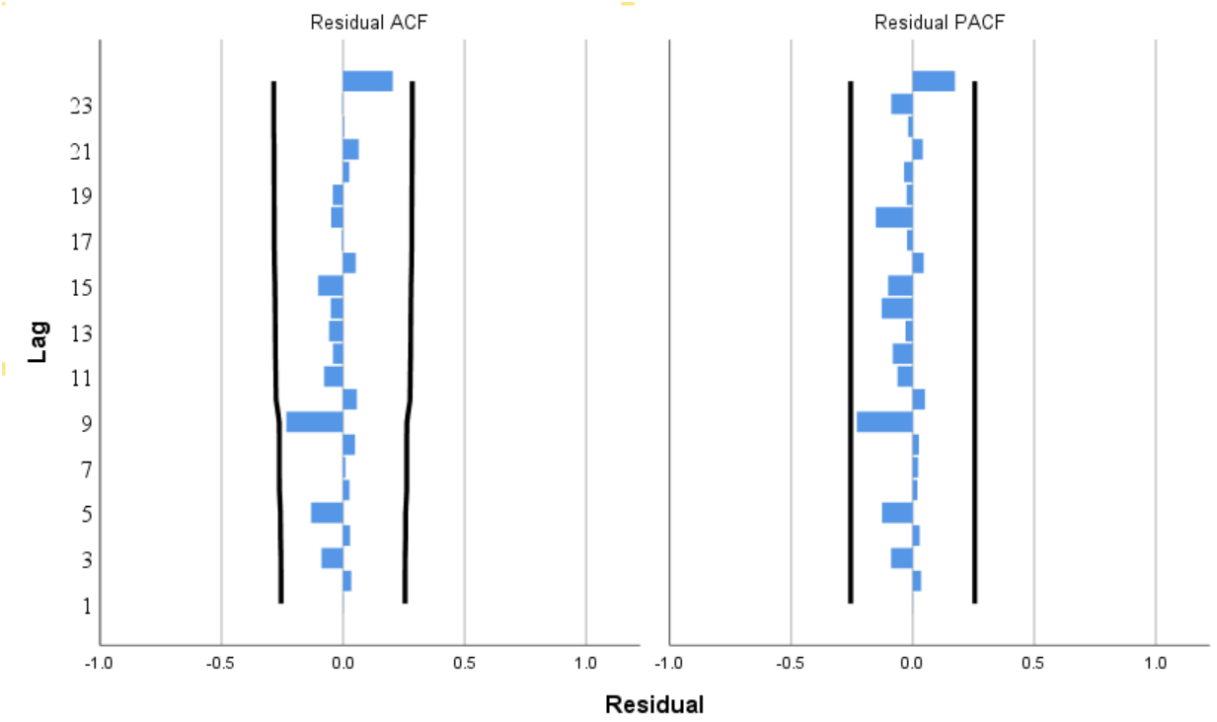

Figure 57 *The results of 2nd order differencing (a) HumST1 CO2 mgl-1- period 1 and the ARIMA model fitting: (b) (2,1,5) HumST1 period 2 CO_2 mgl-1, (c) (1,1,7) WT ^0C*

HumST1 period 3, (d) (1,1,8) WT ^{0}C HumST1 period 4 & (e) (1,1,8) CO_2 mgl^{-1} HumST1 period 4.

The ARIMA (2,1,2) was used to remove autocorrelations from natural log transformed CO_2 and WT times series (ST2, period 1). The results were R^2 = 0.628 (mean) and RMSE = 0.734 (mean). The model application was appropriate in both instances (p>0.05) (Figure 58a). The autocorrelations were removed (P>0.05) from WT times series (ST2, period 2) by transforming data (natural log) and by applying higher order differencing (2). To remove autocorrelations from ST2 CO_2 time series, seasonal difference (1) was applied and then the ARIMA (2,0,0) was fit. The results were indicative that the model was appropriate (p>0.05): R^2 = 0.256 and RMSE = 0.063 (Figure 58b). The ARIMA (2,1,8) model was fit to remove autocorrelations from natural log transformed time series of CO_2 from ST2 (period 3), this model was appropriate (p>0.05) (Figure 58c). The model results were R^2 = 0.966 and RMSE = 0.341. The autocorrelations were removed (P>0.05) from WT times series (ST2, period 3) by transforming data (natural log) and by applying the differencing (1). Both ST2 (WT and CO_2) time series sets were natural log transformed, then seasonal difference (1) was applied prior to model application. The ARIMA (0,0,0) and (0,0,1) models were applied to CO_2 and WT time series to remove autocorrelations. Each model was successful at eliminating autocorrelations (p>0.05): R^2 = 0.078 (mean) and RMSE = 0.700 (mean). The ARIMA models were used to remove autocorrelations from wind speed time series (period 2) and CO_2 flux at ST1 (periods 2 and 5). In each case the time series were prewhitened (natural log transformed). The following ARIMA models were applies (1,0,1)-wind speed and CO_2 flux from period 2 time series and (1,1,2) – CO_2 flux (period 5). The models were appropriate (p>-0.05) at eliminating autocorrelations and the results were R^2 = 0.118, 0.043 and 0.196 (the order of time series

as above) and RMSE =1.504, 0.259 and 0.161. The wind speed time series from period 3 were just prewhitened (natural log transformation) and that was enough to remove autocorrelations ($p>0.05$). The CO_2 flux time series (periods 3 and 4) were prewhitened (natural log transformation) and the difference (1) was applied. In each case the autocorrelations were removed ($p>0.05$) as results of these adjustments.

a)

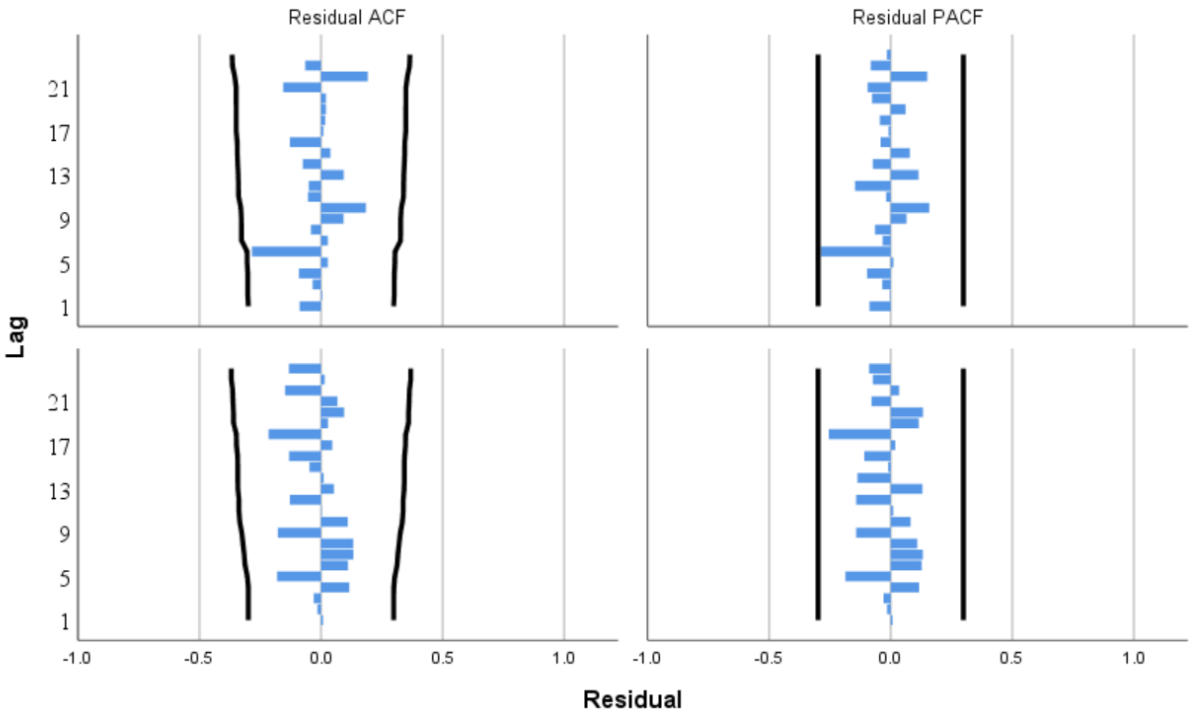

b)

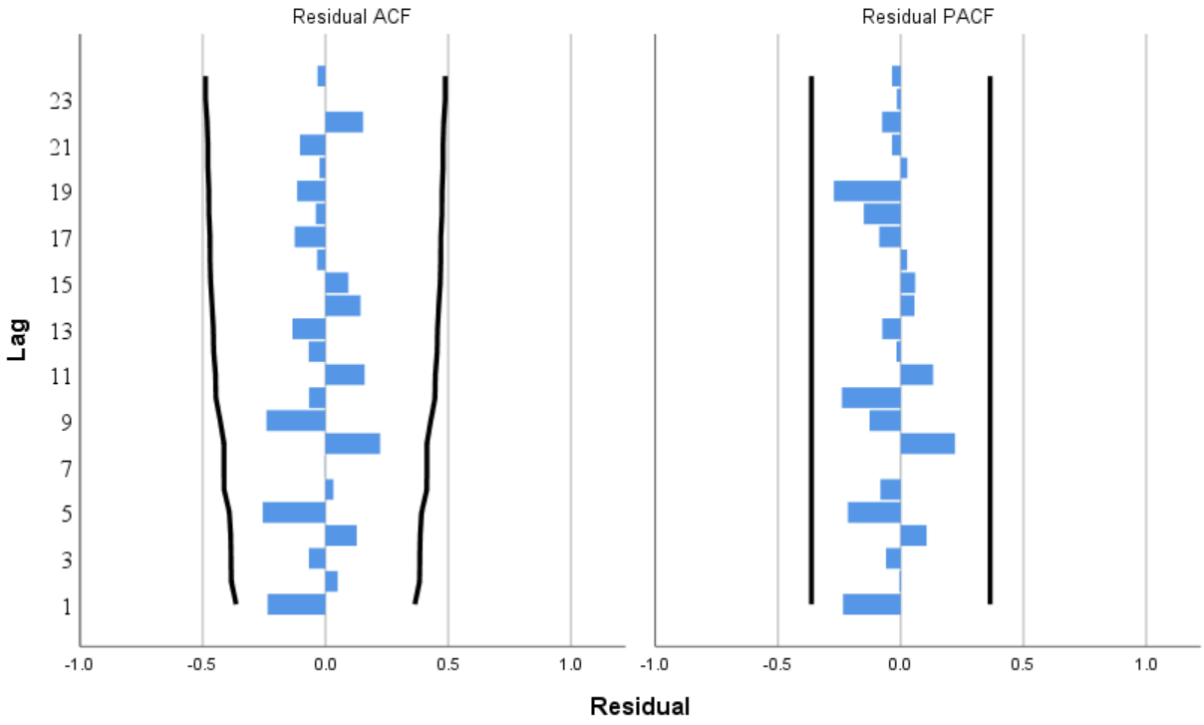
Residual ACF
Residual PACF
Lag
23
21
19
17
15
13
11
9
7
5
3
1
-1.0
-0.5
0.0
0.5
1.0
Residual

c)

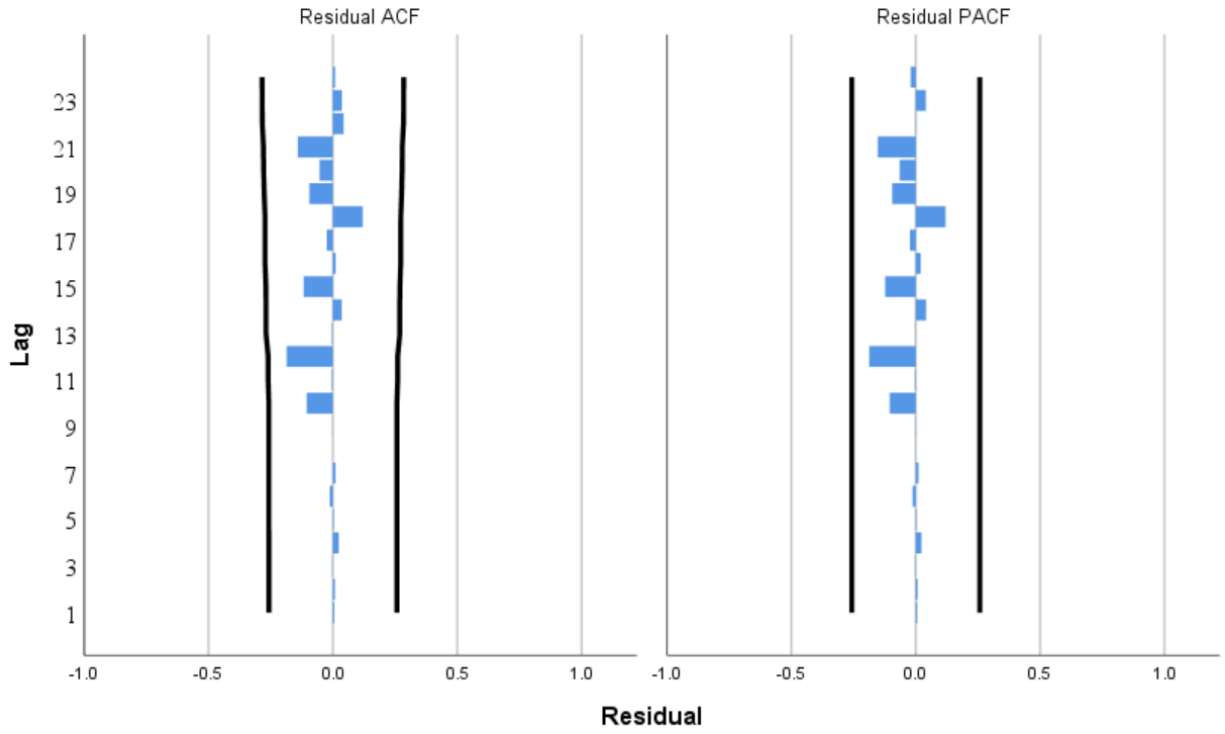

Figure 58 *The results of ARIMA modelling: (a) (2,1,2) ST2 period 1 (top -CO_2; bottom WT); (b) (2,0,0) ST2 period 2 (CO_2) & (c) (2,1,8) ST2 CO_2 period 3. NB: CO_2 mgl^{-1} & WT ^0C.*

The WT time series at ST3 (period 1) were transformed (natural log) and the higher order differencing (2) was applied to remove autocorrelations. The outcome was positive ($p>0.05$). Both CO_2 and WT time series from ST3 (period 2) were transformed (natural log), then the ARIMA models (1,1,13) and (2,1,5) were applied to remove autocorrelations. Both models were appropriate ($p>0.05$) (Figure 59a & b). The results were: R^2 = 0.849 and 0.733 (CO_2 and WT) and RMSE = 0.082 and 1.446. The ARIMA (1,1,8) model was applied to the transformed (natural log) LawnST2 (CO_2) time series from period 1. The results were: R^2 = 0.930 and RMSE = 0.929 ($p>0.05$), the model was appropriate (Figure 59c). The HumST3 CO_2 (period 1) time series were transformed

(natural log) and then ARIMA (1,1,1) model was applied to remove autocorrelations. The model application was successful (p>0.05). The results were: R^2 = 0.749 and RMSE = 20.145. The air temperature, air pressure and soil temperature time series were prewhitened (seasonal differencing of order1 – air temperature and natural log transformed – air pressure and the soil temperature). Then the following ARIMA models were applied: (1,0,1) – air temperature, (2,1,7) – air pressure and (1,1,5) – soil temperature. All models were appropriate (p>0.05) (Figure 59d-f). The model results were: R^2 = 0.184, 0.753 and 0.726 and RMSE = 2.243, 6.829 and 1.147 (air temperature, air pressure and the soil temperature).

a)

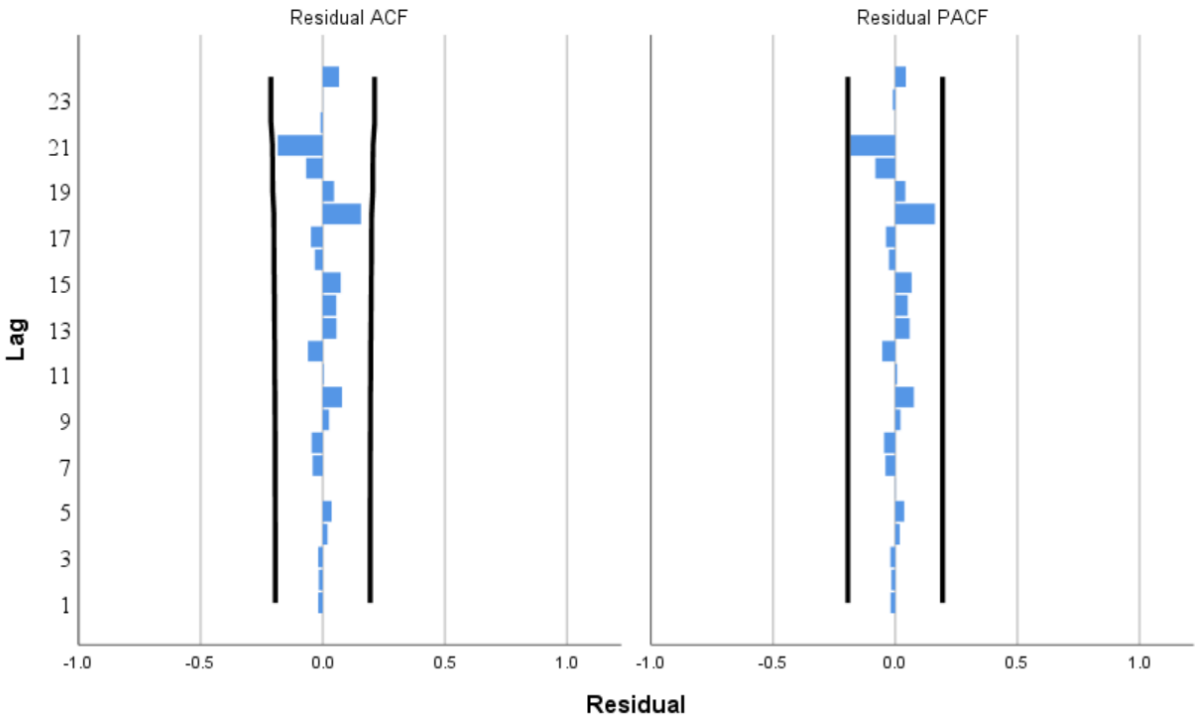

b)

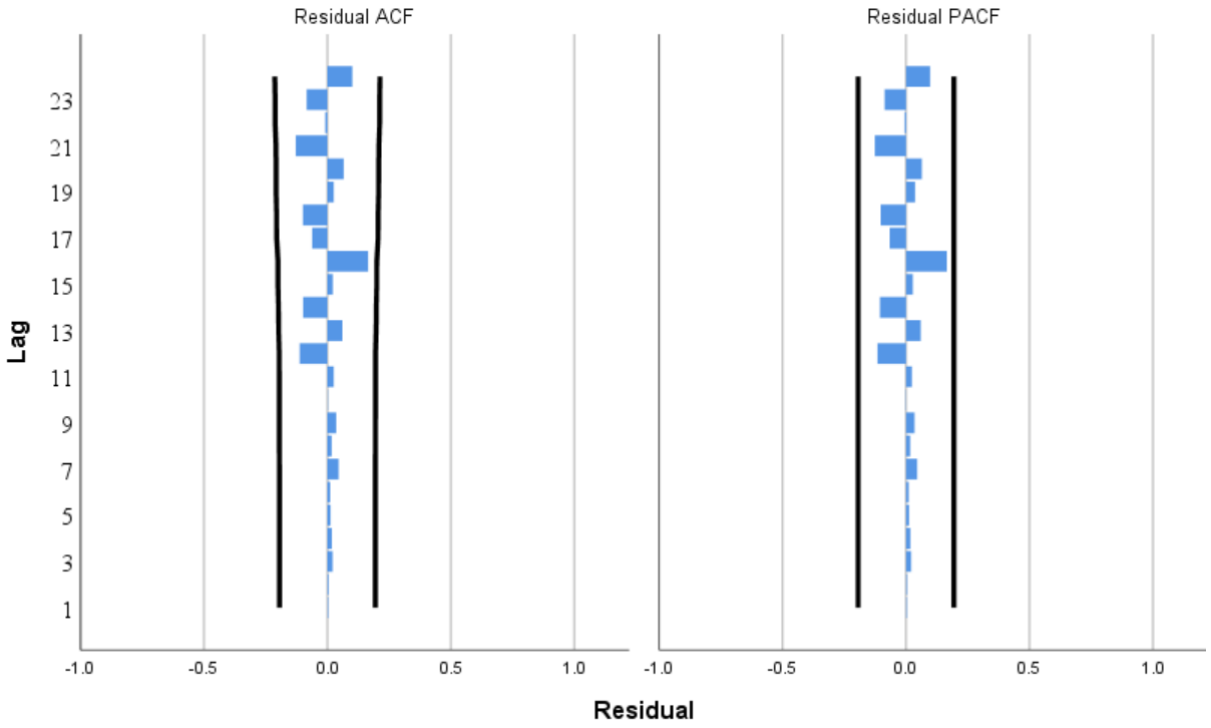
Residual ACF
Residual PACF
Lag
23
21
19
17
15
13
11
9
7
5
3
1
-1.0
-0.5
0.0
0.5
1.0
Residual

c)

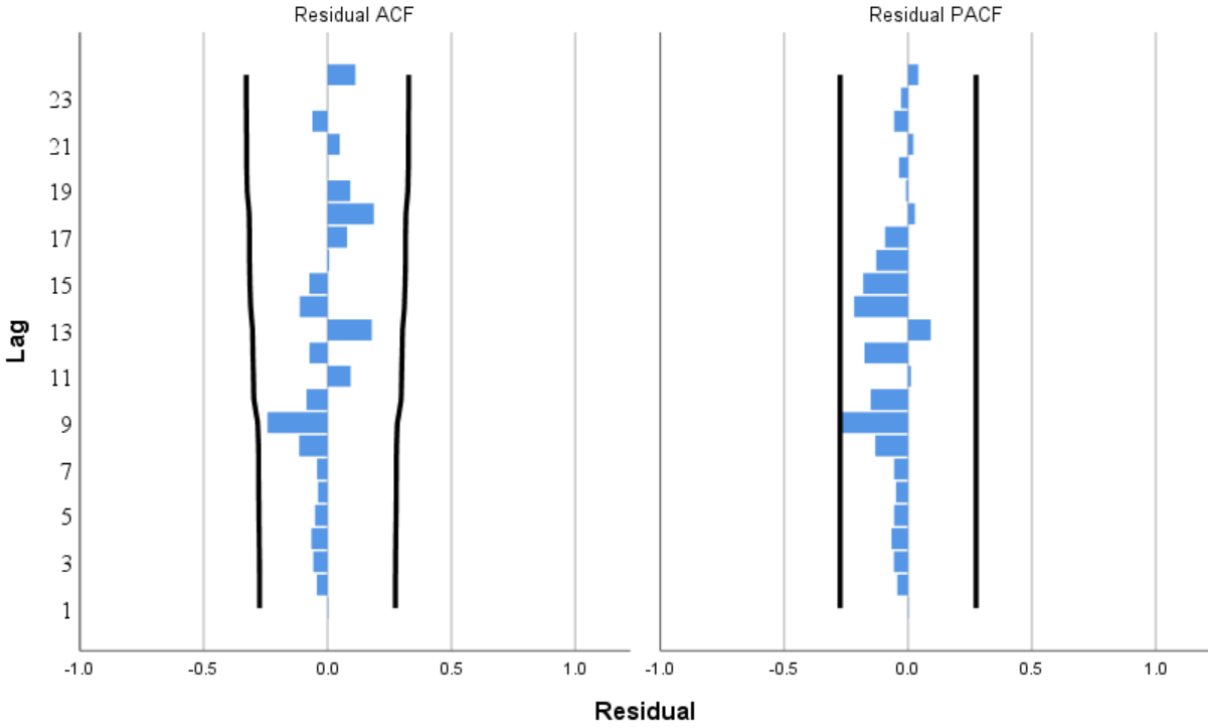
Residual ACF
Residual PACF
Lag
23
21
19
17
15
13
11
9
7
5
3
1
-1.0
-0.5
0.0
0.5
1.0
Residual

d)

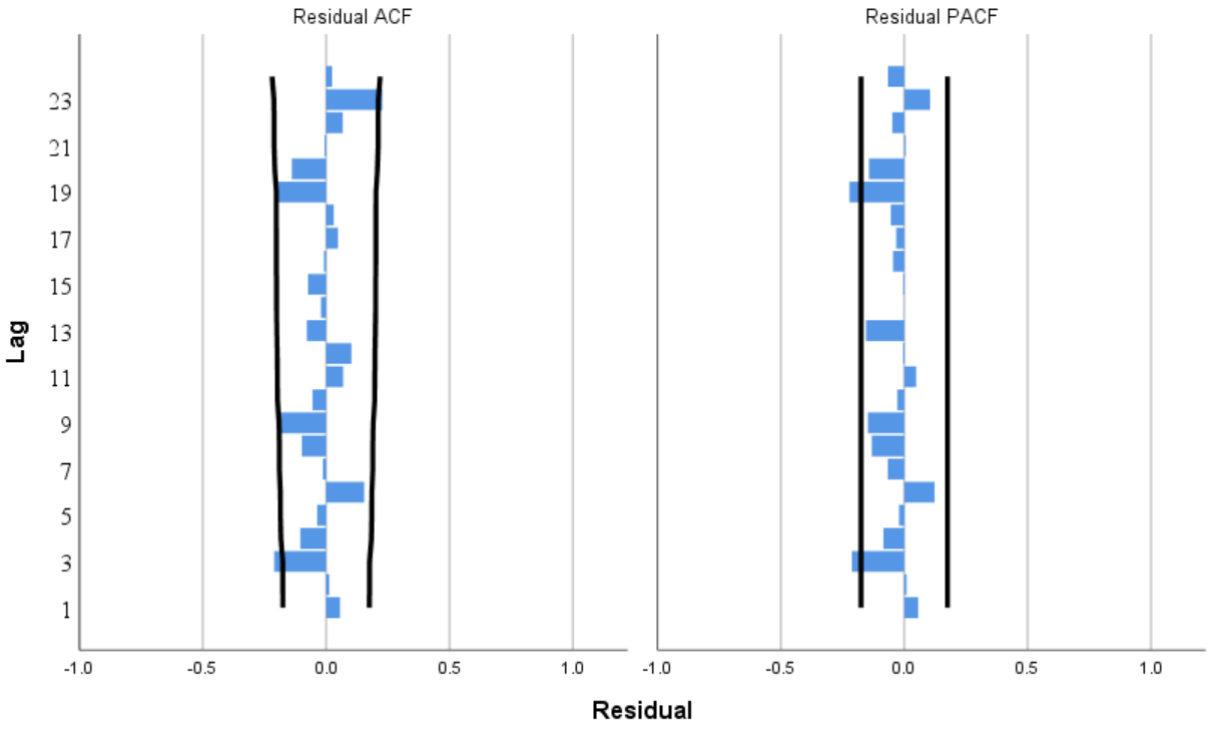
Residual ACF
Residual PACF
Lag
23
21
19
17
15
13
11
9
7
5
3
1
-1.0
-0.5
0.0
0.5
1.0
Residual

e)

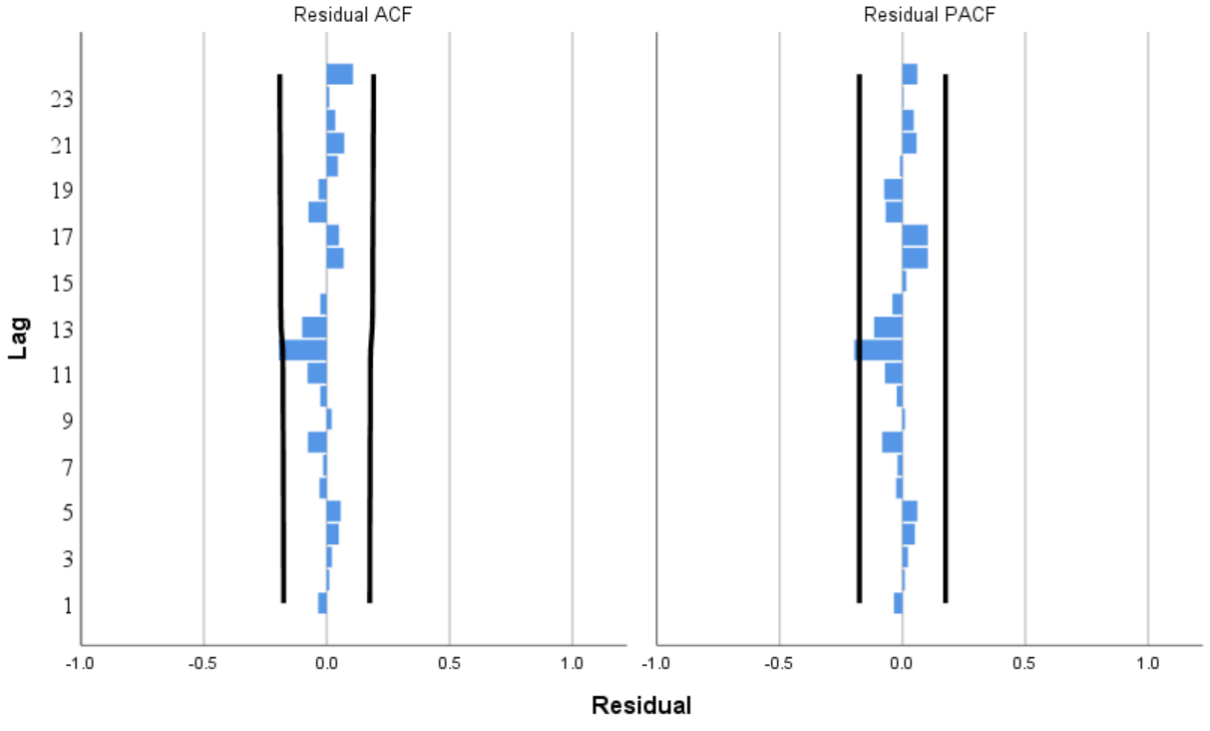
Residual ACF
Residual PACF
Lag
23
21
19
17
15
13
11
9
7
5
3
1
-1.0
-0.5
0.0
0.5
1.0
Residual

f)

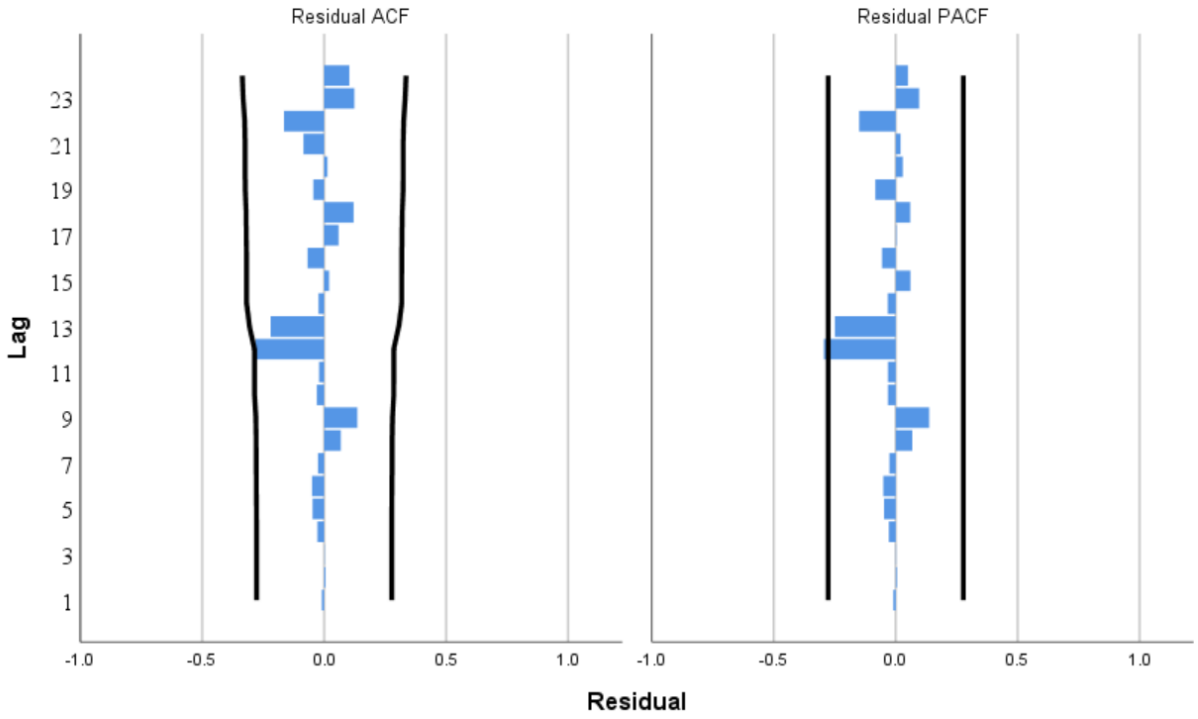

Figure 59 *The results of the ARIMA models fitting: (a) & (b) ST3 period 2 CO_2 mgl^{-1}(1,1,13) and WT ^0C period 2 ST3 (2,1,5); (c) LawnST2 CO_2 mgl^{-1}period 1 (1,1,8); (d) Air temperature ^0C (1,0,1); (e) The air Pressure hPa (2,1,7) and (f) The soil temperature ^0C (1,1,5).*

4.5 CO_2 concentrations

CO_2 concentrations were measured in blanket peatland pools (ST1-ST3), hummocks (HumST1 & HumST3) and a lawn (LawnST2) from 2016 until 2018 as per methods (Study sites) (Table 6; Figure 60; Table 8Table **33**– Appendix B). Average concentrations of CO_2 between years 2016-2018 were 0.63 mgl^{-1} [C] (ST1) and 41.36 mgl^{-1} [C] (HumST1). Winter levels of CO_2 (ST1-ST3, HumST1, LawnST2 and HumST3) were monitored and graphed (Figure 60-61; Table 6). November, December and January (2016 & 2017) CO_2 concentrations (ST1-3) were on average between 0.44±0.01 (SE-standard error) mgl^{-1} [C] and 0.58±0.08 mgl^{-1} [C] (Table 6). The ST1 levels recorded in December 2016 were significantly higher ($p<0.05$) than in January 2017 (Table 8 - Appendix B). The following levels were measured between January and March 2018: 1.14±0.04 mgl^{-1} [C] and 1.38±0.04 mgl^{-1} [C] at ST1 and ST2 (Table 6). Higher average concentrations ($P<0.05$) were recorded in March 2018 (ST1-ST2) then in January - February (Figure 60(a) & 61). This sudden elevation of CO_2 gas (Figure 60(a) & 61) could be potentially linked with pressure build up and entrapment of gas under ice. HumST1 CO_2 concentrations were varying substantially throughout the monitoring period (Table 6). Levels were significantly lower ($p<0.05$) in December 2016, comparing to January 2017 (combined average of 26.24±2.33 mgl^{-1} [C]), then substantially higher in December 2017 (average of 292.12±1.74 mgl^{-1}) (Table 6; Figure 60b,c & 62). In 2018 (January-March), levels of CO_2 were on average 4.14±0.05 mgl^{-1} [C] at HumST1 (Table 6). Levels at LawnST2 & HumST3 were lower than at HumST1 between months of November-December 2017 (1.00±0.02 and 85.74±1.53 mgl^{-1} [C]) (Table 6). Wintertime (2016-2018) $epCO_2$ values at ST1-ST2, HumST1, LawnST2 and HumST3 were >1. Wintertime CO_2 levels from all stations were compared statistically. Significantly higher ($P<0.05$) quantities were measured in HumST1, LawnST2 and HumST3 comparing to ST1-ST3.

***Table** 6 Summary of CO_2 concentrations (winter periods 2016-2018). Averages across ST1-ST3 and HumST1, LawnST2 and HumST3.*

Sample	Winter 2016-2018		
	December-January 2016-2017	November-December 2017	January-March 2018
ST1 CO_2/mgl^{-1} [C]	0.44±0.01 (SE-standard error)	0.51±0.06	1.14±0.04
ST2 CO_2/mgl^{-1}[C]		0.58±0.08	1.38±0.04
ST3 CO_2/mgl^{-1}[C]		0.44±0.11	
HumST1 CO_2/mgl^{-1}[C]	26.24±2.33	292.12±1.74	4.14±0.05
LawnST2 CO_2/mgl^{-1}[C]		1.00±0.02	
HumST3 CO_2/mgl^{-1}[C]		85.74±1.53	

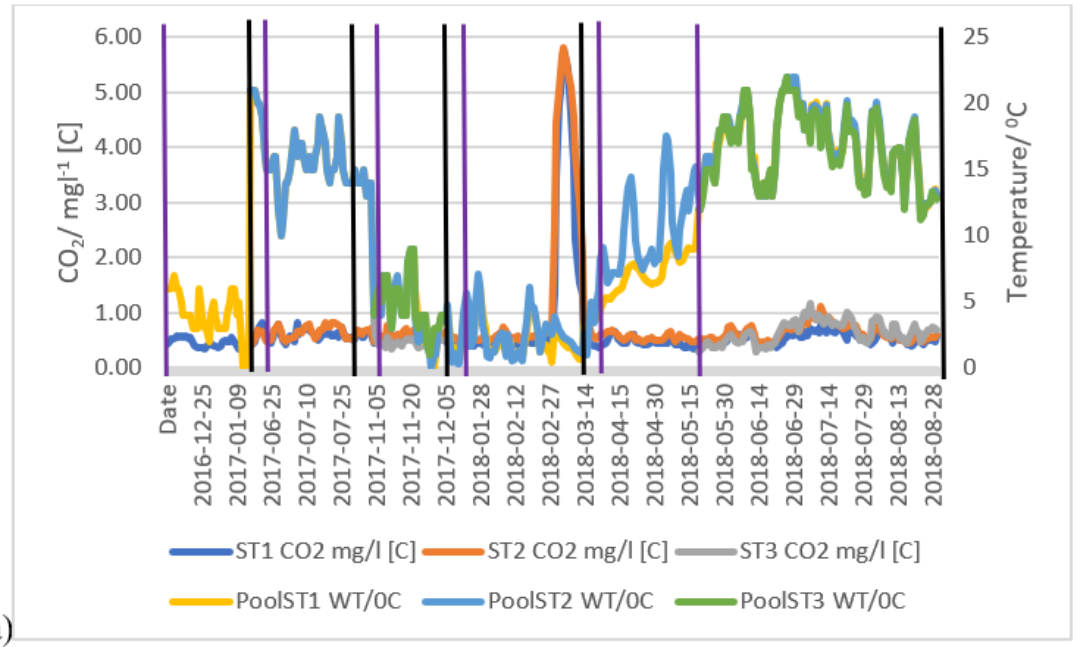
6.00
5.00
4.00
3.00
2.00
1.00
0.00
CO_2/ mgl^{-1} [C]
25
20
15
10
5
0
Temperature/ °C
Date
2016-12-25
2017-01-09
2017-06-25
2017-07-10
2017-07-25
2017-11-05
2017-11-20
2017-12-05
2018-01-28
2018-02-12
2018-02-27
2018-03-14
2018-04-15
2018-04-30
2018-05-15
2018-05-30
2018-06-14
2018-06-29
2018-07-14
2018-07-29
2018-08-13
2018-08-28
ST1 CO2 mg/l [C]
ST2 CO2 mg/l [C]
ST3 CO2 mg/l [C]
PoolST1 WT/0C
PoolST2 WT/0C
PoolST3 WT/0C

a)

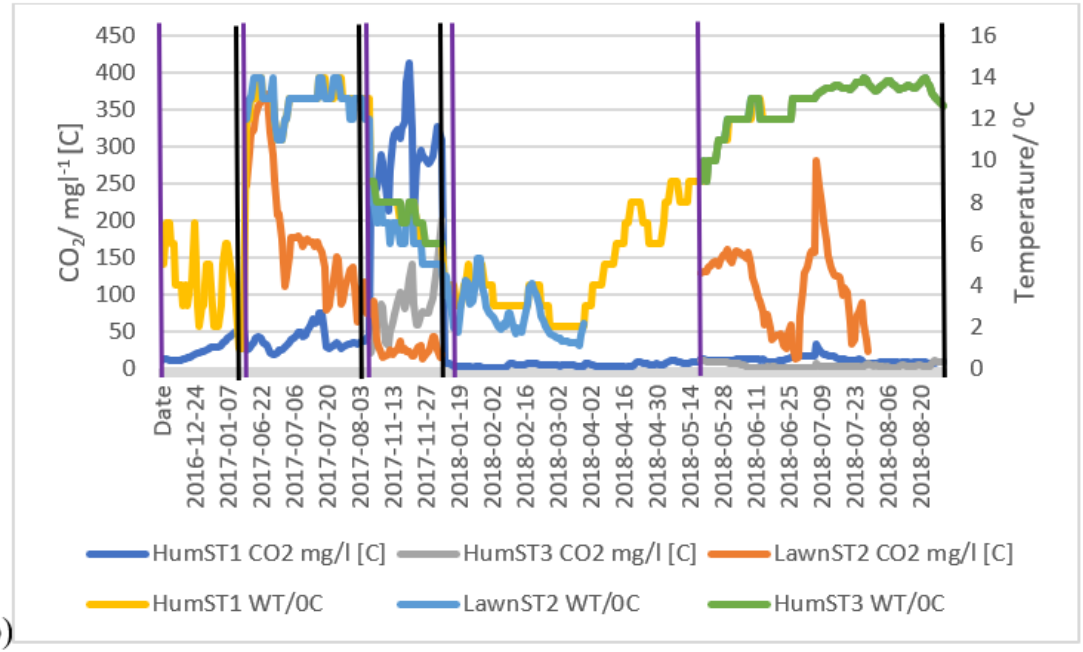
450
400
350
300
250
200
150
100
50
0
CO_2/ mgl^{-1} [C]
16
14
12
10
8
6
4
2
0
Temperature/ °C
Date
2016-12-24
2017-01-07
2017-06-22
2017-07-06
2017-07-20
2017-08-03
2017-11-13
2017-11-27
2018-01-19
2018-02-02
2018-02-16
2018-03-02
2018-04-02
2018-04-16
2018-04-30
2018-05-14
2018-05-28
2018-06-11
2018-06-25
2018-07-09
2018-07-23
2018-08-06
2018-08-20
HumST1 CO2 mg/l [C]
HumST3 CO2 mg/l [C]
LawnST2 CO2 mg/l [C]
HumST1 WT/0C
LawnST2 WT/0C
HumST3 WT/0C

b)

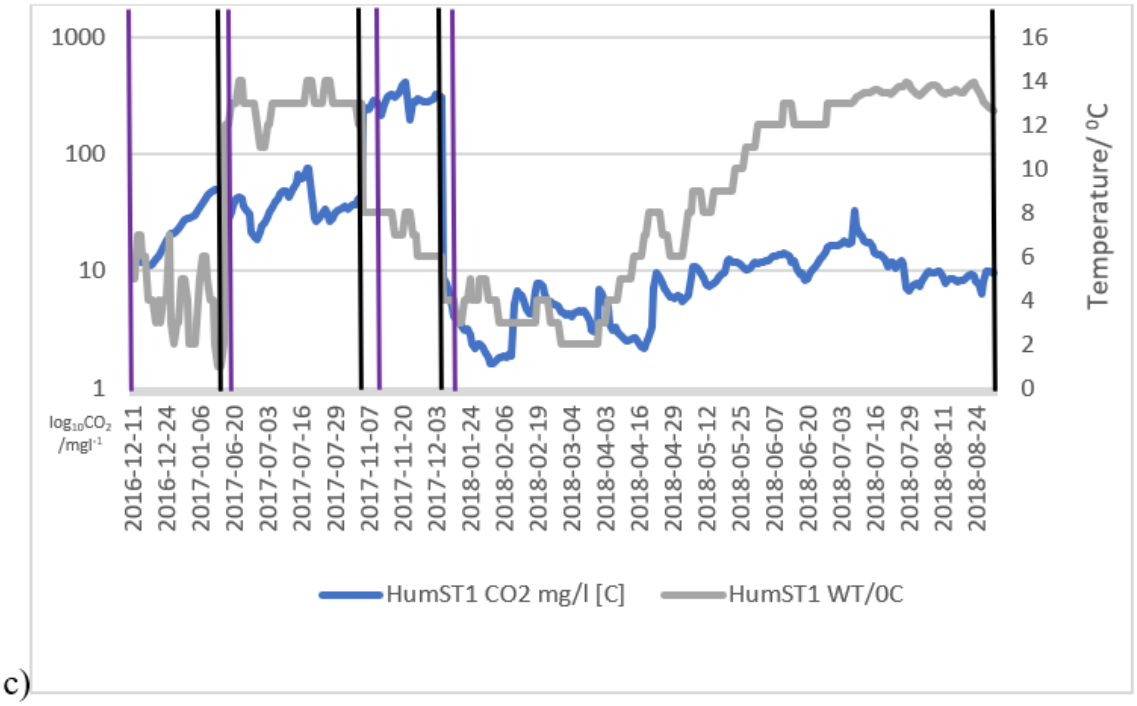

c)

Figure 60 *Showing continuous CO_2 and water temperature data from: a) ST1-3; b) HumST1, LawnST2 and HumST3; c) HumST1. Monitoring periods are indicated on graphs: vertical purple lines – beginning & black lines - ending of study periods.*

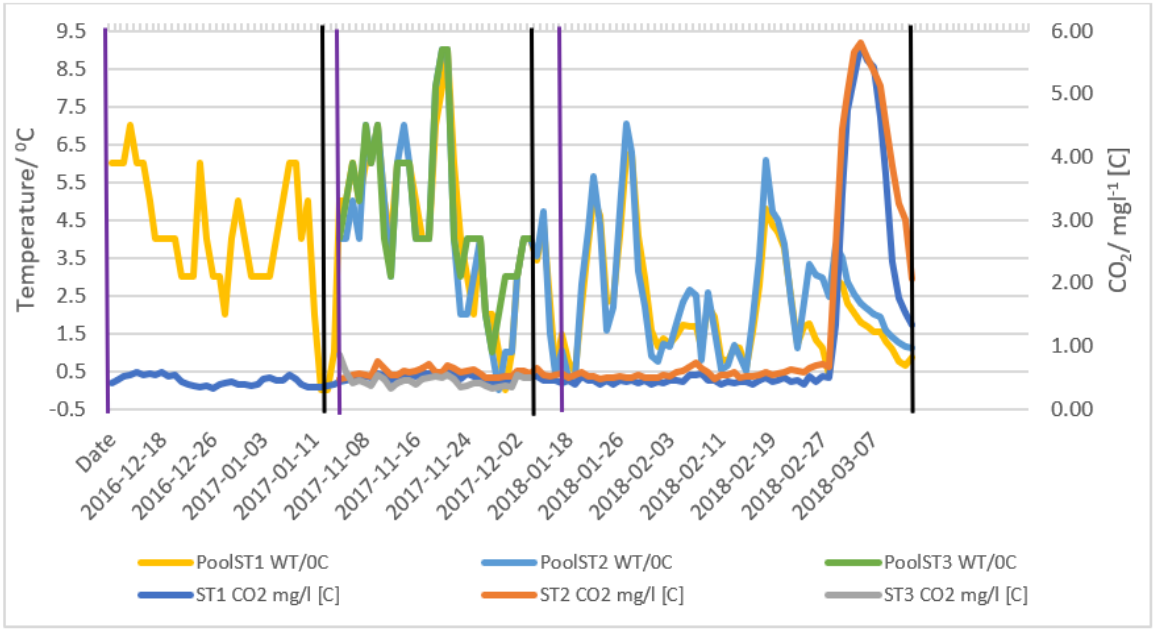

Figure 61 *Showing winter concentrations of CO_2 along with trends in water temperatures from ST1-3 (year 2016-2018).*

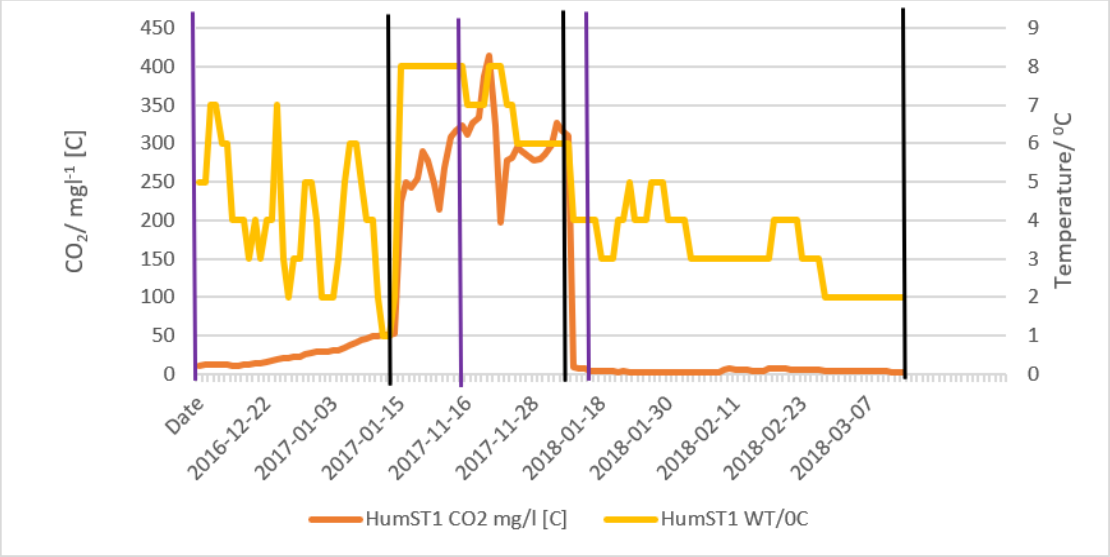

Figure 62 *Showing winter concentration of CO_2 along with trends in water temperature from HumST1 (year 2016-2018).*

Summertime trends of CO_2 across all stations were recorded between years 2017-2018 (Figure 63). The CO_2 concentrations (averages) data are presented in Table 7. Across all conditions there was variability (Table 7). ST1 and 2 CO_2 levels (on average) did not vary substantially in summer months of 2017 (Table 7; Figure 63a). Slightly lower levels were recorded between April and July 2018 (ST1-ST3) comparing to 2017 data (Table 7). Comparison of monthly trends across ST1-3 (May-June 2018) indicated significantly higher ($P<0.05$) levels of CO_2 in June (Figure 63a). The average levels of CO_2 in July-August 2018 were comparable with 2017 averages (Table 7). July levels (ST1-ST3) were higher than August concentrations (Figure 63a). Highest average level was recorded at ST3 (0.71 ± 0.25 mgl^{-1} [C]) during July-August 2018 period (Table 7; Figure 63a). In case of peat soil water average values of CO_2, both HumST1 and LawnST2 exhibited similar pattern where levels were higher in summer months of 2017, lower in early spring-

summer months of 2018 and higher again towards end of summer 2018 (Table 7; Figure 63b). HumST3 CO_2 data (averages) in both summer periods of 2018 did not differ substantially (Table 7; Figure 63b). Highest values were recorded at HumST1 (38.12±0.37 (SE) mgl^{-1} [C] – 2017) (Table 7; Figure 63b).

Comparison of monthly data sets (LawnST2) indicated that in year 2017, CO_2 concentrations were significantly higher ($P<0.05$) in June than in July (Figure 63b). Between April and June 2018 concentrations were significantly higher ($P<0.05$) in June comparing to April-May (HumST1). LawnST2 and HumST3 concentrations were higher in May comparing to June. HumST1 July CO_2 levels were higher than August concentrations (Figure 63b). Opposite was recorded at HumST3, where levels were lower in July. epCO_2 values were >1 across all conditions (Figure 63). The only one period where epCO_2<1 was between 21st of May and the 14th of June 2018 (ST3) (Figure 64). Comparison of CO_2 average levels from pools (ST1-ST3) and peat soils (HumST1, LawnST2 and HumST3) suggested that peat pore waters contained significantly ($P<0.05$) higher concentrations of CO_2 between June-July 2017 and April-August 2018 periods (Figure 65).

Table 7 *Summary of CO_2 concentrations (summer periods 2017-2018). Averages across ST1-ST3 and HumST1, LawnST2 and HumST3.*

Sample	Summer 2017-2018		
	June-July 2017	April-July 2018	July-August 2018
ST1 CO_2/mgl^{-1} [C]	0.59±0.13 (SD – standard deviation)	0.48±0.11	0.57±0.15
ST2 CO_2/mgl^{-1}[C]	0.63±0.11(SD)	0.58±0.16	0.66±0.23
ST3 CO_2/mgl^{-1}[C]		0.55±0.26	0.71±0.25
HumST1 CO_2/mgl^{-1}[C]	38.12±0.37 (SE)	9.37±0.09	11.22±0.14
LawnST2 CO_2/mgl^{-1}[C]	6.52±0.44 (SE)	3.81±0.05	4.20±0.10
HumST3 CO_2/mgl^{-1}[C]		3.74±0.11	3.94±0.06

a)

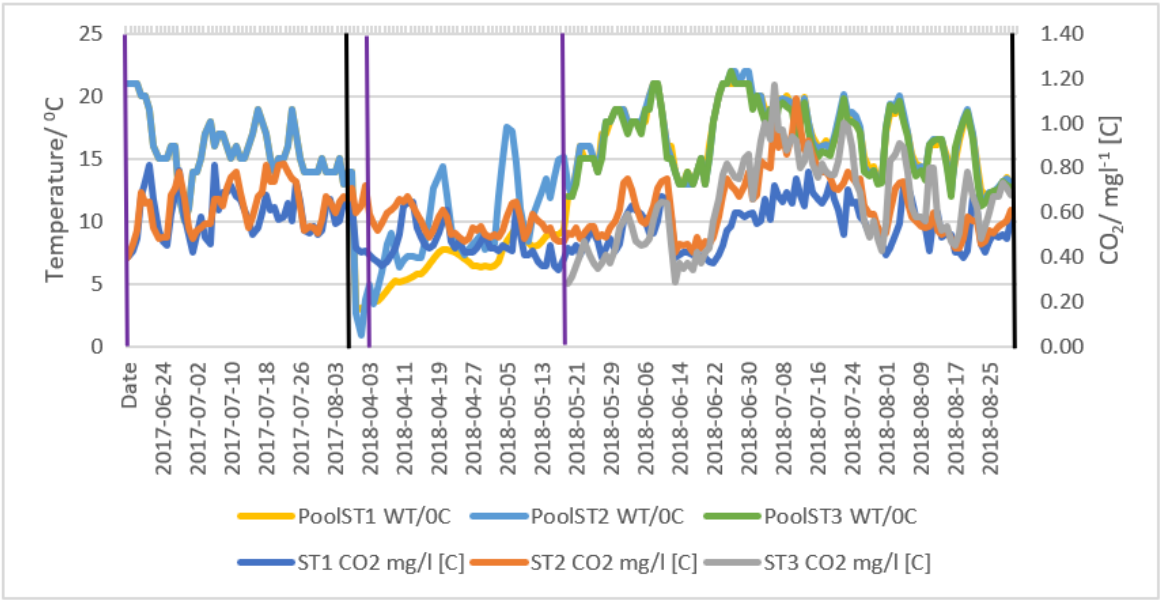

b)

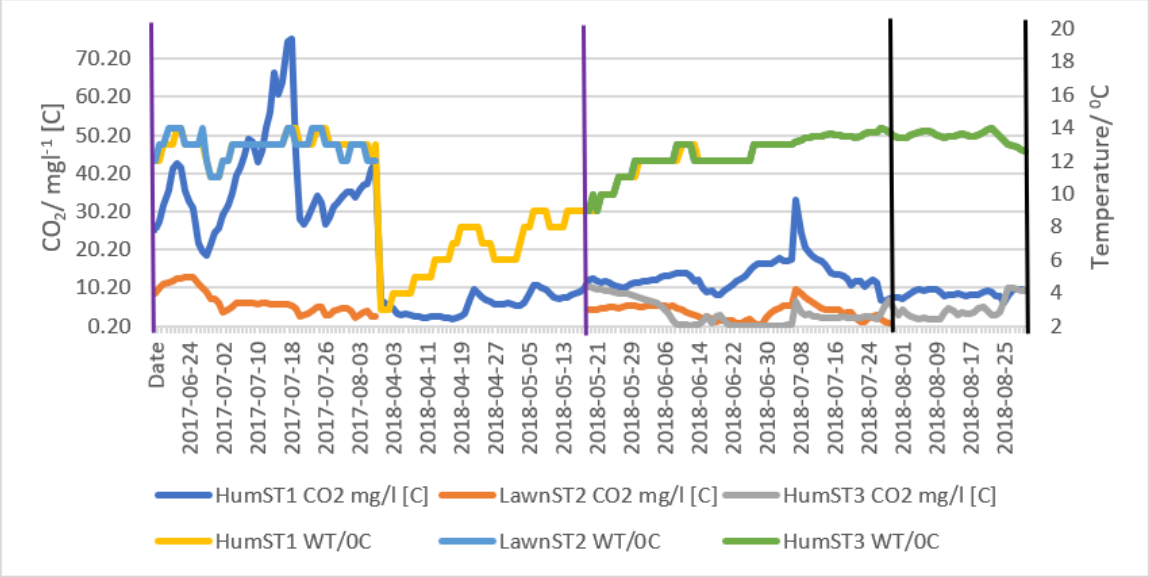

Figure 63 *Showing summer CO_2 trends and water temperature data from: a) ST1-3; b) HumST1, LawnST2 and HumST3.*

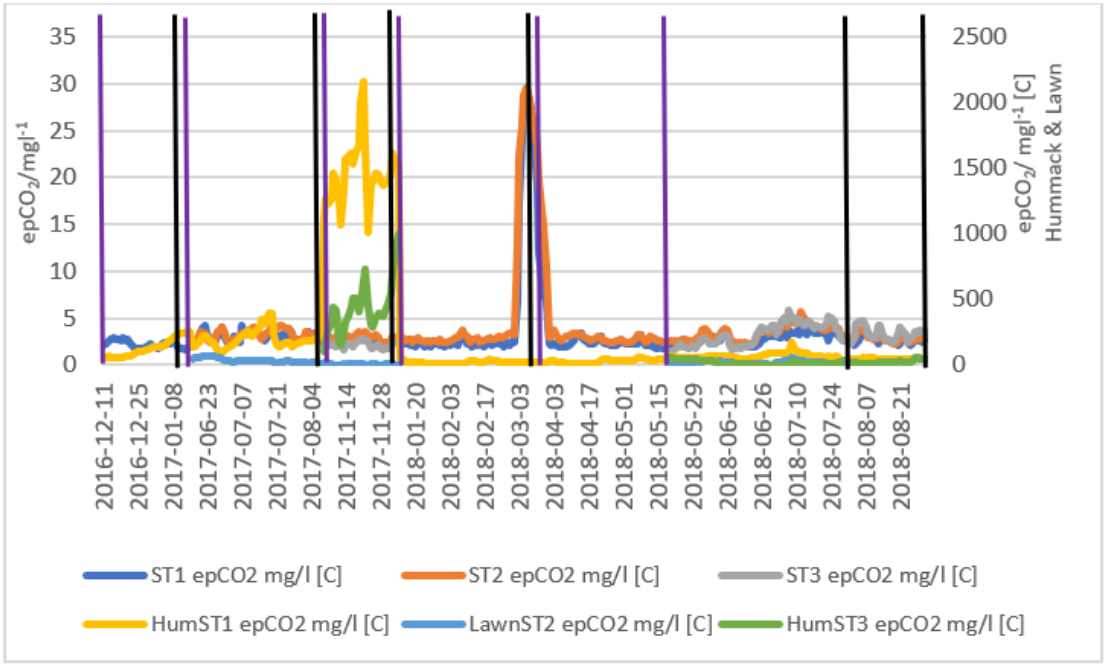

Figure 64 *Showing $epCO_2$ values across ST1-3 & HumST1, LawnST2 and HumST3.*

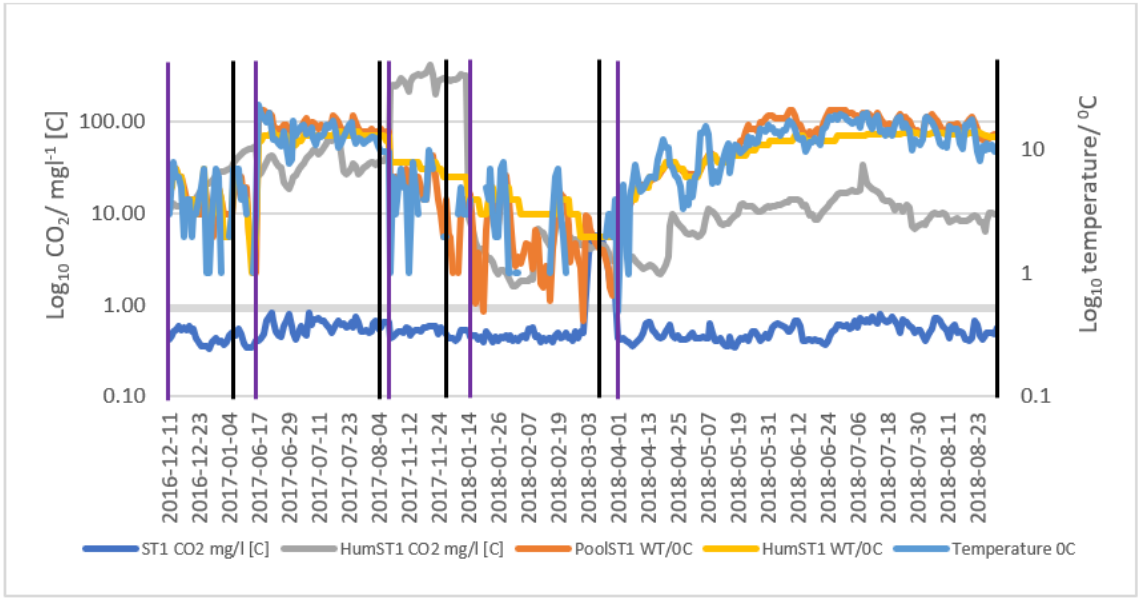

Figure 65 *Showing extent of CO_2 concentration difference between ST1 and HumST1 between years 2016-2018 along with changes in water and air temperatures.*

4.6 The cross-correlation analysis: WT and CO_2 levels comparison

Relationship between water temperature and CO_2 levels (adjusted time series with no autocorrelations) was analysed applying the cross-correlation method. The CO_2 time series from ST1-ST3 and HumST1, LawnST2 and HumST3 were plotted against the corresponding water temperatures. The ST1 CO_2 time series (periods 1-3) were cross-correlated with WT ST1 (periods 1-3). The cross-correlation test results were indicative that WT ST1 was weakly correlated (0.269) with ST1 CO_2 with a lag of -21 (95% confidence level) (Figure 66a). The correlation was positive. Therefore, increases and or decreases of WT were weakly correlated with increases or decreases of ST1 CO_2 with a delay of 20 days. There was also another weak negative correlation (-0.208). Where increases and or decreases of WT were weakly correlated with decreases or increases of ST1 CO_2 with a delay of 6 days. When period 4 times series (ST1) were cross-correlated, all cross-correlations (at lags -7 to 7) were significant (95% confidence level)(Figure 66b). The correlations were negative and medium strength. The greatest correlation coefficients were found at lags 6 and 7 (-0.509 and -0.511) indicating a 6-7 days delay in CO_2 response. In this period, lower than average values of water temperature were correlated with higher than average values of CO_2. The cross-correlation analysis of time series from period 5 was indicative that these series significantly correlated (95% confidence level) across lags -7 to 7(Figure 66c). All correlations were positive (medium strength). The greatest correlation coefficients were detected at lags -3 and -2 (0.582 & 0.577). This finding was indicative that CO_2 concentrations were lagging after WT by up to 3 days.

a)

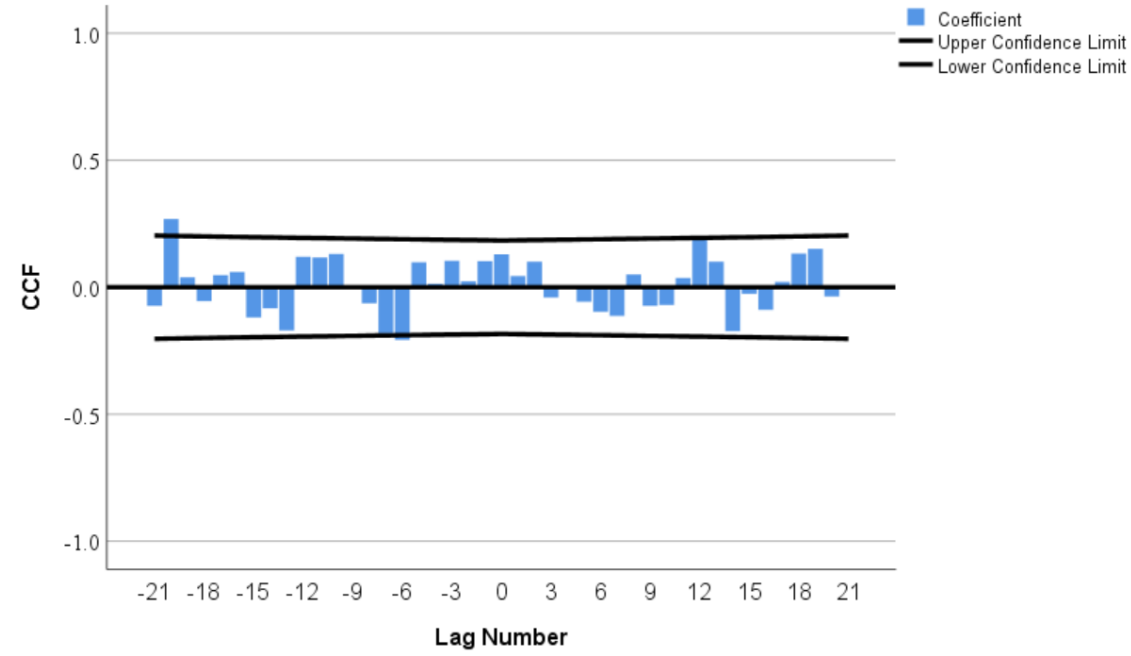
Coefficient
Upper Confidence Limit
Lower Confidence Limit
CCF
1.0
0.5
0.0
-0.5
-1.0
-21 -18 -15 -12 -9 -6 -3 0 3 6 9 12 15 18 21
Lag Number

b)

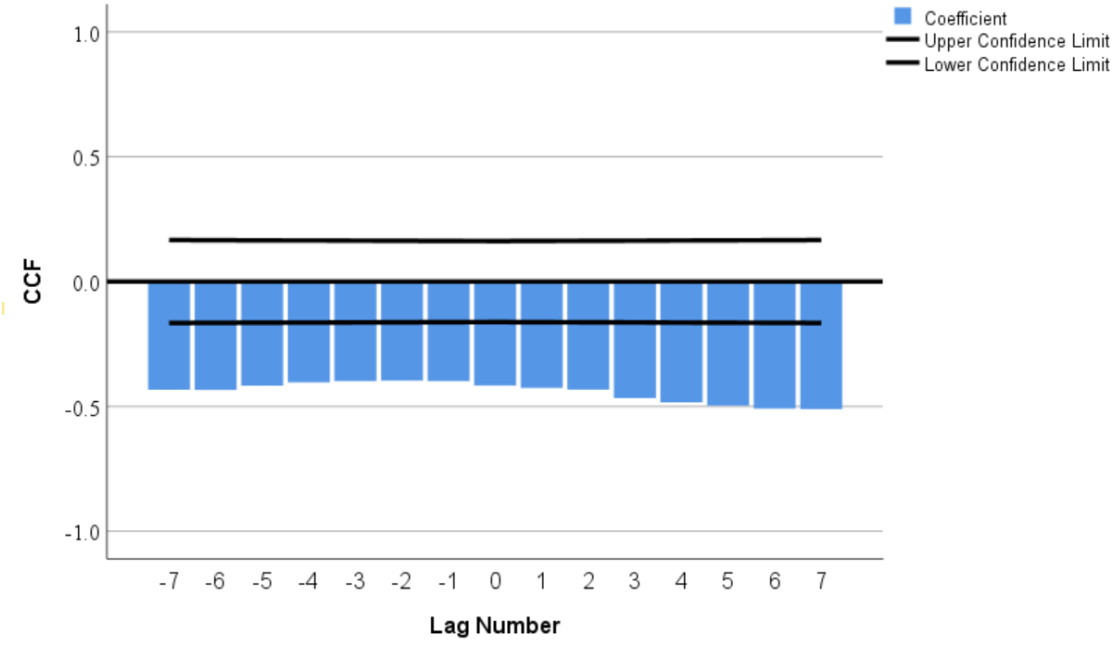
Coefficient
Upper Confidence Limit
Lower Confidence Limit
CCF
1.0
0.5
0.0
-0.5
-1.0
-7 -6 -5 -4 -3 -2 -1 0 1 2 3 4 5 6 7
Lag Number

c)

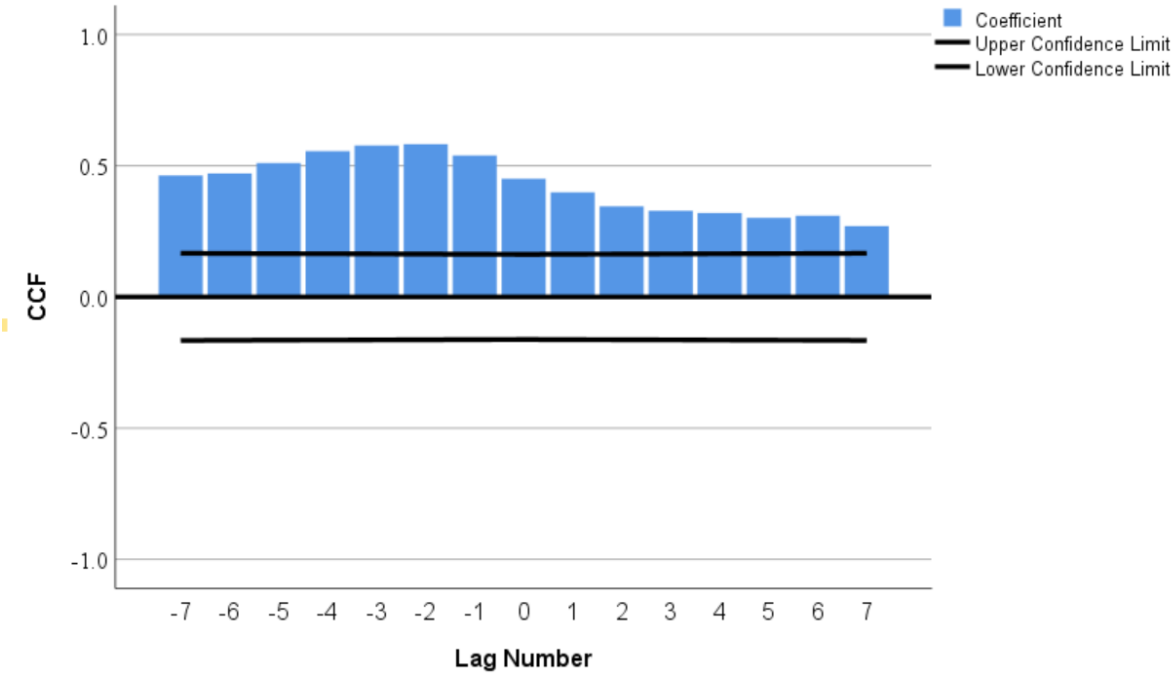

Figure 66 *The cross-correlation analyses of CO_2 versus WT at ST1: (a) Periods 1-3;(b) Period 4 (ARIMA 2,1, 7 adjusted time series) & (c) Period 5 (CO_2 ARIMA 1, 1,11 and WT ARIMA 0,0,4 adjusted time series).*

At HumST1 the cross-correlation results were indicating a significant (95% confidence level) correlation between CO_2 levels and WT (Figure 67). The strongest correlation was observed in period 3 (-0.925) at lag 0, followed by period 2 (0.795) at lag 0 and period 4 (-0.661) at lag -6 (Figure 67). The time series from the period 1 were correlated moderately (-0.377) at lag 0 (Figure 67a). And the time series from period 5 correlated weakly (-0.206) at lag 6 (Figure 67e). The correlation graphs from all periods are indicative that during winter months, correlations are negative. The lag delay of 6 days was observed when analysing time series from period 4 (Figure 67d). That result was indicative that temperature decrease was followed by increase in CO_2 with the delay of 6

days. The time series from ST2 cross-correlation analysis was performed on data from periods 1-4. The results were significant at 95% confidence level. The strongest correlation between CO_2 levels and WT was found when period 1 time series were compared (-0.869 at lag 0). The time series from periods 2, 3 and 4 were moderately correlated (-0.340 at lag -3; 0.418 at lag -1; 0.487 at lag -1). In case of time series analyses from periods 2-4 there was a delay in CO_2 response of up to 3 days. The results from ST3 cross-correlation analysis were indicative of significant (95% confidence level) correlations between CO_2 and WT. When two sets of time series were compared (two periods) the c0rrelations were present at lag 0 and in case of period 1 the correlation was negative (-0.452) and in case of period two, the correlation was positive (0.546). Both correlation coefficients were moderate. Lastly, the time series from LawnST2 and HumST3 were analysed. When LawnST2 time series were cross-correlated only period 1 data sets were correlating significantly (95% confidence level). The correlation was weak and negative at lag 7 (-0.229). That was indicative of a very substantial delay in CO_2 response. Likewise, HumST3 time series were only significantly correlating (95% confidence level) when period 1 time series were analysed. However, in this case, the correlation was evident at lag 0, and it was moderate (-0.462).

a)

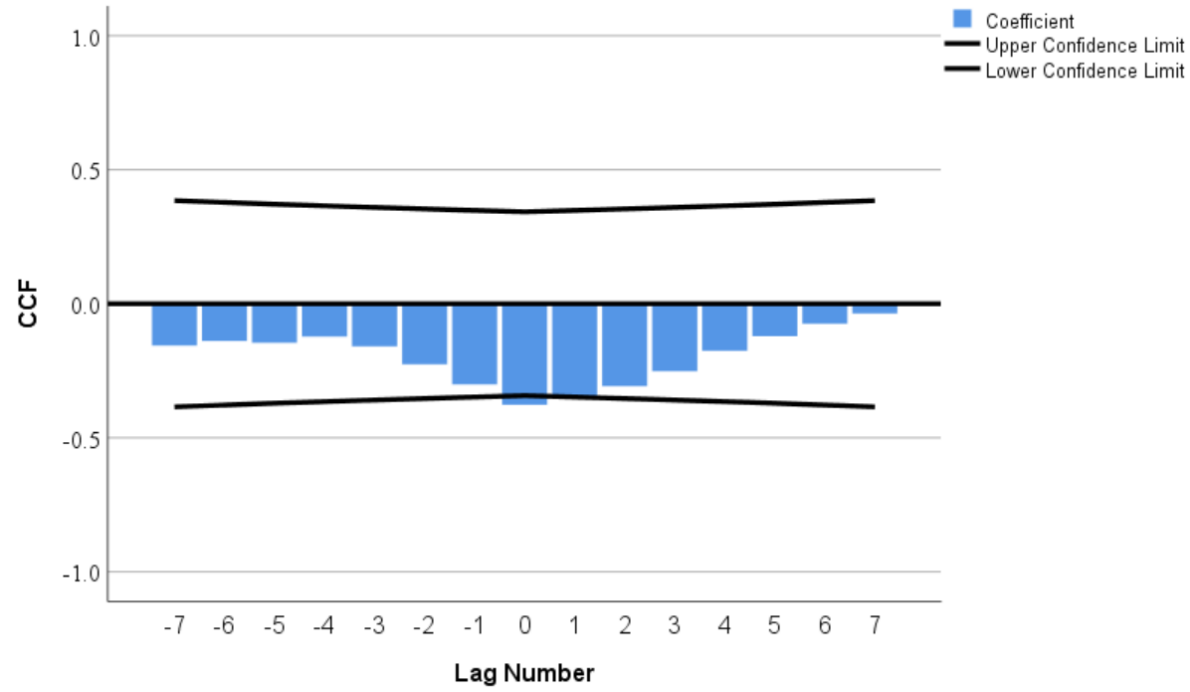
Coefficient
Upper Confidence Limit
Lower Confidence Limit
CCF
1.0
0.5
0.0
-0.5
-1.0
-7 -6 -5 -4 -3 -2 -1 0 1 2 3 4 5 6 7
Lag Number

b)

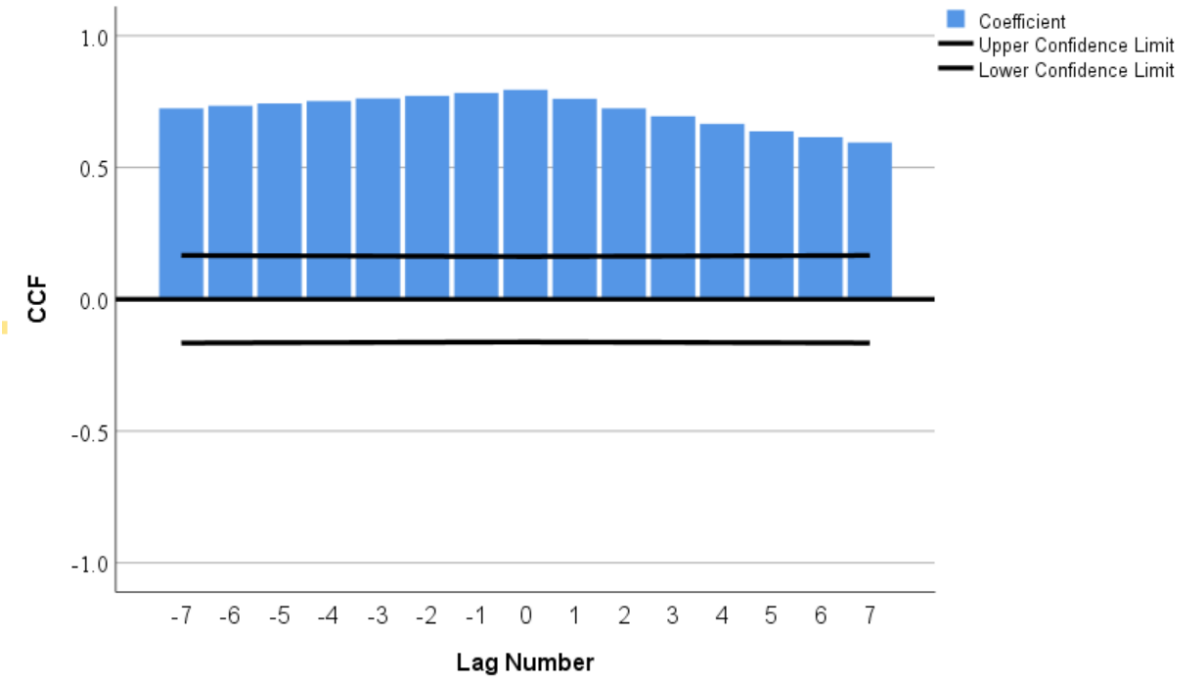
Coefficient
Upper Confidence Limit
Lower Confidence Limit
CCF
1.0
0.5
0.0
-0.5
-1.0
-7 -6 -5 -4 -3 -2 -1 0 1 2 3 4 5 6 7
Lag Number

c)

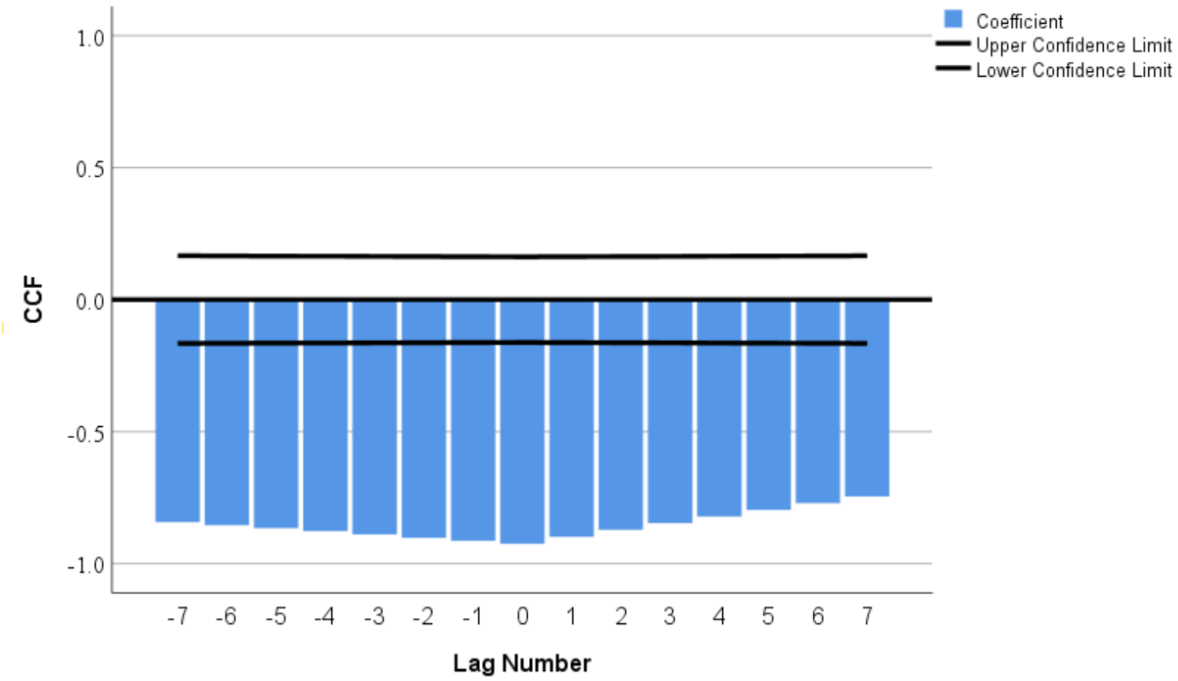
Coefficient
Upper Confidence Limit
Lower Confidence Limit
CCF
1.0
0.5
0.0
-0.5
-1.0
-7 -6 -5 -4 -3 -2 -1 0 1 2 3 4 5 6 7
Lag Number

d)

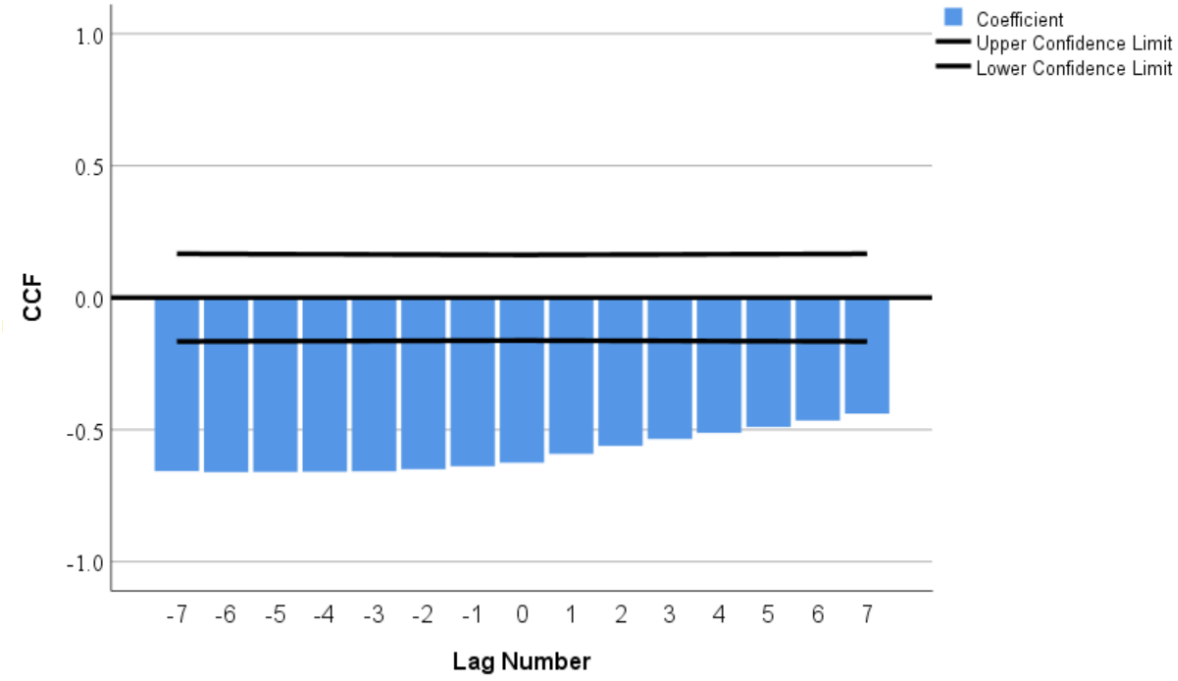
Coefficient
Upper Confidence Limit
Lower Confidence Limit
CCF
1.0
0.5
0.0
-0.5
-1.0
-7 -6 -5 -4 -3 -2 -1 0 1 2 3 4 5 6 7
Lag Number

e)

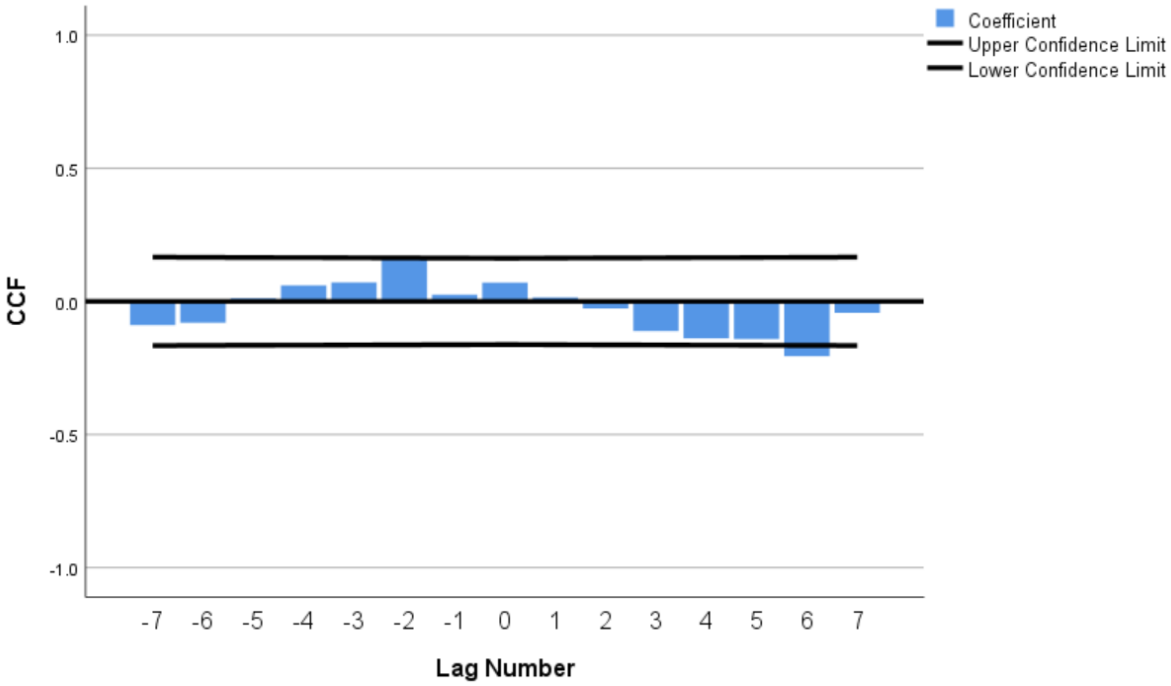

Figure 67 *The cross-correlation results from HumST1 CO_2 vs WT analysis: (a) Period 1; (b) Period 2 (ARIMA 2,1,5 predicted residuals); (c) Period 3 (WT – ARIMA (1,1,7) predicted residuals); (d) Period 4 (ARIMA (1,1,8) predicted residuals); (e) Period 5.*

4.7 The cross-correlation analysis: Air pressure, air temperature and CO_2 levels comparison

Those CO_2 time series that did not correlate significantly with WT series or where correlations were negative were analysed against the air pressure time series. The ST1 CO_2 time series were cross-correlated with the air pressure time series, there was a moderate negative correlation (-0.321) at lag 1. Strong negative correlation (-0.792 at lag 0) was detected when ST1 period 4 time series were compared (Figure 68a). When HumST1 time series were cross-correlated several strong correlations were identified. The period 2 and 3 time series were strongly correlated at lag 0 (-0.794; 0.909) (Figure

68b,c). The correlations were negative and positive. Moderate correlation at lag -3 (0.664) was detected when period 5 time series were analysed (Figure 68d). When period 4 time series were analysed, the moderate correlation was found at lag 0 (-0.380). Period 1 time series were analysed, and only weak correlation was detected at lag 0 (0.194). All correlations were significant (95% confidence level). When ST2 time series from periods 1 and 2 were compared two strong correlations were detected at lag 0 (-0.962; 0.838) (Figure 68e). Both correlations were significant (95% confidence level). ST3 period 1 time series were cross-correlated and the result suggested that CO_2 and air pressure were correlated at lag 0 (-0.887) (95% confidence level) (Figure 68f). LawnST2 (period 1-3) and HumST3 (periods 1-2) time series were analysed. Strong correlations were detected when LawnST2 period 1 and 2 time series were cross-correlated (0.832 at lag 0 and -0.713 at lag 1) (Figure 68g). Moderate correlations (0.696 at lag 0 and -0.353 at lag -3) were detected when HumST3 time series (periods 1 and 2) were analysed (Figure 68h). The time series from period 3 (LawnST2) were correlated only weakly (-0.187 at lag 7). All correlations were significant (95% confidence level). The air temperature time series were cross-correlated with time series from ST1 and HumST1 (entire monitoring period). The results were indicative that these time series were correlating significantly (95% confidence level) but moderately (ST1: 0.368 at lag 0; HumST1: 0.538 at lag -2) (Figure 68i,j). In both cases the correlation was positive.

a)

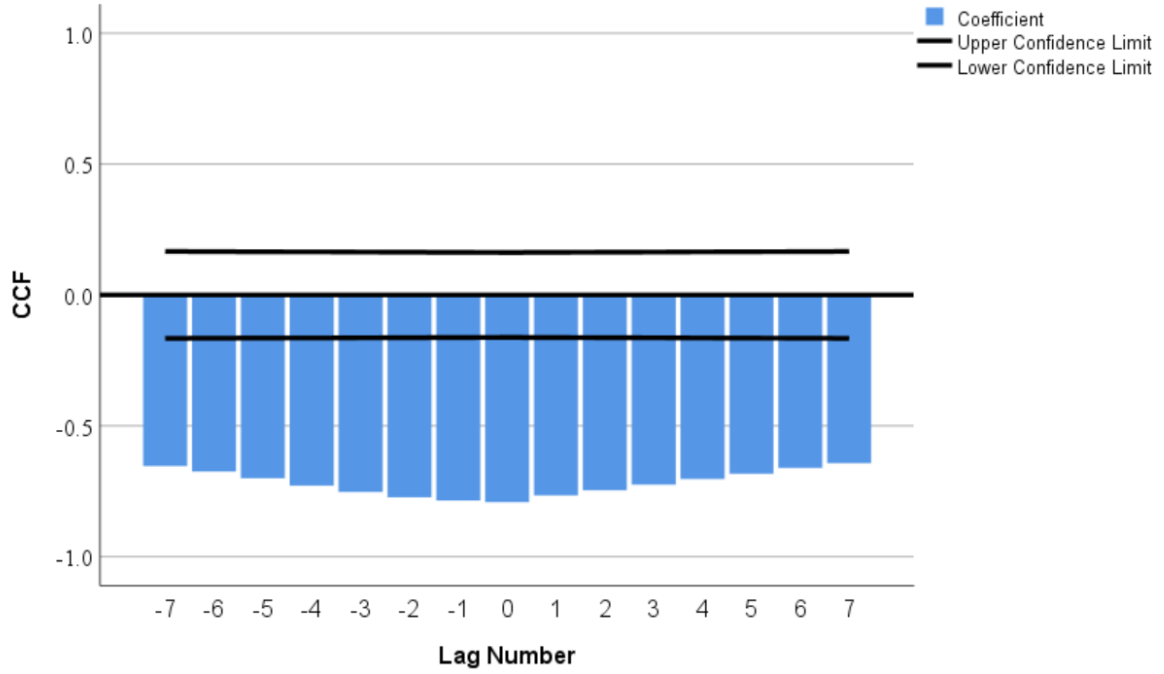
Coefficient
Upper Confidence Limit
Lower Confidence Limit
1.0
0.5
0.0
-0.5
-1.0
CCF
-7 -6 -5 -4 -3 -2 -1 0 1 2 3 4 5 6 7
Lag Number

b)

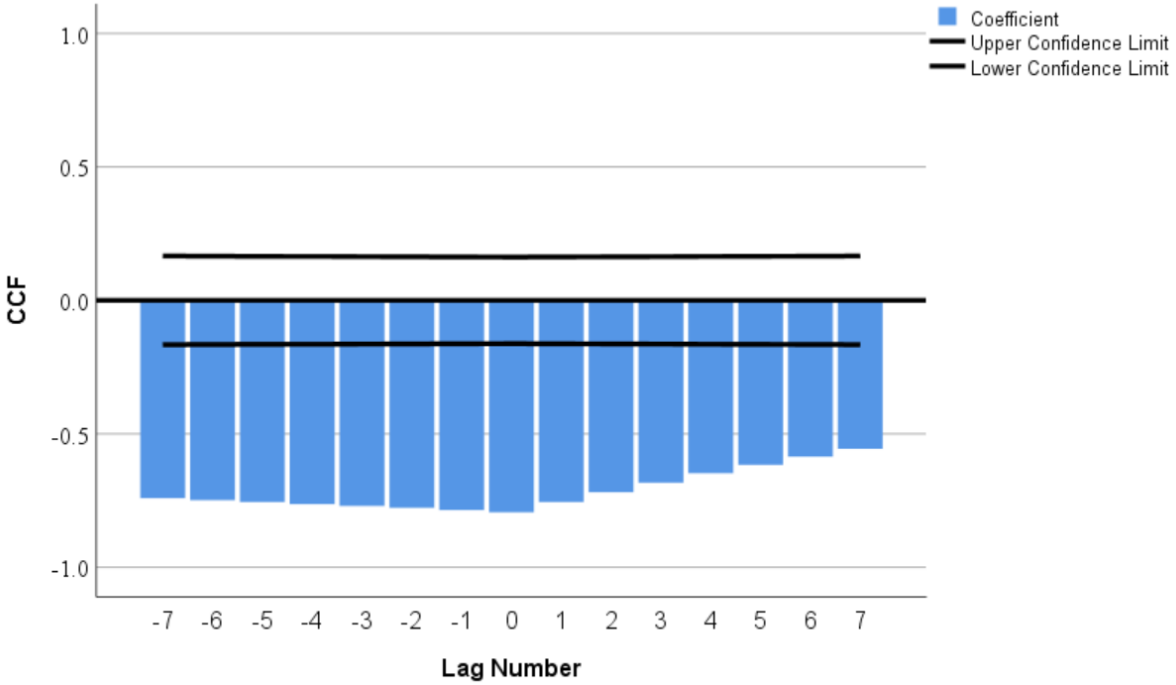
Coefficient
Upper Confidence Limit
Lower Confidence Limit
1.0
0.5
0.0
-0.5
-1.0
CCF
-7 -6 -5 -4 -3 -2 -1 0 1 2 3 4 5 6 7
Lag Number

c)

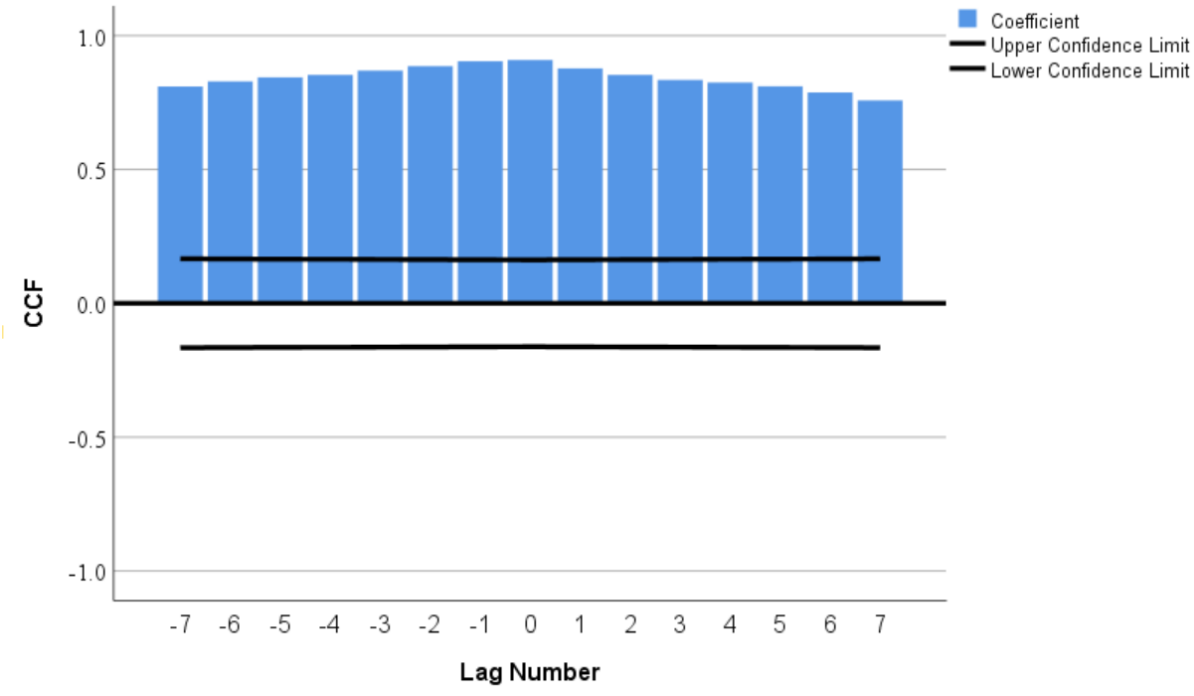
Coefficient
Upper Confidence Limit
Lower Confidence Limit
CCF
1.0
0.5
0.0
-0.5
-1.0
-7 -6 -5 -4 -3 -2 -1 0 1 2 3 4 5 6 7
Lag Number

d)

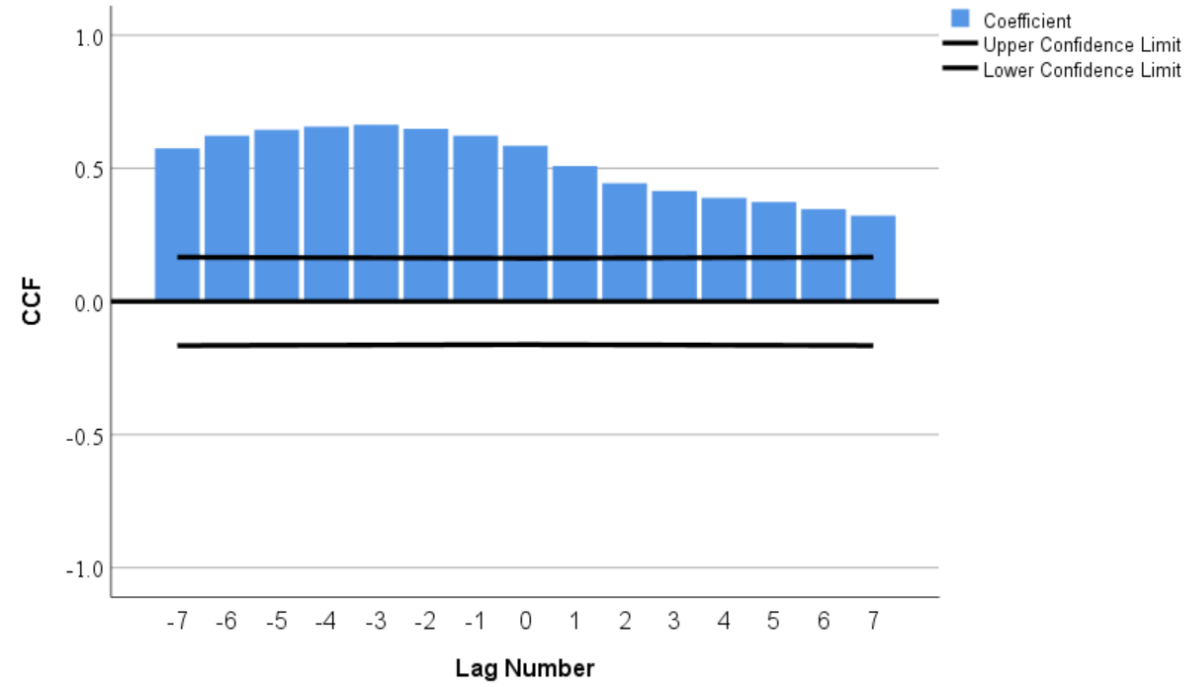
Coefficient
Upper Confidence Limit
Lower Confidence Limit
CCF
1.0
0.5
0.0
-0.5
-1.0
-7 -6 -5 -4 -3 -2 -1 0 1 2 3 4 5 6 7
Lag Number

e)

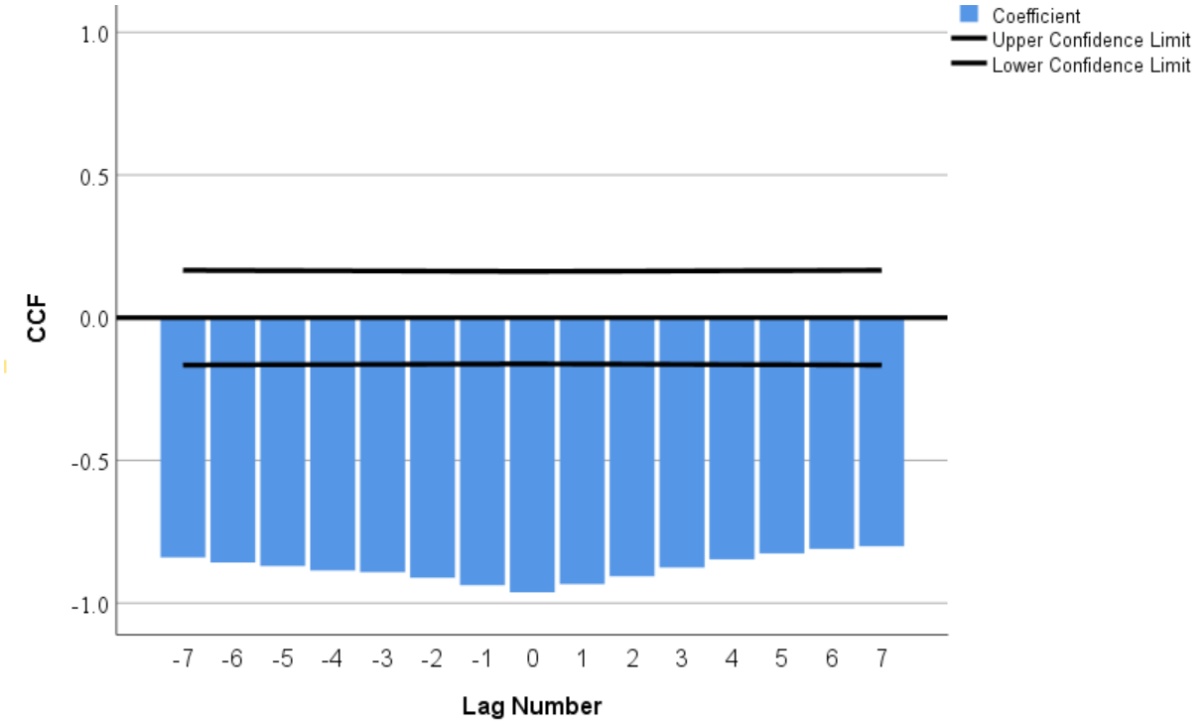
Coefficient
Upper Confidence Limit
Lower Confidence Limit
1.0
0.5
0.0
-0.5
-1.0
CCF
-7 -6 -5 -4 -3 -2 -1 0 1 2 3 4 5 6 7
Lag Number

f)

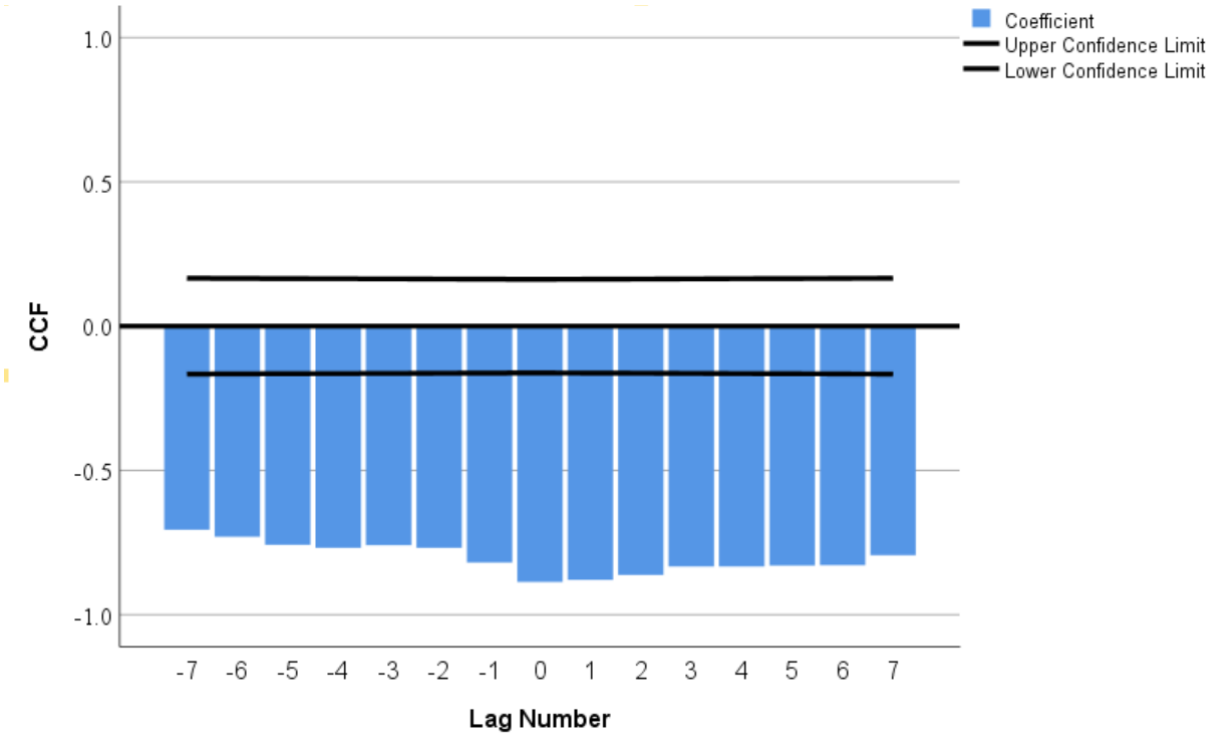
Coefficient
Upper Confidence Limit
Lower Confidence Limit
1.0
0.5
0.0
-0.5
-1.0
CCF
-7 -6 -5 -4 -3 -2 -1 0 1 2 3 4 5 6 7
Lag Number

g)

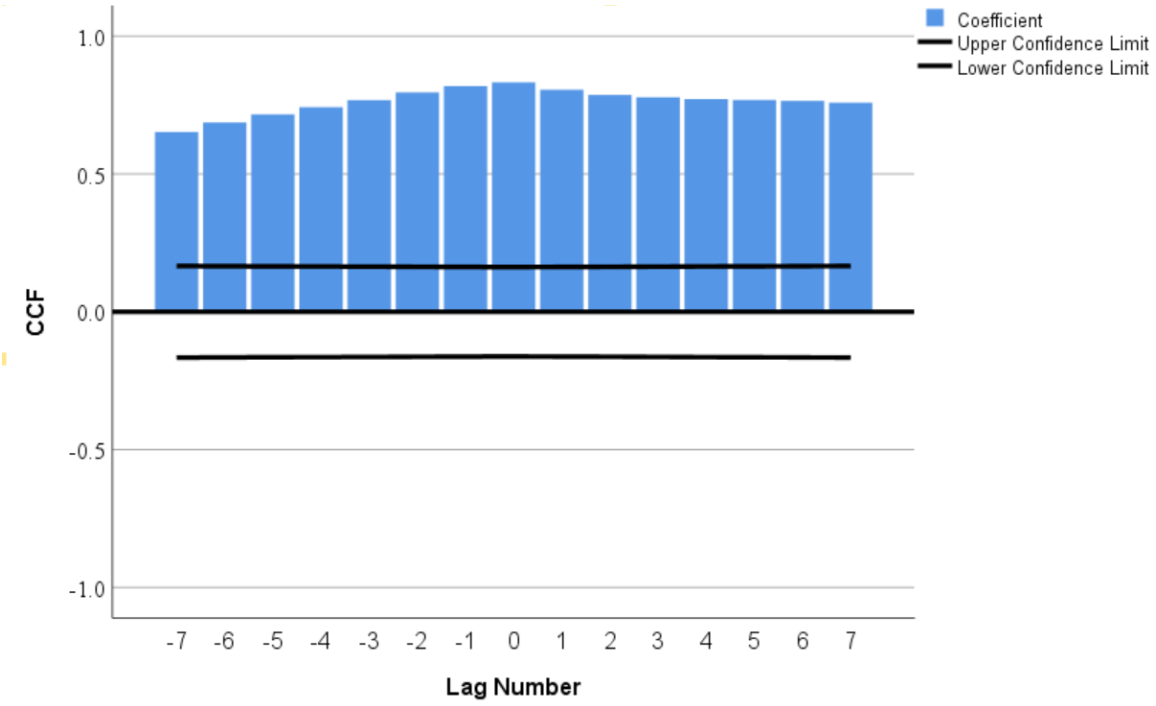
Coefficient
Upper Confidence Limit
Lower Confidence Limit
CCF
1.0
0.5
0.0
-0.5
-1.0
-7 -6 -5 -4 -3 -2 -1 0 1 2 3 4 5 6 7
Lag Number

h)

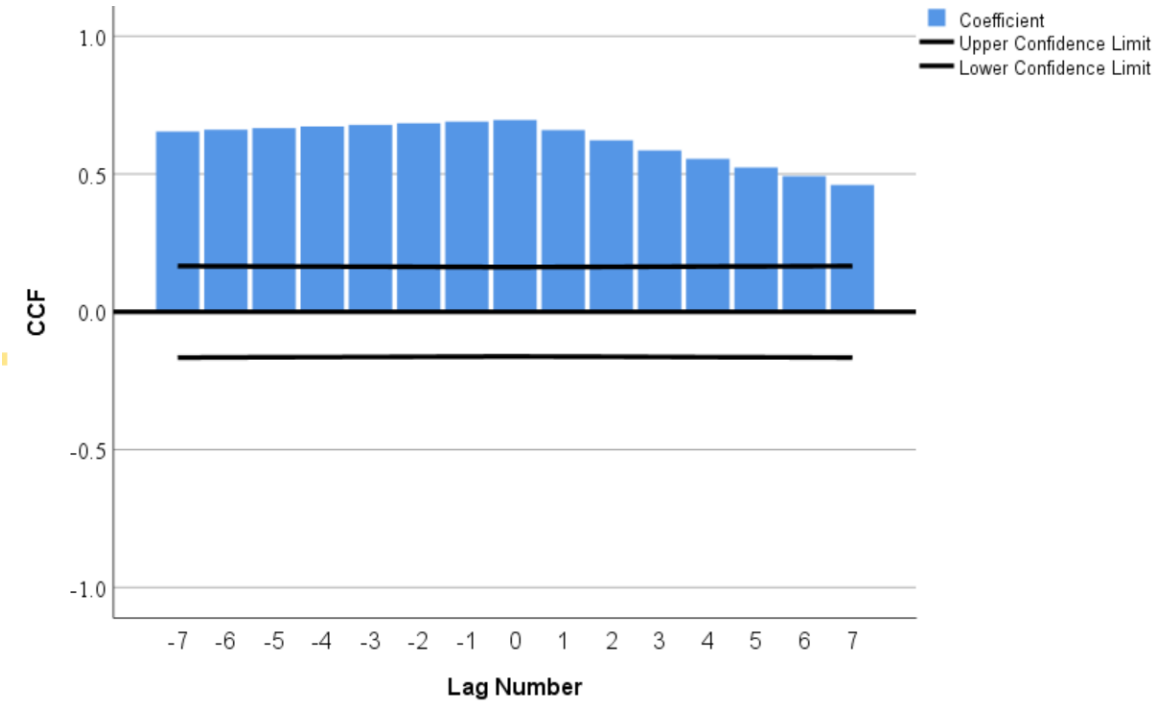
Coefficient
Upper Confidence Limit
Lower Confidence Limit
CCF
1.0
0.5
0.0
-0.5
-1.0
-7 -6 -5 -4 -3 -2 -1 0 1 2 3 4 5 6 7
Lag Number

i)

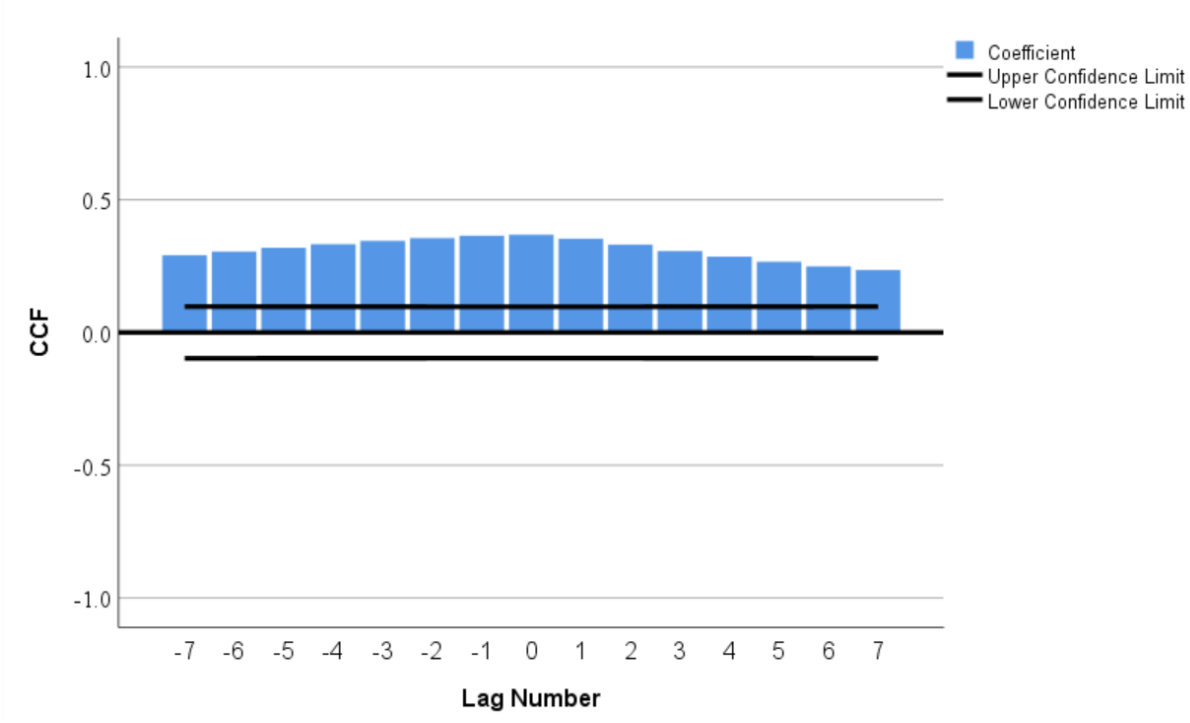
Coefficient
Upper Confidence Limit
Lower Confidence Limit
CCF
1.0
0.5
0.0
-0.5
-1.0
-7 -6 -5 -4 -3 -2 -1 0 1 2 3 4 5 6 7
Lag Number

j)

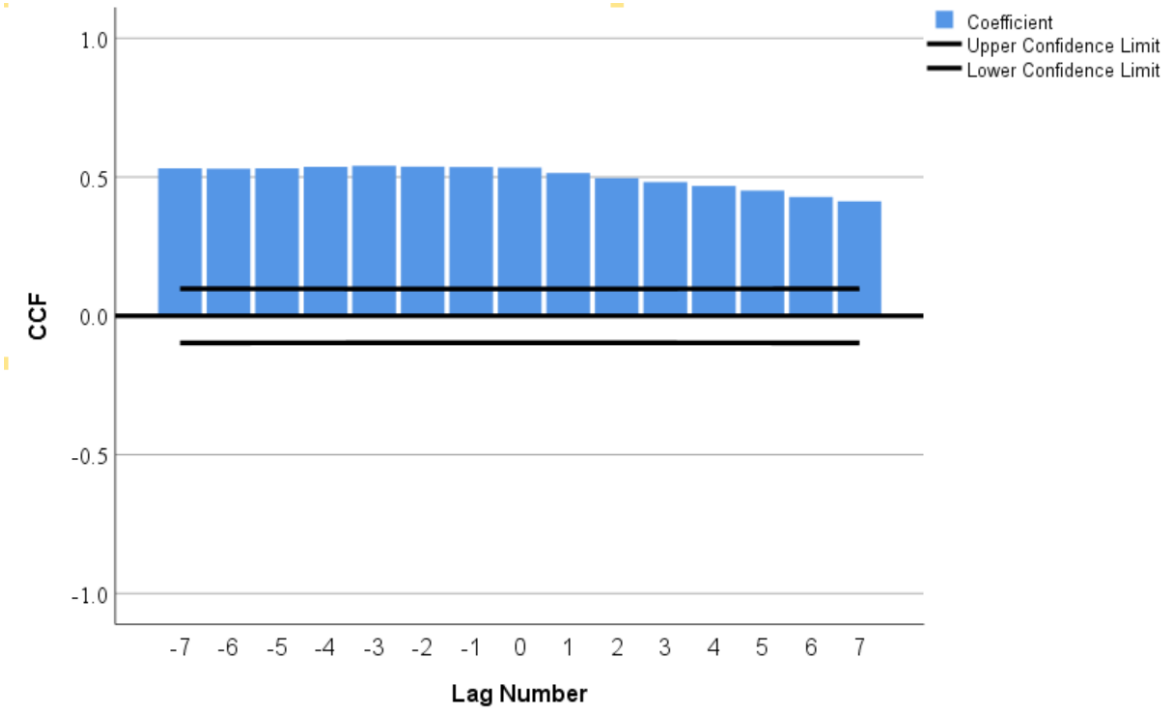

Figure 68 *The cross-correlation analysis of time series (CO_2 versus air pressure and air temperature): (a) ST1 CO_2 versus air pressure (period 4); (b) HumST1 CO_2 versus air pressure (period 2); (c) HumST1 CO_2 versus air pressure (period 3); (d) HumST1 CO_2 versus air pressure (period 5); (e) ST2 CO_2 versus air pressure (period 1); (f) ST3 CO_2 versus air pressure (period 1);(g) LawnST2 CO_2 versus air pressure (period 1);(h) HumST3 CO_2 versus air pressure (period 1); (i) ST1 CO_2 versus air temperature (all);(j) HumST1 CO_2 versus air temperature (all).*

4.8 Diurnal cycles

Open pool water results (ST1-ST3) across all seasons between years of 2016-2018 were suggestive that there was a clear diurnal cycling of CO_2. Significantly higher levels ($p<0.05$) of CO_2 were recorded between 03:00-09:00 (Figure 69). The lowest concentrations were recorded between hours of 17:00-20:00 (Figure 69). Depression and diurnal cycling of CO_2 was more apparent in summer months (Figure 69). HumST1,

LawnST2 and HumST3 hourly CO_2 trends were indicative that the concentrations were lower than average between hours of 03:00-11:00 (Figure 70). Concentrations were higher than average between hours of 10:00-17:00 (year 2017 all seasons and winter period of 2018) and between hours of 20:00-00:00 (summer periods of 2018) (Figure 70).

a)

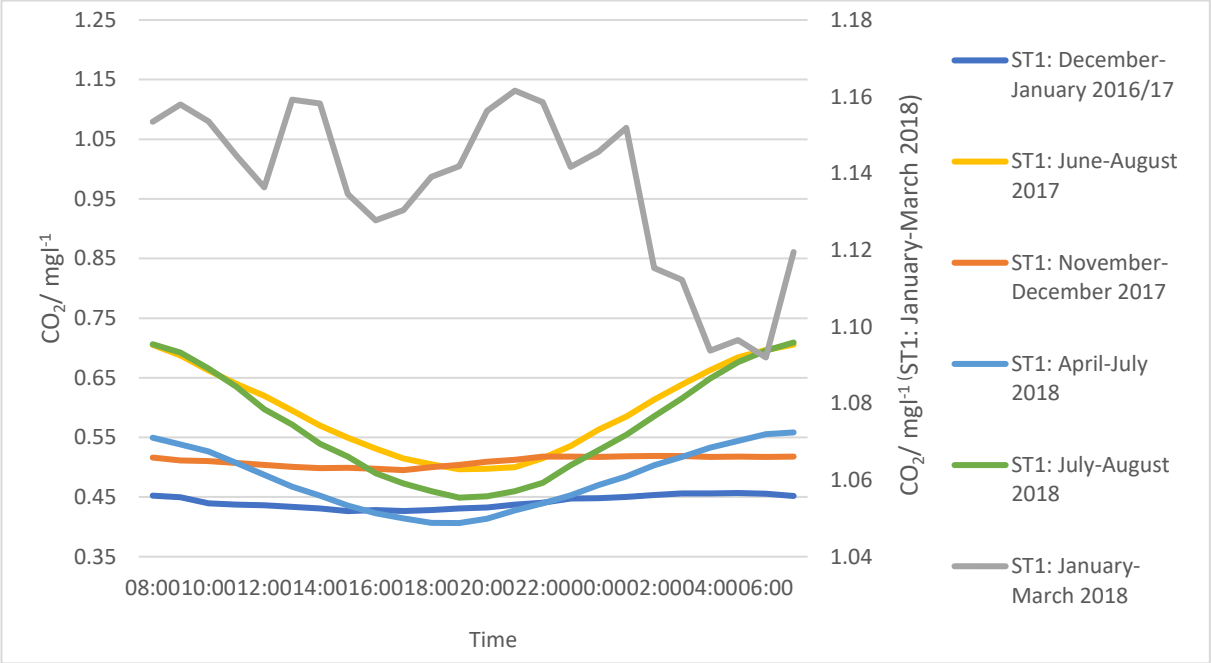

b)

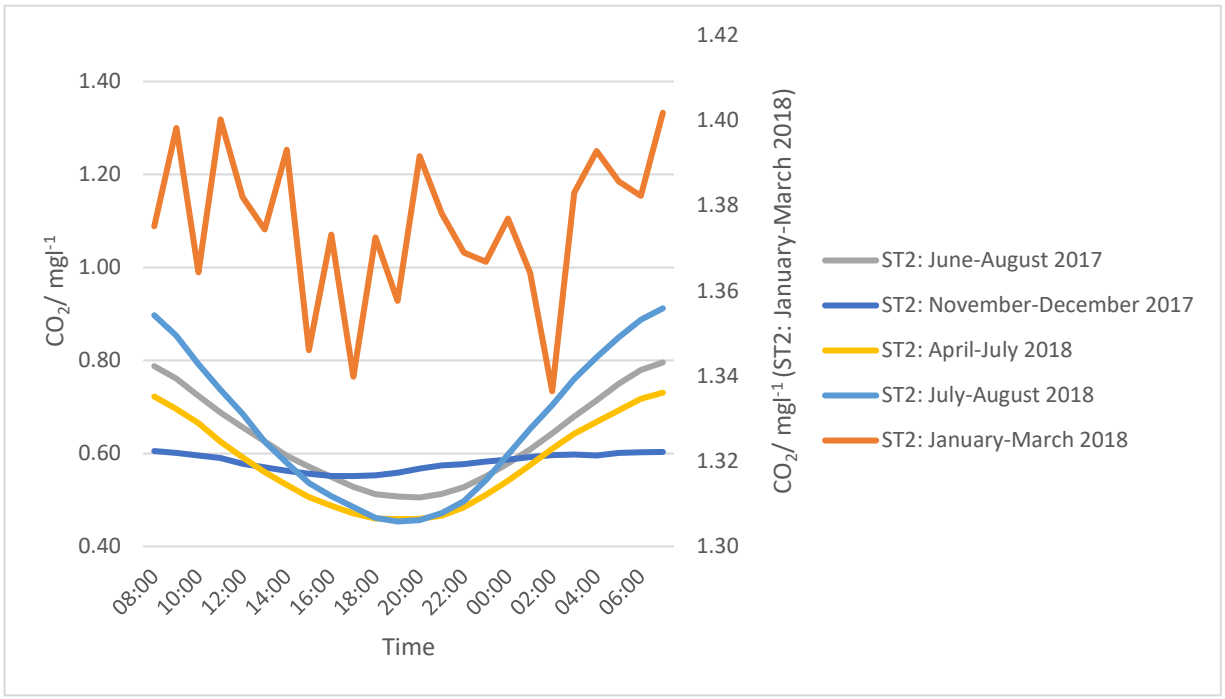

c)

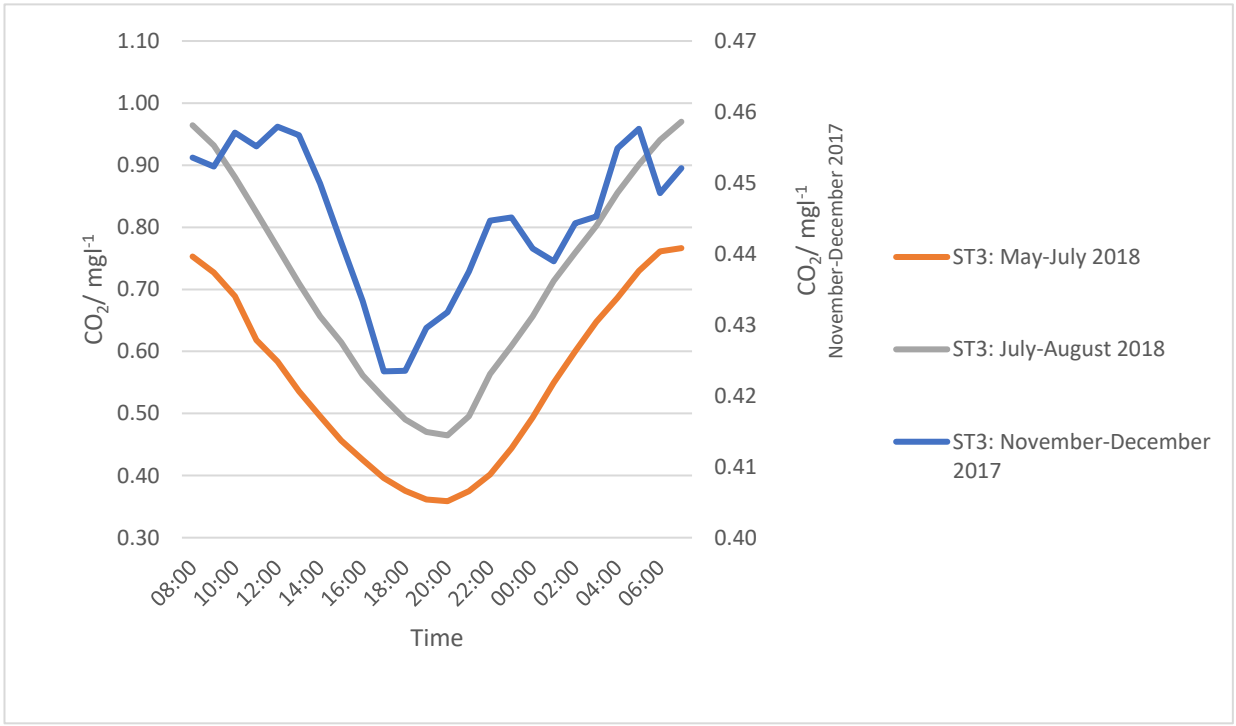

Figure 69 *Illustrating diurnal patterns of CO_2 concentrations on seasonal basis: a) ST1; b) ST2; c) ST3.*

a)

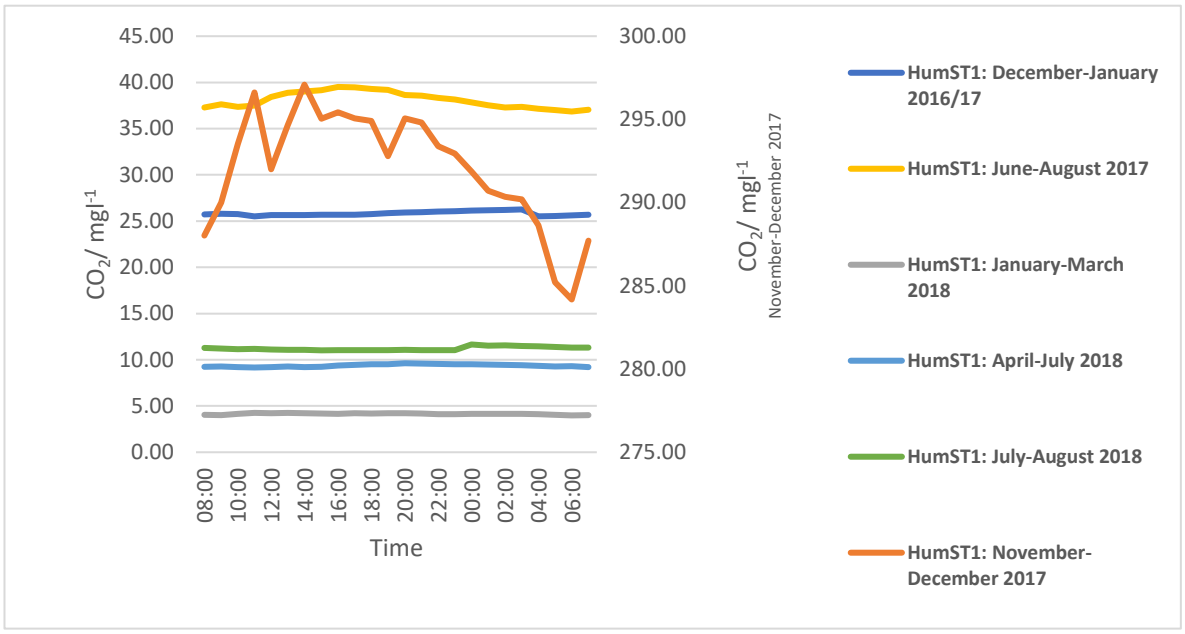
45.00
40.00
35.00
30.00
25.00
20.00
15.00
10.00
5.00
0.00
300.00
295.00
290.00
285.00
280.00
275.00
08:00
10:00
12:00
14:00
16:00
18:00
20:00
22:00
00:00
02:00
04:00
06:00
Time
CO2/ mgl-1
CO2/ mgl-1
November-December 2017
HumST1: December-January 2016/17
HumST1: June-August 2017
HumST1: January-March 2018
HumST1: April-July 2018
HumST1: July-August 2018
HumST1: November-December 2017

b)

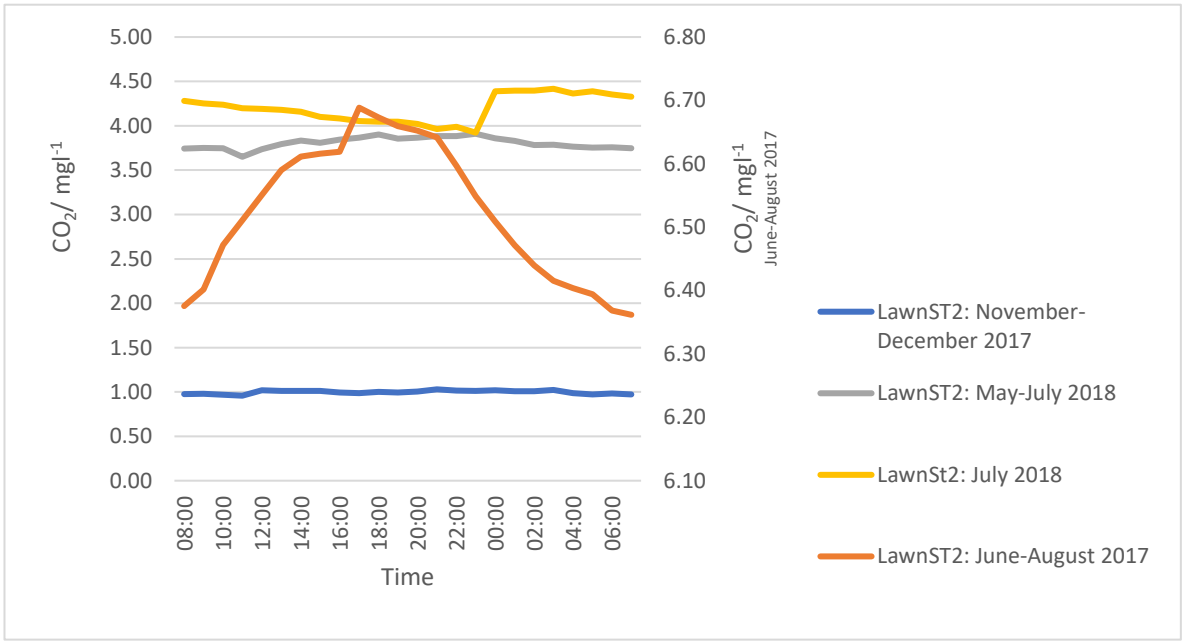
5.00
4.50
4.00
3.50
3.00
2.50
2.00
1.50
1.00
0.50
0.00
6.80
6.70
6.60
6.50
6.40
6.30
6.20
6.10
08:00
10:00
12:00
14:00
16:00
18:00
20:00
22:00
00:00
02:00
04:00
06:00
Time
CO2/ mgl-1
CO2/ mgl-1
June-August 2017
LawnST2: November-December 2017
LawnST2: May-July 2018
LawnSt2: July 2018
LawnST2: June-August 2017

c)

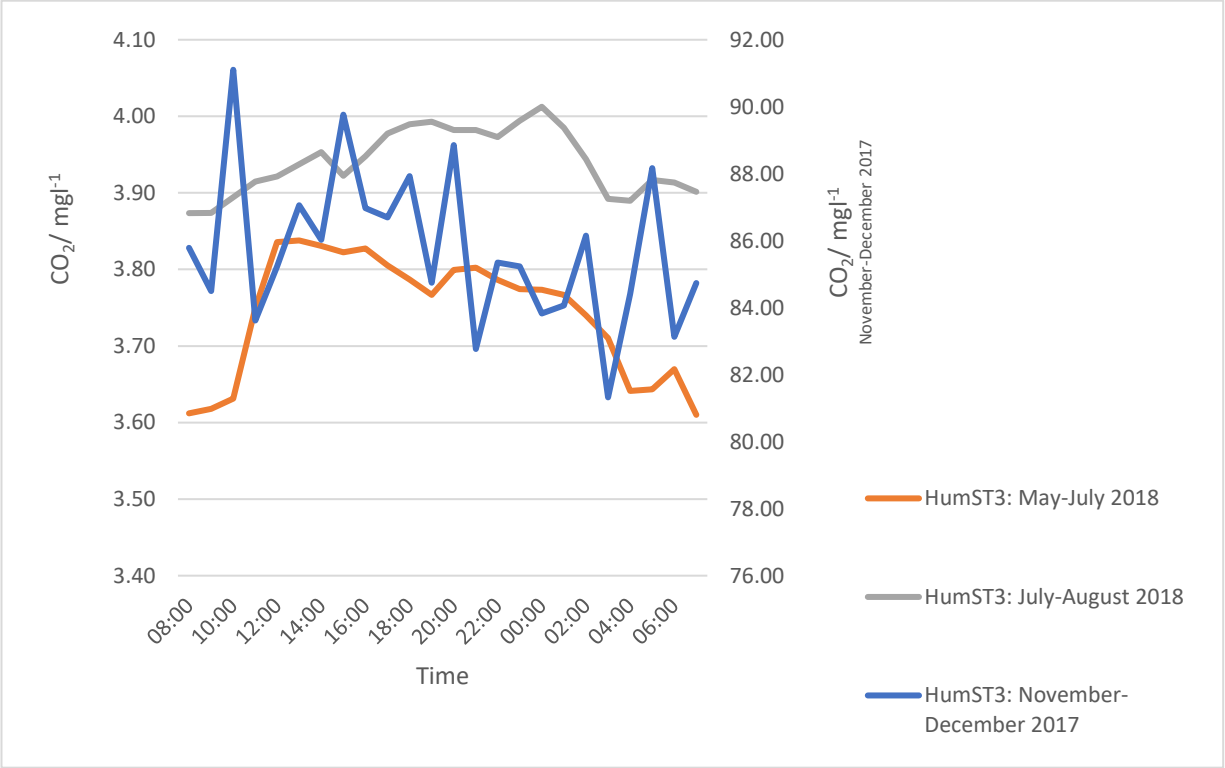

Figure 70 *Illustrating diurnal patterns of CO_2 concentrations on seasonal basis: a) HumST1; b) LawnST2; c) HumST3.*

4.9 Pool-atmosphere CO_2 fluxing

Fluxes of CO_2 from ST1-ST3 were modelled (Methods) for years from 2016 to 2018 (Table 8-33 – Appendix B). Flux data from ST1 suggested that fluxes varied between 0.05-5.54 $gm^{-2}d^{-1}$ (2016-2018) (Figure 71). Maximum and minimum flux rates were estimated to occur in March (7^{th}) and February (5^{th}) 2018 (Figure 71). Results were suggestive that average winter fluxes of CO_2 were between 0.26-0.38 $gm^{-2}d^{-1}$ between years of 2016-2017 (ST1-3). The flux time series (ST1) were cross-correlated with wind speed time series. There was a strong positive correlation (lag 0) between wind speed and CO_2 fluxing (0.943) (Figure 72a). This cross-correlation was significant at 95% confidence level. High mean flux values of 0.86 $gm^{-2}d^{-1}$ and 1.17$gm^{-2}d^{-1}$ were modelled

for ST1 & 2 between January-March 2018.The cross-correlation analysis (ST1) results were indicating a strong positive correlation at lag 0 (0.859) and weaker negative correlation at lag -2 (-0.308). The weak negative correlation indicates that fluxing was potentially higher than average although wind speeds did not exhibit similar pattern, they were lower than average. There was a lag of two days between the wind speed time series and fluxes of CO_2. Overall, these cross-correlations were significant at 95% confidence level. Average July-August fluxes of CO_2 were between 0.41-0.51 $gm^{-2}d^{-1}$ between years of 2017-2018 (ST1-3). At ST1 the cross-correlation analysis was indicative that these time-series significantly (95% confidence level) correlated at lag 0 (0.911). Between April-July 2018, fluxes were lower 0.28- 0.36 $gm^{-2}d^{-1}$ (ST1-2). At ST1 the cross-correlation analysis was indicative that these time-series significantly (95% confidence level) correlated at lags: -2 (0.223), -1 (0.385), 0 (0.742) and 1(0.203) (Figure 72b). All correlations were positive, and the strongest correlation was at lag 0.

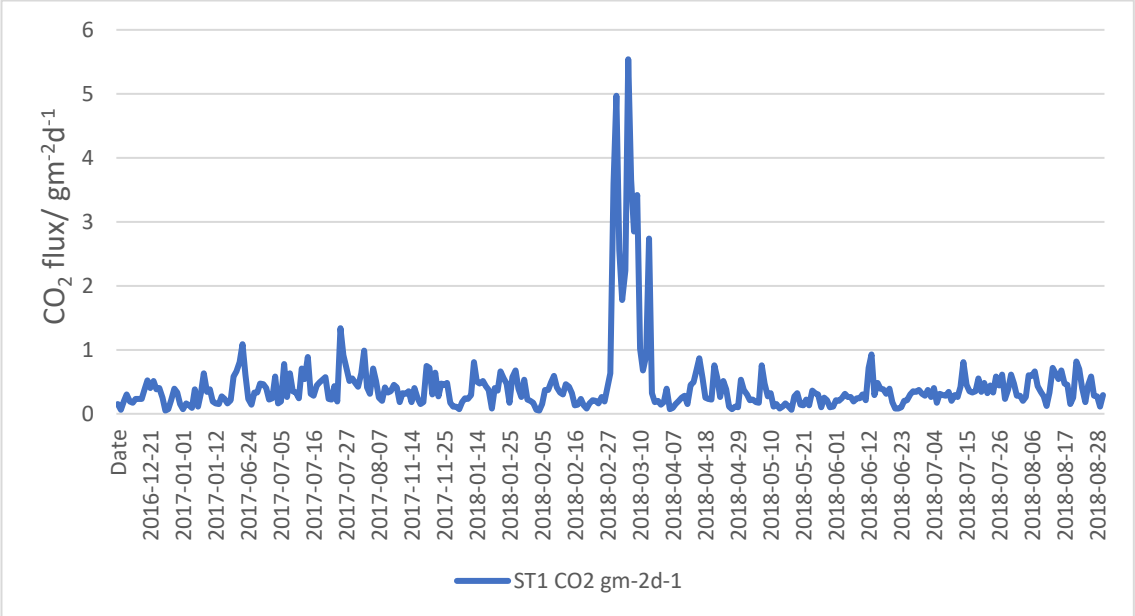

Figure 71 *Showing CO_2 flux data modelled for 2016-2018 study periods (ST1).*

a)

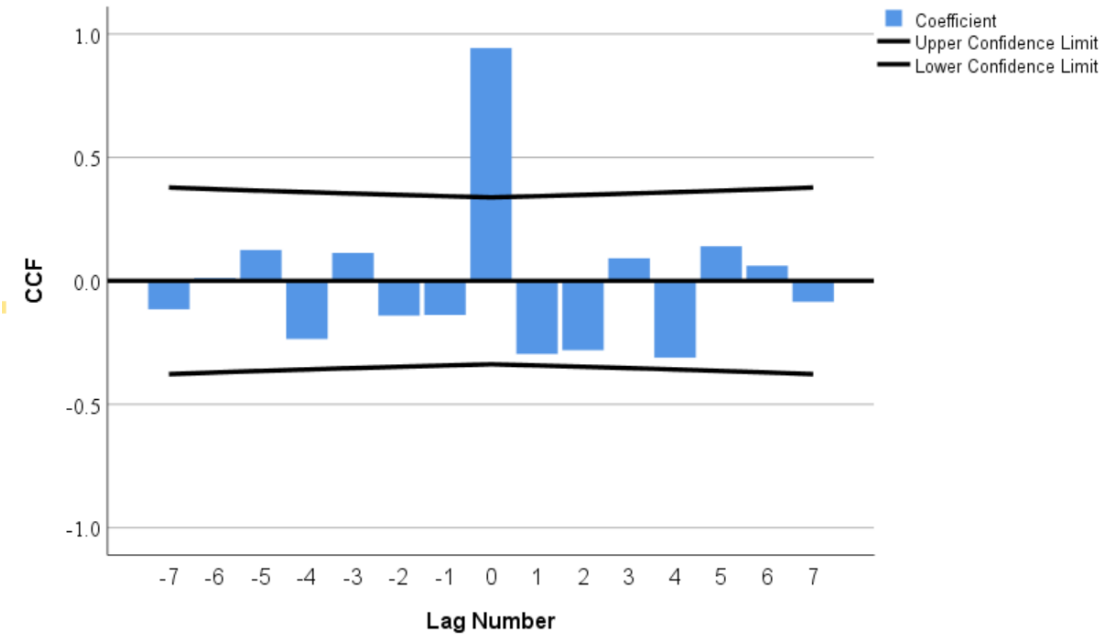

b)

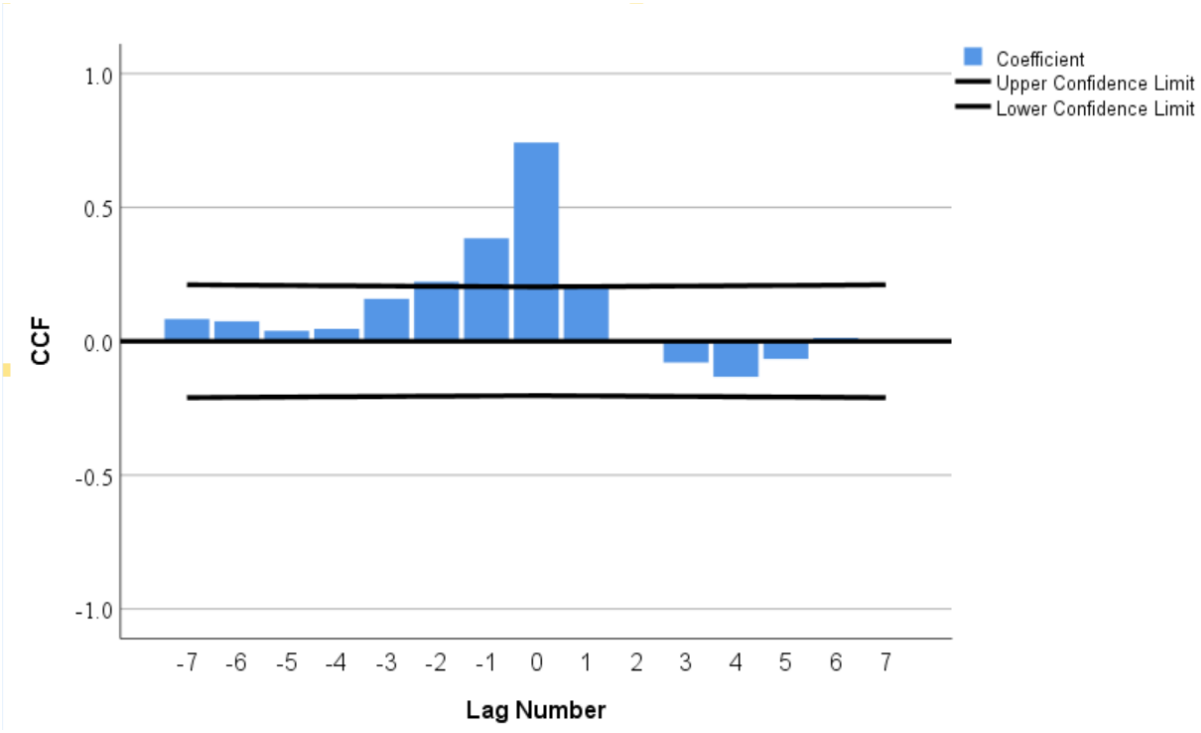

Figure 72 *Showing cross-correlation analysis results for correlation between wind speed and CO_2 flux from ST1: (a) December-January 2016-17; (b) April-July 2019 (ARIMA corrected time series).*

4.10 Precipitation, runoff, organic carbon and CO_2

DOC (ST1-ST3 & HumST1, LawnST2, HumST3) levels were ranging from 4-34 mgl^{-1} (greatest from September sample). TOC levels were between 6-53 mgl^{-1} (greatest from September sample). Levels of POC were between 0-39 mgl^{-1} (greatest from September sample). SUVA method (Hydrochemical monitoring) results were: SUVA254= (absorbance at 254 nm/DOC mgl^{-1})*100 =14.98 (ST1); SUVA254= 13.56 (ST2); SUVA254= 9.1 (HumST1) and SUVA254= 4.89 (LawnST2) (Appendix B: Figure 78). These results were indicative that most aromatic materials were present in pools at that time.

Comparison of trends in precipitation (totals) across different months (years 2016-2018) (Figure 73; Table 9;Table 34;Table 35 – Appendix B) showed a weak negative (-0.18) correlation with CO_2 (ST1) and stronger negative (-0.45) correlation with CO_2 at HumST1. A more detailed analysis of precipitation events against concentration of CO_2, DOC, TOC and pH showed the following results for ST1 and HumST1 (Figure 74; Figure 75). Generally, for data from ST1, there was a strong positive correlation between pH and CO_2 (0.81) and strong negative correlation between precipitation deposition and CO_2 level (-0.81). Precipitation deposition was also correlated negatively with levels of DOC, TOC, and with pH (-0.55, -0.49 & -0.37). For data from HumST1, results suggested that there was a strong negative correlation between precipitation deposition and level of CO_2 (-0.65). Negative correlation was also observed between levels of DOC, TOC and precipitation deposition (-0.34). Correlation between pH and CO_2 was positive (0.55) and between pH and TOC/DOC – negative (-0.64; -0.53). There was also a positive correlation between DOC and CO_2 levels (0.41).

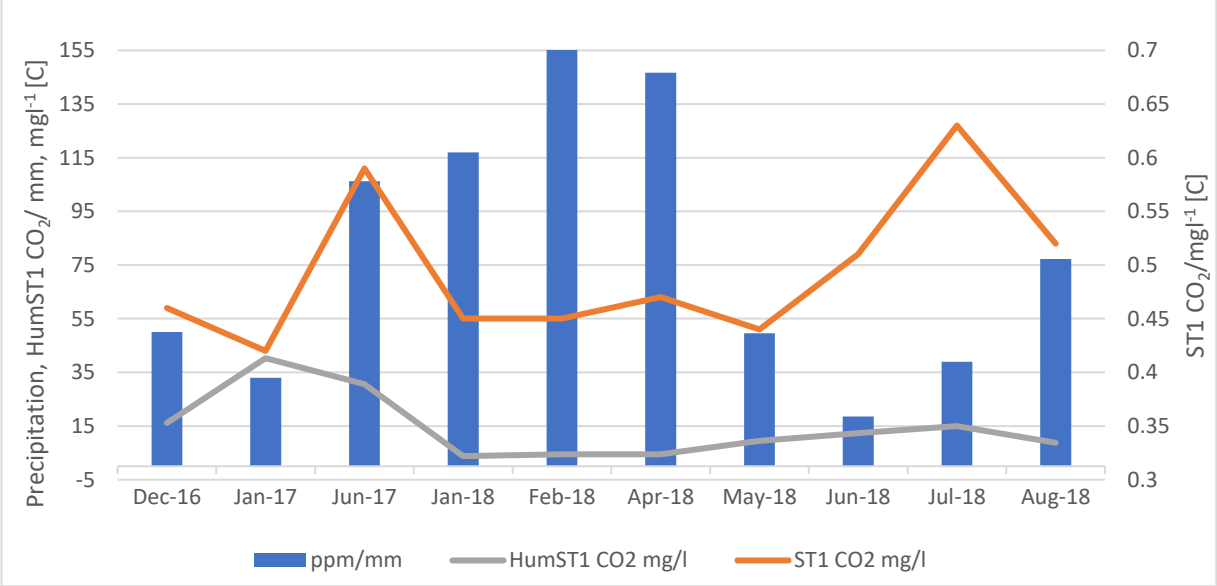

Figure 73 *Showing monthly precipitation totals (year 2016-2018) along with levels of CO_2 (ST1 & HumST1).*

a)

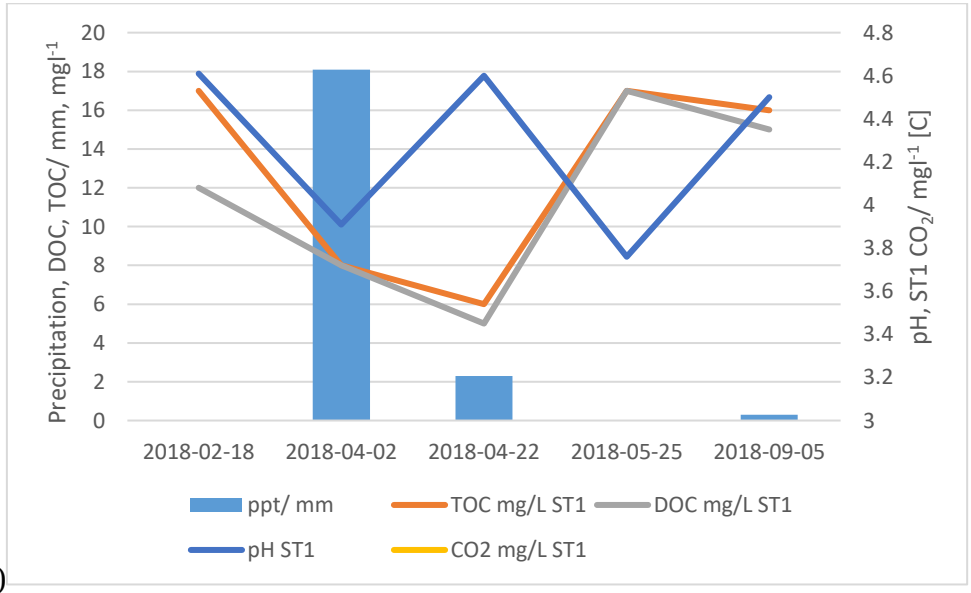

b)

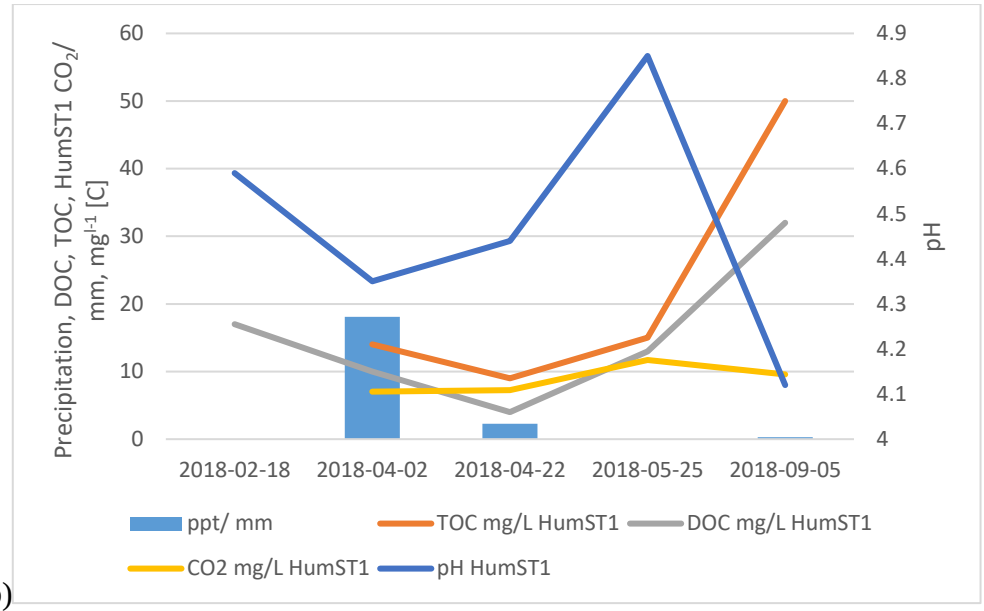

Figure 74 *Illustrating correlations between variables: pH, ppt - precipitation TOC, DOC, CO_2 concentrations: a) ST1; b) HumST1.*

a)

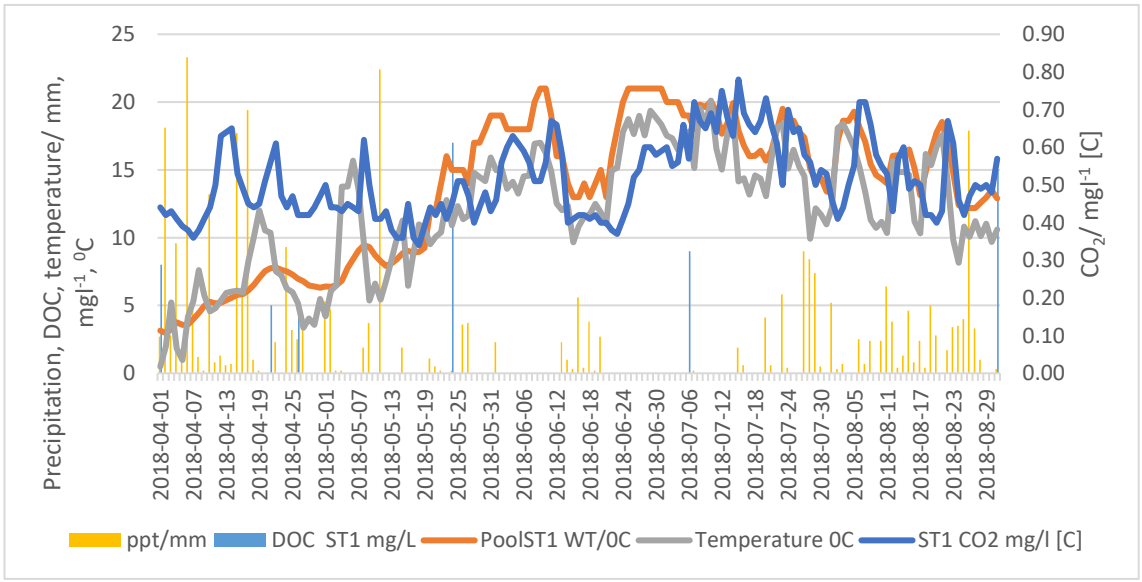

b)

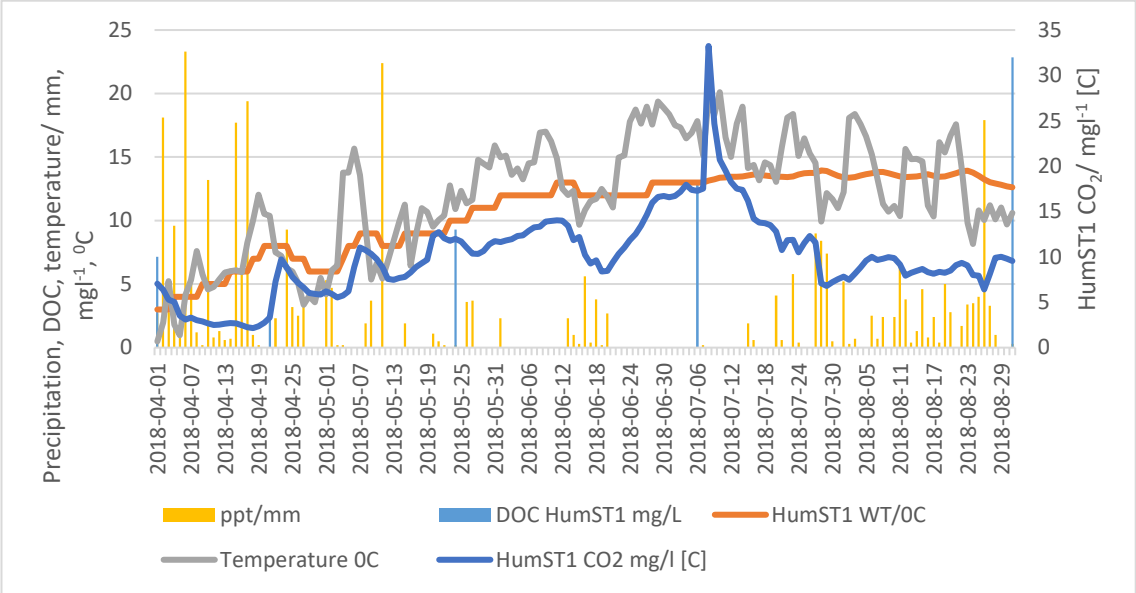

Figure 75 *Showing levels of CO_2, precipitation events, point DOC concentrations, water and air temperatures: a) ST1; b) HumST1 – April to September 2018.*

CHAPTER 5: DISCUSSION

5.1 Kippure blanket peatland – significance of carbon dynamics

Reservoirs of carbon stored in the upland blanket peatlands of Ireland are important as peat soils act as a highly concentrated store of biogenic carbon, which could be delivered to fluvial systems and the atmosphere via processes of leaching, run-off and degassing. To comply with carbon emission requirements and with water quality standards it is crucial to be able to assess carbon stocks accurately. Additionally, it is of paramount importance to understand where potential carbon fluxes or discharges can occur from the peatlands. The upland blanket peatlands at Kippure and Liffey Head in Co Wicklow represent a significant example of the type of mountain blanket peatland that is extensive along the eastern mountain ranges of Ireland. The proximity of these areas close to major urban population centres only adds to the pressures that these systems are subjected to in terms of land use management, land-use change and climate change. These pressure scan have a direct bearing on the flux dynamics of carbon and CO_2. Kippure peatland is also an area where many major headwaters originate, therefore water quality in the Dublin / Wicklow area is closely related to the status and dynamics of these peatlands. If mountain blanket peatlands are managed responsibly, they have the potential to act as net sinks of carbon and as such can represent nature-based system for water quality control and optimisation.

5.1.1 Sustainability of the Kippure peatland

There are significant challenges associated with GHG compliance at both a European, national and local level and many of these issues are addressed within the National Policy Position on Climate Action and Low Carbon Development (2014) and the Climate Action and Low Carbon Development Act 2015 (Department of Communications, Climate Action and Environment, 2019). The low carbon transition agenda is a key aspect of these documents. The principal issue addressed within these policies is the achievement of a competitive, low carbon, climate-resilient and environmentally sustainable economy by 2050 (Department of Communications, Climate Action and Environment, 2019). These documents additionally contextualize and clarify the level of GHG mitigation sought and set out the procedure and processes that need to be addressed in order to advance this agenda (Department of Communications, Climate Action and Environment, 2019). A more in-depth approach to GHG mitigation focuses on the need to reduce CO_2 emissions to at least 80% (compared to 1990 levels) by 2050 across the electricity generation, built environment and transport sectors along with carbon neutrality in the agriculture and land-use sector (forestry) (Department of Communications, Climate Action and Environment, 2019). In parallel, GHG gas mitigation and adaptation measures have been addressed in National Mitigation Plans and the National Climate Change Adaptation Frameworks (Department of Communications, Climate Action and Environment, 2019). The process of compliance has focused on early identification and ongoing updating of possible transition pathways to 2050 intended to inform sectoral strategic choices (Department of Communications, Climate Action and Environment, 2019). Climate action plans are also closely aligned with water related regulatory provisions. The main European water management framework is the Water Framework Directive (WFD) where one of the core aims is to protect and enhance all water bodies

(surface, ground and coastal waters). The WFD is linked with the birds and habitats, drinking water, bathing waters and urban wastewater directives, industrial emissions and environmental impact assessment directives, floods and the marine strategy framework. It is also linked with the priority substances directive and the groundwater directive, nitrates directive, sustainable use of pesticides and the sewage sludge directives. At a national level the WDF is linked with a suite of European Communities regulations and legislation (European Communities Water Policy Regulations (S.I. No. 722 of 2003), European Communities Environmental Objectives (Surface Waters) Regulations, 2009 (S.I. No. 272 of 2009), European Communities Environmental Objectives (Groundwater) Regulations, 2010 (S.I. No. 9 of 2010), European Communities (Good Agricultural Practice for Protection of Waters) Regulations, 2010 (S.I. No. 610 of 2010), European Communities (Technical Specifications for the Chemical Analysis and Monitoring of Water Status) Regulations, 2011 (S.I. No. 489 of 2011) and European Union (Water Policy) Regulations 2014 (S.I. No. 350 of 2014)).

Carbon in water from a water quality perspective needs to be regulated through the implementation of measures that seek to achieve ongoing improvements in the environmental status of water bodies from source to sea (Trodd and O'Boyle, 2018). It has been recognized that the threats to water quality and its relationship to land carbon mobility is substantial. According to recent reports, water quality decline has been envisaged to become a major issue associated with climate change and is likely to be evident in diffuse riverine pollution (Trodd and O'Boyle, 2018). The current River Basin Management Plan 2018–2021, has been developed to address these issues through protecting water bodies that are currently showing high or good quality status (by 2027) (Trodd and O'Boyle, 2018). What is on the agenda for years to come includes: water conservation and leakage reduction, improved level of scientific assessments, and the

development of water and planning guidance for local authorities (Trodd and O'Boyle, 2018). There is also a view that nature-based technologies (wetlands for instance) could be used as a tool to enhance water quality and conserve biodiversity and hence become a valuable approach in the response to climate change adaptation and in addressing sustainability. Given all these frameworks, policies and strategies, it is important to view blanket peatlands as key determinants influencing water quality and in promoting sustainability: environmentally, economically and socially. The development of a deeper understanding of the dynamics of the Kippure blanket peatland system provides greater knowledge on the role these systems play in advancing sustainability particularly in relation to the role of carbon in climate change regulation and water quality.

5.1.2 Blanket peatland microtopography – dynamic and open systems

Blanket peatlands can be seen as dynamic open systems where GHG exchanges must be understood more accurately under different climatic and spatial conditions and settings. With respect to water – blanket peatland interactions and peatland drainage systems represent a setup where water bodies such as pools, lakes and streams are well connected leading to lateral outflow and significant evasion of CO_2 (Johnson *et al*., 2010). Ignoring fluxes through the aquatic pathway can lead to significant underestimation of total catchment carbon losses (Dinsmore, 2008). Benthic respiration and pelagic mineralization, terrestrial respiration and weathering products delivered by subsurface or groundwater inflow are among the reasons for peatland pool supersaturation with respect of CO_2 (Johnson *et al*., 2010). Fluvial carbon exports constitute primarily POC, DOC and to some extent CO_2 and CH_4 (Stimson *et al*., 2017). Interaction where peatlands and air link constitute atmospheric fluxes of CO_2 and CH_4 via effluxion and degassing.

Variations in blanket peatland microtopography such as patterns of hummock-lawn-pool have been associated with gradients of carbon concentration and fluxing. Hummocks have been known to act as hot spots of carbon transformation (Stimson *et al*., 2017). Hummock soil and soil water conditions can be affected by changes in temperature, pressure, pH and water levels. These changes can not only influence the physical structure of the peat, but also affect microbial activity (Bell *et al.*, 2018). Microbial activity could be driven by plant root activity, which can also be influenced by climatic and chemical factors. The CO_2 dynamics of lawns are likely to be intermediate in its nature between pools and hummocks. This is because lawns are wetter than hummocks (water tables are higher). The concentrations of CO_2 are likely to be greater than observed in pools because lawns are not completely waterlogged, and decomposition is still possible where soil is exposed to oxygen. However, the main difference with hummocks is that the portion of soil that is under water is rich in aromatic organic matter that is not easily degradable, and therefore, the speed of carbon cycling and conditions influencing CO_2 production are closely related to the conditions observed within pools. As noted, these similarities could be explained partially by hydrological conditions. Water levels and absence of oxygen in these environments can cause anaerobic decomposition and preferential production of methane, with lower levels of CO_2 forming at later stages. Pool dynamics, DOC production and mineralization, along with low pH and supersaturated conditions, could result in overall lower levels of CO_2 compared with lawns and hummocks. Disturbances such as shear effect of winds and pool degassing could promote losses of CO_2 from pool surfaces.

In this study it was hypothesised that across pools, hummocks and lawns concentrations were greater during the summer periods. It was also suggested that summertime peatland

pore water under hummocks contains highest levels of CO_2 comparing with peatland pore water from lawns and pools. The following model 'Kippure-PeatHydro-CO_2' (Figure 76; Figure 77) was proposed to explain the differences in the levels of CO_2 across different seasons in different spatial settings and to explain diurnal variability driven by explanatory variables such as air, water and soil temperatures and air pressure. Effects of precipitation deposition on hydrology, microbiological activity, production of DOC, changes in pH and as a result CO_2 levels. To complete field-based monitoring, a model was proposed to explain degassing of CO_2 from pool surfaces largely driven by pool turbulence and disequilibrium driven by winds.

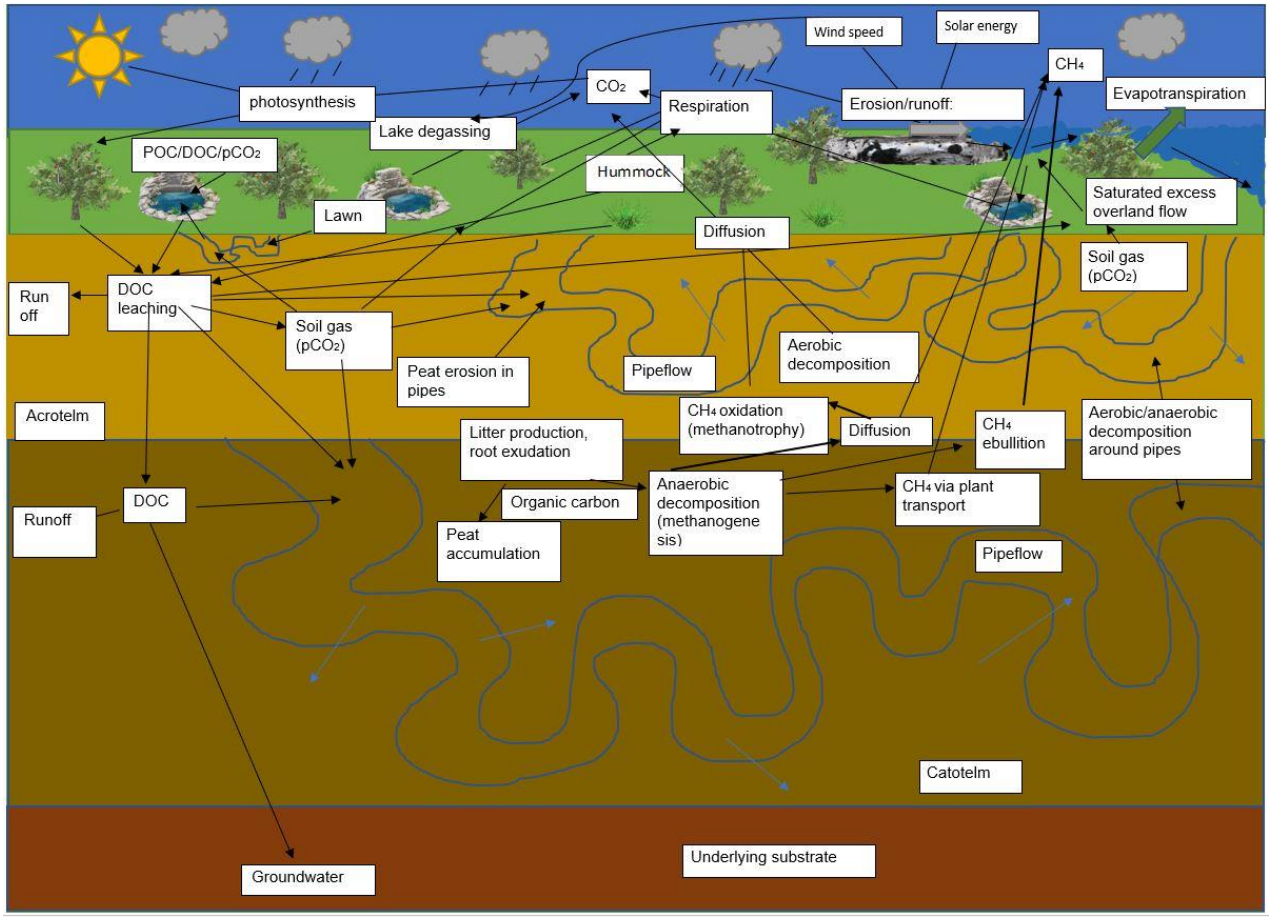

Figure 76 *'Kippure-PeatHydro-CO_2' conceptual model of carbon cycling in Liffey Head Bog, Wicklow Mountains National Park.*

a)

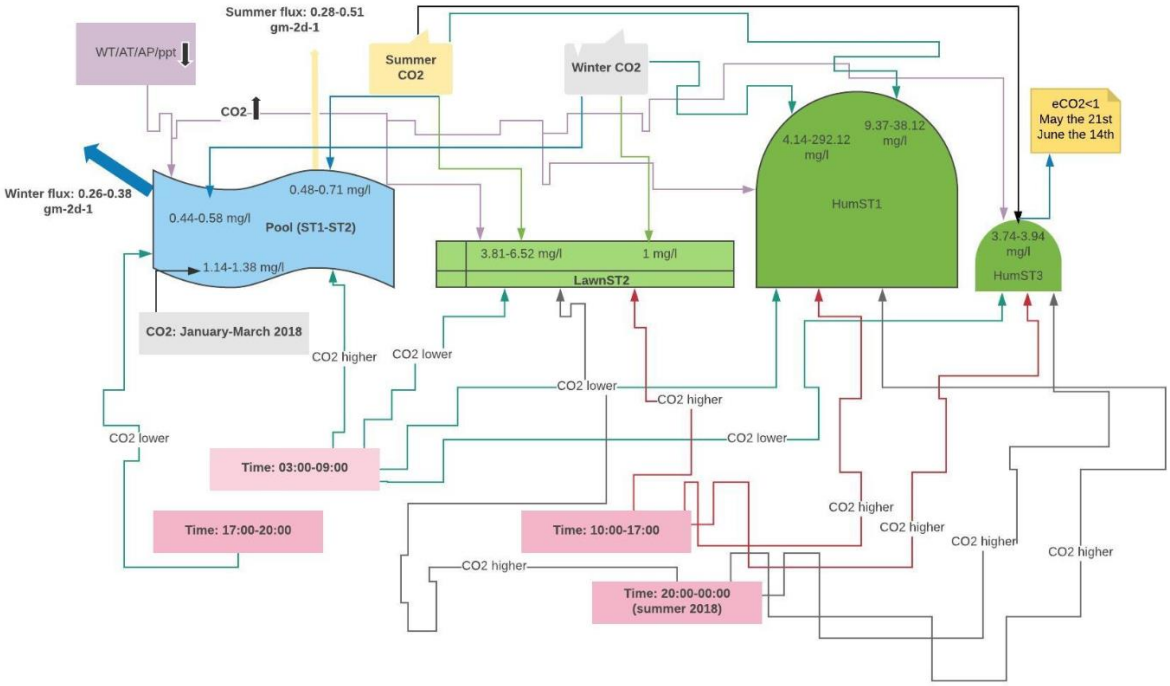

b)

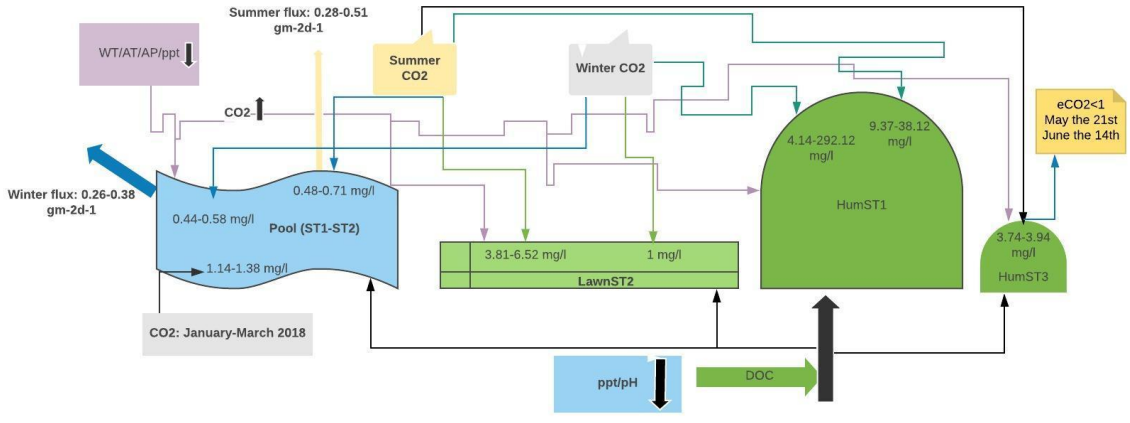

Figure 77 *Illustrating model of carbon dynamics in Kippure peatland: a)CO_2 dynamics; b) including DOC dynamics.*

5.2 Conceptual Model describing carbon dynamics of Kippure peatland

'Kippure-PeatHydro-CO_2' conceptual model was developed to illustrate water-air and soil interactions across the surface and within body of Kippure peatland (Figure 76). Elements depicted as part of this model (Figure 76) illustrate sources of carbon: organic matter, litter, precipitation (carbonic acid), some mineral forms (carbonate material) and wind-blown forms (dusts and organic materials). Schematic lists forms of carbon: methane, carbon dioxide in the atmosphere, dissolved organic/inorganic carbon, particulate organic carbon and soil/water carbon dioxide gas (Figure 76). Pathways of carbon transport are also visible on the schematic. These include aerial (wind-blown; pool degassing), fluvial (erosion, saturated excess overland flow, leaching underground, via lateral peat pipe flow and uplift via methane ebullition and subsequent breakdown) (Figure 76). The model illustrates factors influencing production of various forms of carbon: climatic (temperature, solar radiation, precipitation, evapotranspiration), biological (photosynthetic activity, microbial activity – aerobic and anaerobic decomposition, production of plant root exudates), physical factors (role of pH, turbulence and pressure) and spatial setting (hummocks, lawns and pools – water table gradient) (Figure 63). This conceptual model was further altered and developed to depict seasonal and diurnal trends in CO_2 (Figure 77). Key variables (temperature, pH, wind strength, water table level, precipitation, and organic carbon level) were illustrated to show correlation with carbon dioxide within Kippure peatland in this study (Figure 77).

5.2.1 Integrating project results into conceptual model

5.2.1.1 Correlation with temperature and water table – spatial orientation (hummocks, lawns and pools)

In general, NEE-CO_2 varies significantly in space, both within and between different peatlands. Results of this study suggest that CO_2 concentrations were greater in peat pore waters from hummocks (3.74-292.12 mgl^{-1} [C]) and a lawn microform (1-6.52 mgl^{-1} [C]) comparing to pool levels (0.44-0.71 mgl^{-1} [C]) (Figure 65; Figure 77). This difference observed at Kippure blanket peatland site when comparing hummocks, lawns and pools was primarily attributed to environmental controls such as water table levels (pool>lawn>hummock). Difference between levels of CO_2 within hummocks and a lawn were additionally potentially influenced/correlated with presence of different types of plant species (Pelletier, 2014). Hummocks are naturally drier, vegetation cover is denser (GEP & ER are higher), CO_2 sequestration is greater and more efficient (Waddington and Rouler, 2000). Although, downside of it, if hummocks are to be disturbed, they could potentially emit more CO_2. Summertime concentrations of CO_2 were found to be greater (maximum of 0.71 mgl^{-1} [C] in pool condition and maximum of 6.52 mgl^{-1} [C] in a lawn) than wintertime concentrations (maximum of 0.58 mgl^{-1} [C] in pool and 1 mgl^{-1} [C] in a lawn) in waters from pools and a lawn when looking at trends from entire study period 2016-2018 (Figure 65; Figure 77).

With regards to hummock conditions it was originally hypothesised that they would exhibit similar behaviour (e.g. greater summertime values of CO_2), however comparison of CO_2 levels at HumST1 throughout entire study period did not reflect correlation with the hypothesis (Figure 63). However, when CO_2 data from HumST1 were segmented (year 2016 until January 2018 and January 2018 until September 2018) and were plotted

against water temperature at HumST1, it was found that between January 2018-Septemeber 2018, there was a statistically significant ($P<0.05$) positive correlation between variables, summertime values were higher than wintertime values (Figure 65). The maximum level (33.24 mgl^{-1} [C]) of CO_2 was recorded on 8th of July 2018 and the lowest value (1.61 mgl^{-1} [C]) was recorded 2nd of February 2018. In work by Dinsmore *et al*. (2009a) it was noted that solar radiation, temperature and CO_2 production and consumption during summer months were correlated. Greater levels were observed under warmer conditions (Dinsmore *et al*., 2009a). This is consistent with what was modelled in this project. Solar radiation is a physical parameter positively linked with an air temperature. Higher temperatures promoting evaporation and naturally lowering water table of hummocks. Under warmer conditions plants uptake more water as well, root zone become drier and that triggers microbial decomposition in the root zone. Microbial activity intensifies under oxic conditions and stretches deeper into lower zones of acrotelm. Decomposition of organic matter and activity of plants (uptake of water, uptake of nutrients and production of carbon rich exudates) results in production of excess of CO_2.

Going back to peat pool summer dynamics, the summer levels were reflective of what was measured in analogous environments in Canada in 2011-2012 applying headspace technique (Pelletier, 2014). However, in Pelletier (2014) study, researchers additionally noted that concentrations were greater in smaller pools. Researchers also commented that levels varied temporally with levels increasing between June and August (Pelletier, 2014). Levels were decreasing from November onwards (Pelletier, 2014). These findings are in line with what was observed in this study. Concentrations of CO_2 were also measured using NDIR (Vaisala) between months of August-September 2011 and May-

August 2012 and were found to be on average between 0.7-1.35 mgl^{-1} [C] (Pelletier, 2014). Which is of similar magnitude to currently described project findings. Pelletier (2014) noted that drops in CO_2 in years 2011-2012 corresponded with declines in water temperature and air temperature. In line with current study, Pelletier (2014) observed that levels of CO_2 were higher at greater depths (1 m) and this relationship was even stronger during the summer. Similar findings were described by Dinsmore (2008a; 2009a). In one of papers by Dinsmore (2009a) it was established that summer CO_2 concentrations differ at different depths, at 10 cm mean value recoded using NDIR sensor was 17, 323 µatm and at 70 cm value was 50, 137 µatm. Soil air CO_2 values ranged between 8418 ppmV (shallow wells: 10-50 cm) and >90, 000 ppmV (deep wells: 50-90 cm) (Dinsmore, 2009a). This does support finding that levels of CO_2 were greater in lawn and hummocks waters as dip wells were 0.8 m in depth and sensor position was lower as opposed to surface position of pool-based sensors. Potential reasons behind this observation is that water tables under hummocks are generally lower and that stimulates breakdown of organic matter. Additionally, dip wells in these conditions were deeper stretching into catotelm where more resistant organic matter was stored, drying of the catotelm soil could have potentially activated enzymatic activity and breakdown of significant amount of recalcitrant organic matter producing large volumes of CO_2.

March 2018 spiking of CO_2 in pools (levels up to 6-7 mgl^{-1} [C]) related to snow and ice cover recorded in this study was consistent with what was recorded in similar study by Pelletier (2014). However, in his case, values measured by head space method were up to maximum of 8.1 mgl^{-1} [C] (Pelletier, 2014). NDIR records for the same period of ice cover were indicating that levels of CO_2 were up to a maximum of 3.25 mgl^{-1} [C] (Pelletier, 2014). In this study, our measurements were of intermediate extent. Researcher

had experienced a sensor failure due to extremely cold conditions similar to what was experienced in our study. This does indicate that under conditions of extreme freezing Vaisala sensors could perform less accurately and that can give underestimates in pools and or increased readings in peat pore water conditions. Perhaps this is a reason for seeing extremely high reading during wintertime between 2016-2017 in HumST1. Post ice melt values were found to be lowest and this could be attributed to significant dilution of CO_2 concentration (Dinsmore *et al*., 2009a). The mechanism of that phenomenon is that under ice cover, CO_2 has no way of escaping into atmosphere, as soon as ice cover disappears, CO_2 escapes into air. Additionally, ice meltdown produces excess water and that water dilutes existing CO_2 in the water. Overall, the effect of such processes is lowering of CO_2 levels.

Variability in CO_2 exchange between microforms is explained by different controls on the GEP and ER. GEP is variable spatially and this is due to a vegetation biomass and presence of groups of plant species. Plant species variability is influenced by water table (e.g. heather communities would establish in places that are drier; mosses would thrive where conditions are moist) (Pelletier, 2014). ER factor is a combination of both autotrophic and heterotrophic respiration, and these include plant respiration and organic matter decomposition. Vegetation biomass and types of plant species directly influence photosynthetic rates and therefore autotrophic respiration variability in different spatial settings (Pelletier, 2014). Water table position across different microforms is the main factor influencing carbon dynamics via affecting decomposition rates. As water table level reduces or increases the thickness of peat soil changes and therefore has direct influence on microbial activity, and breakdown of soil organic matter. Water table changes are directly linked with climatic conditions. That is a rationale behind seeing

greater levels of CO_2 produced during summertime in hummocks and lawns. Lower water table, greater microbial activity and as result higher respiration. In pools, greater levels of CO_2 in summertime could be to certain extent be due to evaporation of pool water under extreme air temperatures conditions, followed by pool volume reduction and overconcentration of CO_2 per that given volume (opposite to dilution post ice melt). Similar trend was observed in study by Dinsmore *et al*. (2009a). Furthermore, more in depth investigation carried by Dinsmore *et al*. (2009a) revealed that in standing water at 10 cm depth, with water rich in CO_2, with high levels of light, high temperature environment specially during the summer periods had a different diurnal dynamic of carbon when comparing with lower levels at about 60 cm. Pool of water developed a strong thermocline during the day associated with a significant increase in CO_2 with depth (Dinsmore *et al*., 2009a). As clearly pointed by Dinsmore *et al*. (2009a) diurnal patterns of CO_2 are driven by variability of microclimatic and hydrological factors. In line with that, the main observation of currently described study is that temperature is not a singular factor influencing on CO_2 production. In this described study, hummock soils were thick peat soils with drier acrotelms exposed to oxidation. Water present was likely to partition forming thermocline, where gases were concentrating. Depending on the depth where NDIR sensors were positioned they would read significantly different levels of carbon dioxide at that given time (e.g. closer to surface – greater).

5.2.1.2 Aromaticity of organic matter and correlation with extent of CO_2 production

Comparison of pool and hummock/lawn CO_2 concentrations were carried by various researchers. In these studies, it was mentioned that not only microbial decomposition is accountable solely for differences between CO_2 dynamics of pools, hummocks and lawns but in fact decomposition potential itself is a factor influenced by presence of certain types of organic matter and that is dependent on plant species present. Lower values of CO_2 observed in pools in general were explained by the fact, that pools contain higher levels of aromatic polymers that are characterised by structural and chemical recalcitrance and that leads to lower decomposition rates relative to other substrates from other microforms (Bell *et al*., 2018). This observation in fact was supported in this study, where water samples were analysed for aromaticity and samples of pool water were found to be more aromatic in nature than peat pore water samples (SUVA tests). The picture is different in hummocks and lawns. Dominance of certain plant groups like *Sphagnum* or *Calluna* is the key in explaining excess of CO_2. It was shown that *Sphagnum* produced lower levels of DOC but slightly more levels of CO_2 than *Calluna*, because *Sphagnum* is more recalcitrant (Bell *et al*., 2018). Opposite is true to *Calluna* (Bell *et al*., 2018). Therefore, variability in carbon fixation between peatland types and regions has been linked to a site's vegetation biomass, leaf index and plant functional type (Laine *et al*., 2011). In studies conducted by Lund *et al*. (2010) it was shown that higher leaf index corresponds with greater photosynthetic rates and CO_2 sinks. Plant functional groups influence NEE of peatland and that was observed by Laine *et al.* (2011) even though the biomass was significantly different when comparing two sites that they were working at.

Vascular plants have stronger photosynthetic capacity and are associated with stronger fixing properties of CO_2 (Pelletier, 2014). However, such trend could have a downside

when peatland state is under stress. Significant portion of fixed CO_2 from hummocks and lawns may be lost through CO_2 respiration over the winter. According to Roulet *et al*. (2007) on an annual basis almost 60% of the CO_2 taken up during the growing season was lost during the winter via heterotrophic respiration. Additionally, about 50% of the remaining portion was lost through methane emissions and DOC export during the snow free season (Roulet *et al*., 2007). This could be another explanation for observing less CO_2 in summer 2017 at HumST1, comparing with winter of 2016-17, stronger photosynthetic activity of *Calluna* plants. In this period climatic conditions were mild; no extreme weather events were recorded, and the growing season was long to sustain productivity of *Calluna*. This specific hummock site had dominant *Calluna* community.

5.2.1.3 Microbial activity and correlation with CO_2

Another parameter that needs to be considered when comparing CO_2 dynamics of hummocks, lawns and pools is presence of distinct microbial communities. Higher surface soil respiration could be attributed to oxidation of methane by methanotrophic bacteria, that process could led to production of up to 71% of CO_2 (Dinsmore, 2008). In addition to this, vascular plant roots could transport oxygen that can leak into rhizosphere, which can stimulate oxidation of methane (Dinsmore, 2008). The product of methane oxidation is CO_2. This is an important link between plants and carbon dynamics. The link that is important to investigate further if to establish a rationale behind spatial variability in GHG in Kippure Bog. Another process that has same effect on methane breakdown is the level of water table that was variable at different times of year and was changing across hummocks and lawns. The commonly adopted diplotelmic view of peatland structure has another implication for spatial and seasonal variability in GHG across

Wicklow blanket bog. Peatland flow paths for solutes and dissolved gases include saturation and infiltration-excess overland flow, near surface throughflow, throughflow from deeper peat layer and groundwater flow through the underlying mineral and bedrock layers (Holden *et al.* 2001). It was earlier assumed that runoff production and solute transfer occurs primarily in the near surface acrotelm. However, although catotelm has lower hydraulic conductivity, presence of peatland pipes and wider channels has potential for causing flash distribution of carbon laterally. In places where these soil pipes are bridging hummocks and pools such interconnection could result in post drought enrichment of pools with freshly produced DOC that can further decompose either along the way or when released into pools. In a study by Dinsmore (2008) it was emphasised that lateral water movement could be even more important than vertical movement. In his work, it was highlighted that low vertical hydraulic conductivity could result in a build-up of dissolved and gaseous solutes in peat pore water which then could be transported to pools via lateral throughflow or soil pipe flow (Dinsmore, 2008). However, such theory is largely unclear and under investigated (Dinsmore, 2009a). Nevertheless, this finding theoretically could help explaining higher levels of CO_2 at the end of summer in this study.

5.2.1.4 Diurnal variability of CO_2

Comparison of diurnal dynamics across pools and lawn/hummocks revealed that CO_2 concentrations were at their minimum between hours of 17:00-20:00 (pools) and 03:00-09:00 (hummocks/lawn). Greatest levels were detected between hours of 10:00-17:00; 20:00-00:00 (hummocks/lawn) and 03:00-09:00 (pools). Hamilton *et al*. (1994) observed that pool concentrations were greater at nights and lower during the day, but they have failed to find explanation to this as their data did not correlate with temperature, wind

speed or pressure. The work described in this study revealed similar pattern for pools. Levels were in general greater during dark hours and progressively decreasing toward daytime. It was also noted that levels of CO_2 were at their greatest in early morning time and that could be linked with photooxidation of DOC at the pool surface (Bertilsson and Tranvik, 2000). Photooxidation was noted to be an important factor in lake CO_2 supersaturation and the reaction has been linked to energy absorption which decreases with water depth (Bertilsson and Tranvik, 2000). In hummocks and lawn CO_2 levels did not vary as significantly and drops and rises of CO_2 were not as sharp as in pools on diurnal scale. Although CO_2 values were greater during daytime hours such trend could be explained by the limited light penetration at depth where sensors were, organic matter was not as exposed to photooxidation. To support pool based diurnal CO_2 cycling further, in work by Pelletier (2014) it was noted that diurnal variation was more pronounced at the surface than at 1 metre and the extent of that variation was greater in August and September 2011. They had established a positive correlation with cumulative daily photosynthetic active radiation. Additionally, Pelletier (2014) established that peatland pools were producing less CO_2 between 10:00-14:00 (up taking-fixing) and releasing more between 00:00-04:00 and 20:00-24:00. This does correlate with finding from all microforms in this study. In peat soil settings, the course of carbon production, consumption and release was linked with cycles of photosynthetic activity (during daytime) and respiration both microbial and autotrophic (during night-time).

In paper by Dinsmore (2009a) clear diurnal cycles of CO_2 were evident in both surface and deep water in peatland. Peak CO_2 concentration in deep water was at 16:00 and minimum was detected at 06:00 (Dinsmore, 2009a). This clearly aligns with finding in this study. Where greatest levels of CO_2 were recorded between 10:00-00:00 and lowest

values between 03:00-09:00. As of pool dynamics multiple peaking in CO_2 was only detected in March 2018 under snow cover, however in work by Dinsmore (2009a) they recorded two distinct daytime peaks at approximately 10:00 and 19:00. The minimum occurred at approximately 02:00 (Dinsmore, 2009a). These results to some extent correlate with results from our study. Dinsmore (2009a) also measured soil air CO_2 concentrations and they observed diurnal pattern; the peak occurred at midnight with a minimum at approximately 13:00 (Dinsmore, 2009a). In another study by Dinsmore (2008b) they have studied riverine diurnal cycling, and their observations could be useful here as well. In this riverine environment outlined in paper by Dinsmore (2008b) a clear diurnal cycling was identified, maximum concentration of CO_2 occurred between 13:00-14:00 and this was approximately 8 hours after daily minimum water temperature. From the data presented by Dinsmore (2008b) it could be clearly seen that water temperature rise was correlated with spiking of CO_2 on that diurnal scale.

5.2.1.5 CO_2 variability on diurnal scale correlation with temperature and air pressure

Summer and winter diurnal variations were correlated with air, soil, water temperatures, and air pressure. Correlation analysis revealed potential for temperature and air pressure to exert an influence on CO_2 dynamics on diurnal basis. Some of correlation trends were statistically significant. Certain temperature and air pressure levels were correlated with greater CO_2 levels. This trend was more significant when analysing summer data sets of diurnal CO_2 fluctuations. Water and air temperatures were factors that were more significantly correlating with trends of CO_2 ($P<0.05$). Fluvial fluxes of CO_2 were greater in summer. When wintertime data sets from peat-based locations were correlated with air pressure, the correlation between CO_2 diurnal dynamics and air pressure was positive. It

is likely that different process operated in pools and peat-soil conditions. It could be seen that effect of temperature on gas solubility linked with vapor pressure increases with temperature. Increased temperature caused an increase in kinetic energy. Higher kinetic energy caused more motion in molecules which break intermolecular bonds and escape from solution. Therefore, extent of CO_2 dissolved in pool water in this described study possibly was not captured as accurately, as higher temperatures were causing degassing. With regards to air pressure, decreased pressure in pool water allowed more gas molecules to be present in the air, with very little being dissolved in pool water. In peat-soils the conditions were not always as uniform, and water tables were changing, therefore at times, sensors were not completely submerged. Effects of temperatures on CO_2 levels on diurnal scale were more of prerequisite of biological activity. Warmer temperatures were stimulating decomposition. In work by Neff and Hooper (2002) it was noted that effects of temperature on production of CO_2, were largely dependent on vegetation community. Regarding air pressure effects, observations were consistent with the fact that more pressure was causing greater solubility of CO_2, by forcing gas molecules into solution, relieving the pressure that was applied, caused fewer gas molecules to be present in the air and more in solution.

In paper by Dinsmore (2008b) the researcher commented that temperature dependent changes in gas solubility cannot fully explain diurnal variation in CO_2. In his work there were no significant correlations between these parameters, and that suggested that effect of temperature was possibly masked or complicated by other factors – inputs from surrounding soils (Dinsmore, 2008b). Among complications referred to in this chapter were effects of periodic inundation of the sensor following fluctuations in water table (Dinsmore, 2008b). This could be possibly a reason for lower level of correlation between

water temperature and CO_2 fluctuations on diurnal scale in peat-based sites (HumST1). Nevertheless, Dinsmore (2008b) commented in his paper, that correct way of adjusting for time lags is considering transport of soil water and that may help explaining the signal in CO_2 in soil water.

In book by Strack (2008) it was mentioned that peat mineralisation is greatest between months of June-September and this is linked with highest temperatures experienced during this period. Greater level of CO_2 emissions is linked with that time. Similar trends were observed in currently described study and in work by Pelletier (2014) where researcher observed spiking of CO_2 that was more profound in August-September months. In work conducted by Ilnicki & Iwaszyniec (2002) highest values of CO_2 were recorded between 12:00-00:00 at depth of 90 cm, the monitoring was carried between June-September. This finding corresponds well with observations recorded in this study at HumST1. Similar to Ilnicki & Iwaszyniec (2002), in the paper by Johnson *et al*. (2010) it was noted that secondary diurnal change in CO_2 was attributed to differences between day and night temperatures.

5.2.1.6 CO_2 concentrations in water and peat soil – role of DOC.

In paper by Dinsmore (2009a) it was found that soil concentrations of CO_2 were lagging after water concentrations indicating that CO_2 was unlikely produced in adjacent peat. More likely explanation for correlation between soil and water CO_2 concentrations was temperature and the observed lag could be explained by the different thermal properties of soil and water (Dinsmore, 2009a). Short-wave radiation and both air and surface water temperatures were the key factors influencing aquatic CO_2 cycles (Dinsmore, 2009a).

Therefore, the main control on carbon levels in his study was biological activity of aquatic plants and algae (Dinsmore, 2009a). These effects could also explain diurnal trends (Dinsmore, 2009a). Double peaks in CO_2 were absent from data derived from deep waters and that is due to light inability to penetrate these depth and also due to higher photosynthetic activity in shallow layers (Dinsmore, 2009a). The main drivers for CO_2 production in surface waters were autotrophic and heterotrophic respiration (Dinsmore, 2009a). Autochtonous DOC was the primary substrate for CO_2 production, since this peatland had low soil-water connectivity (Dinsmore, 2009a). However, the author stressed that such dynamics could be different in spring, during or post snow melt, where dissolved CO_2 could be flushed into water from adjacent peat (Dinsmore, 2009a). Opposite, to findings by Dinsmore (2009a), in this study, the surface CO_2 dynamics on diurnal scale was different, there were no double peaks observed during the summertime, wintertime dynamics was not all linear as summertime. High CO_2 concentrations in northern temperate peatlands where conditions are restrictive of in-stream in water carbon processing (e.g. low temperatures and low pH), are of allochthonous in origin (Dinsmore, 2009). Lake CO_2 concentrations were linked with DOC levels in many studies (Jonsson *et al*., 2003; Roehm *et al*., 2009; Stimson *et al*., 2017), but pool dynamics did not receive as thorough attention and correlation is still missing for Irish blanket mires.

5.2.1.7 Role of precipitation, pH and organic acidity on fluvial CO_2 levels

Precipitation, pH and organic acidity were correlated with carbon concentrations in conceptual model described in this study (Figure 73 & 74). Precipitation was negatively correlated with levels of DOC and CO_2 (Figure 73 & 74). Drier conditions were promoting DOC accumulation and breakdown into CO_2. Pool waters contained more

aromatic materials. Similar trend was observed in Dinsmore (2008b), where researcher concluded that in dry period model a significant negative correlation between CO_2 and pH was dominant. In case of wet period – discharge model, both variables were decreasing with increasing discharge (Dinsmore, 2008b). Researcher outlined, that diurnal fluctuation in pH in peatland streams could have been influenced by presence of different forms of organic matter during the day and that is a direct factor affecting dynamics of CO_2, however he did also pointed that this relationship is still largely unclear (Dinsmore, 2008b).

In this study pH was negatively correlated with aromaticity and organic acidity. Water routed through the peat has low pH, and that causes losses of CO_2 and that is the reason for higher CO_2 levels at lower monthly rainfall because carbon concentrations are not diluted (Stimson *et al*., 2017). Peatland reservoirs like pools that accumulated large areas of organic sediments act as hotspots for carbon transformations (Stimson *et al*., 2017). Following breakdown of DOC into CO_2, pH was positively correlated with levels of CO_2 in this study (Figure 75). Levels of CO_2 in all microforms were likely be correlated with organic carbon levels originated in these environments and not with leaching of DIC from surrounding grounds that is usually a post-precipitation event outcome. Peatland pools described in this project were not connected to each other or to a stream and their basins were composed almost uniquely of organic matter, providing an almost unlimited amount of substrate for decomposition. In addition to this, pools in this study were located on the interfluve, and their sizes were small, the water inputs were likely to come dominantly from atmosphere in form of rain. CO_2 production is therefore pool driven, as a product of decomposing DOC. Another factor that was potentially important in this study was depth of pools, in study by Pelletier (2014) it was argued that deeper, permanent pools were releasing larger levels of carbon from sediments. Those peatlands that have deep,

permanent pools that cover more than 37% of area of peatland could act as sources of carbon (Pelletier, 2014). Limited emergent vegetation to uptake CO_2, and microbial and photodegradation of DOC were possibly among additional factors promoting production of CO_2 in this currently described study.

In study by Bell *et al*. (2018) it was found that there was a statistically significant interaction between rainfall and substrate with the proportion of carbon lost as CO_2 generally increasing under drier rainfall scenario. This finding is in line with observation from this described study (Figure 75). In study by Bell *et al*. (2018) it was revealed that drier conditions were significant in changing the partitioning between gas and aquatic carbon fluxes for the peat and *Sphagnum*. However, it was noted that partitioning between CO_2 and DOC in *Molinia*, *Calluna* and mixed litter was not affected by temperature and rainfall treatments (Bell *et al*., 2018). Drought induced acidification was proposed as a process responsible for reduced mobility of DOC observed in case of *Sphagnum* (Bell *et al*., 2018). In case of *Calluna* the opposite was true (Bell *et al*., 2018). In support of aforementioned, in the paper by Dinsmore (2008b) it was noted that carbon dioxide dynamics was linked with rainfall and pH in streams in peatland catchments. Although in stream and soil CO_2 levels were mirroring one another, rainfall-discharge trends were linked with trends in CO_2, in such that post discharge the levels of CO_2 were higher this was also correlated with pH, that was higher at the same time. Riverine concentration of CO_2 was on average 2.04 mgl^{-1} (Dinsmore, 2008b).

Similar was observed by Pelletier (2014) where CO_2 levels were found to correlate with dry periods where precipitation was minimal. In paper by Dinsmore (2008b) researcher

observed that CO_2 was spiking initially fast after rainfall and that was likely due to near surface throughflow transporting CO_2-rich water from peatland soil to the stream. It was noted that at the time of the study, peatland soils contained approximately 52 times more CO_2 comparing with atmosphere (approximately 21, 350 ppmV) (Dinsmore, 2008b). Secondary spiking of CO_2 post rainfall was lower, and that was explained by possible depletion of CO_2 or as result of change of flow path to saturation-excess overland flow) (Dinsmore, 2008b). Interestingly, the author hypothesise that because concentration of CO_2 in that incoming water was lower than concentration of CO_2 when river is at its baseflow, it means that primary source of CO_2 in stream is from deep peat/groundwater (Dinsmore, 2008b).

With regards to DOC, Pelletier (2014) noted that levels varied between 8-26 mgl^{-1} over the study period and that there was a significant relationship between levels of DOC and that of CO_2 but not in every pool. In the smallest pool (128 m^2) CO_2 decreased with increasing DOC and in bigger pool (1866 m^2) DOC increased and CO_2 increased as well. In the project described in this study similar DOC values were measured and there was a similar trend between DOC and CO_2 (positive correlation), pools were of intermediate size comparing to those described by Pelletier (2014). $SUVA_{254}$ and CO_2 relationship was found positive in study by Pelletier (2014). Peatland pool morphology was found to be a significant in driving CO_2 fluxes. In studies by McEnroe *et al*. (2009), Roehm *et al.* (2009) and Pelletier (2014) negative correlation was observed between pool area and fluxes. This could be due to loading of dissolved CO_2 and DOC from the surrounding landscape.

Linking CO_2 with DOC, it is further possible to speculate why would DOC levels rise in these environments at certain time periods. In study conducted by Freeman *et al*. (2001a) it was shown that temperature increases could contribute to higher levels of DOC. In work performed by Worrall *et al*. (2004) it was argued that temperature increase is not the only factor influencing DOC production. Freeman *et al*. (2001b) proposed that an enzymatic latch coupled with land management, temperature variability and nutrient enrichment is a mechanism responsible for driving production of DOC. This does correlate with proposed dynamics at Kippure peatland. In peat soil environment under hummocks and lawns it would be expected to experience variations in water table depending on the season. As water table falls, the phenol oxidase activity increases destroying phenolic compounds that supress the hydrolase activity (Worrall *et al*., 2005). That triggers decomposition event after water table has risen again (Worrall *et al*., 2005). That mechanism is an enzymatic latch (Worrall *et al*., 2005). This can cause increased peat decomposition, and as result increased DOC release following periods of drought or water-table drawdown (Worrall *et al*., 2005). DOC releases are also coinciding with autumn when water tables beginning to increase again in these types of environments (Worrall *et al*., 2005; Hannigan & Kelly-Quinn, 2014). In study by Hannigan & Kelly-Quinn (2014) carried at Kippure Bog, it was estimated that DOC values were greater in autumn than in spring. Increases of pH and decreases in ionic strength were correlated with DOC solubility (Hannigan & Kelly-Quinn, 2014). It was noted that thick mats of submerged *Sphagnum* moss could increase the amount of organic matter and DOC as a result (Hannigan & Kelly-Quinn, 2014). Temperature changes could promote decomposition of organic matter and DOC (Hannigan & Kelly-Quinn, 2014). These findings are in support of conceptual model proposed in this study (Figure 76 & 77).

Soil solution DOC values were found to be highest from samples under *Calluna* (33 mgl^{-1}), followed by *Sedge*/Hummock and *Juncus*/Hummock (23.8 and 22.6 mgl^{-1}) between years 2006-2007 (Dinsmore, 2009b). Soil air CO_2 was also highest under *Calluna* (4488 ppmV), followed by Hollow (3852 ppmV) and Juncus/Hummock (3149 ppmV) (Dinsmore, 2009b). In paper by Dinsmore (2009c), as part of mesocosm study, hummocks and depressions were evaluated, and respiration rates were measured, it was stated that respiration was greatest in the 'Sedge/Hummock' condition. It was also noted, when water table variability was simulated, both conditions had higher respiration rates when water tables were low (Dinsmore, 2009c). In paper by Dinsmore (2009c) it was noted that soil air CO_2 concentrations between months of February-May 2007 were higher with depth of soil and were on average 764 and 680 ppmV (deep and shallow) conditions. Comparing to peat pore water concentrations, these were significantly lower, but still higher than atmospheric levels. The combination of depth of well, water table level and plant type growing within microform were all drivers of carbon production and evasion. In condition where deep soil well was studied, where water table was low, and Juncus was growing production of CO_2 was greatest, opposite to this, lowest concentration in soil air was detected from condition where well was shallow, water level was highest and the microform was a depression (Dinsmore, 2009c). Therefore, lower water table causing higher respiration rates and reduces photosynthetic activity. Lowering of water table causes increased oxic respiration-decomposition (Dinsmore, 2009c). If deeper soil layers are to be continuously exposed to atmosphere as in this study (HumST1 & ST3) during dry periods (summer 2018), aerobic decomposition will be intensified and that will produce initially high volumes of carbon dioxide, but after time when water table will be restored, some of DOC could leach into water and be transported via pipework into pools, however, this DOC and some remaining organic matter will be highly recalcitrant and

aromatic. Therefore, decomposition to CO_2 in these deep wells at higher water tables post draught is likely to reduce significantly as observed in year 2018 comparing to years 2016-2017 in HumST2 condition. In paper by Dinsmore (2009c), GHG fluxes were modelled using 100-year global warming potentials, and the author found that CO_2 fluxes were dominating at the time. According to his simulation, under low table water conditions all three microforms (Sedge/Hummock>Depression>Juncus/Hummock) were fluxing CO_2 into atmosphere, and under high water table condition depression and Sedge/Hummock were fluxing CO_2 (Dinsmore, 2009c). Interestingly to see that both depression and Sedge/Hummock were sources of CO_2 under variable water tables and that Sedge/Hummock was significantly more productive in terms of decomposition under low water table (10, 608 CO2-eq $m^{-2}d^{-1}$) (Dinsmore, 2009c). Juncus/Hummock was the only one sinking CO_2 under high water table (Dinsmore, 2009c). At the time of study, DOC levels were quantified, and the values varied between 8.0-124 mgl^{-1} (Dinsmore, 2009c).

5.2.1.8 Correlation of wind caused turbulence and CO_2 fluxing into atmosphere

Peatland pools were found to act as net sources of carbon to the atmosphere, fluxing between 23 and 419 g C m^{-2} yr^{-1} (McEnroe *et al*., 2009; Pelletier *et al*., 2014). Wind speed controls the rate at which air is removed from near the water surface and helps to maintain the concentration gradient. In many systems, turbulence itself is regarded as a function of wind speed. Turbulence is crucial, as it determines the rate at which water is degassing. Turbulence is a driving force for water mixing, and it brings CO_2 from deeper profiles to surface layers within pools. The physical disturbance that turbulence causes is paramount as it increases the rate at which CO_2 can travel across the water-air boundary. At times, when wind speeds are high and therefore turbulence is great, pools could act as hotspots

of carbon evasion into atmosphere. In this described study, modelled fluxing of CO_2 from pools was greater in summer (Figure 77). Modelled summer levels were in range 0.28-0.51 $gm^{-2}d^{-1}$. Hamilton *et al*. (1994) observed higher fluxes in autumn, at the end of growing season. Higher fluxes in his opinion were supported by degradation of underlying peat, death and decay of algal mats (Hamilton *et al*., 1994). In other studies, the levels of CO_2 emission from peatland pools during ice-free periods were between 0.14-16.6 $gm^{-2}d^{-1}$ CO_2-C (Hamilton *et al*., 1994; Cliché Trudeau *et al.*, 2013). The levels modelled in this study were of similar extend.

'Thin layer boundary model' used in described study did not correlate with spiking of CO_2 during the month of March 2018, when there was extreme snowfall and negative air temperatures. There was significant accumulation of CO_2, that was later released into air and soil water post snow melt. Therefore, it is difficult to suggest based on model along what was the main driver causing greater fluxing in summer comparing to winter, release of stored CO_2 under snow cover or turbulence patterns created by winds or in fact mixture of two. In study by Pelletier (2014), pools were described to be constantly supersaturated in CO_2, and the fluxes were ranging between 0.06-2.48 $gm^{-2}d^{-1}$. These values were closer to levels modelled in currently described study. According to Pelletier (2014) fluxes were increasing from August to September 2011 and were decreasing until ice cover formed. In year 2012 maximum flux was lower than in 2011, as estimated from data using NDIR it was approximately 1.9 $gm^{-2}d^{-1}$ (Pelletier, 2014). Researcher also mentioned that strong wind patterns correlated with lower water concentrations as wind caused turbulence was affecting water-air interface exchange promoting fluxing of carbon into atmosphere (Pelletier, 2014). Similar trends were modelled described study (Figure 72). Summer evasion peaks (July and August) were observed in paper by Dinsmore (2009a). The author

explained this by suggesting that higher temperatures could have been promoting lower gas solubility (Dinsmore, 2009a). Similar explanation was suggested for higher evasion post snow melt in early spring, where flow of gas was increased in general under the ice and gas was also building prior to being released when snow and ice started to melt (Dinsmore, 2009a). Like what was modelled for March 2018 fluxing as part of this described study. Some spatial evasion variability was observed in paper by Dinsmore (2009a). Researcher explained such variability in two ways: firstly he proposed that summer evasion hot spots appeared to relate to *in situ* respiration and likely appeared where water was stagnant and where water contained high plant and algal biomass, and secondly, he proposed that turbulence caused by wind patterns in spring and autumn was another factor promoting evasion hot spots and high gas flow (Dinsmore, 2009a).

5.2.1.9 Spatial variability, climatic changes and future perspectives on carbon fluxing at Kippure peatland

Mostly, throughout entire period of monitoring all described macroforms were acting as sources of CO_2 into atmosphere ($epCO_2>1$) as modelled in the study described in this study. This finding is supported globally (Hamilton *et al*., 1994; Repo *et al*., 2007). Pools studied in this study in general contained less CO_2 comparing with other microforms, but still were effusing CO_2 into atmosphere (as per model) because of wind caused disturbance and surface turbulence. In general, according to Pelletier (2014) pools are not acting as sinks of CO_2 due to fact that their presence reduces vegetation biomass that could potentially develop on blanket peatland surface and would overwise fix CO_2.

With the global climate warming, future rainfall patterns would be going to some extremes in some localities (e.g. increases and decreases would be observed for northern latitudes) (Bell *et al*., 2018). Droughts would be more common, and temperatures would rise (Bell *et al*., 2018). Therefore, the projections are as such that under these changes, warmer summer temperatures, decrease rainfalls will stimulate decomposition, because water tables in peatlands will be reduced, fluxes of DOC in soils will be reduced and DOC will eventually breakdown into CO_2 (Bell *et al*., 2018). As for pools, similar events will occur, but also, post drought rainfall events would deliver carbon rich waters into pools via lateral flows. These scenarios could be applicable to peatlands such as Kippure blanket bog.

CHAPTER 6: CONCLUSIONS

Although Kippure Bog is a SAC site, the presence of Dublin city has affected this peatland site significantly putting anthropogenic pressures such as peat extraction, afforestation and vegetation burning which were all practiced in past (Tallis, 1998). Results of this continuous *in situ* study provided information that allowed to get a better understanding of carbon dynamics in upland blanket peatland system in Ireland. Irish peatlands are significant landscape unit covering approximately 20.6 % of land. They are reservoirs of carbon. Knowledge of carbon footprint associated with Kippure Blanket Peatland (SAC 002122) is of paramount importance. Rising concentrations of DOC globally are concerning. In the UK, a 12th year study cited in Freeman *et al*. (2001a) has shown an increase of 65% in levels of DOC from stream and lake catchment. This increased transport of DOC and excessive production of labile organic matter is indicative of shifting in global carbon budgets towards decreasing storage of carbon. Breakdown of DOC into CO_2 along the way, in the soil water and in peatland pools could represent a significant pathway for losses of carbon into atmosphere. Surface to atmosphere carbon exchanges at the microform level (hummock/lawn/pool) received limited attention in Ireland specially with regards to upland blanket peatland ecosystem scale. According to National Peatland Strategy (2016) it is essential to preserve and restore these peatlands (National Peatlands Strategy Progression Report, 2017). Knowing the state and carbon balance of Kippure peatlands, responsible stakeholders could be informed and that could potentially affect the way these environments are currently being management. It is essential to ensure that these peatlands are utilised environmentally friendly to allow future generations to enjoy visiting these landscapes. Proper management practices would result in gaining other benefits, such as compliance with EU environmental law, climate change, forestry, flood control, energy, nature conservation, planning, and agriculture.

Mitigation of climate change is at the forefront worldwide. In Ireland, there is a progressive goal set to minimise carbon emissions by 2050 as set as part of Climate Action and Low Carbon Development Act 2015 (Irish Statute Book, 2015). One of key elements in achieving this target is accurate quantification of peatland carbon budgets, and restoration of peatlands that are now contributing to atmospheric carbon levels.

In this study it was attempted to model the seasonal and spatial dynamics of carbon in upland blanket peatlands of Wicklow Mountains National Park. Findings of this study were indicating that these peatlands at the time of investigation were likely emitting carbon into water and air. Globally, such long-term records of dissolved CO_2 did not exist, as researchers were focusing on DOC primarily. This study provided records of dissolved CO_2 from upland blanket peatland in Ireland, and it is behaviour under changing climate. In year 2018, weather patterns experienced in Ireland were extreme. March 2018 was the coldest month with snow cover for a period of two weeks and negative temperatures up to -10 ^{0}C. Opposite to this, end of August was the driest and warmest period. With significant number of days with no precipitation deposition. Such extremes in weather simulate the effects of global climate warming on Kippure peatlands and on its capability at fixing and storing carbon. Findings of this study illustrated that Kippure peatland under changing climate cannot act as carbon sink and likely to progressively breakdown and emit CO_2 if restorative measures are not going to be implemented. To understand carbon dynamics in greater details in this environment there is a need to investigate with greater level of details certain unanswered topics. Find a different model or tool that will allow to monitor CO_2 under ice cover. Design experiments to compare effects of different vegetation species and microbial organisms on carbon dynamics. Quantify the proportion of pools per peatland site to establish sinking or sourcing potential of peatland. According

to Dinsmore (2008) largely unclear and under investigated is the role of soil pipes in transfer of solutes and gases. It is essential to model hydrological connectivity of Kippure peatland. Finally, according to Tranvik *et al*. (2009) deep water carbon sinking needs to be studied to better understand CO_2 cycling in pools, as they could be potentially be sinking carbon into sediments. All this question could help answer the question of how Kippure peatland will respond to global climate warming in the nearest future and will help to put the mitigation strategy in place not only to reduce losses of carbon but also to preserve this pristine environment from further degradation.

The monitoring method that was applied in this study was only able to capture a very local and limited carbon dynamics of Kippure peatland. Based on findings in this study it could be concluded that at that local point Kippure peatland was possible still disturbed. To understand the condition of the entire peatland site there is a need to implement a more accurate method of monitoring of carbon fluxing. One of suggested actions would be to increase the number of monitoring points (e.g. establish more stations and use more sensors). These should be spread across the entire area of Kippure peatland. To more accurately estimate the fluxing extent of carbon dioxide, there is a need to be able to measure wind speed directly and continuously across entire site. One of possible methods is Eddy Covariance tower technique (Patel *et al*., 2019). Another useful mean of monitoring carbon dynamic of peatlands is an application of satellite data-driven modelling approaches (Patel *et al*., 2019). The best option would be although to combine Eddy Covariance flux method, remote sensing modelling and hydrological sampling of organic carbon species this approach will allow to optimize the ecosystem model parameters, validation of its outputs, and up-scaling of CO_2 flux across spatial or temporal scales (Patel *et al*., 2019). The management recommendation would be to restore these environments, their hydrological function, vegetation cover and peat forming vegetation.

The key monitoring strategies to assess the success of restoration are surveys to assess vegetation biodiversity, measuring water tables to assess the effects of rewetting. In blanket peatlands the restoration in theory should reduce peak flow and increase lag times (e.g. attenuating storm hydrographs) because these bogs are 'flashy' in nature. Based on literature, the restored sites even after 8-12 years still indicate rising water tables, however variability is great between sites, but the stand is positive in general.

There is no statistically significant pattern of change in DOC concentrations over five years. This is surprising as the addition of significant labile carbon to the system through re-vegetation might be expected to increase DOC directly, or through the priming effect (Kuzyakov et al., 2000). Previous work has also shown that re-wetting of previously drained peat can produce spikes in DOC concentration (Worrall et al., 2007). In contrast, the slowly rising water tables discussed previously might be expected to reduce DOC concentrations, by minimising the proportion of the peat mass subject to aerobic decomposition, a standard concept of the diplotelmic model (Ingram, 1978). It should be noted that despite there being no statistically significant change, DOC at the sites studied was slightly elevated relative to control five years after restoration. Relatively slow response of DOC concentrations to re-vegetation might be expected in the same manner as hypothesised for the water table; i.e. changes in DOC production are likely to be a function of slow change in sub-surface conditions, rather than rapid change observed at the peatland surface.

REFERENCES/BIBLIOGRAPHY

- Aalen, F.H.A., Whelan, K. & Stout, M. (Ed.) (2011) *Atlas of the Irish Rural Landscape*. Cork: Cork University Press.
- Abouleish, M.Y.Z. & Wells, M.J.M. (2015) Trihalomethane formation potential of aquatic and terrestrial fulvic and humic acids: Sorption on activated carbon, *Science of the Total Environment*, **521–522**, 293–304.
- Amundson, R. (2001) The carbon budget in soils, *Annu Rev Earth Planet Sci*, **29**, 535–562.
- Andersson, S., Nilsson, S. & Saetre, P. (2000) Leaching of dissolved organic carbon (DOC) and organic nitrogen (DOM) in mor humus as affected by temperature and pH, *Soil Biology and Biochemistry*, **32**, 1-10.
- Anderson, R. (2001) *Deforesting and Restoring Peat Bogs*. A Review. Forestry Commission, Edinburgh, UK.
- Angell, J.K. & Korshover, J. (1981) Comparison between sea surface temperature in the Equatorial Eastern Pacific and United states surface temperatures, *Journal of Applied Meteorology*, **20**, 1105-1110.
- Aon, M.A. & Colaneri, A.C. (2001) Temporal and spatial evolution of enzymic activities and physico-chemical properties in an agricultural soil, *Applied Soil Ecology*, **18**, 255–270.
- ArcGIS (2020) *My Map*. Available online at: http://www.arcgis.com/home/webmap/viewer.html?url=http://services6.arcgis.c

om/uWTLlTypaM5QTKd2/ArcGIS/rest/services/Regional/FeatureServer/8&source=sd [Accessed 11 January 2020].

- Armstrong, A., Holden, J., Luxton, K. & Quinton, J.N. (2012) Multi-scale relationship between peatland vegetation type and dissolved organic carbon concentration, *Ecological Engineering*, **47**, 182– 188.
- Artz, R.R.E., Anderson, I., Chapman, S., Hagn, A., Schloter, M., Potts, J. & Campbell, C. (2007) Changes in fungal community composition in response to vegetational succession during the natural regeneration of cutover peatlands, *Microb. Ecol*, **54,** 508–522.
- Artz, R.R.E., Chapman, S.J., Siegenthaler, A., Mitchell, E.A.D., Buttler, A., Bortoluzzi, E., Gilbert, D., Yli-Petays, M., Vasander, H. & Francez, A.-J. (2008) Functional microbial diversity in regenerating cutover peatlands responds to vegetation succession, *J. Appl. Ecol*, **45**, 1799–1809.
- Baehr, M.M., DeGrandpre, M.D. (2004) In situ pCO2 and O2 measurements in a freshwater lake during turnover and stratification: observations and a model, *Limnology and Oceanography*, **49**: 330–340.
- Barthelmes, A., Couwenberg, J., Risager, M., Tegetmeyer, C., Joosten, H. (2015) *Peatlands and climate in a Ramsar context*. A Nordic-Baltic Perspective. Nordic Council of Ministers. Denmark.
- Battin, T.J., Kaplan, L.A., Findlay, S., Hopkinson, C.S., Marti, E., Packman, A.I., Newbold, J.D. & Sabater, F. (2008) Biophysical controls on organic carbon fluxes in fluvial networks, *Nat. Geosci.*, **1** (2), 95–100.
- Bell E, Lamminmäki T, Alneberg J, Andersson AF, Qian C, Xiong W, Hettich RL, Balmer L, Frutschi M, Sommer G and Bernier-Latmani R (2018)

Biogeochemical Cycling by a Low-Diversity Microbial Community in Deep Groundwater, *Front. Microbiol*. 9:2129. doi: 10.3389/fmicb.2018.02129.

- Belyea, L. R. (1996) Separating the effects of litter quality and microenvironment on decomposition rates in a patterned peatland, *Oikos*, **77**(3), 529-539.
- Belyea, B. & Clymo, A. (1999) *Do hollows control the rate of peat bog growth? Patterned Mires and Mire Pools*, (ed.) Standen, V., Tallis, J., Meade, R., pp. 55-65, Br. Soc., London.
- Belyea, L. R. & Clymo, R. S. (2001) Feedback control of the rate of peat formation, Proc. *R. Soc. Lond. Ser. B-Biol. Sci*., **268**, 1315-1321.
- Bertilsson, S., and L. J. Tranvik (2000), Photochemical transformation of dissolved organic matter in lakes, *Limnol. Oceanogr*., **45**, 753–762.
- Bhavani, R. (2013) Comparison of mean and weighted annual rainfall in Ananrapuram district, *International Journal of Innovative Research in Science, Engineering and Technology*, **2** (7).
- Bieroza, M.Z. & Heathwaite, A.L. (2016) Unravelling organic matter and nutrient biogeochemistry in groundwater-fed rivers under baseflow conditions: uncertainty in in situ high-frequency analysis, *Sci. Total Environ*. http://dx.doi.org/10.1016/j. scitotenv.2016.02.046.
- Billett, M.F., Palmer, S.M., Hope, D., Deacon, C., Storeton-West, R., Hargreaves, K.J., Flechard, C., Fowler, D. (2004) Linking land-atmosphere-stream carbon fluxes in a lowland peatland system, *Global Biogeochemical Cycles*, **18**, GB1024, doi: 10.1029/2003GB002058.
- Billett, M.F., Dinsmore, K.J., Smart, R.P., Garnett, M.H., Holden, J., Chapman, P., Baird, A.J., Grayson, R., Stott, A.W. (2012) Variable source and age of

different forms of carbon released from natural peatland pipes, *Journal of geophysical research*, **117**, GO2003, doi:10.1029/2011JG001807.

- Blodau, C., Basiliko, N. & Moore, T.R. (2004) Carbon turnover in peatland mesocosms exposed to different water table levels, *Biogeochemistry*,**67**, 331–51.
- Bridgeman,J., Gulliver,P., Roe,J. & Baker, A. (2014) Carbon isotopic characterisation of dissolved organic matter during water treatment, *Water Research*,**48**,119-125.
- Briones, M.J.I., Ineson, P. & Piearce, T.G. (1997) Effects of climate change on soil fauna; responses of enchytraids, Diptera larvae and tardigrades in a transplant experiment, *Appl. Soil Ecol.*, **6**, 117- 34.
- Briones, M.J.I., Ineson, P. & Poskitt, J. (1998) Climate change and *Cognettia sphagnetorum*: effects on carbon dynamics in organic soils, *Functional Ecology*, **12**, 528–535.
- Bonnett, S.A.F., Ostle, N. & Freeman, C. (2006) Seasonal variations in decomposition processes in a valley-bottom riparian peatland, *Science of the Total Environment*, **370**, 561-573.
- Borcard, D. & Matthey, W. (1995) Effect of a controlled trampling of Sphagnum mosses on their oribatid mites assemblages (*Acari, Oribatei*), *Pedobiologia*, **39**, 219–230.
- Boylan, N., Jennings, P. & Long, M. (2008) Peat slope failure in Ireland, *Quarterly Journal of Engineering Geology and Hydrogeology*, **41** (1): 93-108.
- Bullock, C.H., Collier, M.J. & Convery, F. (2012) Peatlands, their economic value and priorities for their future management – The example of Ireland, *Land Use Policy*, **29**, 921-928.

- Buondonno, A., Capra, G.F., Coppola, E., Dazz, C., Grilli, E., Odierna, P., Rubino, M. & Vacca, S. (2014) Aspects of soil phenolic matter (SPM): An explorative investigation in agricultural, agroforestry and wood ecosystems, *Geoderma*, **213**, 235-244.
- Buckmaster, C., R., Bain, S., Reed, M. C. (Eds) (2014) *Global Peatland Restoration demonstrating SUCCESS*. IUCN UK National Committee Peatland Programme, Edinburgh.
- Cabezas, A., Gelbrecht, J. & Zak, D. (2013) The effect of rewetting drained fens with nitrate-polluted water on dissolved organic carbon and phosphorus release, *Ecological Engineering*, **53**, 79– 88.
- Campos, J. R. da R., Silva, A. C., Fernandes, J. S. C., Ferreira, M. M., & Silva, D. V. (2011) Water retention in a peatland with organic matter in different decomposition stages. *Revista Brasileira de Ciência do Solo*, **35**(4), 1217-1227. Doi: https://dx.doi.org/10.1590/S0100-06832011000400015.
- Carrera, N., Barreal, M.E., Gallego, P.P. & Briones, M.J.I. (2009) Soil invertebrates control peatland C fluxes in response to warming, *Functional Ecology*, **23**, 637-648.
- CC-GAP (2005) *Peatlands. Do you Care?* Coordinating Committee for Global Action on Peatlands. Available at: http://www.imcg.net/docum/Peat_ccgap.pdf.
- Chakravarti, Laha, and Roy (1967) *Handbook of Methods of Applied Statistics*, Volume I, John Wiley and Sons, pp. 392-394.
- Chow, A.T., Tanji, K.K., Gao, S. & Dahlgren, R.A. (2006) Temperature, water content and wet–dry cycle effects on DOC production and carbon mineralisation in agricultural peat soils, *Soil Biol. Biochem.*, **38**, 477–488.

- Clair, T.A., Arp, P., Moore, T.R., Dalva, M., Meng, F.-R. (2002) Gaseous carbon dioxide and methane, as well as dissolved organic carbon losses from a small temperate wetland under a changing climate, *Environmental Pollution*, **116**, S143-S148.
- Clark, J.M., Chapman, P.J., Adamson, J.K. & Lane, S.N.(2005) Influence of drought-induced acidification on the mobility of dissolved organic carbon in peat soils, *Glob Change Biol*, **11** (5):791–809.
- Clark, J.M., Ashley, D., Wagner, M., Chapman, P.J., Lane, S.N., Evans, C.D., *et al*. (2009) Increased temperature sensitivity of net DOC production from ombrotrophic peat due to water table draw-down, *Glob Change Biol*, **15**(4):794–807.
- Clark, J.M., Bottrell, S.H., Evans, C.D., *et al*. (2010) The importance of the relationship between scale and process in understanding long-term DOC dynamics, *Science of the Total Environment*, **408**, 2768-2775.
- Clark, J.M., Heinemeyer, A., Martin, P., *et al*. (2012) Processes controlling DOC in pore water during drought cycles in six different UK peats, *Biogeochemistry*, **109**, 253-270.
- Cliche Trudeau, N., M. Garneau, and L. Pelletier (2013), Methane fluxes from a patterned fen of the northeastern part of the La Grande river watershed, James Bay, Canada, *Biogeochemistry*, **113(1-3)**: 409–422, doi:10.1007/s10533-012-9767-3.
- Cliché Trudeau, N., Garneau, M., Pelletier, L. (2014) Interannual variability in the CO2 balance of a boreal patterned fen, James Bay, Canada, *Biogeochemistry*, **118**(1-3), 371-387.

- Clymo, R.S. (1984) The limits to peat bog growth, *Philosophical Transactions of the Royal Society of London B,* **303**, 605-654.
- Clymo, R.S. (1987) *Interactions of Sphagnum with water and air*. In: Hutchinson, T.C., Meema, K.M. (Eds.) *Effects of Atmospheric Pollutants on Forests, Wetlands and Agricultural Ecosystems*, **16**, Springer, Heidelberg, 513–529.
- Cole, JJ. and Caraco, NF. (1998) Atmospheric exchange of carbon dioxide in a low-wind oligotrophic lake measured by the addition of SF6, *Limnology and Oceanography,* **43(4)**: 647-656. http://dx.doi.org/10.4319/lo.1998.43.4.0647.
- Cole J.J., Prairie Y.T., Caraco N.F., McDowell W.H., Tranvik L.J., Striegl R.G., Duarte C.M., Kortelainen P., Downing J.A., Middelburg J.J.& Melack J. (2007) Plumbing the global carbon cycle: integrating inland waters into the terrestrial carbon budget. *Ecosystems 10, 172–185*.
- Conaghan, J., Douglas, C., Grogan, H., O' Sullivan, A., Kelly, L., Garvey, L., Van Doorslaer, L., Scally, L., Dunnells, D., & Wyse Jackson, M., Goodwillie, R. & Mooney, E. (2000) *Distribution, ecology and conservation of Blanket Bog in Ireland, A synthesis of the reports of the blanket bog surveys carried out between 1987 and 1991 by the National Parks & Wildlife Service. Galway*: Enviroscope Environmental Consultancy.
- Cong, R.-G. & Brady, M. (2012) The interdependence between rainfall and temperature: Copula Analyses, *The Scientific world journal*, Article ID 405675, 1-11. Doi:10.1100/2012/405675.
- Connolly, J. & Holden, N.M. (2013) Classification of peatland disturbance, *Land degradation & development,* **24**, 548–555. Cole, J.J., Prairie, Y.T., Caraco, N.F., McDowell, W.H., Tranvik, L.J., Striegl, R.G., Duarte, C.M., Kortelainen, P., Downing, J.A., Middelbugh, J.J., Melack, J. (2007) Plumbing the global carbon

cycle: integrating inland waters into the terrestrial carbon budget, *Ecosystems,* **10**:172–185.

- Connolly, J. & Holden, N. (2013) *Identification, Mapping, Assessment and Quantification of the Effects of Disturbance of the Peat soil carbon stock in Ireland.* STRIVE synthesis report. Environmental Protection Agency Programme 2007-2013. University College Dublin.
- Cory, R.M., Boyer, E.W., McKnight, D.M., (2011) Spectral methods to advance understanding of dissolved organic carbon dynamics in forested catchments, *Forest Hydrology and Biogeochemistry: Synthesis of past Research and Future Directions*, 117–135.
- Council directive 1992/43/EEC on the conservation of natural habitats and of wild fauna and flora (1992). *Official Journal* L 206, p. 7–50.
- Council directive 2000/60/EU establishing a framework for community action in the field of water policy (2000). *Official Journal* L 327, p. 1–73.
- Crow., S. E. & Wieder, R. K. (2005) Sources of CO2 emission from a northern peatland: root respiration, exudation, and decomposition, *Ecology*, **86**(7), 1825-1834.
- Crowther, T.W., Sokol, N.W., Oldfield, E.E., Maynard, D.S.,Thomas, S.M. & Bradford, M. A. (2015) Environmental stress response limits microbial necromass contributions to soil organic carbon, *Soil Biology & Biochemistry*, **85,** 153-161.
- Curtis, C.J., Battarbee, R.W., Monteith, D.T. & Shilland, E. M. (2014) The future of upland water ecosystems of the UK in the 21st century: A synthesis, *Ecological Indicators*, **37,** 412-430.

- Davidson, E. A., K. Savage, L. V. Verchot, and R. Navarro (2002) Minimizing artifacts and biases in chamber-based measurements of soil respiration, *Agric. For. Meteorol.*, **113**, 21–37.
- Dawson, J. J. C., Billett, M.F., Neal, C. & Hill, S. (2002), A comparison of particulate, dissolved and gaseous carbon in two contrasting upland streams in the UK, *J. Hydrol*., **257**, 226–246.
- De Deyn, G.B., Cornelissen, J.H.C. & Bardgett, R.D. (2008) Plant functional traits and soil carbon sequestration in contrasting biomes, *Ecol. Lett*, **11**, 516–531.
- Department of Environment, Community and Local Government (2012) *'Our Sustainable Future, A Framework for Sustainable Development',* Dublin: Stationary office, Available at: http://www.sd-network.eu/?k=country%20profiles&s=single%20country%20profile&country=Ireland [Accessed 22 May 2015].
- Department of Communications, Climate Action and Environment (2019) *National Climate Policy* [available online] https://www.dccae.gov.ie/en-ie/climate-action/topics/climate-action-at-a-national-level/Pages/default.aspx (Accessed 20th June 2019).
- Dinsmore, K. J. (2008a) *Atmosphere-soil-stream greenhouse gas fluxes from peatlands*. PhD thesis. University of Edinburgh.
- Dinsmore, K.J., Billett, M.F. (2008b) Continuous measurement and modelling of CO2 losses from a peatland stream during stormflow events, *Water Resour Res*, **44**: W12417.

- Dinsmore, K.J., Billett, M.F., Moore, T.R. (2009a) Transfer of carbon dioxide and methane through the soil-water-atmosphere system at Mer Bleue peatland, Canada, *Hydrological Processes*, **23**, 330-341.
- Dinsmore, K.J., Skiba, U.M., Billett, M. F., Rees, R.M., Drewer, J. (2009b) Spatial and temporal variability in CH4 and N2O fluxes from a Scottish ombrotrophic peatland; implications for modelling and upscaling, *Soil Biology and Biochemistry*, **41**(6), 1315-1323.
- Dinsmore, K.J., Skiba, U. M., Billett, M. F., Rees, R.M. (2009c) Effect of water table on greenhouse gas emissions from peatland mesocosms, *Plant and Soil*, 318:229. https://doi.org/10.1007/s11104-008-9832-9.
- Dinsmore, K.J., Smart, R.P., Billett, M.F., Holden, J., Baird, A.J., Chapman, P.J. (2011a) Greenhouse gas losses from peatland pipes: a major pathway for loss to the atmosphere? *J Geophys Res Biogeosci*, **116**: G03041. doi:10.1029/2011JG001646.
- Dinsmore, K.J., Billett, M.F., Dyson, K.E., Harvey, F., Thomson, A.M., Piirainen, S., Kortelainen, P. (2011b) Stream water hydrochemistry as an indicator of carbon flow paths in Finnish peatland catchments during a spring snowmelt events, *Science of the total environment*, **409**, 4858-4867.
- Donnelly, D.P. & Boddy, L. (1997) Development of mycelial systems of *Stropharia caerulea* and *Phanerochaete velutina* on soil: effect of temperature and water potential, *Mycological Research*, **101**, 705–713.
- Dorrepaal, E. (2007) Are plant growth-form-based classifications useful in predicting northern ecosystem carbon cycling feedbacks to climate change? *J. Ecol*, **95**, 1167–1180.

- Douglas, C., Valverde, F.F. & Ryan, J. (2008) Peatland habitat conservation in Ireland. In: Farrell, C.A. & Feehan, J. (Eds.), After Wise Use – The Future of Peatlands. Proceedings of the 13th International Peat Congress Tullamore, Co. Offaly, Ireland: The International Peat Society, Finland. pp. 681–685.
- Drollinger, S., Maier, A., Glatzel, S. (2019) Interannual and seasonal variability in carbon dioxide and methane fluxes of a pine peat bog in the Eastern Alps, Austria, *Agricultural and Forest Meteorology*, **275**, 69-78.
- Elayouty, A., Scott, M., Miller, C., Waldron, S., Franco-Villoria, M. (2016) Challenges in modelling detailed and complex environmental data sets: a case study modelling the excess partial pressure of fluvial CO_2, *Environmental and Ecological Statistics*, **23(1)**: 65-87.
- European Commission (2003) *Interpretation Manual of European Union Habitats – EUR 25*. Habitats Committee, Commission of the European Communities, Brussels, Belgium.
- European Commission (2009) *Mainstreaming Sustainable Development into EU Policies: 2009*, Review of the European Union Strategy for Sustainable Development. European Communities, Brussels, Belgium.
- European Council (2006) *Review of the EU Sustainable Development Strategy (EU SDS) – Renewed Strategy*. Council of the European Union, Brussels, Belgium.
- Fasching, C., Behounek, B., Singer, G.A., Battin, T.J. (2014) Microbial degradation of terrigenous dissolved organic matter and potential consequences for carbon cycling in brown water streams, *Sci Rep*, **4:4981**. doi:10.1038/srep04981.

- Feeley, H.B., Bruen, M., Blacklocke, S. Baars & Kelly-Quinn, M. (2012) Significant changes in the hydrochemistry and drivers of episodic acidity in headwater streams draining plantation forest in Ireland: increasing role of organic acidity with the reduction of anthropogenic deposition, Science *of the Total Environment,* **443**, 173-183.
- Feeley, H.., Bruen, M., Blacklocke, S. & Kelly-Quinn,M. (2013) A regional examination of episodic acidification response to reduced acidic deposition and the influence of plantation forests in Irish headwater streams, *Science of the Total Environment,***443**, 173-183.
- Fellman, J.B., Hood, E., Spencer, R.G.M. (2010) Fluorescence spectroscopy opens new windows into dissolved organic matter dynamics in freshwater ecosystems: a review, *Limnol. Oceanogr*, **55** (6), 2452–2462.
- Fenner, N., Freeman, C. & Reynolds, B. (2005a) Hydrological effects on the diversity of phenolic degrading bacteria in a peatland: implications for carbon cycling, *Soil Biology & Biochemistry*, **37**, 1277–1287.
- Fenner, N., Freeman, C. & Reynolds, B. (2005b). Observations of a seasonally shifting thermal optimum in peatland carbon-cycling processes; implications for the global carbon cycle and soil enzyme methodologies, *Soil Biology & Biochemistry*, **37**, 1814–1821.
- Fenner, N. & Freeman, C. (2011) Drought-induced carbon loss in peatlands, *Nature Geoscience*, **4,** 895-900.
- Fiedler, S., Holl, B.S., Freibauer, A., Stahr, K., Drosler, M., Sehloter, M., Jungkunst, H. F. (2008) Particulate organic carbon (POC) in relation to other pore water carbon fractions in drained and rewetted fens in Southern Germany, *Biogeosciences,* **5**, 1615-1623.

- Fortuniak, K., Pawlak, W., Bednorz, L., Grygoruk, M., Siedlecki, M., Zielinski, M. (2017) Methane and carbon dioxide fluxes of a temperate mire in Central Europe, *Agricultural and Forest Meteorology*, **232**, 306-318.
- Frank, S., Tiemeyer, B., Gelbrecht, J. & Freibauer, A. (2013) High soil solution carbon and nitrogen concentrations in a drained Atlantic bog are reduced to natural levels by 10 yr of rewetting, *Biogeosciences*, **11**, 2309–2324.
- Freeman, C., Ostle, N. & Kang, H. (2001a) An enzymic 'latch' on a global carbon store, *Nature,* **409**, 149.
- Freeman, C., Evans, C.D., Monteith, D.T., Reynolds, B. & Fenner, N. (2001b) Export of organic carbon from peat soils, *Nature,* **412**, 785.
- Freeman, C., Fenner, N., Ostle, N.J., Kang, H., Dowrick, D.J., Reynolds, B., *et al*. (2004) Export of dissolved organic carbon from peatlands under elevated carbon dioxide levels, *Nature*, **430**(6996):195–8.
- Friedlingstein, P., Cox, P.M., Betts, R. A., et al. (2006) Climate-carbon cycle feedback analysis: results from the C^4MIP model intercomparison, *J. Clim*., **19**, 3337-3353.
- Frolking, S., Bubier, J.L., Moore, T.R., Ball, T., Bellisario, L.M., Bhardwaj, A., Carroll, P., Crill, P.M., Lafleur, P.M., McCaughey, J.H., Roulet, N.T., Suyker, A.E., Verma, S.B., Waddington, J.M., Whiting, G.J. (1998) Relationship between ecosystem productivity and photosynthetically active radiation from northern peatlands, *Global Biogeochemical Cycles*, **12**, 115-126.
- Frolking, S., Roulet, N.T. & Fuglestvedt, J. (2006) How northern peatlands influence the Earth's radiative budget: sustained methane emission versus sustained carbon sequestration, *Journal of Geophysical Research*, **111**: G01008.

- Gao, Y., Zhang, Z., Liu, X., Yi, N., Zhang, L., Song, W., Wang, Y. (2016) Seasonal and diurnal dynamics of physicochemical parameters and gas production in vertical water column of a eutrophic pond, *Ecological Engineering*, **87**, 313-323.
- GeoHive (2017) *Mapviewer*. Available online at: http://map.geohive.ie/mapviewer.html [Accessed 11 January 2020].
- Ghasemi, A. & Zahediasl, S. (2012) Normality tests for statistical analysis: A guide for non-statisticians, *Endocrinology & Metabolism*, **10(2):** 486-489.
- Global Peatland Initiative (2016) *What is the global peatlands initiative?* Available [online] at: https://www.globalpeatlands.org/ (Accessed 17 January 2020).
- Gunnarsson, U., Malmer, N. & Rydin, H. (2002) Dynamics or constancy in Sphagnum dominated mire ecosystems? A 40-year study, *Ecography*, **25**, 685–704.
- Hach (2015) *Carbon dioxide* [available online] at: file:///C:/Users/d14123766/Downloads/DOC316.53.01152_8ed.pdf (Accessed on the 4th of January 2017).
- Hach (2015) *DR 2800 spectrophotometer* [available online] at: http://au.hach.com/dr-2800-portable-spectrophotometer-with-lithium-ion-battery/product-downloads?id=14533795902 (Accessed on 8th of January 2017).
- Hamilton, J. D., Kelly, C. A., Rudd, J. W. M., Hesslein, R. H., Roulet, N. T. (1994) Flux to the atmosphere of CH4 and CO2 from wetland ponds on the Hudson-Bay Lowlands (Hbls), *J. Geophys. Res.- Atmospheres*, **99**, 1495-1510.

- Hammond, R.F. (1979) *The Peatlands of Ireland.* Soil Survey Bulletin 35, An Foras Talúntais, Dublin.
- Hannigan, E., Mangan, R., Kelly-Quinn, M. (2011) Evaluation of the sorces of Montain Blanket Bog Pool restoration in terms of aquatic macroinvertebrates, *Biology and Environment: Proceedings of the Royal Irish Academy*, **11(B)**: 1-11.
- Hannigan, E. & Kelly-Quinn, M. (2014) Hydrochemical characteristics of the open-water habitats of selected Irish peatlands, *Biology and Environment: Proceedings of the Royal Irish Academy*, **114 (2)**: 109-116.
- Heathwaite, A.L., Göttlich, K.H., Burmeister, E.G., Kaule, G. & Grospietsch, T.H. (1993) *Mires: definitions and form.* In: Heathwaite, A.L., Göttlich, K.H. (Eds.), Mires: Processes, Exploitation and Conservation. Wiley, Chichester, 1–75.
- Helago (2016) Eutech pH 700 - pH meter, pH electrode, ATC probe, electrode holder, available [online] at: https://www.helago-cz.com/eshop-eutech-ph-700-143446.html (Accessed 18 January 2020).
- Hess, D. (ed.) (2011) *McKnight's Physical Geography. A landscape Appreciation.* Pearson.
- Hodzic, M. & Kennedy, I.R. (2019) Time and frequency analysis of Vostok ice core climate data, *Periodicals of Engineering and Natural Sciences*, **7(2)**:907-923.
- Holden, J., Burt, T.P. & Cox, N.J. (2001). Macroporosity and infiltration in blanket peat: the implications of tension disc infiltrometer measurements, *Hydrol. Process*,**15**, 289–303.
- Holden, J. & Burt, T.P. (2003) Hydrological studies on blanket peat: the significance of the acrotelm-catotelm model, *Journal of Ecology*, **91,** 86-102.

- Holden, J. (ed.) (2004) *An Introduction to Physical Geography and the Environment*. Pearson.
- Holden, J. (2005) Piping and woody plants in peatlands: cause or effect? *Water Resour. Res*, **41**, W06009.
- Holden, J. (2009) Flow through macropores of different size classes in blanket peat, *J. Hydrol*, **364**, 342–348.
- Höll, B.S., Fiedler, S., Jungkunst, H.F., Kalbitz, K., Freibauer, A., Drösler, M. & Stahr, K. (2009) Characteristics of dissolved organicmatter following 20 years of peatland restoration, *Sci. Total Environ*, **408** (1): 78–83.
- Hongve D, Riise G. & Kristiansen J.F. (2004) Increased colour and organic acid concentrations in Norwegian forest lakes and drinking water — a result of increased precipitation, *Aquat Sci*, **66,** 231–8.
- Howard, T. & Clark, P. (2007) Correction and downscaling of NWP wind speed forecasts, *Meteorological Applications*, **14**, 105-116.
- IBM Corp. (2019) IBM SPSS Statistics for Windows, Version 26.0. Armonk, NY: IBM Corp.
- Ilnicki, P. & Iwaszyniec, P. (2002) *Emissions of greenhouse gases (GHG) from peatland*, In Restoration of Carbon Sequestration Capacity and Biodiversity in Abandoned Grassland on Peatland in Poland, Ilnicki, P. (ed.), Wydawnictwo AR PoznaĔ, pp.19-57.
- International Mire Conservation Group (2020) *About IMCG*. Available [online] at: http://www.imcg.net/pages/home.php (Accessed 17 January 2020).
- IPCC (2007) *Climate change 2007: the physical science basis summary for policymakers*. Contribution of Working Group I to the Fourth Assessment report of the IPCC.

- Irish Statute Book (2015) Climate Action and Low Carbon Development Act 2015. Available: http://www.irishstatutebook.ie/eli/2015/act/46/enacted/en/pdf. Accessed [11 May 2019].
- Jager, D.F., Wilmking, M. & Kukkonen, J.V.K. (2009) The influence of summer seasonal extremes on dissolved organic carbon export from a boreal peatland catchment: evidence from one dry and one wet growing season, *Science of the Total Environment*, **407**, 1373-1382.
- Jenkins, G.L., Murphy, J.M., Sexton, D.M.H., *et al*. (2009) *UK Climate Projections: Briefing Report*. Met Office Hadley Centre, Exeter, UK.
- Jenway (2020) 4510 and 4520 Bench conductivity meters, available [online] at: http://www.jenway.com/product.asp?dsl=248 (Accessed 18 January 2020).
- Johnson, J., Aherne, J., Cummins, T., Farrell, E.P., Neville, P., Harrington, F. & O'Dea, P. (2010) *Long-term trends in deposition and soil water chemistry at intensively monitored forest plots in Ireland: Results of 20 years of forest monitoring*. Ballinastoe, Wicklow: Workshops.
- Johnson, M.S., Billett, M.F., Dinsmore, K.E., Jassal, R.S. (2010) Direct and continuous measurement of dissolved carbon dioxide in freshwater aquatic systems – method and applications, *Ecohydrology*, **3**, 68-78.
- Jonsson, A., J. Karlsson, and M. Jansson (2003), Sources of carbon dioxide supersaturation in clearwater and humic lakes in northern Sweden, *Ecosystems*, **6**, 224–235.
- Joosten, H. & Clarke, D. (2002) *Wise Use of Mires and Peatlands*. International Mire Conservation Group and International Peat Society, Finland.

- Kaiser, K., Guggenberger, G., Haumaier, L. & Zech, W. (2001) Seasonal changes in the chemical composition of dissolved organic matter in organic forest floor leachates of old-growth Scots pine (*Pinus sylvestries* L.) and European beech (*Fagus sylvatica* L.) stand in northeastern Bavaria, *Germany. Biogeochemistry*, **55**, 103–43.
- Kalmykova, Y., Strömvalla,A-M. & Steenarib, B-M. (2008) Adsorption of Cd, Cu, Ni, Pb and Zn on Sphagnum peat from solutions with low metal concentrations, *Journal of Hazardous Materials*, **152** (2), 885-891.
- Kechavarzi, C., Dawson,Q., Bartlett, M. & Leeds-Harrison, P.B. (2010) The role of soil moisture, temperature and nutrient amendment on CO_2 efflux from agricultural peat soil microcosms, *Geoderma*, **154**, 203-210.
- Kiely, G., Leahy, P., McVeigh, P., Lewis, C., Sottocornola, M., Laine, A., Koehler, A.-K. (2018) *PeatGHG-Survey of GHG Emission and Sink Potential of Blanket Peatlands (2012-CCRP-MS.9)*, EPA Research Programme 2014-2020. EPA & UCC & Waterford IT.
- Koehler, A.-K., Sottocornola, M. and Kiely, G. (2011) How strong is the current carbon sequestration of an Atlantic blanket bog? *Global Change Biology*, **17**, 309–319.
- Koster, E., Koster, K., Berninger, F., Pumpanen, J. (2015) Carbon dioxide, methane and nitrous oxide fluxes from podzols of a fire chronosequence in the boreal forests in Varrio, Finnish Lapland, *Geoderma Regional*, **5**, 181-187.
- Kuhry, P., Nicholson, B.J., Gignac, L.D., Vitt, D.H. & Bayley, S.E. (1993) Development of Sphagnum-dominated peatlands in boreal continental Canada, *Can. J. Bot*, **71**, 10–22.

- Kuzyakov, Y. (2002) Review: factors affecting rhizosphere priming effects, *J Plant Nutri Soil Sc*, **165**(4):382–96.
- Laas, A., Cremona, F., Meinson, P., Room, E.-I., Noges, T., Noges, P. (2016) Summer depth distribution profiles of dissolved CO2 and O2 in shallow temperate lakes reveal trophic state and lake type specific differences, *Science of the Total Environment*, 566-567, 63-75.
- Laine, A., Byrne, K.A., Kiely, G. and Tuittila, E.-S. (2007) Patterns in vegetation and CO2 dynamics along a water level gradient in a lowland blanket bog, *Ecosystems*, **10**, 890–905.
- Laine, A. M., J. Bubier, T. Riutta, M. B. Nilsson, T. R. Moore, H. Vasander, and E.-S. Tuittila (2011), Abundance and composition of plant biomass as potential controls for mire net ecosytem CO2 exchange, *Botany*, **90(1)**: 63–74, doi:10.1139/b11-068.
- Ledesma, J.L.J., Kohler, S.J. & Futter, M.N. (2012) Long-term dynamics of dissolved organic carbon: implications for drinking water supply, *Science of the Total Environment*, **432**, 1-11.
- Li, C., Grayson, R., Holden, J., Li, P. (2018) Erosion in peatlands: Recent research progress and future directions, *Earth-Science Reviews*, **185**, 870-886.
- Limpens, J., Berendse, F., Blodau, C., Canadell, J.A., Freeman, C., Holden, J., Roulet, N., Rydin, H. & Schaepman-Strub, G. (2008) Peatlands and the carbon cycle: from local processes to global implications — a synthesis, *Biogeosciences*, **5**, 1475–1491.
- Lindsay, R. (1995) *Bogs: the Ecology, Classification and Conservation of Ombrotrophic Mires*. Scottish Natural Heritage, Edinburgh, Scotland.

- Lindsay, R.A. & Bragg, O.M. (2004) *Wind Farms and Blanket Peat*. The Bog Slide of 16th October 2003 at Derrybrien, Co. Galway, Ireland. University of East London, London, UK.
- Lorke, A., Bodmer, P., Noss, C., Alshboul, Z., Koschorreck, M., Somlai, C., Bastviken, D., Flury, S., McGinnis, D., and Maeck, A. (2015) Technical Note: *Drifting vs. anchored flux chambers for measuring greenhouse gas emissions from running waters*, vol. 12, no. 17.
- Lund, M. *et al*. (2010) Variability in exchange of CO2 across 12 northern peatland and tundra sites, *Glob. Change Biol*., **16**, 2436–2448.
- Malone, S. & O'Connell, C. (2009*) Ireland's Peatland Conservation Action Plan 2020 – Halting the Loss of Peatland Biodiversity.* Irish Peatland Conservation Council, Rathangan, Co. Kildare, Ireland.
- Manahan, S.E. (2011) *Water Chemistry. Green Science and Technology of Nature's most renewable resource*. US: Taylor and Francis Group, LLC.
- MathWorks (1994-2020) Documentation: autocorr, available [online]: https://uk.mathworks.com/help/econ/autocorr.html (Accessed 27 January 2020).
- MATLAB (2018) 9.7.0.1190202 (R2019b), Natick, Massachusetts: The MathWorks Inc.
- Mattsson, T., Kortelainen, P., Lepisto, A. & Raike, A. (2007) Organic and mineralogical acidity in Finnish rivers in relation to land use and deposition, *Science of the Total Environment*, **383**, 183-192.
- McEnroe, N. A., N. T. Roulet, T. R. Moore, and M. Garneau (2009), Do pool surface area and depth control CO2 and CH4 fluxes from an ombrotrophic raised

bog, James Bay, Canada?, *J. Geophys. Res. Biogeosciences*, **114(G1)**: G01001, doi:10.1029/2007JG000639.

- McKnight, D.M., Boyer, E.W., Westerhoff, P.K., Doran, P.T., Kulbe, T., Andersen, D.T. (2001) Spectrofluorometric characterization of dissolved organic matter for indication of precursor organic material and aromaticity, *Limnol. Oceanogr*, **46** (1), 38–48.
- McNamara, N.P., Plant, T., Oakley, S., Ward, S., Wood, C. & Ostle, N. (2008) Gully hotspot contribution to landscape methane (CH4) and carbon dioxide (CO2) fluxes in a northern peatland, *Sci. Total Environ*, **404**, 354–360.
- Medvedeff, C.A., Bridgham, S.D., Pfeifer-Meister, L. & Keller, J.K. (2015) Can Sphagnum leachate chemistry explain differences in anaerobic decomposition in peatlands? *Soil Biology & Biochemistry*, **86**, 34-41.
- MET Eireann (2019) *Historical data* [available online] at: https://www.met.ie/climate/available-data/historical-data (Accessed 29 August 2020).
- Monteith, D.T., Evans, C.D., Henrys, P.A., Simpson, G.L. & Malcolm, I.A. (2014) Trends in the hydrochemistry of acid-sensitive surface waters in the UK 1988-2008, *Ecological Indicators*, **37**, 287-303.
- Moore, T.R. & Dalva, M. (2001) Some controls on the release of dissolved organic carbon by plant tissues and soils, *Soil Science*, **166**, 38-47.
- Moss, B. (fourth ed.) (2010) *Ecology of fresh waters: A view for the twenty-first century*, John Wiley & Sons.
- Murphy, G., Collier, M. & Feehan, J. (2008) *Opinions of upland walkers on socio-cultural and environmental impacts on blanket bog habitats: cultural aspects of peat and peatlands.* In: Farrell, C.A. & Feehan, J. (Eds,), After Wise Use – The

Future of Peatlands. Proceedings of the 13th International Peat Congress Tullamore, Co. Offaly, Ireland. The International Peat Society, Finland. pp. 549–551.

- NASA Global Climate Change (2018) *Carbon Dioxide*, available [online] at: https://climate.nasa.gov/ (Accessed 16 January 2020).
- National Committee United Kingdom (2020) *Peatland Programme*. Available [online] at: https://www.iucn-uk-peatlandprogramme.org/about-us/global-peatland-initiatives (Accessed 17 January 2020).
- National Parks & Wildlife Service (2015) *Draft National Peatland Strategy.* Available at: http://www.npws.ie/search-results?as_q=draft [Accessed 22 May 2015].
- Neal, C., House, W.A., Down, C. (1998) An assessment of excess carbon dioxide partial pressures in natural waters based on pH and alkalinity measurements, *Sci Total Environ*, **210–211**:173–185.
- Neff, J.C., Hooper, D.U. (2002) Vegetation and climate controls on potential CO2, DOC and DON production in northern latitude soils, *Glob. Chang. Biol*., **8**, 872-884.
- Oke, T.R. (second ed.) (1987) *Boundary Layer Climates*, Talor & Frances e-Library.
- Omega (2017) *pH and Temperature Data Logger with LCD Display* [available online] at: http://www.omega.com/pptst/OM-CP-PHTEMP2000.html#description

(Accessed on 8th of January 2017).

- Onset Computer corporation (2005-2011) *Data logging rain gauge RG3 and RG3-M User's manual* [available online] at: http://www.onsetcomp.com/files/manual_pdfs/10241-D-MAN-RG3.pdf (Accessed on 8th of January 2017).
- Orellana, G., Cano-Raya, C., Lopez-Gejo, J. & Santos, AR. (2011) *Online Monitoring Sensors*, Treatise in water science: Aquatic Chemistry and Microbiology, **3**, pp. 221-236. ELSEVIER: UK.
- Otte (ed.)(2003*) Wetlands of Ireland. Distribution, ecology, uses and economic value*. University College Dublin Press, Dublin 2, Ireland.
- Pastor, J., Solin, J., Bridgham, S.D., *et al*. (2003) Global warming and the export of dissolved organic carbon from boreal peatlands, *Oikos*, **100**, 380-386.
- Patel, N.R., Padalia, H., Kushwaha, S.P.S., Nandy, S., Watham, T., Ahongshangbam, J., Kumar, R., Dadhwal, V.K., Kumar, A.S. (2019) *CO_2 flux tower and remote sensing: Tools for monitoring carbon exchange over ecosystem scale in Northwest Himalaya.* Project: Assessment of Forest productivity of Northwest Himalayan region. Chapter 14. Doi: 10.1007/978-981-13-2128-3_14.
- Peixeiro, M. (2019) *About time series* [available online] at: https://towardsdatascience.com/almost-everything-you-need-to-know-about-time-series-860241bdc578 (Accessed 10 February 2020).
- Pelletier, L. (2014) *Surface to atmosphere carbon exchange in peatlands with permanent open water pools*. PhD thesis. Dept. of Natural Resource Sciences, Macdonald Campus of McGill University, St.-Anne-de-Bellevue.

- Pfeiffer, T., Summerfelt, S.T., Watten, B.J. (2011) Comparative performance of CO2 measuring methods: Marine aquaculture recirculation system application, *Aquacultural Engineering*, **44(1)**, 1-9.
- Pind, A., Freeman, C. & Lock, M.A. (1994) Enzymatic degradation of phenolic materials in peatlands-measurement of phenol oxidase activity, *Plant and Soil*, **159**, 227–231.
- Plummer, L.N. & Busenberg, E. (1982) The solubilities of calcite, aragonite and vaterite in CO_2-H_2O solutions between 0 and 90 ^{0}C, and an evaluation of the aqueous model for the system $CaCO_3$-CO_2-H_2O, *Geochimica et Cosmochimica Acta*, **46**, 1011-1040.
- Poll, C., Ingwersen, J., Stemmer, M., Gerzabek, M.H. & Kandeler, E. (2006) Mechanisms of solute transport affect small-scale abundance and function of soil microorganisms in the detritusphere, *European Journal of Soil Science*, **57**, 583–595.
- Preston, M.D., Eimers, M.C. & Watmough, S.A. (2011) Effect of moisture and temperature variation on DOC release from a peatland: Conflicting results from laboratory, field and historical data analysis, *Science of the Total Environment*, **409**, 1235-1242.
- Probst, W. N., Stelzenmuller, V., Fock, H. O. (2012) Using cross-correlations to assess the relationship between time lagged pressure and state indicators: an exemplary analysis of North Sea fish population indicators, *ICES Journal of Marine Science*, **69(4)**: 670-681. Doi:10.1093/icesjms/fss015.
- Qassim, S.M., Dixon, S.D., Rowson, J.G., Worrall, F., Evans, M.G., Bonn, A. (2014) A 5-year study of the impact of peatland revegetation upon DOC concentrations, *Journal of Hydrology*, **519**, 3578–3590.

- Radomski, S. (2018) *'Peat-Hydro' carbon data code*. The C++ language. Ireland.
- Ramsar Convention Secretariat (2016) *The Fourth Ramsar Strategic Plan 2016–2024*. Ramsar handbooks for the wise use of wetlands, 5th edition, vol. 2. Ramsar Convention Secretariat, Gland, Switzerland.
- Renou-Wilson, F. & Farrell, C.A. (2009) Peatland vulnerability to energy-related developments from climate change policy in Ireland: the case of wind farms, *Mires and Peat*, **4**, 1-11.
- Renou-Wilson, F., Bolger, T., Bullock, C., Convery, F., Curry, J., Ward, S., Wilson, D. & Muller, C. (2011) *BOGLAND: Sustainable Management of Peatlands in Ireland*. STRIVE Environmental Protection Agency Programme 2007-2013. Prepared by University College Dublin. Ireland. Environmental Protection Agency, 157pp.
- Rezanezhad, F., Price, J.S., Quinton, W.L., Lennartz, B., Milojevic, T., Cappellen, P.V. (2016) Structure of peat soils and implications for water storage, flow and solute transport: A review update for geochemists, *Chemical Geology*, **429**, 75-84.
- Riley, J.L. (1986) *Laboratory methods for testing Peat-Ontario Peatland Inventory Project;* Open File Report 5572, 108 p.
- Ritson, J.P., Bell, M., Graham, N.J.D., Templeton, M.R., Brazier, R.E., Verhoef, A., Freeman, C. & Clark, J.M.(2014) Simulated climate change impact on summer dissolved organic carbon release from peat and surface vegetation: Implications for drinking water treatment, *Water Research*, **67**, 66 -7 6.
- RMS (2020) pH 700 bench meter kit [available online] at: https://rmsupply.co.uk/ph-meter-kits/81-eutech-ph-700-ph-tester.html (Accessed 28 August 2020).

-
- Robinson, J. W. (1996) *Atomic Spectroscopy*. CRC Press.
- Roehm, C. L., Y. T. Prairie, and P. A. del Giorgio (2009), The pCO2 dynamics in lakes in the boreal region of northern Quebec, Canada, Glob. *Biogeochem. Cycles*, 23.
- Roulet, N. T., P. M. Lafleur, P. J. H. Richard, T. R. Moore, E. R. Humphreys, and J. Bubier (2007), Contemporary carbon balance and late Holocene carbon accumulation in a northern peatland, *Glob. Change Biol.*, **13**, 397–411, doi:10.1111/J.1365-2486.2006.01292.
- Rowe, E.C., Tipping, E., Posch, M., Oulehle, F., Cooper, D.M., Jones, T.G., Burden, A., Hall, J. & Evans, C.D. (2014) Predicting nitrogen and acidity effects on long-term dynamics of dissolved organic matter, *Environmental Pollution*, **184**, 271-282.
- Ruhala, S.S & Zarnetske, J.P. (2017) Using in-situ optical sensors to study dissolved organic carbon dynamics of streams and watersheds: A review, *Science of the Total Environment*, **575**, 713-723.
- Ryder, E., de Eyto, E., Dillane, M., Poole, R. & Jennings, E. (2014) Identifying the role of environmental drivers in organic carbon export from a forested peat catchment, *Science of the Total Environment*, **490**, 28-36.
- Rydin, H. & Jeglum, J.K. (2013) *The biology of peatlands*. OUP Oxford.
- Saraceno, J.F., Pellerin, B.A., Downing, B.D. (2009) High-frequency in situ optical measurements during a storm event: assessing relationships between dissolved organic matter, sediment concentrations, and hydrologic processes, *J. Geophys. Res*, 114.

- Sarkkola, S., Koivusalo, H., Laurén, A., Kortelainen, P., Mattsson, T., Palviainen, M., *et al.* (2009) Trends in hydrometeorological conditions and stream water organic carbon in boreal forested catchments, *Sci Total Environ*, **408**(1):92-101.
- Schwalm, M. & Zeitz, J. (2015) Concentrations of dissolved organic carbon in peat soils as influenced by land use and site characteristics — A lysimeter study, *Catena*, **127**, 72-79.
- Scoones, I. (2007) Sustainability, *Development in Practice,* **17**(4-5): 589-596.
- Scott, M.J., Woof, C., Jones, M.N. & Tipping, E. (1998) Concentrations and fluxes of dissolved organic carbon in drainage water from an upland peat system, *Environ. Int*., **24**, 537-546.
- Shapiro, S. S. and Wilk, M. B. (1965) *Biometrika*, 52, 591-611.
- Sharma, P.D. (2005) *Environmental Microbiology*. Alpha Science International, Ltd, 382pp.
- Schneider, J., L. Kutzbach, S. Schulz, and M. Wilmking (2009) Overestimation of CO2 respiration fluxes by the closed chamber method in low-turbulence nighttime conditions, *J. Geophys. Res. Biogeosciences*, **114(G3)**, G03005, doi:10.1029/2008JG000909.
- Schulze, E.D. & Freibauer, A. (2005) Environmental science—carbon unlocked from soils, *Nature*, **437**, 205–206.
- Spiro, T.G., Purvis-Roberts, K.L., Stigliani, W.M. (ed.) (2012) *Chemistry of the Environment*. Uviversity Science Books.
- Sottocornola, M., Kiely, G. (2005) An Atlantic blanket bog is a modest CO2 sink, *Geophysical Research Letters*, **32**, L23804, doi: 10.1029/2005GL024731.

- Stimson, A.G., Allott, T.E.H., Boult, S., Evans, M.G. (2017) Reservoirs as hotspots of fluvial carbon cycling in peatland catchments, *Science of the total environment*, **580**, 398-411.
- Stojanova, D. (2012) *Considering autocorrelation in predictive models*. Doctoral Dissertation. JOŽEF STEFAN INTERNATIONAL POSTGRADUATE SCHOOL, Ljubljana, Slovenia.
- Strack, M. (ed.) (2008) *Peatlands and Climate change*. International Peat society. Finland.
- Strack, M.& Zuback, Y. C. A. (2013) Annual carbon balance of a peatland 10 years following restoration, *Biogeosciences*, **10**, 2885–2896.
- Strack, M., Zuback, Y., McCarter, C., Price, J. (2015) Changes in dissolved organic carbon quality in soils and discharge 1o years after peatland restoration, *Journal of Hydrology*, **527**, 345-354.
- Stroustrup, B. (fourth ed.) (2013) *The C++ programming language*. Addison-Wesley. Pearson Education.
- Sun, Y., Liu, C., Xie, P., Hartl, A., Chan, K., Tian, Y., Wang, W., Qin, M., Liu, J., Liu, W. (2016) Industrial SO2 emission monitoring through a portable multichannel gas analyzer with an optimized retrieval algorithm, *Atmos. Meas. Tech*., **9**, 1167-1180.
- Tallis, J.H. (1998) Growth and degradation of British and Irish blanket mires, *Environmental Reviews*, **6(2)**: 81-122.
- Takeda, K., Moriki, M., Oshiro, W. & Sakugawa, H. (2013) Determination of phenolic concentration in dissolved organic matter pre-concentrate using solid phase extraction from natural water, *Marine Chemistry,***157**, 208-215.

- Takeshita, Y., Johnson, K. S., Martz, T. R., Plant, J. N., & Sarmiento, J. L. (2018) Assessment of autonomous pH measurements for determining surface seawater partial pressure of CO2, *Journal of Geophysical Research: Oceans*, **123**, 4003–4013. https://doi.org/10.1029/2017JC013387.
- Tang, R., Clark, J.M., Bond, T., Graham, N., Hughes, D. & Freeman, C. (2013) Assessment of potential climate change impacts on peatland dissolved organic carbon release and drinking water treatment from laboratory experiments, *Environmental Pollution,* **173,** 270-277.
- Tang, J., Baldocchi, D.D., Qi, Y. & Xu, L. (2003) Accessing soil CO2 efflux using continuous measurements of CO2 profiles in soils with small solid-state sensors, *Agricultural and Forest Meteorology*, **118**, 207-220.
- The Irish Meteorological service (2016a) *Rainfall* [available online] at: http://www.met.ie/climate-ireland/rainfall.asp (Accessed 25 March 2017).
- The Irish Meteorological service (2016b) *Historical Data* [available online] at: http://www.met.ie/climate-request/ (Accessed 25 March 2017).
- The Irish Meteorological service (2016c) *Air temperature* [available online] at: http://www.met.ie/climate-ireland/surface-temperature.asp (Accessed 25 March 2017).
- Thurman E. M. (1985) *Organic Geochemistry of Natural Waters*. Martinus Nijhoff/Dr W. Junk Publishers, Dordrecht, The Netherlands.
- Tian, J., McCormack, L., Wang, J., Guo., D., Wang, Q., Zhang, X., Yu, G., Blagodatskaya, E. & Kuzyakov, Y. (2015) Linkages between the soil organic matter fractions and the microbial metabolic functional diversity within a broad-leaved Korean pine forest, *European Journal of Soil Biology*, **66**,57-64

- Toberman, H., Freeman, C., Evans, C., *et al*. (2008) Summer drought decreases soil fungal diversity and associated phenol oxidase activity in upland *Calluna* heathland soil, *FEMS Microbiology Ecology*, **66** (2): 426-436.
- Toivonen, J., Osterholm, P. & Frojdo, S. (2013) Hydrological processes behind annual and decadal-scale variations in the water quality of runoff in Finnish catchments with acid sulphate soles, *Journal of Hydrology*,**487**, 60-69.
- Tomassen, H.B.M., Smolders, A.J.P., Limpens, J., Lamers, L. and Roelofs, J.G.M. (2004) Expansion of invasive species on ombrotrophic bogs: desiccation of high N deposition, *Journal of Applied Ecology*, **41**, 139–150.
- Toosi, E.R., Schmidt, J.P. & Castellano, M.J. (2014) Soil temperature is an important regulatory control on dissolved organic carbon supply and uptake of soil solution nitrate, *European Journal of Soil Biology,* **61***,* 68-71.
- Tranvik, L. J., J. A. Downing, J. B. Cotner, S. A. Loiselle, R. G. Striegl, T. J. Ballatore, P. Dillon, K. Finlay, K. Fortino, and L. B. Knoll (2009), Lakes and reservoirs as regulators of carbon cycling and climate, *Limnol. Oceanogr*., **54(6_part_2)**: 2298–2314, doi:10.4319/lo.2009.54.6_part_2.2298.
- Trixie (2019) Thermometer. Available online at: https://www.trixie.de/heimtierbedarf/en/shop/Reptile/TerrariumAccessories/MonitoringControlling/?card=26756

  Accessed 18th April 2019.
- Trodd, W. and O'Boyle, S. (2018) *Water Quality in 2017: An indicators report*, Environmental Protection Agency. Ireland.

- Tsai, Y.I. & Kuo, S-C. (2013) Contributions of low molecular weight carboxylic acids to aerosols and wet deposition in a natural subtropical broad-leaved forest environment, *Atmospheric Environment,* **81,** 270-279.
- Turetsky, M.R. & St. Louis, V.L. (2006) *Disturbance in boreal peatlands*. In: Wieder, R.K. & Vitt, D.H. (Eds.), Boreal Peatland Ecosystems. Springer-Verlag Ecological Study Series. Vol. 188. Springer-Verlag, Berlin, Heidelberg, pp. 360–379.
- Turner, E.K., Worrall, F. & Burt, T.P. (2013) The effect of drain blocking on the dissolved organic carbon (DOC) budget of an upland peat catchment in the UK, *Journal of Hydrology*, **479,** 169-179.
- Uhlmann, D., Paul, L., Hupfer, M., Fischer, R. (2011) *Lakes and reservoirs*, Treatise on Water Science: Hydrology, **2**, pp. 157-211. Elsevier: UK.
- UNEP (United Nations Environment Programme), 2015. *The United Nations Environment Programme and the 2030 Agenda: Global Action for People and the Planet.* Resolution adopted by the General Assembly on 25 September 2015. United Nations, Washington, DC. Available online: https://wedocs.unep.org/handle/20.500.11822/9851 (accessed 18 April 2019).
- Vachon, D., Y. T. Prairie, and J. J. Cole (2010) The relationship between near-surface turbulence and gas transfer velocity in freshwater systems and its implications for floating chamber measurements of gas exchange, *Limnol. Oceanogr.*, **55**, 1723– 1732.
- Vaisala (2012) *How to measure carbon dioxide* [available online] at: http://www.vaisala.com/Vaisala%20Documents/Application%20notes/CEN-TIA-Parameter-How-to-measure-CO2-Application-note-B211228EN-A.pdf (Accessed on the 4th of January 2017).

- Vaisala (2013) *GMM220 Carbon Dioxide Modules for demanding OEM applications*. http://www.vaisala.com/Vaisala%20Documents/Brochures%20and%20Datasheets/GMM220_Datasheet-B210856EN-E.pdf (Accessed 25 March 2017).
- Van den Berg, L.J.L., Shotbolt, L. & Ashmore, M.R. (2012) Dissolved organic carbon (DOC) concentrations in UK soils and the influence of soil, vegetation type and seasonality, *Sci Total Environ,* **427-428,** 269-276.
- Van Seters, T.E. & Price, J.S. (2002) Towards a conceptual model of hydrological change on an abandoned cutover bog, Quebec, *Hydrol. Proced*, **16**, 1965–1981.
- Verry, E.S., Boelter, D.H., Paivanen, J., Nichols, D.S., Malterer, T., Gafni, A. (2011) *Physical properties of organic soils*. Peatland Biogeochemistry and Watershed Hydrology. Taylor and Francis Group, LLC.
- Vestgarden, L.S., Austnes, K. & Strand, L.T. (2010) Vegetation control on DOC, DON, and DIN concentrations in soil water from a montane system, southern Norway, *Boreal Environ. Res*, **15**.
- Waddington, J.M., Griffs, T.J., Rouse, W.R. (1998) Northern Canadian wetlands: Net ecosystem CO2 exchange and climatic change, *Climatic Change*, **40**, 267-275.
- Waddington, J.M., Roulet, N.T. (2000) Carbon balance of a boreal patterned peatland, *Global Change Biology*, **6**, 87-97.
- Waddington, J.M., Tóth, K., Bourbonniere, R. (2008) Dissolved organic carbon export from a cutover and restored peatland, *Hydrol. Process*., **22**, 2215–2224.
- Wallin, M.B., Oquist, M.G., Buffam, I., Billett, M.F., Nisell, J., Bishop, K.H. (2011) Spatiotemporal variability of the gas transfer coefficient (KCO2) in boreal

streams; implications for large scale estimates of CO2 evasion, *Global Biogeochem Cycles*, GB3025. doi:10.1029/2010GB003975.

- Wang, M., Wu, J., Lafleur, P.M., Luan, J. (2019) Investigation of the climatological impacts of agricultural management and abandonment on a boreal bog in western Newfoundland, Canada, *Science of the Total Environment*, in Press, Corrected Proof.
- Wanninkhof, R. (1992), Relationship between wind speed and gas exchange over the ocean, J. *Geophys. Res.,* **97**, 7373–7382.
- Ward, S.E., Bardgett, R.D., McNamara, N.P. & Ostle, N.J. (2009) Plant functional group identity influences short-term peatland ecosystem carbon flux: evidence from a plant removal experiment, *Funct. Ecol***, 23**, 454–462.
- Watts, C.D., Naden, P.S., Machell, J., *et al*. (2001) Long term variation in water colour from Yorkshire catchments, *Science of the Total Environment*, **278**, 57-72.
- WCED (World Commission on Environment and Development), 1987. Our Common Future. Oxford University Press, New York.
- Wellock, M.L., Reidy, B., Laperle, C.M., Bolger, T. & Kiely, G.(2011) Soil organic carbon stocks of afforested peatlands in Ireland, *Forestry***, 84** (4).
- Whitfield, C.J., Aherne, J., Baulch, H.M. (2011) Controls on greenhouse gas concentrations in polymictic headwater lakes in Ireland, *Sci Total Environ*, **410–411**:217–225.
- Wicklow Mountains National Parks (2016) *Blanket Bog* [available online] at: http://www.wicklowmountainsnationalpark.ie/images/downloads/Blanket%20Bog.pdf (Accessed 26 December 2016).
- Wilson, D., Muller, C., Renou-Wilson, F. (2013) Carbon emissions and removals from Irish peatlands: present trends and future mitigation measures, *Irish*

Geography, **46**(1-2), 1-23.

- Wooda, C.M., Al-Reasi, H.A. & Smith, D.S. (2011) The two faces of DOC, *Aquatic Toxicology*, **105S**, 3–8.
- Worrall, F., Reed, M., Warburton, J., Burt, T. (2003) Carbon budget for a British upland peat catchment, *The Science of the Total Environment*, **312,** 133-146.
- Worrall, F., Harriman, R., Evans, C.D., Watts, C.D., Adamson, J., Neal, C., Tipping, E., Burt, T., Grieve, I., Monteith, D., Naden, P.S., Nisbet, T., Reynolds, B., Stevens, P. (2004) Trends in Dissolved Organic Carbon in UK Rivers and Lakes, *Biogeochemistry*, **70**, 369-402.
- Worrall F, Burt T, Adamson J. (2005) Fluxes of dissolved carbon dioxide and inorganic carbon from an upland peat catchment: implications for soil respiration, *Biogeochemistry*, **73**, 515-539.
- Worrall, F., Burt, T. & Adamson, J. (2006) Trends in drought frequency — the fate of DOC export from British peatlands, *Climatic Change*, **76**, 339–59.
- Worrall, F. & Burt, T.P. (2007) Trends in DOC concentration in Great Britain, *J Hydrol*, **346**, 81–92.
- Wright, R.F. & Jenkins, A. (2001) Climate change as a confounding factor in reversibility of acidification: RAIN and CLIMEX projects, *Hydrology and Earth System Sciences*, **5** (3): 379-390.
- Yan, W., Artz, R.R.E. & Johnson, D. (2008) Species-specific effects of plants colonising cutover peatlands on patterns of carbon source utilisation by soil microorganisms, *Soil Biol. Biochem*, **40,** 544–549.
- Yang, R., Chen, B., Liu, H., Liu, Z. & Yan, H. (2015) Carbon sequestration and decreased CO2 emission caused by terrestrial aquatic photosynthesis: Insights

from diel hydrochemical variations in an epikarst spring and two spring-fed ponds in different seasons, *Applied Geochemistry*, **63**, 248-260.

- Yu, Z. (2011) Holocene carbon flux histories of the world's peatlands: global carbon-cycle implications, *The Holocene*, **21**(5), 761-774.
- Yu-Lai, W. Chang-Ming, Y., Li-Min, Z., & Heng-Zhao, C. (2015) Spatial Distribution and Fluorescence Properties of Soil Dissolved Organic Carbon Across a Riparian Buffer Wetland in Chongming Island, China, *Pedosphere*, **25**(2): 220–229.
- Zak, D. & Gelbrecht, J. (2007) The mobilisation of phosphorus, organic carbon and ammonium in the initial stage of fen rewetting (a case study from NE Germany), *Biogeochemistry*, **85**, 141–151.
- Zsolnay, A. (1996) *Dissolved humus in soil waters*. In: Piccolo, A., editor. Humic Substances in Terrestrial Ecosystems. Amsterdam: Elsevier.

APPENDICES

APPENDIX A

VAISALA

Certificate report no. H40-17270015

CALIBRATION CERTIFICATE

Instrument GMP221 Carbon dioxide probe
Serial number N2710029
Manufacturer Vaisala Oyj, Finland
Calibration date 6th July 2017

The carbon dioxide probe was calibrated against accurate gas concentrations. Gas concentrations were made by mixing pure carbon dioxide and nitrogen gases with mass flow controller factory working standards. Communication with the probe was achieved via a Vaisala GMB220ACB module. Pressure and temperature compensation was made by using the compensation parameters of a non-volatile memory in the probe and by using actual ambient pressure and temperature values read from a Vaisala PTU transmitter. At the time of shipment, the probe met its operating specifications.

The factory working standards have been calibrated at Vaisala Measurement Standards Laboratory (MSL).
The mass flow controllers have been calibrated using MSL Primary flow standard and the PTU transmitter using MSL pressure and temperature working standards.
The measurement results are traceable to the international system of units (SI) through national metrology institutes (NIST USA, MIKES Finland, or equivalent) or accredited calibration laboratories.

Calibration results

Reference % CO_2	Observed* % CO_2	Difference % CO_2	Permissible difference % CO_2
0.000	0.000	0.000	± 0.15
10.000	10.000	0.000	± 0.35

*Reading after pressure and temperature compensation.

Ambient conditions / Humidity 32 ± 5 %RH, Temperature 24.1 ± 1 °C, Pressure 1011 ± 1 hPa.

Equipment used in calibration

Type	Serial number	Calibration date	Certificate number
SEC-Z512MGX	3484321641	2017-02-17	A00336
SEC-Z512MGX	3411006991	2017-02-17	A00338
PTU30T	E2520011	2017-05-10	A00994
Vaisala GMB220ACB	X1330019	2016-12-01	H40-15500068

Gas cylinders used in calibration

Type	Purity classification	Cylinder number	Reference number
Scientific nitrogen	5.0	48453000011	0ZZ1X4/0/001/0
Scientific carbon dioxide	5.2	7523112138013	315666217-40

Technician

Vaisala Oyj | PO Box 26, FI-00421 Helsinki, Finland
Phone +358 9 894 91 | Fax +358 9 8949 2227
Email firstname.lastname@vaisala.com | www.vaisala.com
Domicile Vantaa, Finland | VAT FI01244162 | Business ID 0124416-2

VAISALA

Certificate report no. H40-16110076

CALIBRATION CERTIFICATE

Instrument	GMP221 Carbon dioxide probe
Serial number	M1140039
Manufacturer	Vaisala Oyj, Finland
Calibration date	17th March 2016

The carbon dioxide probe was calibrated against accurate gas concentrations. Gas concentrations were made by mixing pure carbon dioxide and nitrogen gases with mass flow controller factory working standards. Communication with the probe was achieved via a Vaisala GMB220ACB module. Pressure and temperature compensation was made by using the compensation parameters of a non-volatile memory in the probe and by using actual ambient pressure and temperature values read from a Vaisala transmitter. At the time of shipment, the probe met its operating specifications.

The mass flow controller factory working standards have been calibrated at Vaisala Measurement Standards Laboratory (MSL) by using Vaisala's mass flow primary standards. The mass flow primary standards are traceable to the National Institute of Standards and Technology (NIST). The pressure and temperature readings of the Vaisala transmitter have been calibrated at an ISO/IEC 17025 accredited calibration laboratory (FINAS), MSL by using working standards traceable to NIST.

Calibration results

Reference $\%\ CO_2$	Observed* $\%\ CO_2$	Difference $\%\ CO_2$	Permissible difference $\%\ CO_2$
0.000	0.000	0.000	± 0.15
10.000	9.976	-0.024	± 0.35

*Reading after pressure and temperature compensation.

Ambient conditions / Humidity 34 ± 5 %RH, Temperature 23.5 ± 1 °C, Pressure 1001 ± 1 hPa.

Equipment used in calibration

Type	Serial number	Calibration date	Certificate number
SEC-Z512MGX	3488748591	2016-01-19	Z00082
SEC-Z512MGX	3487509853	2016-01-13	Z00083
PTU30T	C2050002	2014-05-06	K008-X00984
GMB 220 ACB	D2810037	2015-12-11	H40-15500125

Gas cylinders used in calibration

Type	Purity classification	Cylinder number	Reference number
Scientific nitrogen	6.0	7527010212324	100399464
Scientific carbon dioxide	5.2	2703077	103000384986

Technician

Vaisala Oyj | PO Box 26, FI-00421 Helsinki, Finland
Phone +358 9 894 91 | Fax +358 9 8949 2227
Email firstname.lastname@vaisala.com | www.vaisala.com
Domicile Vantaa, Finland | VAT FI01244162 | Business ID 0124416-2

VAISALA

Certificate report no. H40-16110074

CALIBRATION CERTIFICATE

Instrument	GMP221 Carbon dioxide probe
Serial number	M1140037
Manufacturer	Vaisala Oyj, Finland
Calibration date	17th March 2016

The carbon dioxide probe was calibrated against accurate gas concentrations. Gas concentrations were made by mixing pure carbon dioxide and nitrogen gases with mass flow controller factory working standards. Communication with the probe was achieved via a Vaisala GMB220ACB module. Pressure and temperature compensation was made by using the compensation parameters of a non-volatile memory in the probe and by using actual ambient pressure and temperature values read from a Vaisala transmitter. At the time of shipment, the probe met its operating specifications.

The mass flow controller factory working standards have been calibrated at Vaisala Measurement Standards Laboratory (MSL) by using Vaisala's mass flow primary standards. The mass flow primary standards are traceable to the National Institute of Standards and Technology (NIST). The pressure and temperature readings of the Vaisala transmitter have been calibrated at an ISO/IEC 17025 accredited calibration laboratory (FINAS), MSL by using working standards traceable to NIST.

Calibration results

Reference % CO_2	Observed* % CO_2	Difference % CO_2	Permissible difference % CO_2
0.000	0.001	0.001	± 0.15
10.000	9.980	-0.020	± 0.35

*Reading after pressure and temperature compensation.

Ambient conditions / Humidity 34 ± 5 %RH, Temperature 23.5 ± 1 °C, Pressure 1001 ± 1 hPa.

Equipment used in calibration

Type	Serial number	Calibration date	Certificate number
SEC-Z512MGX	3488748591	2016-01-19	Z00082
SEC-Z512MGX	3487509853	2016-01-13	Z00083
PTU30T	C2050002	2014-05-06	K008-X00984
GMB 220 ACB	D2810032	2015-12-11	H40-15500123

Gas cylinders used in calibration

Type	Purity classification	Cylinder number	Reference number
Scientific nitrogen	6.0	7527010212324	100399464
Scientific carbon dioxide	5.2	2703077	103000384986

Technician

DOC210567-D

Vaisala Oyj | PO Box 26, FI-00421 Helsinki, Finland
Phone +358 9 894 91 | Fax +358 9 8949 2227
Email firstname.lastname@vaisala.com | www.vaisala.com
Domicile Vantaa, Finland | VAT FI01244162 | Business ID 0124416-2

VAISALA

Certificate report no. H40-17270016

CALIBRATION CERTIFICATE

Instrument	GMP221 Carbon dioxide probe
Serial number	N2710030
Manufacturer	Vaisala Oyj, Finland
Calibration date	6th July 2017

The carbon dioxide probe was calibrated against accurate gas concentrations. Gas concentrations were made by mixing pure carbon dioxide and nitrogen gases with mass flow controller factory working standards. Communication with the probe was achieved via a Vaisala GMB220ACB module. Pressure and temperature compensation was made by using the compensation parameters of a non-volatile memory in the probe and by using actual ambient pressure and temperature values read from a Vaisala PTU transmitter. At the time of shipment, the probe met its operating specifications.

The factory working standards have been calibrated at Vaisala Measurement Standards Laboratory (MSL).
The mass flow controllers have been calibrated using MSL Primary flow standard and the PTU transmitter using MSL pressure and temperature working standards.
The measurement results are traceable to the international system of units (SI) through national metrology institutes (NIST USA, MIKES Finland, or equivalent) or accredited calibration laboratories.

Calibration results

Reference $\%\ CO_2$	Observed* $\%\ CO_2$	Difference $\%\ CO_2$	Permissible difference $\%\ CO_2$
0.000	0.000	0.000	± 0.15
10.000	9.995	-0.005	± 0.35

*Reading after pressure and temperature compensation.

Ambient conditions / Humidity 32 ± 5 %RH, Temperature 24.1 ± 1 °C, Pressure 1011 ± 1 hPa.

Equipment used in calibration

Type	Serial number	Calibration date	Certificate number
SEC-Z512MGX	3484321641	2017-02-17	A00336
SEC-Z512MGX	3411006991	2017-02-17	A00338
PTU30T	E2520011	2017-05-10	A00994
Vaisala GMB220ACB	X1330025	2016-12-01	H40-16480065

Gas cylinders used in calibration

Type	Purity classification	Cylinder number	Reference number
Scientific nitrogen	5.0	48453000011	0ZZ1X4/0/001/0
Scientific carbon dioxide	5.2	7523112138013	315666217-40

Technician

DOC210567-F

ala Oyj | PO Box 26, FI-00421 Helsinki, Finland
e +358 9 894 91 | Fax +358 9 8949 2227
firstname.lastname@vaisala.com | www.vaisala.com
le Vantaa, Finland | VAT FI01244162 | Business ID 0124416-2

VAISALA

Certificate report no. H40-16110077

CALIBRATION CERTIFICATE

Instrument	GMP221 Carbon dioxide probe
Serial number	M1140040
Manufacturer	Vaisala Oyj, Finland
Calibration date	17th March 2016

The carbon dioxide probe was calibrated against accurate gas concentrations. Gas concentrations were made by mixing pure carbon dioxide and nitrogen gases with mass flow controller factory working standards. Communication with the probe was achieved via a Vaisala GMB220ACB module. Pressure and temperature compensation was made by using the compensation parameters of a non-volatile memory in the probe and by using actual ambient pressure and temperature values read from a Vaisala transmitter. At the time of shipment, the probe met its operating specifications.

The mass flow controller factory working standards have been calibrated at Vaisala Measurement Standards Laboratory (MSL) by using Vaisala's mass flow primary standards. The mass flow primary standards are traceable to the National Institute of Standards and Technology (NIST). The pressure and temperature readings of the Vaisala transmitter have been calibrated at an ISO/IEC 17025 accredited calibration laboratory (FINAS), MSL by using working standards traceable to NIST.

Calibration results

Reference % CO_2	Observed* % CO_2	Difference % CO_2	Permissible difference % CO_2
0.000	0.002	0.002	± 0.15
10.000	9.966	-0.034	± 0.35

*Reading after pressure and temperature compensation.

Ambient conditions / Humidity 34 ± 5 %RH, Temperature 23.5 ± 1 °C, Pressure 1001 ± 1 hPa.

Equipment used in calibration

Type	Serial number	Calibration date	Certificate number
SEC-Z512MGX	3488748591	2016-01-19	Z00082
SEC-Z512MGX	3487509853	2016-01-13	Z00083
PTU30T	C2050002	2014-05-06	K008-X00984
GMB 220 ACB	D2810034	2015-12-11	H40-15500126

Gas cylinders used in calibration

Type	Purity classification	Cylinder number	Reference number
Scientific nitrogen	6.0	7527010212324	100399464
Scientific carbon dioxide	5.2	2703077	103000384986

Technician

DOC210567-D

Vaisala Oyj | PO Box 26, FI-00421 Helsinki, Finland
Phone +358 9 894 91 | Fax +358 9 8949 2227
Email firstname.lastname@vaisala.com | www.vaisala.com
Domicile Vantaa, Finland | VAT FI01244162 | Business ID 0124416-2

APPENDIX B

Table 8 Summary of results: 1) ST1 used in the modelling of CO_2 fluxes & 2) HumST1 condition expressed as CO_2 mg/l [C] and epCO_2 mg/l [C].

Date	Average ST1 CO_2 as mg/l [C]	Average air CO_2 as mg/l [C]	Average epCO_2 as mg/l [C]	Average CO_2 flux g/m^2d
11-12-16	0.42	0.20	2.10	0.15
12-12-16	0.46	0.20	2.32	0.06
13-12-16	0.51	0.20	2.59	0.19
14-12-16	0.53	0.20	2.69	0.30
15-12-16	0.58	0.20	2.91	0.19
16-12-16	0.54	0.20	2.67	0.17
17-12-16	0.57	0.21	2.75	0.23
18-12-16	0.54	0.20	2.63	0.23
19-12-16	0.58	0.20	2.85	0.23
20-12-16	0.52	0.20	2.61	0.38
21-12-16	0.55	0.20	2.74	0.52
22-12-16	0.44	0.20	2.17	0.40
23-12-16	0.39	0.20	1.96	0.51
24-12-16	0.36	0.20	1.80	0.38
25-12-16	0.35	0.20	1.79	0.40
26-12-16	0.36	0.20	1.75	0.25
27-12-16	0.33	0.21	1.61	0.05
28-12-16	0.39	0.20	1.90	0.07
29-12-16	0.41	0.20	1.99	0.21
30-12-16	0.44	0.20	2.18	0.39
31-12-16	0.39	0.20	1.92	0.33
01-01-17	0.40	0.20	1.95	0.15
02-01-17	0.37	0.21	1.78	0.07
03-01-17	0.39	0.21	1.88	0.16
04-01-17	0.47	0.21	2.30	0.13
05-01-17	0.49	0.20	2.37	0.09
06-01-17	0.46	0.20	2.30	0.38
07-01-17	0.46	0.20	2.26	0.11
08-01-17	0.55	0.20	2.71	0.32
09-01-17	0.48	0.20	2.37	0.63
10-01-17	0.38	0.20	1.90	0.34
11-01-17	0.34	0.20	1.70	0.38
12-01-17	0.34	0.20	1.69	0.19
13-01-17	0.34	0.20	1.67	0.16
14-01-17	0.36	0.20	1.75	0.15
15-01-17	0.40	0.20	1.97	0.27

Date	Average HumST1CO_2 as mg/l [C]	Average air CO_2 as mg/l [C]	Average epCO_2 as mg/l [C]
11-12-16	10.78	0.20	53.31
12-12-16	12.20	0.20	61.29
13-12-16	12.55	0.20	63.78
14-12-16	12.06	0.20	60.91
15-12-16	12.04	0.20	60.86
16-12-16	11.82	0.20	58.79

17-12-16	11.19	0.21	54.35
18-12-16	11.09	0.20	54.39
19-12-16	11.66	0.20	57.63
20-12-16	12.50	0.20	62.18
21-12-16	13.53	0.20	67.40
22-12-16	14.31	0.20	70.85
23-12-16	16.00	0.20	80.05
24-12-16	18.01	0.20	89.91
25-12-16	19.92	0.20	100.63
26-12-16	20.86	0.20	101.77
27-12-16	21.27	0.21	102.85
28-12-16	22.27	0.20	108.74
29-12-16	23.28	0.20	114.31
30-12-16	25.34	0.20	126.06
31-12-16	27.66	0.20	138.00
01-01-17	28.47	0.20	139.38
02-01-17	28.56	0.21	138.05
03-01-17	28.81	0.21	139.67
04-01-17	30.16	0.21	147.13
05-01-17	31.71	0.20	154.83
06-01-17	34.42	0.20	171.08
07-01-17	37.96	0.20	187.69
08-01-17	41.39	0.20	205.19
09-01-17	43.68	0.20	217.75
10-01-17	46.72	0.20	234.32
11-01-17	48.60	0.20	242.28
12-01-17	49.40	0.20	244.82
13-01-17	50.35	0.20	245.73
14-01-17	51.67	0.20	252.93
15-01-17	52.57	0.20	258.37

Table 9 Precipitation data – event records/mm taken from M. Moanbane #4 station.

Date	Precipitation/mm
11-Dec-16	0.1
12-Dec-16	3.4
13-Dec-16	12.8
14-Dec-16	11.7
15-Dec-16	11.4
16-Dec-16	2.1
17-Dec-16	0
18-Dec-16	0.2
19-Dec-16	2
20-Dec-16	8.2
21-Dec-16	0.5

22-Dec-16	0.2
23-Dec-16	7.4
24-Dec-16	4.6
25-Dec-16	3.5
26-Dec-16	0.1
27-Dec-16	0
28-Dec-16	0
29-Dec-16	0
30-Dec-16	0
31-Dec-16	12
01-Jan-17	1.9
02-Jan-17	0.2
03-Jan-17	1.1
04-Jan-17	0.4
05-Jan-17	1.5
06-Jan-17	4.6
07-Jan-17	2.8
08-Jan-17	3.3
09-Jan-17	0.2
10-Jan-17	2.3
11-Jan-17	2.2
12-Jan-17	3.2
13-Jan-17	0.2
14-Jan-17	3
15-Jan-17	6.3

Table 10 Summary of results from ST: 17th of June to 8th of August 2017 (daily averages).

Date	**WT1/ ^{0}C**	**Air Pressure/ hPa**	**CO_2 mg/l [C]**	**Wind speed m/s**	**Air CO_2 mg/l [C]**	**epCO_2 mg/l [C]**	**CO_2 flux/gm^{-2}d^{-1}**
17-06-2017	21	962	0.40	3.9	0.19	2.08	0.23
18-06-2017	21	960	0.43	2.6	0.19	2.20	0.16
19-06-2017	21	958	0.48	2.6	0.19	2.45	0.21
20-06-2017	20	956	0.67	4.6	0.20	3.42	0.58
21-06-2017	20	950	0.74	4.1	0.19	3.89	0.66

22-06-2017	19	949	0.81	4.9	0.19	4.15	0.81
23-06-2017	16	948	0.66	7.4	0.19	3.42	1.09
24-06-2017	15	949	0.52	6.8	0.19	2.69	0.61
25-06-2017	15	949	0.47	3.6	0.20	2.42	0.23
26-06-2017	15	950	0.45	2.5	0.20	2.29	0.14
27-06-2017	16	941	0.59	3.3	0.19	3.08	0.33
28-06-2017	16	938	0.68	2.8	0.19	3.51	0.33
29-06-2017	12	938	0.79	3.8	0.19	4.07	0.47
30-06-2017	10	947	0.58	5.2	0.20	2.94	0.46
01-07-2017	11	953	0.50	5.7	0.20	2.57	0.40
02-07-2017	14	956	0.42	4.3	0.20	2.16	0.22
03-07-2017	14	953	0.50	3.1	0.19	2.55	0.24
04-07-2017	15	952	0.58	5.4	0.19	2.99	0.58
05-07-2017	17	953	0.49	2.2	0.19	2.55	0.16
06-07-2017	18	950	0.46	2.8	0.19	2.38	0.19
07-07-2017	16	951	0.81	4.8	0.19	4.19	0.78
08-07-2017	17	953	0.61	2.7	0.19	3.15	0.26
09-07-2017	17	947	0.69	4.8	0.19	3.58	0.63
10-07-2017	16	944	0.69	2.8	0.19	3.58	0.35
11-07-2017	15	942	0.72	2.7	0.19	3.73	0.33

12-07-2017	16	951	0.67	2.4	0.19	3.41	0.24
13-07-2017	15	953	0.66	5.5	0.19	3.42	0.71
14-07-2017	15	954	0.61	4.8	0.19	3.15	0.54
15-07-2017	16	952	0.57	7.6	0.19	3.00	0.89
16-07-2017	17	957	0.50	4.1	0.19	2.58	0.31
17-07-2017	19	958	0.53	3.3	0.19	2.74	0.28
18-07-2017	18	950	0.60	4.1	0.19	3.15	0.44
19-07-2017	17	939	0.68	4.0	0.19	3.56	0.49
20-07-2017	15	940	0.61	5.0	0.19	3.15	0.53
21-07-2017	14	932	0.62	5.2	0.19	3.25	0.57
22-07-2017	15	940	0.57	2.7	0.19	2.98	0.23
23-07-2017	15	947	0.58	2.6	0.19	3.00	0.22
24-07-2017	16	953	0.64	3.8	0.19	3.33	0.43
25-07-2017	19	950	0.56	2.1	0.19	2.91	0.19
26-07-2017	17	937	0.73	7.3	0.19	3.83	1.34
27-07-2017	15	936	0.65	7.1	0.19	3.37	0.92
28-07-2017	14	936	0.52	7.5	0.19	2.70	0.73
29-07-2017	14	938	0.51	5.9	0.19	2.65	0.51
30-07-2017	14	936	0.54	6.0	0.19	2.80	0.55
31-07-2017	14	940	0.50	5.8	0.19	2.58	0.48

01-08-2017	15	944	0.52	5.0	0.19	2.72	0.42
02-08-2017	14	937	0.62	5.4	0.19	3.28	0.63
03-08-2017	14	935	0.66	7.2	0.19	3.51	0.99
04-08-2017	14	945	0.55	4.7	0.19	2.84	0.41
05-08-2017	15	951	0.56	3.6	0.19	2.90	0.31
06-08-2017	13	951	0.65	5.9	0.19	3.32	0.71
07-08-2017	14	949	0.65	4.5	0.19	3.35	0.51
08-08-2017	14	948	0.64	2.7	0.19	3.32	0.25

Table 11 Summary of results from HumST1: 17th of June to 8th of August 2017 (daily averages).

Date	**WT1 / ^{0}C**	**Air Pressure/ hPa**	**CO_2 mg/l [C]**	**epCO_2 mg/l [C]**
17-06-2017	12	962	25.37	131.81
18-06-2017	12	960	27.51	141.29
19-06-2017	13	958	31.72	163.75
20-06-2017	13	956	35.85	183.62
21-06-2017	13	950	41.35	216.94
22-06-2017	14	949	42.94	221.16
23-06-2017	14	948	41.58	213.99

24-06-2017	13	949	35.70	183.34
25-06-2017	13	949	32.90	168.25
26-06-2017	13	950	31.17	158.41
27-06-2017	13	941	21.83	113.74
28-06-2017	13	938	19.75	102.02
29-06-2017	12	938	18.52	95.15
30-06-2017	11	947	21.35	108.80
01-07-2017	11	953	24.71	126.06
02-07-2017	11	956	25.80	131.98
03-07-2017	12	953	29.15	149.87
04-07-2017	12	952	31.90	165.33
05-07-2017	13	953	34.81	179.71
06-07-2017	13	950	39.53	205.36
07-07-2017	13	951	41.80	215.92
08-07-2017	13	953	44.93	231.67
09-07-2017	13	947	49.06	255.25
10-07-2017	13	944	48.28	250.20
11-07-2017	13	942	43.25	223.65
12-07-2017	13	951	46.02	236.23
13-07-2017	13	953	51.88	267.16

14-07-2017	13	954	56.38	290.30
15-07-2017	13	952	66.60	347.65
16-07-2017	13	957	60.93	313.24
17-07-2017	13	958	64.00	329.72
18-07-2017	14	950	74.80	391.69
19-07-2017	14	939	75.33	397.03
20-07-2017	14	940	45.68	235.95
21-07-2017	13	932	28.33	148.12
22-07-2017	13	940	26.78	139.58
23-07-2017	13	947	28.61	148.79
24-07-2017	13	953	31.14	161.32
25-07-2017	14	950	34.19	177.61
26-07-2017	14	937	32.33	169.59
27-07-2017	14	936	26.89	140.11
28-07-2017	13	936	28.45	148.86
29-07-2017	13	938	31.31	163.35
30-07-2017	13	936	32.59	169.71
31-07-2017	13	940	34.07	176.92
01-08-2017	13	944	35.29	183.91
02-08-2017	13	937	35.39	186.73

03-08-2017	13	935	33.83	178.75
04-08-2017	13	945	35.74	185.64
05-08-2017	13	951	37.11	190.80
06-08-2017	13	951	37.56	193.18
07-08-2017	12	949	41.34	213.81
08-08-2017	13	948	42.77	220.69

Table 12 Summary of results from ST2: 17th of June to 8th of August 2017 (daily averages).

Date	**WT2/ ^{0}C**	**Air Pressure/ hPa**	**CO_2 mg/l [C]**	**Wind speed m/s**	**Air CO_2 mg/l [C]**	**epCO_2 mg/l [C]**	**CO_2 flux/gm^{-2}d^{-1}**
17-06-2017	21	962	0.40	3.9	0.19	2.05	0.22
18-06-2017	21	960	0.46	2.6	0.19	2.34	0.18
19-06-2017	21	958	0.52	2.6	0.19	2.68	0.23
20-06-2017	20	956	0.69	4.6	0.20	3.54	0.60
21-06-2017	20	950	0.64	4.1	0.19	3.34	0.53
22-06-2017	19	949	0.65	4.9	0.19	3.37	0.60
23-06-2017	16	948	0.53	7.4	0.19	2.71	0.76
24-06-2017	15	949	0.48	6.8	0.19	2.44	0.49
25-06-2017	15	949	0.49	3.6	0.20	2.52	0.24

26-06-2017	15	950	0.49	2.5	0.20	2.51	0.16
27-06-2017	16	941	0.68	3.3	0.19	3.57	0.43
28-06-2017	16	938	0.71	2.8	0.19	3.68	0.34
29-06-2017	12	938	0.78	3.8	0.19	4.00	0.45
30-06-2017	10	947	0.66	5.2	0.20	3.36	0.55
01-07-2017	11	953	0.53	5.7	0.20	2.68	0.42
02-07-2017	14	956	0.48	4.3	0.20	2.47	0.28
03-07-2017	14	953	0.52	3.1	0.19	2.67	0.25
04-07-2017	15	952	0.53	5.4	0.19	2.74	0.51
05-07-2017	17	953	0.55	2.2	0.19	2.82	0.19
06-07-2017	18	950	0.55	2.8	0.19	2.84	0.26
07-07-2017	16	951	0.66	4.8	0.19	3.39	0.58
08-07-2017	17	953	0.66	2.7	0.19	3.40	0.29
09-07-2017	17	947	0.63	4.8	0.19	3.29	0.56
10-07-2017	16	944	0.71	2.8	0.19	3.67	0.35
11-07-2017	15	942	0.76	2.7	0.19	3.92	0.35
12-07-2017	16	951	0.78	2.4	0.19	4.02	0.31
13-07-2017	15	953	0.69	5.5	0.19	3.55	0.69
14-07-2017	15	954	0.61	4.8	0.19	3.13	0.52

15-07-2017	16	952	0.53	7.6	0.19	2.75	0.77
16-07-2017	17	957	0.58	4.1	0.19	2.99	0.39
17-07-2017	19	958	0.67	3.3	0.19	3.46	0.39
18-07-2017	18	950	0.69	4.1	0.19	3.60	0.53
19-07-2017	17	939	0.81	4.0	0.19	4.25	0.60
20-07-2017	15	940	0.74	5.0	0.19	3.80	0.68
21-07-2017	14	932	0.74	5.2	0.19	3.86	0.73
22-07-2017	15	940	0.81	2.7	0.19	4.24	0.37
23-07-2017	15	947	0.82	2.6	0.19	4.25	0.35
24-07-2017	16	953	0.78	3.8	0.19	4.04	0.56
25-07-2017	19	950	0.75	2.1	0.19	3.91	0.29
26-07-2017	17	937	0.74	7.3	0.19	3.86	1.30
27-07-2017	15	936	0.63	7.1	0.19	3.28	0.86
28-07-2017	14	936	0.52	7.5	0.19	2.74	0.74
29-07-2017	14	938	0.54	5.9	0.19	2.80	0.55
30-07-2017	14	936	0.53	6.0	0.19	2.74	0.53
31-07-2017	14	940	0.51	5.8	0.19	2.65	0.49
01-08-2017	15	944	0.57	5.0	0.19	2.98	0.48
02-08-2017	14	937	0.67	5.4	0.19	3.51	0.70

03-08-2017	14	935	0.65	7.2	0.19	3.44	0.96
04-08-2017	14	945	0.60	4.7	0.19	3.11	0.46
05-08-2017	15	951	0.65	3.6	0.19	3.34	0.38
06-08-2017	13	951	0.67	5.9	0.19	3.43	0.73
07-08-2017	14	949	0.66	4.5	0.19	3.42	0.51
08-08-2017	14	948	0.71	2.7	0.19	3.69	0.30

Table 13 Summary of results from LawnST2: 17th of June to 8th of August 2017 (daily averages).

Date	**WT2/ ^{0}C**	**Air Pressure/ hPa**	**CO_2 mg/l [C]**	**epCO_2 mg/l [C]**
17-06-2017	12	962	8.77	45.56
18-06-2017	13	960	10.32	52.96
19-06-2017	13	958	11.30	58.32
20-06-2017	14	956	11.52	58.97
21-06-2017	14	950	12.10	63.49
22-06-2017	14	949	12.62	65.01
23-06-2017	14	948	12.83	66.03
24-06-2017	13	949	12.89	66.19
25-06-2017	13	949	12.99	66.44

26-06-2017	13	950	13.16	66.89
27-06-2017	13	941	11.31	58.95
28-06-2017	14	938	10.28	53.09
29-06-2017	12	938	9.09	46.73
30-06-2017	11	947	7.38	37.62
01-07-2017	11	953	7.46	38.03
02-07-2017	11	956	6.24	31.83
03-07-2017	12	953	3.95	20.28
04-07-2017	12	952	4.36	22.61
05-07-2017	13	953	5.36	27.66
06-07-2017	13	950	6.27	32.59
07-07-2017	13	951	6.28	32.45
08-07-2017	13	953	6.31	32.51
09-07-2017	13	947	6.40	33.29
10-07-2017	13	944	6.15	31.85
11-07-2017	13	942	5.89	30.45
12-07-2017	13	951	6.15	31.56
13-07-2017	13	953	6.21	31.99
14-07-2017	13	954	6.11	31.46

15-07-2017	13	952	6.07	31.64
16-07-2017	13	957	5.90	30.32
17-07-2017	13	958	6.05	31.15
18-07-2017	14	950	5.88	30.79
19-07-2017	14	939	5.62	29.60
20-07-2017	13	940	4.86	25.12
21-07-2017	13	932	2.84	14.82
22-07-2017	13	940	3.00	15.64
23-07-2017	13	947	3.57	18.59
24-07-2017	14	953	4.29	22.25
25-07-2017	14	950	5.40	28.06
26-07-2017	14	937	5.24	27.50
27-07-2017	13	936	3.11	16.23
28-07-2017	13	936	3.23	16.89
29-07-2017	13	938	3.99	20.80
30-07-2017	13	936	4.48	23.34
31-07-2017	12	940	4.74	24.60
01-08-2017	12	944	4.91	25.60
02-08-2017	13	937	4.04	21.31

03-08-2017	13	935	2.28	12.04
04-08-2017	13	945	3.10	16.10
05-08-2017	13	951	3.87	19.87
06-08-2017	12	951	4.17	21.43
07-08-2017	12	949	2.64	13.65
08-08-2017	12	948	2.60	13.40

Table 14 Summary of results from ST1: 5th of November to 5th of December 2017 (daily averages).

Date	**WT1/ ^{0}C**	**Air Pressure/ hPa**	**CO_2 mg/l [C]**	**Wind speed m/s**	**Air CO_2 mg/l [C]**	**epCO_2 mg/l [C]**	**CO_2 flux/gm^{-2}d^{-1}**
05-11-2017	5	956	0.44	5	0.20	2.18	0.20
06-11-2017	5	952	0.45	7	0.20	2.28	0.41
07-11-2017	6	949	0.48	6	0.20	2.42	0.33
08-11-2017	5	957	0.52	5	0.20	2.60	0.35
09-11-2017	6	957	0.51	6	0.20	2.60	0.45
10-11-2017	6	954	0.49	6	0.20	2.46	0.41
11-11-2017	7	947	0.56	3	0.20	2.86	0.18

12-11-2017	5	953	0.55	5	0.20	2.74	0.32
13-11-2017	4	959	0.46	6	0.20	2.30	0.31
14-11-2017	6	956	0.51	6	0.20	2.60	0.35
15-11-2017	6	956	0.53	3	0.20	2.68	0.18
16-11-2017	6	957	0.54	5	0.20	2.70	0.40
17-11-2017	5	962	0.51	4	0.20	2.49	0.24
18-11-2017	4	957	0.56	3	0.20	2.81	0.15
19-11-2017	4	955	0.56	2	0.20	2.82	0.18
20-11-2017	7	946	0.59	8	0.19	3.06	0.75
21-11-2017	8	939	0.58	8	0.19	3.03	0.72
22-11-2017	9	922	0.59	4	0.19	3.08	0.30
23-11-2017	6	929	0.58	7	0.20	2.94	0.64
24-11-2017	4	944	0.48	5	0.20	2.37	0.27
25-11-2017	3	951	0.56	7	0.20	2.76	0.47
26-11-2017	2	955	0.51	7	0.20	2.52	0.45
27-11-2017	4	946	0.48	8	0.20	2.43	0.48
28-11-2017	2	947	0.44	4	0.20	2.18	0.17
29-11-2017	2	951	0.43	3	0.20	2.12	0.11
30-11-2017	1	952	0.43	3	0.20	2.12	0.11

01-12-2017	0	961	0.41	3	0.21	1.98	0.07
02-12-2017	1	962	0.44	5	0.20	2.17	0.18
03-12-2017	3	964	0.53	5	0.20	2.61	0.24
04-12-2017	4	968	0.53	4	0.20	2.60	0.23
05-12-2017	4	966	0.53	5	0.20	2.61	0.29

Table 15 Summary of results from ST2: 5th of November – 5th of December 2017.

Date	**WT2/ ^{0}C**	**Air Pressure/ hPa**	**CO_2 mg/l [C]**	**Wind speed m/s**	**Air CO_2 mg/l [C]**	**epCO_2 mg/l [C]**	**CO_2 flux/gm^{-2}d^{-1}**
05-11-2017	4	956	0.47	5	0.20	2.32	0.21
06-11-2017	4	952	0.49	7	0.20	2.51	0.47
07-11-2017	5	949	0.54	6	0.20	2.72	0.41
08-11-2017	4	957	0.57	5	0.20	2.85	0.39
09-11-2017	7	957	0.53	6	0.20	2.67	0.47
10-11-2017	6	954	0.52	6	0.20	2.63	0.46
11-11-2017	7	947	0.76	3	0.20	3.83	0.25
12-11-2017	5	953	0.65	5	0.20	3.24	0.40
13-11-2017	3	959	0.55	6	0.20	2.73	0.37
14-11-2017	6	956	0.55	6	0.20	2.78	0.40
15-11-2017	7	956	0.61	3	0.20	3.07	0.22

16-11-2017	6	957	0.58	5	0.20	2.90	0.44
17-11-2017	4	962	0.60	4	0.20	2.95	0.30
18-11-2017	4	957	0.65	3	0.20	3.26	0.19
19-11-2017	4	955	0.71	2	0.20	3.55	0.23
20-11-2017	8	946	0.59	8	0.19	3.06	0.78
21-11-2017	9	939	0.58	8	0.19	3.01	0.74
22-11-2017	9	922	0.68	4	0.19	3.57	0.37
23-11-2017	4	929	0.64	7	0.20	3.26	0.71
24-11-2017	2	944	0.58	5	0.20	2.89	0.36
25-11-2017	2	951	0.61	7	0.20	3.01	0.53
26-11-2017	3	955	0.63	7	0.20	3.15	0.67
27-11-2017	4	946	0.56	8	0.20	2.85	0.63
28-11-2017	2	947	0.49	4	0.20	2.45	0.20
29-11-2017	1	951	0.49	3	0.20	2.42	0.14
30-11-2017	0	952	0.50	3	0.20	2.49	0.15
01-12-2017	1	961	0.51	3	0.21	2.47	0.11
02-12-2017	1	962	0.52	5	0.20	2.56	0.24
03-12-2017	3	964	0.61	5	0.20	3.03	0.31
04-12-2017	4	968	0.61	4	0.20	2.98	0.28

05-12-2017	4	966	0.56	5	0.20	2.76	0.32

Table 16 Summary of results from ST3: 5th of November – 5th of December 2017.

Date	**WT3 / ^{0}C**	**Air Pressure/ hPa**	**CO_2 mg/l [C]**	**Wind speed m/s**	**Air CO_2 mg/l [C]**	**epCO_2 mg/l [C]**	**CO_2 flux/gm^{-2}d^{-1}**
05-11-2017	4	956	0.86	5	0.20	4.30	0.53
06-11-2017	5	952	0.58	7	0.20	2.93	0.52
07-11-2017	6	949	0.42	6	0.20	2.13	0.27
08-11-2017	5	957	0.45	5	0.20	2.23	0.27
09-11-2017	7	957	0.42	6	0.20	2.13	0.32
10-11-2017	6	954	0.37	6	0.20	1.86	0.25
11-11-2017	7	947	0.55	3	0.20	2.78	0.16
12-11-2017	4	953	0.48	5	0.20	2.38	0.26
13-11-2017	3	959	0.33	6	0.20	1.65	0.17
14-11-2017	6	956	0.42	6	0.20	2.11	0.25
15-11-2017	6	956	0.46	3	0.20	2.30	0.14
16-11-2017	6	957	0.45	5	0.20	2.24	0.30
17-11-2017	4	962	0.38	4	0.20	1.88	0.15

18-11-2017	4	957	0.48	3	0.20	2.42	0.12
19-11-2017	4	955	0.50	2	0.20	2.51	0.16
20-11-2017	8	946	0.52	8	0.19	2.67	0.64
21-11-2017	9	939	0.50	8	0.19	2.61	0.59
22-11-2017	9	922	0.53	4	0.19	2.78	0.25
23-11-2017	4	929	0.47	7	0.20	2.42	0.46
24-11-2017	3	944	0.35	5	0.20	1.73	0.15
25-11-2017	4	951	0.37	7	0.20	1.83	0.23
26-11-2017	4	955	0.42	7	0.20	2.08	0.39
27-11-2017	4	946	0.42	8	0.20	2.14	0.39
28-11-2017	2	947	0.36	4	0.20	1.81	0.11
29-11-2017	1	951	0.33	3	0.20	1.61	0.06
30-11-2017	2	952	0.35	3	0.20	1.72	0.07
01-12-2017	3	961	0.37	3	0.21	1.80	0.06
02-12-2017	3	962	0.34	5	0.20	1.69	0.11
03-12-2017	3	964	0.53	5	0.20	2.61	0.25
04-12-2017	4	968	0.50	4	0.20	2.45	0.21
05-12-2017	4	966	0.49	5	0.20	2.43	0.26

Table 17 Summary of results from HumST1: 5th of November to 5th of December 2017 (daily averages).

Date	WT1/ ^{0}C	Atir Pressure/ hPa	CO_2 mg/l [C]	epCO_2 mg/l [C]
05-11-2017	8	956	223.95	1117.18
06-11-2017	8	952	248.64	1262.46
07-11-2017	8	949	243.01	1223.16
08-11-2017	8	957	253.85	1266.01
09-11-2017	8	957	289.78	1465.67
10-11-2017	8	954	278.61	1405.03
11-11-2017	8	947	246.95	1252.49
12-11-2017	8	953	213.78	1062.83
13-11-2017	8	959	267.07	1323.11
14-11-2017	8	956	308.58	1565.56
15-11-2017	8	956	316.34	1592.36
16-11-2017	8	957	323.17	1615.61
17-11-2017	7	962	311.11	1532.09
18-11-2017	7	957	325.89	1625.92
19-11-2017	7	955	333.62	1667.12

20-11-2017	7	946	386.26	1992.15
21-11-2017	8	939	413.66	2152.49
22-11-2017	8	922	322.84	1688.67
23-11-2017	8	929	197.99	1007.83
24-11-2017	7	944	278.47	1387.17
25-11-2017	7	951	281.53	1390.27
26-11-2017	6	955	294.66	1466.35
27-11-2017	6	946	287.14	1448.86
28-11-2017	6	947	282.77	1406.82
29-11-2017	6	951	277.49	1367.13
30-11-2017	6	952	279.74	1382.92
01-12-2017	6	961	286.27	1391.64
02-12-2017	6	962	298.57	1470.91
03-12-2017	6	964	326.24	1617.54
04-12-2017	6	968	316.00	1554.74
05-12-2017	6	966	309.93	1528.85

Table 18 Summary of results from LawnST2: 5th of November to 5th of December 2017 (daily averages).

Date	WT2/ ^{0}C	Air Pressure/ hPa	CO_2 mg/l [C]	epCO_2 mg/l [C]
05-11-2017	8	956	2.95	14.72
06-11-2017	8	952	3.22	16.37
07-11-2017	7	949	1.40	7.10
08-11-2017	7	957	1.11	5.55
09-11-2017	8	957	0.75	3.81
10-11-2017	7	954	0.55	2.79
11-11-2017	7	947	0.61	3.09
12-11-2017	7	953	0.70	3.47
13-11-2017	6	959	0.93	4.59
14-11-2017	7	956	0.68	3.43
15-11-2017	7	956	0.84	4.22
16-11-2017	7	957	0.91	4.56
17-11-2017	6	962	1.30	6.41
18-11-2017	6	957	0.92	4.59
19-11-2017	6	955	0.94	4.69

20-11-2017	7	946	0.82	4.25
21-11-2017	8	939	0.80	4.16
22-11-2017	8	922	0.63	3.30
23-11-2017	6	929	0.58	2.95
24-11-2017	6	944	0.87	4.35
25-11-2017	6	951	1.05	5.21
26-11-2017	6	955	1.14	5.65
27-11-2017	5	946	0.49	2.49
28-11-2017	5	947	0.67	3.34
29-11-2017	5	951	0.80	3.96
30-11-2017	5	952	1.00	4.92
01-12-2017	5	961	1.51	7.35
02-12-2017	5	962	1.55	7.65
03-12-2017	5	964	0.86	4.26
04-12-2017	5	968	0.57	2.83
05-12-2017	5	966	0.68	3.38

Table 19 Summary of results from HumST3: 5th of November to 5th of December 2017 (daily averages).

Date	WT3/ ^{0}C	Air Pressure/ hPa	CO_2 mg/l [C]	epCO_2 mg/l [C]
05-11-2017	9	956	20.42	101.82
06-11-2017	9	952	34.25	174.29
07-11-2017	8	949	54.59	274.68
08-11-2017	8	957	62.44	311.64
09-11-2017	8	957	87.48	442.42
10-11-2017	8	954	83.56	421.42
11-11-2017	8	947	35.15	178.55
12-11-2017	8	953	30.84	153.30
13-11-2017	8	959	48.43	240.23
14-11-2017	8	956	63.70	323.13
15-11-2017	8	956	72.45	364.78
16-11-2017	8	957	89.03	444.55
17-11-2017	8	962	102.36	504.09
18-11-2017	7	957	102.13	509.69
19-11-2017	7	955	81.77	408.35

20-11-2017	7	946	88.93	458.64
21-11-2017	8	939	121.30	631.42
22-11-2017	8	922	140.34	733.55
23-11-2017	8	929	87.82	448.37
24-11-2017	7	944	59.66	297.19
25-11-2017	7	951	59.07	291.67
26-11-2017	7	955	73.06	363.80
27-11-2017	7	946	77.44	390.74
28-11-2017	6	947	75.90	377.60
29-11-2017	6	951	75.05	369.82
30-11-2017	6	952	82.33	406.88
01-12-2017	6	961	94.43	459.01
02-12-2017	6	962	111.33	548.48
03-12-2017	6	964	140.90	698.60
04-12-2017	6	968	181.81	894.44
05-12-2017	6	966	201.92	995.97

Table 20 Summary of results from ST1&ST2: 14th of January– 14th of March 2018.

Date	ST1 CO_2 mg/l [C]	Wind speed m/s	Air CO_2 mg/l [C]	ST1 epCO_2 mg/l [C]	ST1 CO_2 flux/$gm^{-2}d^{-1}$	ST2 CO_2 mg/l [C]	ST2 epCO_2 mg/l [C]	ST2 CO_2 flux/$gm^{-2}d^{-1}$
14/01	0.52	8.64	0.20	2.65	0.81	0.65	3.30	1.00
15/01	0.45	8.53	0.19	2.31	0.50	0.54	2.76	0.69
16/01	0.46	8.32	0.20	2.33	0.47	0.52	2.64	0.57
17/01	0.46	9.07	0.20	2.33	0.51	0.54	2.70	0.68
18/01	0.42	8.60	0.20	2.11	0.43	0.56	2.81	0.68
19/01	0.45	7.52	0.20	2.22	0.37	0.50	2.49	0.44
20/01	0.39	2.96	0.20	1.93	0.08	0.53	2.68	0.14
21/01	0.52	6.62	0.20	2.65	0.40	0.58	2.94	0.54
22/01	0.46	6.67	0.20	2.31	0.36	0.52	2.61	0.42
23/01	0.45	9.99	0.19	2.29	0.66	0.51	2.62	0.83
24/01	0.39	10.78	0.20	1.98	0.55	0.48	2.48	0.84
25/01	0.45	8.51	0.20	2.29	0.47	0.50	2.55	0.56
26/01	0.40	4.69	0.20	2.00	0.17	0.50	2.47	0.24
27/01	0.45	9.41	0.20	2.29	0.57	0.52	2.64	0.78
28/01	0.44	10.37	0.20	2.21	0.68	0.50	2.54	0.89
29/01	0.46	7.03	0.20	2.26	0.39	0.49	2.41	0.47
30/01	0.42	6.00	0.20	2.07	0.26	0.54	2.69	0.39

31/01	0.46	9.05	0.20	2.33	0.53	0.49	2.44	0.58
01/02	0.40	6.11	0.20	1.97	0.22	0.50	2.46	0.31
02/02	0.44	4.99	0.20	2.18	0.20	0.49	2.42	0.23
03/02	0.41	4.93	0.20	2.02	0.17	0.53	2.62	0.27
04/02	0.45	1.80	0.21	2.18	0.06	0.51	2.50	0.07
05/02	0.46	1.37	0.21	2.23	0.05	0.58	2.84	0.08
06/02	0.44	4.12	0.21	2.12	0.15	0.61	2.96	0.27
07/02	0.55	5.36	0.20	2.67	0.37	0.66	3.22	0.45
08/02	0.54	6.02	0.20	2.75	0.37	0.74	3.72	0.59
09/02	0.56	6.82	0.20	2.79	0.49	0.65	3.20	0.59
10/02	0.45	9.86	0.20	2.29	0.59	0.59	2.99	0.96
11/02	0.46	7.67	0.20	2.29	0.41	0.48	2.38	0.45
12/02	0.39	8.45	0.20	1.92	0.33	0.54	2.67	0.61
13/02	0.44	6.58	0.20	2.21	0.30	0.53	2.66	0.42
14/02	0.41	9.17	0.20	2.10	0.46	0.58	2.97	0.81
15/02	0.44	8.72	0.20	2.22	0.42	0.49	2.46	0.54
16/02	0.44	7.40	0.20	2.18	0.32	0.51	2.56	0.45
17/02	0.39	4.44	0.20	1.92	0.13	0.51	2.55	0.23
18/02	0.46	3.37	0.20	2.31	0.14	0.54	2.72	0.21
19/02	0.49	4.42	0.20	2.48	0.23	0.58	2.93	0.32
20/02	0.43	3.37	0.20	2.11	0.13	0.54	2.67	0.19
21/02	0.45	2.08	0.20	2.21	0.08	0.57	2.76	0.12
22/02	0.49	3.56	0.20	2.44	0.16	0.58	2.87	0.22

23/02	0.44	4.93	0.20	2.19	0.21	0.62	3.05	0.37
24/02	0.45	4.87	0.20	2.22	0.20	0.60	2.97	0.32
25/02	0.40	5.06	0.20	1.94	0.16	0.58	2.86	0.35
26/02	0.51	5.06	0.21	2.47	0.26	0.65	3.16	0.40
27/02	0.43	5.04	0.21	2.09	0.19	0.69	3.34	0.45
28/02	0.51	6.73	0.21	2.46	0.41	0.71	3.43	0.67
01/03	0.50	9.88	0.20	2.43	0.63	0.67	3.27	1.09
02/03	1.33	12.20	0.20	6.61	3.59	2.55	12.73	7.84
03/03	3.40	7.67	0.20	17.10	4.97	4.44	22.32	6.93
04/03	4.73	3.58	0.20	24.05	2.56	5.02	25.49	2.80
05/03	5.26	2.36	0.20	26.78	1.78	5.65	28.78	1.94
06/03	5.77	2.89	0.20	29.38	2.24	5.80	29.52	2.29
07/03	5.54	5.83	0.20	28.13	5.54	5.57	28.28	5.71
08/03	5.42	4.31	0.20	27.35	3.66	5.35	26.98	3.66
09/03	4.63	3.94	0.20	23.23	2.85	5.12	25.70	3.18
10/03	3.73	5.47	0.19	19.26	3.42	4.54	23.44	4.33
11/03	2.34	3.36	0.20	12.00	1.02	3.87	19.82	1.78
12/03	1.77	3.11	0.20	9.04	0.68	3.25	16.60	1.34
13/03	1.53	4.42	0.20	7.68	0.91	3.00	15.09	1.94
14/03	1.33	10.29	0.19	6.85	2.74	2.06	10.58	4.21

Table 21 Summary of results from HumST1: 14th of January to 14th of March 2018 (daily averages).

Date	WT1/ ^{0}C	CO_2 mg/l [C]	epCO_2 mg/l [C]
14/01	4	8.72	44.27
15/01	4	7.94	40.73
16/01	4	6.60	33.26
17/01	4	4.81	24.19
18/01	4	4.08	20.60
19/01	3	4.05	20.17
20/01	3	4.02	20.16
21/01	3	3.44	17.48
22/01	4	3.10	15.65
23/01	4	3.22	16.55
24/01	5	2.88	14.80
25/01	4	2.35	11.92
26/01	4	2.15	10.63
27/01	4	2.36	11.88
28/01	5	2.35	11.85

29/01	5	2.22	11.04
30/01	5	1.97	9.74
31/01	4	1.82	9.14
01/02	4	1.62	8.06
02/02	4	1.61	7.99
03/02	4	1.69	8.39
04/02	3	1.81	8.81
05/02	3	1.82	8.83
06/02	3	1.85	9.01
07/02	3	1.84	9.00
08/02	3	1.93	9.70
09/02	3	1.90	9.39
10/02	3	5.14	26.30
11/02	3	6.76	33.56
12/02	3	6.37	31.69
13/02	3	6.16	30.97
14/02	3	5.22	26.74
15/02	3	4.67	23.35
16/02	3	4.34	21.55

17/02	3	4.33	21.53
18/02	3	6.69	33.56
19/02	4	7.76	39.07
20/02	4	7.74	37.95
21/02	4	7.40	36.15
22/02	4	6.45	31.93
23/02	4	5.43	26.82
24/02	3	5.43	26.67
25/02	3	5.11	25.06
26/02	3	5.14	24.92
27/02	3	4.95	24.02
28/02	2	4.44	21.55
01/03	2	4.48	21.94
02/03	2	4.21	20.97
03/03	2	4.29	21.57
04/03	2	4.09	20.77
05/03	2	4.28	21.77
06/03	2	4.40	22.41
07/03	2	4.63	23.51

08/03	2	4.49	22.62
09/03	2	4.57	22.95
10/03	2	4.23	21.83
11/03	2	3.71	19.03
12/03	2	3.12	15.97
13/03	2	3.03	15.24
14/03	2	2.98	15.34

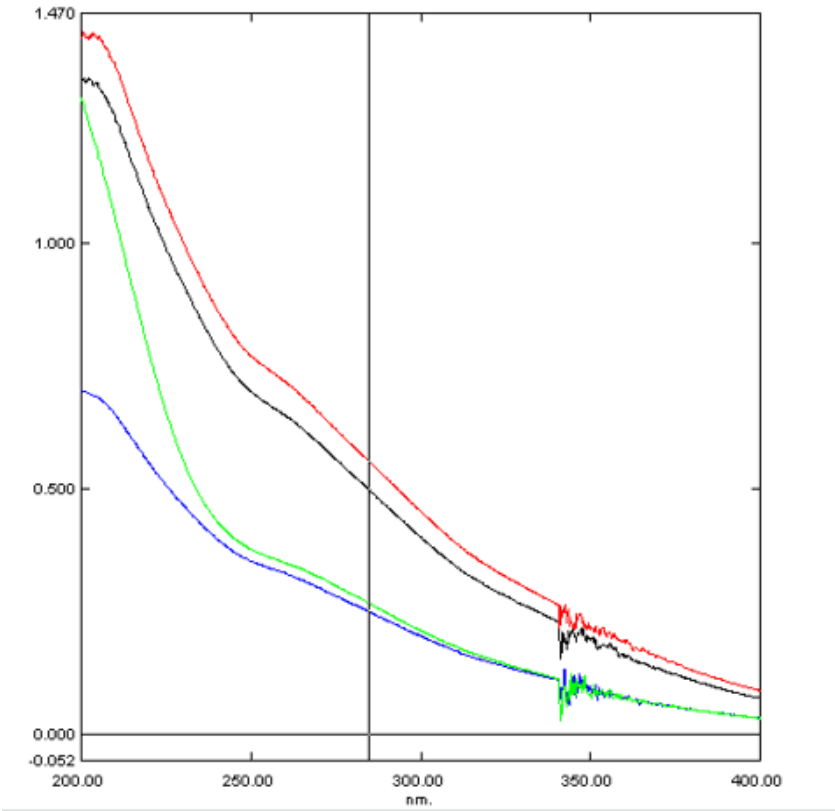

Figure 78 SUVA spectra showing absorbance curves (pool conditions one and two – red and black lines and peat pore water samples – green and blue lines).

Table 22 Summary of results from ST1: 1st of April to 7th of July 2018 (daily averages).

Date	Wind speed m/s	CO_2 mg/l [C]	Air CO_2 mg/l [C]	epCO_2 mg/l [C]	CO_2 flux/gm^{-2}d^{-1}
01-04-2018	6.90	0.44	0.20	2.18	0.32
02-04-2018	4.57	0.42	0.20	2.11	0.18
03-04-2018	4.44	0.43	0.19	2.24	0.20
04-04-2018	3.79	0.41	0.20	2.09	0.14

05-04-2018	4.61	0.39	0.20	1.95	0.18
06-04-2018	8.85	0.38	0.20	1.94	0.39
07-04-2018	2.64	0.36	0.20	1.85	0.07
08-04-2018	2.74	0.38	0.20	1.94	0.09
09-04-2018	3.58	0.41	0.20	2.06	0.15
10-04-2018	4.46	0.44	0.20	2.21	0.20
11-04-2018	4.33	0.50	0.20	2.51	0.25
12-04-2018	3.60	0.63	0.20	3.15	0.28
13-04-2018	2.01	0.64	0.20	3.22	0.15
14-04-2018	5.02	0.65	0.20	3.31	0.45
15-04-2018	6.67	0.53	0.20	2.72	0.49
16-04-2018	9.13	0.49	0.20	2.51	0.68
17-04-2018	11.17	0.45	0.20	2.32	0.87
18-04-2018	8.66	0.44	0.20	2.24	0.56
19-04-2018	4.54	0.45	0.20	2.25	0.25
20-04-2018	3.45	0.51	0.20	2.55	0.23
21-04-2018	2.96	0.56	0.20	2.81	0.22
22-04-2018	7.27	0.61	0.20	3.11	0.76
23-04-2018	8.17	0.47	0.20	2.37	0.56

24-04-2018	4.97	0.44	0.20	2.20	0.26
25-04-2018	7.95	0.47	0.20	2.35	0.51
26-04-2018	6.75	0.42	0.20	2.09	0.38
27-04-2018	2.77	0.42	0.20	2.09	0.11
28-04-2018	2.12	0.42	0.20	2.07	0.07
29-04-2018	2.83	0.44	0.20	2.18	0.11
30-04-2018	2.10	0.47	0.20	2.36	0.10
01-05-2018	7.44	0.50	0.20	2.52	0.53
02-05-2018	6.82	0.44	0.20	2.23	0.37
03-05-2018	6.07	0.44	0.20	2.20	0.30
04-05-2018	4.22	0.43	0.20	2.17	0.21
05-05-2018	3.97	0.45	0.20	2.29	0.22
06-05-2018	3.19	0.44	0.20	2.22	0.18
07-05-2018	3.26	0.43	0.20	2.17	0.17
08-05-2018	6.28	0.62	0.20	3.18	0.76
09-05-2018	6.07	0.50	0.20	2.53	0.47
10-05-2018	5.53	0.41	0.20	2.06	0.27
11-05-2018	6.09	0.41	0.20	2.09	0.32
12-05-2018	2.49	0.43	0.20	2.18	0.11
13-05-2018	3.92	0.38	0.20	1.93	0.15
14-05-2018	2.29	0.36	0.20	1.80	0.08

15-05-2018	3.19	0.36	0.20	1.83	0.11
16-05-2018	3.45	0.45	0.20	2.22	0.16
17-05-2018	3.19	0.36	0.20	1.80	0.11
18-05-2018	2.04	0.34	0.20	1.70	0.06
19-05-2018	4.84	0.39	0.20	1.99	0.27
20-05-2018	5.49	0.44	0.20	2.23	0.32
21-05-2018	3.02	0.42	0.20	2.12	0.14
22-05-2018	2.47	0.45	0.20	2.26	0.13
23-05-2018	4.09	0.41	0.20	2.08	0.22
24-05-2018	2.14	0.45	0.20	2.27	0.13
25-05-2018	4.50	0.51	0.20	2.58	0.36
26-05-2018	4.27	0.51	0.20	2.60	0.32
27-05-2018	4.22	0.47	0.20	2.39	0.30
28-05-2018	2.29	0.40	0.20	2.01	0.10
29-05-2018	3.86	0.44	0.20	2.24	0.25
30-05-2018	3.22	0.48	0.20	2.45	0.21
31-05-2018	1.63	0.43	0.19	2.23	0.10
01-06-2018	1.41	0.46	0.20	2.36	0.11
02-06-2018	2.40	0.56	0.20	2.86	0.21
03-06-2018	2.10	0.60	0.20	3.08	0.20
04-06-2018	2.12	0.63	0.20	3.22	0.24
05-06-2018	3.09	0.61	0.20	3.08	0.31
06-06-2018	2.77	0.59	0.20	3.02	0.26

07-06-2018	2.83	0.56	0.20	2.89	0.26
08-06-2018	2.38	0.51	0.19	2.63	0.19
09-06-2018	2.77	0.51	0.19	2.62	0.24
10-06-2018	2.57	0.56	0.19	2.86	0.24
11-06-2018	2.64	0.67	0.20	3.45	0.30
12-06-2018	1.97	0.66	0.20	3.35	0.21
13-06-2018	6.62	0.58	0.20	2.98	0.72
14-06-2018	10.95	0.40	0.19	2.05	0.93
15-06-2018	5.53	0.41	0.20	2.07	0.29
16-06-2018	7.31	0.42	0.20	2.16	0.48
17-06-2018	6.60	0.42	0.20	2.14	0.39
18-06-2018	6.60	0.41	0.20	2.09	0.38
19-06-2018	5.04	0.42	0.20	2.14	0.31
20-06-2018	6.45	0.40	0.20	2.04	0.39
21-06-2018	4.05	0.40	0.20	1.97	0.18
22-06-2018	2.01	0.38	0.20	1.90	0.08
23-06-2018	1.78	0.37	0.20	1.86	0.08
24-06-2018	1.84	0.41	0.20	2.08	0.10
25-06-2018	2.98	0.45	0.19	2.33	0.20
26-06-2018	2.51	0.52	0.20	2.66	0.21
27-06-2018	3.19	0.54	0.19	2.76	0.30
28-06-2018	3.11	0.60	0.19	3.07	0.35
29-06-2018	3.34	0.60	0.19	3.09	0.34

30-06-2018	3.49	0.58	0.19	3.01	0.37
01-07-2018	3.02	0.59	0.19	3.03	0.31
02-07-2018	2.96	0.60	0.19	3.08	0.28
03-07-2018	3.84	0.55	0.19	2.82	0.37
04-07-2018	2.79	0.56	0.19	2.92	0.26
05-07-2018	3.26	0.66	0.19	3.39	0.40
06-07-2018	1.74	0.57	0.19	2.94	0.17
07-07-2018	2.53	0.72	0.20	3.69	0.31

Table 23 Summary of results (daily averages) from ST2: 1st of April to 7th of July 2018.

Date	**Wind speed m/s**	**CO_2 mg/l [C]**	**Air CO_2 mg/l [C]**	**epCO_2 mg/l [C]**	**CO_2 flux/gm^{-2}d^{-1}**
01-04-2018	6.90	0.60	0.20	2.97	0.53
02-04-2018	4.57	0.63	0.20	3.17	0.33
03-04-2018	4.44	0.72	0.19	3.72	0.43
04-04-2018	3.79	0.59	0.20	2.99	0.25
05-04-2018	4.61	0.55	0.20	2.75	0.31
06-04-2018	8.85	0.52	0.20	2.64	0.68
07-04-2018	2.64	0.55	0.20	2.81	0.15
08-04-2018	2.74	0.60	0.20	3.05	0.19

09-04-2018	3.58	0.61	0.20	3.06	0.28
10-04-2018	4.46	0.63	0.20	3.18	0.37
11-04-2018	4.33	0.66	0.20	3.32	0.37
12-04-2018	3.60	0.65	0.20	3.27	0.29
13-04-2018	2.01	0.67	0.20	3.37	0.16
14-04-2018	5.02	0.63	0.20	3.20	0.43
15-04-2018	6.67	0.59	0.20	3.04	0.60
16-04-2018	9.13	0.56	0.20	2.88	0.84
17-04-2018	11.17	0.52	0.20	2.66	1.13
18-04-2018	8.66	0.49	0.20	2.51	0.72
19-04-2018	4.54	0.52	0.20	2.66	0.35
20-04-2018	3.45	0.58	0.20	2.89	0.30
21-04-2018	2.96	0.61	0.20	3.10	0.27
22-04-2018	7.27	0.58	0.20	2.95	0.69
23-04-2018	8.17	0.50	0.20	2.51	0.62
24-04-2018	4.97	0.51	0.20	2.55	0.32
25-04-2018	7.95	0.49	0.20	2.47	0.56
26-04-2018	6.75	0.47	0.20	2.34	0.45
27-04-2018	2.77	0.48	0.20	2.42	0.15

28-04-2018	2.12	0.53	0.20	2.64	0.12
29-04-2018	2.83	0.52	0.20	2.59	0.18
30-04-2018	2.10	0.54	0.20	2.68	0.13
01-05-2018	7.44	0.50	0.20	2.54	0.55
02-05-2018	6.82	0.49	0.20	2.46	0.46
03-05-2018	6.07	0.50	0.20	2.49	0.40
04-05-2018	4.22	0.49	0.20	2.49	0.27
05-05-2018	3.97	0.52	0.20	2.65	0.32
06-05-2018	3.19	0.58	0.20	2.95	0.30
07-05-2018	3.26	0.64	0.20	3.23	0.35
08-05-2018	6.28	0.65	0.20	3.30	0.79
09-05-2018	6.07	0.58	0.20	2.91	0.58
10-05-2018	5.53	0.48	0.20	2.40	0.34
11-05-2018	6.09	0.52	0.20	2.62	0.46
12-05-2018	2.49	0.59	0.20	2.99	0.20
13-05-2018	3.92	0.56	0.20	2.82	0.30
14-05-2018	2.29	0.55	0.20	2.79	0.17
15-05-2018	3.19	0.52	0.20	2.63	0.23
16-05-2018	3.45	0.53	0.20	2.63	0.23
17-05-2018	3.19	0.48	0.20	2.37	0.20
18-05-2018	2.04	0.47	0.20	2.34	0.13
19-05-2018	4.84	0.47	0.20	2.37	0.33

20-05-2018	5.49	0.51	0.20	2.61	0.42
21-05-2018	3.02	0.50	0.20	2.50	0.18
22-05-2018	2.47	0.53	0.20	2.64	0.17
23-05-2018	4.09	0.48	0.20	2.42	0.29
24-05-2018	2.14	0.51	0.20	2.56	0.17
25-05-2018	4.50	0.54	0.20	2.76	0.37
26-05-2018	4.27	0.54	0.20	2.74	0.34
27-05-2018	4.22	0.49	0.20	2.51	0.33
28-05-2018	2.29	0.50	0.20	2.53	0.15
29-05-2018	3.86	0.49	0.20	2.48	0.27
30-05-2018	3.22	0.53	0.20	2.71	0.25
31-05-2018	1.63	0.56	0.19	2.87	0.15
01-06-2018	1.41	0.61	0.20	3.14	0.18
02-06-2018	2.40	0.73	0.20	3.72	0.31
03-06-2018	2.10	0.75	0.20	3.82	0.27
04-06-2018	2.12	0.70	0.20	3.57	0.26
05-06-2018	3.09	0.63	0.20	3.21	0.33
06-06-2018	2.77	0.56	0.20	2.87	0.23
07-06-2018	2.83	0.55	0.20	2.81	0.23
08-06-2018	2.38	0.58	0.19	2.97	0.22
09-06-2018	2.77	0.63	0.19	3.26	0.30
10-06-2018	2.57	0.71	0.19	3.62	0.32
11-06-2018	2.64	0.74	0.20	3.80	0.34

12-06-2018	1.97	0.75	0.20	3.79	0.25
13-06-2018	6.62	0.60	0.20	3.08	0.64
14-06-2018	10.95	0.42	0.19	2.15	1.00
15-06-2018	5.53	0.46	0.20	2.35	0.36
16-06-2018	7.31	0.45	0.20	2.31	0.51
17-06-2018	6.60	0.46	0.20	2.37	0.43
18-06-2018	6.60	0.42	0.20	2.15	0.40
19-06-2018	5.04	0.49	0.20	2.48	0.33
20-06-2018	6.45	0.44	0.20	2.25	0.49
21-06-2018	4.05	0.47	0.20	2.33	0.25
22-06-2018	2.01	0.46	0.20	2.29	0.11
23-06-2018	1.78	0.49	0.20	2.45	0.13
24-06-2018	1.84	0.58	0.20	2.94	0.17
25-06-2018	2.98	0.68	0.19	3.47	0.35
26-06-2018	2.51	0.75	0.20	3.86	0.35
27-06-2018	3.19	0.72	0.19	3.68	0.40
28-06-2018	3.11	0.70	0.19	3.57	0.38
29-06-2018	3.34	0.67	0.19	3.46	0.37
30-06-2018	3.49	0.72	0.19	3.70	0.46
01-07-2018	3.02	0.78	0.19	4.03	0.41
02-07-2018	2.96	0.66	0.19	3.39	0.29
03-07-2018	3.84	0.68	0.19	3.51	0.45
04-07-2018	2.79	0.83	0.19	4.31	0.41

05-07-2018	3.26	0.81	0.19	4.15	0.52
06-07-2018	1.74	0.80	0.19	4.11	0.26
07-07-2018	2.53	1.04	0.20	5.30	0.49

Table 24 Summary of results from ST3: 20th of May to 7th of July 2018.

Date	**Wind speed m/s**	**CO_2 mg/l [C]**	**Air CO_2 mg/l [C]**	**epCO_2 mg/l [C]**	**CO_2 flux/gm^{-2}d^{-1}**
20-05-2018	8	0.28	0.20	1.38	0.17
21-05-2018	6	0.31	0.20	1.51	0.17
22-05-2018	5	0.36	0.20	1.77	0.19
23-05-2018	6	0.41	0.20	2.00	0.33
24-05-2018	6	0.47	0.20	2.31	0.45
25-05-2018	8	0.41	0.20	2.00	0.49
26-05-2018	8	0.37	0.20	1.85	0.37
27-05-2018	7	0.35	0.20	1.74	0.29
28-05-2018	8	0.37	0.20	1.82	0.44
29-05-2018	8	0.41	0.20	2.01	0.53
30-05-2018	8	0.37	0.20	1.81	0.38
31-05-2018	9	0.44	0.20	2.16	0.74
01-06-2018	8	0.53	0.20	2.61	0.93
02-06-2018	8	0.56	0.20	2.75	0.98
03-06-2018	8	0.59	0.20	2.88	0.98

04-06-2018	8	0.54	0.20	2.62	0.86
05-06-2018	7	0.47	0.20	2.33	0.61
06-06-2018	8	0.45	0.20	2.20	0.58
07-06-2018	9	0.46	0.20	2.29	0.73
08-06-2018	9	0.48	0.20	2.36	0.87
09-06-2018	9	0.57	0.20	2.83	1.22
10-06-2018	8	0.63	0.20	3.09	1.27
11-06-2018	8	0.65	0.20	3.21	1.19
12-06-2018	7	0.64	0.20	3.11	0.84
13-06-2018	7	0.46	0.20	2.29	0.53
14-06-2018	8	0.29	0.19	1.54	0.22
15-06-2018	6	0.37	0.20	1.85	0.27
16-06-2018	7	0.35	0.19	1.78	0.28
17-06-2018	7	0.37	0.20	1.86	0.34
18-06-2018	7	0.34	0.20	1.73	0.27
19-06-2018	8	0.42	0.20	2.07	0.45
20-06-2018	7	0.37	0.20	1.86	0.38
21-06-2018	6	0.42	0.20	2.08	0.32
22-06-2018	7	0.44	0.21	2.11	0.43
23-06-2018	8	0.56	0.21	2.71	0.92
24-06-2018	9	0.66	0.21	3.21	1.57
25-06-2018	10	0.77	0.20	3.78	2.26
26-06-2018	10	0.82	0.21	3.98	2.23

27-06-2018	10	0.79	0.20	3.86	2.44
28-06-2018	11	0.76	0.20	3.72	2.30
29-06-2018	10	0.75	0.20	3.66	2.21
30-06-2018	9	0.84	0.20	4.14	2.20
01-07-2018	9	0.86	0.20	4.27	1.99
02-07-2018	9	0.66	0.20	3.28	1.24
03-07-2018	9	0.80	0.20	3.99	1.88
04-07-2018	10	0.92	0.20	4.54	2.78
05-07-2018	9	1.00	0.20	4.96	2.30
06-07-2018	9	0.93	0.20	4.54	2.36
07-07-2018	9	1.17	0.19	5.87	2.78

Table 25 Summary of results from HumST1: 1st of April to 7th of July 2018 (daily averages).

Date	**WT1/ ^{0}C**	**CO_2 mg/l [C]**	**epCO_2 mg/l [C]**
01-04-2018	3	7.03	35.04
02-04-2018	3	6.37	32.28
03-04-2018	3	5.29	27.29
04-04-2018	4	5.03	25.45
05-04-2018	4	3.52	17.45
06-04-2018	4	3.11	15.81

07-04-2018	4	3.32	16.85
08-04-2018	4	3.02	15.26
09-04-2018	5	2.87	14.54
10-04-2018	5	2.67	13.48
11-04-2018	5	2.49	12.52
12-04-2018	5	2.54	12.80
13-04-2018	5	2.62	13.24
14-04-2018	6	2.70	13.66
15-04-2018	6	2.66	13.59
16-04-2018	6	2.46	12.53
17-04-2018	6	2.23	11.43
18-04-2018	7	2.15	10.94
19-04-2018	7	2.37	12.00
20-04-2018	8	2.73	13.69
21-04-2018	8	3.31	16.81
22-04-2018	8	7.25	36.88
23-04-2018	8	9.74	49.31
24-04-2018	8	8.84	44.57
25-04-2018	7	7.77	39.12

26-04-2018	7	7.14	35.77
27-04-2018	7	6.63	33.23
28-04-2018	6	6.03	30.09
29-04-2018	6	5.92	29.47
30-04-2018	6	5.84	29.15
01-05-2018	6	6.19	31.32
02-05-2018	6	5.92	29.94
03-05-2018	6	5.52	27.70
04-05-2018	7	5.74	28.99
05-05-2018	8	6.21	31.45
06-05-2018	8	8.88	45.24
07-05-2018	9	11.03	56.13
08-05-2018	9	10.75	54.71
09-05-2018	9	10.34	52.19
10-05-2018	9	9.75	48.98
11-05-2018	8	8.89	44.87
12-05-2018	8	7.58	38.10
13-05-2018	8	7.46	37.48
14-05-2018	8	7.68	38.69
15-05-2018	9	7.78	39.16
16-05-2018	9	8.28	40.84
17-05-2018	9	8.87	43.99

18-05-2018	9	9.29	46.60
19-05-2018	9	9.70	49.11
20-05-2018	9	12.35	62.79
21-05-2018	9	12.74	64.25
22-05-2018	9	12.07	60.32
23-05-2018	10	11.77	58.92
24-05-2018	10	11.97	60.03
25-05-2018	10	11.71	59.58
26-05-2018	10	11.02	55.78
27-05-2018	11	10.37	52.67
28-05-2018	11	10.33	52.64
29-05-2018	11	10.64	54.27
30-05-2018	11	11.40	58.27
31-05-2018	11	11.74	60.37
01-06-2018	12	11.63	59.52
02-06-2018	12	11.82	60.46
03-06-2018	12	11.94	60.86
04-06-2018	12	12.30	62.80
05-06-2018	12	12.37	62.83
06-06-2018	12	12.85	65.55
07-06-2018	12	13.26	67.97
08-06-2018	12	13.33	68.42
09-06-2018	12	13.89	71.52

10-06-2018	12	13.97	71.72
11-06-2018	13	14.04	71.80
12-06-2018	13	14.01	71.00
13-06-2018	13	13.42	68.64
14-06-2018	13	11.86	61.19
15-06-2018	12	12.21	61.96
16-06-2018	12	10.23	52.34
17-06-2018	12	9.27	47.48
18-06-2018	12	9.61	49.04
19-06-2018	12	8.39	42.82
20-06-2018	12	8.46	43.03
21-06-2018	12	9.41	47.01
22-06-2018	12	10.32	51.50
23-06-2018	12	11.03	55.64
24-06-2018	12	11.84	60.52
25-06-2018	12	12.51	64.19
26-06-2018	12	13.42	68.68
27-06-2018	12	14.64	75.31
28-06-2018	13	15.98	82.39
29-06-2018	13	16.62	85.79
30-06-2018	13	16.71	86.15
01-07-2018	13	16.58	85.66
02-07-2018	13	16.72	86.13

03-07-2018	13	17.18	88.59
04-07-2018	13	17.95	93.78
05-07-2018	13	17.40	89.77
06-07-2018	13	17.29	89.25
07-07-2018	13	17.53	89.65

Table 26 Summary of results from LawnST2: 20th of May to 7th of July 2018 (daily averages).

Date	**WT2/ ^{0}C**	**CO_2 mg/l [C]**	**epCO_2 mg/l [C]**
20-05-2018	9	4.62	23.16
21-05-2018	10	4.65	22.94
22-05-2018	9	4.67	22.86
23-05-2018	10	4.89	24.14
24-05-2018	10	4.97	24.26
25-05-2018	10	5.10	25.31
26-05-2018	10	5.18	25.65
27-05-2018	11	4.95	24.60
28-05-2018	11	5.16	25.26
29-05-2018	11	5.46	27.03

30-05-2018	11	5.47	27.09
31-05-2018	12	5.73	28.09
01-06-2018	12	5.33	26.01
02-06-2018	12	5.07	24.96
03-06-2018	12	5.58	27.33
04-06-2018	12	5.67	27.80
05-06-2018	12	5.60	27.63
06-06-2018	12	5.55	27.37
07-06-2018	12	5.46	26.90
08-06-2018	12	5.31	26.07
09-06-2018	12	5.56	27.47
10-06-2018	13	4.93	24.29
11-06-2018	13	4.37	21.55
12-06-2018	13	3.95	19.35
13-06-2018	13	3.41	17.34
14-06-2018	12	3.27	17.23
15-06-2018	12	2.72	13.72
16-06-2018	12	2.07	10.59
17-06-2018	12	2.59	13.19
18-06-2018	12	1.94	9.84
19-06-2018	12	1.42	7.13
20-06-2018	12	1.56	7.91
21-06-2018	12	1.64	8.08

22-06-2018	12	1.64	7.92
23-06-2018	12	1.71	8.29
24-06-2018	12	1.09	5.29
25-06-2018	12	0.97	4.75
26-06-2018	12	1.69	8.25
27-06-2018	12	2.10	10.29
28-06-2018	13	1.10	5.37
29-06-2018	13	0.49	2.42
30-06-2018	13	0.57	2.82
01-07-2018	13	2.56	12.77
02-07-2018	13	3.75	18.58
03-07-2018	13	4.59	22.90
04-07-2018	13	4.89	24.26
05-07-2018	13	5.51	27.37
06-07-2018	13	5.67	27.78
07-07-2018	13	5.56	28.03

Table 27 Summary of results from HumST3: 20th of May to 7th of July 2018 (daily averages).

Date	**WT3/ ^{0}C**	**CO_2 mg/l [C]**	**epCO_2 mg/l [C]**
20-05-2018	9	10.43	52.25
21-05-2018	10	10.24	50.50

22-05-2018	9	10.00	48.96
23-05-2018	10	9.80	48.37
24-05-2018	10	9.43	46.02
25-05-2018	10	9.36	46.41
26-05-2018	10	8.96	44.41
27-05-2018	11	8.83	43.92
28-05-2018	11	8.82	43.15
29-05-2018	11	8.63	42.74
30-05-2018	11	8.47	41.97
31-05-2018	12	8.20	40.17
01-06-2018	12	7.72	37.68
02-06-2018	12	7.45	36.61
03-06-2018	12	7.07	34.64
04-06-2018	12	6.57	32.22
05-06-2018	12	6.43	31.74
06-06-2018	12	5.74	28.31
07-06-2018	12	4.66	22.96
08-06-2018	12	3.50	17.20
09-06-2018	12	1.62	7.97
10-06-2018	13	0.75	3.69
11-06-2018	13	0.63	3.11
12-06-2018	13	0.55	2.67
13-06-2018	13	0.44	2.23

14-06-2018	12	0.78	4.12
15-06-2018	12	0.56	2.82
16-06-2018	12	1.50	7.72
17-06-2018	12	2.65	13.53
18-06-2018	12	1.14	5.78
19-06-2018	12	2.78	13.93
20-06-2018	12	2.99	15.07
21-06-2018	12	1.85	9.11
22-06-2018	12	0.46	2.22
23-06-2018	12	0.43	2.10
24-06-2018	12	0.39	1.91
25-06-2018	12	0.38	1.85
26-06-2018	12	0.37	1.79
27-06-2018	12	0.34	1.69
28-06-2018	13	0.35	1.73
29-06-2018	13	0.27	1.32
30-06-2018	13	0.32	1.58
01-07-2018	13	0.43	2.15
02-07-2018	13	0.34	1.69
03-07-2018	13	0.27	1.37
04-07-2018	13	0.35	1.74
05-07-2018	13	0.44	2.17
06-07-2018	13	0.60	2.93

07-07-2018	13	0.66	3.35

Table 28 Summary of results from ST1: 8th of July to 31st of August 2018 (daily averages).

Date	**Wind speed m/s**	**CO_2 mg/l [C]**	**Air CO_2 mg/l [C]**	**epCO_2 mg/l [C]**	**CO_2 flux/gm^{-2}d^{-1}**
08-07-2018	2.38	0.67	0.19	3.44	0.29
09-07-2018	2.36	0.65	0.20	3.33	0.28
10-07-2018	2.81	0.69	0.20	3.53	0.34
11-07-2018	1.78	0.64	0.20	3.30	0.20
12-07-2018	2.21	0.75	0.20	3.82	0.29
13-07-2018	2.14	0.68	0.19	3.49	0.26
14-07-2018	3.67	0.63	0.19	3.27	0.42
15-07-2018	5.06	0.78	0.19	4.05	0.81
16-07-2018	3.84	0.69	0.19	3.54	0.45
17-07-2018	3.30	0.66	0.19	3.38	0.35
18-07-2018	3.22	0.64	0.19	3.32	0.33
19-07-2018	3.19	0.67	0.19	3.42	0.35
20-07-2018	3.97	0.73	0.19	3.76	0.55
21-07-2018	3.24	0.66	0.19	3.42	0.34

22-07-2018	4.50	0.61	0.19	3.15	0.48
23-07-2018	3.84	0.50	0.19	2.60	0.32
24-07-2018	3.43	0.70	0.19	3.61	0.44
25-07-2018	3.17	0.64	0.19	3.31	0.33
26-07-2018	4.69	0.65	0.19	3.41	0.58
27-07-2018	4.46	0.58	0.19	3.03	0.44
28-07-2018	5.72	0.56	0.19	2.90	0.61
29-07-2018	3.37	0.50	0.19	2.62	0.23
30-07-2018	4.61	0.54	0.19	2.78	0.38
31-07-2018	6.71	0.53	0.19	2.72	0.61
01-08-2018	6.79	0.46	0.19	2.37	0.47
02-08-2018	4.99	0.41	0.19	2.13	0.28
03-08-2018	4.14	0.44	0.19	2.30	0.28
04-08-2018	2.40	0.50	0.19	2.59	0.20
05-08-2018	2.85	0.55	0.19	2.84	0.26
06-08-2018	4.20	0.72	0.19	3.73	0.60
07-08-2018	4.42	0.72	0.19	3.72	0.59
08-08-2018	5.47	0.66	0.19	3.42	0.66
09-08-2018	4.74	0.58	0.19	2.97	0.43
10-08-2018	4.03	0.55	0.20	2.80	0.34

11-08-2018	3.54	0.53	0.19	2.72	0.27
12-08-2018	2.14	0.43	0.19	2.28	0.12
13-08-2018	3.62	0.57	0.19	2.95	0.33
14-08-2018	6.37	0.60	0.19	3.11	0.72
15-08-2018	6.75	0.49	0.19	2.57	0.63
16-08-2018	6.34	0.51	0.19	2.61	0.54
17-08-2018	7.95	0.50	0.19	2.56	0.68
18-08-2018	7.05	0.42	0.19	2.21	0.47
19-08-2018	5.68	0.42	0.19	2.20	0.45
20-08-2018	3.02	0.40	0.19	2.08	0.15
21-08-2018	4.05	0.43	0.19	2.22	0.25
22-08-2018	5.17	0.67	0.19	3.49	0.82
23-08-2018	6.32	0.61	0.20	3.13	0.70
24-08-2018	5.81	0.46	0.20	2.34	0.40
25-08-2018	3.73	0.42	0.20	2.12	0.18
26-08-2018	5.96	0.47	0.19	2.44	0.45
27-08-2018	6.88	0.50	0.19	2.57	0.58
28-08-2018	4.14	0.49	0.20	2.50	0.28
29-08-2018	3.90	0.50	0.20	2.56	0.27
30-08-2018	1.82	0.48	0.20	2.43	0.11
31-08-2018	3.37	0.57	0.19	2.92	0.29

Table 29 Summary of results from ST2: 8th of July to 31st of August 2018 (daily averages).

Date	Wind speed m/s	CO_2 mg/l [C]	Air CO_2 mg/l [C]	epCO_2 mg/l [C]	CO_2 flux/gm^{-2}d^{-1}
08-07-2018	2.38	0.89	0.19	4.60	0.43
09-07-2018	2.36	0.95	0.20	4.83	0.42
10-07-2018	2.81	0.86	0.20	4.39	0.42
11-07-2018	1.78	0.95	0.20	4.85	0.34
12-07-2018	2.21	1.11	0.20	5.68	0.48
13-07-2018	2.14	0.98	0.19	5.00	0.39
14-07-2018	3.67	0.88	0.19	4.58	0.64
15-07-2018	5.06	0.92	0.19	4.75	0.98
16-07-2018	3.84	0.86	0.19	4.44	0.58
17-07-2018	3.30	0.80	0.19	4.11	0.45
18-07-2018	3.22	0.78	0.19	4.03	0.43
19-07-2018	3.19	0.78	0.19	4.01	0.43
20-07-2018	3.97	0.76	0.19	3.92	0.57
21-07-2018	3.24	0.71	0.19	3.66	0.36
22-07-2018	4.50	0.70	0.19	3.64	0.58

23-07-2018	3.84	0.73	0.19	3.83	0.52
24-07-2018	3.43	0.78	0.19	4.05	0.51
25-07-2018	3.17	0.76	0.19	3.92	0.40
26-07-2018	4.69	0.73	0.19	3.83	0.63
27-07-2018	4.46	0.75	0.19	3.91	0.62
28-07-2018	5.72	0.63	0.19	3.24	0.66
29-07-2018	3.37	0.59	0.19	3.10	0.28
30-07-2018	4.61	0.59	0.19	3.08	0.45
31-07-2018	6.71	0.53	0.19	2.71	0.58
01-08-2018	6.79	0.51	0.19	2.62	0.51
02-08-2018	4.99	0.51	0.19	2.66	0.42
03-08-2018	4.14	0.60	0.19	3.13	0.47
04-08-2018	2.40	0.71	0.19	3.67	0.32
05-08-2018	2.85	0.73	0.19	3.77	0.37
06-08-2018	4.20	0.74	0.19	3.85	0.63
07-08-2018	4.42	0.65	0.19	3.37	0.50
08-08-2018	5.47	0.58	0.19	2.98	0.53
09-08-2018	4.74	0.56	0.19	2.87	0.40
10-08-2018	4.03	0.54	0.20	2.74	0.32
11-08-2018	3.54	0.53	0.19	2.76	0.26

12-08-2018	2.14	0.54	0.19	2.83	0.17
13-08-2018	3.62	0.60	0.19	3.12	0.34
14-08-2018	6.37	0.52	0.19	2.71	0.56
15-08-2018	6.75	0.50	0.19	2.59	0.65
16-08-2018	6.34	0.52	0.19	2.67	0.52
17-08-2018	7.95	0.48	0.19	2.47	0.60
18-08-2018	7.05	0.44	0.19	2.28	0.50
19-08-2018	5.68	0.44	0.19	2.29	0.49
20-08-2018	3.02	0.48	0.19	2.49	0.21
21-08-2018	4.05	0.58	0.19	3.00	0.40
22-08-2018	5.17	0.56	0.19	2.90	0.64
23-08-2018	6.32	0.56	0.20	2.87	0.57
24-08-2018	5.81	0.46	0.20	2.34	0.38
25-08-2018	3.73	0.47	0.20	2.38	0.22
26-08-2018	5.96	0.52	0.19	2.71	0.50
27-08-2018	6.88	0.51	0.19	2.62	0.60
28-08-2018	4.14	0.54	0.20	2.78	0.34
29-08-2018	3.90	0.55	0.20	2.78	0.31
30-08-2018	1.82	0.56	0.20	2.85	0.13
31-08-2018	3.37	0.61	0.19	3.12	0.32

Table 30 Summary of results from ST3: 8th of July to 31st of August 2018 (daily averages).

Date	Wind speed m/s	CO_2 mg/l [C]	Air CO_2 mg/l [C]	epCO_2 mg/l [C]	CO_2 flux/gm^{-2}d^{-1}
08-07-2018	2.38	0.97	0.19	5.00	0.47
09-07-2018	2.36	0.97	0.20	4.96	0.44
10-07-2018	2.81	0.88	0.20	4.46	0.43
11-07-2018	1.78	0.94	0.20	4.79	0.33
12-07-2018	2.21	0.92	0.20	4.71	0.37
13-07-2018	2.14	0.80	0.19	4.12	0.31
14-07-2018	3.67	0.83	0.19	4.29	0.57
15-07-2018	5.06	0.91	0.19	4.73	0.95
16-07-2018	3.84	0.82	0.19	4.22	0.53
17-07-2018	3.30	0.76	0.19	3.93	0.42
18-07-2018	3.22	0.82	0.19	4.21	0.45
19-07-2018	3.19	0.78	0.19	4.01	0.41
20-07-2018	3.97	0.77	0.19	3.97	0.57
21-07-2018	3.24	0.77	0.19	3.96	0.40

22-07-2018	4.50	0.83	0.19	4.31	0.72
23-07-2018	3.84	1.00	0.19	5.23	0.72
24-07-2018	3.43	0.98	0.19	5.08	0.66
25-07-2018	3.17	0.90	0.19	4.65	0.50
26-07-2018	4.69	0.73	0.19	3.83	0.59
27-07-2018	4.46	0.69	0.19	3.61	0.56
28-07-2018	5.72	0.56	0.19	2.91	0.56
29-07-2018	3.37	0.49	0.19	2.58	0.22
30-07-2018	4.61	0.56	0.19	2.92	0.41
31-07-2018	6.71	0.48	0.19	2.49	0.51
01-08-2018	6.79	0.43	0.19	2.25	0.38
02-08-2018	4.99	0.55	0.19	2.87	0.47
03-08-2018	4.14	0.83	0.19	4.34	0.73
04-08-2018	2.40	0.86	0.19	4.45	0.41
05-08-2018	2.85	0.91	0.19	4.69	0.50
06-08-2018	4.20	0.89	0.19	4.62	0.77
07-08-2018	4.42	0.78	0.19	4.05	0.64
08-08-2018	5.47	0.62	0.19	3.22	0.58
09-08-2018	4.74	0.58	0.19	2.95	0.42
10-08-2018	4.03	0.58	0.20	2.97	0.36

11-08-2018	3.54	0.56	0.19	2.90	0.27
12-08-2018	2.14	0.80	0.19	4.21	0.27
13-08-2018	3.62	0.80	0.19	4.19	0.50
14-08-2018	6.37	0.58	0.19	3.00	0.64
15-08-2018	6.75	0.52	0.19	2.69	0.69
16-08-2018	6.34	0.54	0.19	2.78	0.56
17-08-2018	7.95	0.47	0.19	2.42	0.55
18-08-2018	7.05	0.45	0.19	2.36	0.54
19-08-2018	5.68	0.51	0.19	2.64	0.61
20-08-2018	3.02	0.66	0.19	3.43	0.34
21-08-2018	4.05	0.78	0.19	4.04	0.63
22-08-2018	5.17	0.67	0.19	3.50	0.85
23-08-2018	6.32	0.62	0.20	3.15	0.67
24-08-2018	5.81	0.48	0.20	2.42	0.41
25-08-2018	3.73	0.54	0.20	2.75	0.26
26-08-2018	5.96	0.60	0.19	3.10	0.67
27-08-2018	6.88	0.67	0.19	3.49	0.93
28-08-2018	4.14	0.67	0.20	3.42	0.48
29-08-2018	3.90	0.73	0.20	3.71	0.50
30-08-2018	1.82	0.71	0.20	3.59	0.19
31-08-2018	3.37	0.68	0.19	3.50	0.39

Table 31 Summary of results from HumST1: 8th of July to 31st of August 2018 (daily averages).

Date	WT1/ ^{0}C	CO_2 mg/l [C]	epCO_2 mg/l [C]
08-07-2018	13	33.24	171.04
09-07-2018	13	24.69	126.12
10-07-2018	13	20.70	105.56
11-07-2018	13	19.50	99.81
12-07-2018	13	18.28	93.45
13-07-2018	13	17.54	90.04
14-07-2018	13	17.37	90.29
15-07-2018	14	16.18	83.95
16-07-2018	14	14.21	73.35
17-07-2018	14	13.79	71.19
18-07-2018	14	13.72	70.78
19-07-2018	14	13.49	69.21
20-07-2018	13	12.81	66.06
21-07-2018	13	10.75	55.46
22-07-2018	13	11.84	61.80

23-07-2018	13	11.88	62.10
24-07-2018	14	10.50	54.20
25-07-2018	14	11.54	59.79
26-07-2018	14	12.30	64.45
27-07-2018	14	11.60	60.82
28-07-2018	14	7.08	36.75
29-07-2018	14	6.80	35.45
30-07-2018	14	7.22	37.40
31-07-2018	14	7.55	38.97
01-08-2018	13	7.82	40.48
02-08-2018	13	7.46	39.00
03-08-2018	13	8.13	42.29
04-08-2018	14	8.84	45.52
05-08-2018	14	9.60	49.71
06-08-2018	14	10.00	52.06
07-08-2018	14	9.64	50.02
08-08-2018	14	9.78	50.60
09-08-2018	14	9.97	51.21
10-08-2018	14	9.87	50.46
11-08-2018	13	9.17	47.38

12-08-2018	13	7.94	41.66
13-08-2018	13	8.25	42.91
14-08-2018	13	8.46	44.03
15-08-2018	14	8.66	45.30
16-08-2018	14	8.30	42.79
17-08-2018	14	8.13	41.75
18-08-2018	13	8.34	43.62
19-08-2018	13	8.25	42.89
20-08-2018	14	8.48	43.99
21-08-2018	14	9.09	47.32
22-08-2018	14	9.35	48.39
23-08-2018	14	9.06	46.42
24-08-2018	14	8.01	40.82
25-08-2018	14	7.93	40.47
26-08-2018	13	6.40	33.24
27-08-2018	13	8.15	42.12
28-08-2018	13	9.90	50.80
29-08-2018	13	10.00	50.99
30-08-2018	13	9.78	49.50
31-08-2018	13	9.56	49.06

Table 32 Summary of results from LawnST2: 8th of July to 30th of July 2018 (daily averages).

Date	WT2/ ^{0}C	CO_2 mg/l [C]	epCO_2 mg/l [C]
08-07-2018	13	9.99	51.49
09-07-2018	13	8.75	44.71
10-07-2018	13	7.77	39.64
11-07-2018	13	7.11	36.40
12-07-2018	13	6.18	31.58
13-07-2018	13	5.46	28.01
14-07-2018	13	4.90	25.47
15-07-2018	14	4.49	23.28
16-07-2018	14	4.42	22.82
17-07-2018	14	4.47	23.06
18-07-2018	14	4.38	22.59
19-07-2018	14	3.55	18.17
20-07-2018	13	3.85	19.89
21-07-2018	13	3.69	19.05
22-07-2018	13	2.25	11.67
23-07-2018	13	1.16	6.08

24-07-2018	14	1.41	7.29
25-07-2018	14	2.46	12.74
26-07-2018	14	2.72	14.29
27-07-2018	14	3.18	16.67
28-07-2018	14	2.15	11.18
29-07-2018	14	1.37	7.15
30-07-2018	14	0.84	4.35

Table 33 Summary of results from HumST3: 8th of July to 31st of August 2018 (daily averages).

Date	**WT3/ ^{0}C**	**CO_2 mg/l [C]**	**epCO_2 mg/l [C]**
08-07-2018	13	6.58	33.82
09-07-2018	13	3.89	19.88
10-07-2018	13	3.15	16.08
11-07-2018	13	3.46	17.72
12-07-2018	13	2.73	13.96
13-07-2018	13	2.64	13.58
14-07-2018	13	2.50	13.01
15-07-2018	14	2.41	12.53

16-07-2018	14	2.34	12.10
17-07-2018	14	2.31	11.91
18-07-2018	14	2.30	11.84
19-07-2018	14	2.91	14.94
20-07-2018	13	2.30	11.87
21-07-2018	13	2.31	11.91
22-07-2018	13	2.49	13.00
23-07-2018	13	2.36	12.35
24-07-2018	14	2.64	13.64
25-07-2018	14	2.63	13.63
26-07-2018	14	2.29	12.01
27-07-2018	14	2.08	10.88
28-07-2018	14	3.30	17.11
29-07-2018	14	5.67	29.59
30-07-2018	14	6.86	35.54
31-07-2018	14	4.47	23.07
01-08-2018	13	2.97	15.39
02-08-2018	13	4.40	23.03
03-08-2018	13	3.50	18.21

04-08-2018	14	2.79	14.35
05-08-2018	14	2.31	11.94
06-08-2018	14	2.09	10.89
07-08-2018	14	2.25	11.68
08-08-2018	14	2.16	11.20
09-08-2018	14	2.04	10.48
10-08-2018	14	1.96	10.05
11-08-2018	13	2.02	10.47
12-08-2018	13	3.71	19.48
13-08-2018	13	4.97	25.86
14-08-2018	13	4.29	22.34
15-08-2018	14	3.19	16.66
16-08-2018	14	3.95	20.35
17-08-2018	14	3.53	18.14
18-08-2018	13	3.46	18.08
19-08-2018	13	3.80	19.75
20-08-2018	14	5.02	26.05
21-08-2018	14	5.40	28.09
22-08-2018	14	4.00	20.74
23-08-2018	14	3.24	16.61
24-08-2018	14	3.27	16.65
25-08-2018	14	3.81	19.47

26-08-2018	13	6.71	34.98
27-08-2018	13	10.32	53.35
28-08-2018	13	10.09	51.72
29-08-2018	13	9.78	49.90
30-08-2018	13	9.54	48.28
31-08-2018	13	9.53	48.94

Table 34 Showing daily data of precipitation –average of two data sets. From the 1st of April until 7th of July 2018.

Date	Daily precipitation/mm
1-4-18	2.7
2-4-18	18.1
3-4-18	2.8
4-4-18	9.6
5-4-18	1.5
6-4-18	23.3
7-4-18	5.2
8-4-18	1.2
9-4-18	0.2
10-4-18	13.2
11-4-18	0.8
12-4-18	1.3
13-4-18	0.6
14-4-18	0.7
15-4-18	17.7
16-4-18	6.2
17-4-18	19.4
18-4-18	1
19-4-18	0.2
22-4-18	2.3
24-4-18	9.3
25-4-18	3.2
26-4-18	2.5
27-4-18	3.7
1-5-18	5.3
2-5-18	4.7
3-5-18	0.2
4-5-18	0.2
8-5-18	1.9
9-5-18	3.7
11-5-18	22.4
15-5-18	1.9
20-5-18	1.1
21-5-18	0.5
22-5-18	0.2
24-5-18	0.2
26-5-18	3.6
27-5-18	3.7
1-6-18	2.3
13-6-18	2.3
14-6-18	1

15-6-18	0.3
16-6-18	5.6
17-6-18	0.4
18-6-18	3.8
19-6-18	0.2
20-6-18	2.7
7-7-18	0.2

Table 35 Showing daily precipitation –average of two data sets. From 7th of July until 2nd of September 2018.

Date	Daily precipitation/mm
7-7-18	0
15-7-18	1.9
16-7-18	0.6
20-7-18	4.1
21-7-18	0.6
22-7-18	0
23-7-18	5.8
24-7-18	0.4
27-7-18	9
28-7-18	8.4
29-7-18	7.4
30-7-18	0.5
1-8-18	5.2
2-8-18	0.3
3-8-18	0.7
6-8-18	2.5
7-8-18	0.7
8-8-18	2.4
9-8-18	0
10-8-18	2.4
11-8-18	6.4
12-8-18	3.8
13-8-18	0.4
14-8-18	1.3
15-8-18	4.6
16-8-18	0.8
17-8-18	2.4

18-8-18	0.4
19-8-18	5
20-8-18	2.8
22-8-18	1.7
23-8-18	3.4
24-8-18	3.5
25-8-18	4
26-8-18	17.9
27-8-18	3.3
29-8-18	1
1-9-18	0.3
2-9-18	0

LIST OF PUBLICATIONS

1. Radomski, M. (2014) 'The impacts of climatic and anthropogenic variables on production and transport of Dissolved Organic Carbon (DOC) within northern peatlands', 5th Annual Postgraduate Research Symposium: Oral Presentations and Poster Displays by Postgraduate Research Students. Focas Research Institute, 25 November 2014. Dublin: Dublin Institute of Technology, p. 22.
2. Radomski, M., Gilmer, A. & Cassidy, J. (2015) 'Nitrogen Mediated Discharges of Dissolved Organic Carbon from Irish Blanket Peatlands: Space-time Events in Fluvial Distribution Networks', The 25th Environmental Researchers' Colloquium (ENVIRON 2015): Sustainability and Opportunities for Change. Institute of Technology, Sligo, 8-10 April 2015. Sligo: IT Sligo, p.181.
3. Radomski, M., Gilmer, A. & Byers, V. (2016) 'A sensor-based approach to the measurement of carbon fluxes in streams from blanket peatland dominated catchments in Ireland', The 26h Irish Environmental Research Colloquium: Ecosystem Services for a Sustainable Future. University of Limerick, 22-24 March 2016. Limerick: UL, p. 194.
4. Radomski, M., Gilmer, A. (2016) 'An in situ continuous measurement of the carbon fluxes in streams draining blanket peatlands in Ireland using a non-dispersive infrared sensor method', Nordic Water 2016 XXIX Nordic Hydrological conference: The Role of Hydrology towards water resources sustainability, August 8-10 2016, Lithuania: Kaunas, p.86.
5. Radomski, M., Gilmer, A. & Byers, V. (2016) 'Vegetation indices of freshwater carbon dynamics in Irish Blanket peatland catchments', The international water

association regional conference on diffuse pollution and catchment management, 23rd October-27th October 2016, Dublin City University, Ireland, p. 327.

6. Radomski, M. (2017) 'Analysis of the seasonal and diurnal dynamics of dissolved carbon dioxide along the riparian-pond continuum in a blanket peatland catchment of the Wicklow Mountains National Park, using a non-dispersive infrared sensor method', 7th Annual Graduate Research Symposium: Oral Presentations and Poster Displays by Graduate Research Students. Gleeson Theatre, DIT Kevin Street, 16 February 2017, p. 21.
7. Radomski, M., Gilmer, A. & Byers, V. (2017) 'An evaluation of spatio-temporal CO_2 flux gradients across the soil-pond profile in an upland Irish blanket peatland', HydroEco 2017, Ecohydrology on the edge: ecology-hydrology-human interactions in the changing world, 6th International Multidisciplinary conference on Hydrology and Ecology, 18-23rd June 2017, University of Birmingham: UK, p. 132.
8. Radomski, M., Gilmer, A., Byers, V., Cassidy, J. & McGovern, E. (2018) 'Factors affecting the carbon dynamics in blanket peatland – Irish case study', 'Wise use of peatlands, past and future', IPS 50th Anniversary Jubilee Symposium 2018, 11-13 September 2018, Rotterdam: Netherlands, p. 53.
9. Radomski, M. & Gilmer, A. (2018) Factors affecting carbon cycling in Kippure blanket peatland – case study from Ireland, *Peatlands International*, 4, 34-38.
10. Radomski, M., Gilmer, A., Byers, V. & McGovern, E. (2019) Carbon dioxide measurement in Irish blanket peatlands: an assessment of pool-soil flux variability, *Ecohydrology & Hydrobiology*, 19, 487-498.

List of Employability skills and discipline specific skills training

The following employability modules were selected to develop a skill set essential to carry out a more rigorous research and lecturing activity.

Employability Skills training:

1. GRSO1008 Communication skills,

2. GRSO1003 Project Management,

3. GRSO1001 Research Methods,

4. THED H1001 Teaching in Higher Education.

The discipline specific modules listed below were selected based on three factors: data analysis methodology, chemical techniques and environmental management.

Discipline Specific Skills training:

1. NMAD1005 NMR and molecular recognition,

2. BIOL9223 Research Methods / Biostatistics,

3. CIVL9007 Waste and Environmental Management Systems.